TEXTBOOK OF
MACHINES
HYDRAULIC

Prof. Dr. Magdy Abou Rayan
President of Mansoura University

Prof. Dr. Nabil H . Mostafa
Dept. of Mechanical Engineering
Zagazig University

Prof.Dr. Purage Ohans

This course designed to students
In the (3rd) year, Department of Mechanical Engineering
Faculity of Engineering - Zagazig University

CONTENTS

CHAPTER (I)   BASIC THEORY

CHAPTER (II)   DIMENSIONAL ANALYSIS AND SIMILITUDE OF TURBOMACHINES

CHAPTER (III) CASCADE MECHANICS
"TWO-DIMENSIONAL APPROACH"

B

CHAPTER (IV)   INCOMPRESSIBLE FLOW TURBOMACHINES (PUMPS)

CHAPTER (V)   INCOMPRESSIBLE FLOW TURBINES (Hydraulic Turbines)

D

CHAPTER (VI)   COMPRESSIBLE FLOW TURBOMACHINES
(Thermodynamic Principles)

CHAPTER (VII)   FANS, BLOWERS, and TURBO-COMPRESSORS

F

CHAPTER (VIII)   VOLUMETRIC MACHINES

APPENDIX "I"   Pressure Recovery Devices

APPENDIX "II"   Theory of Cavitation in Centrifugal Pumps

APPENDIX "III"   Solved Examples and Problems

H

<u>APPENDIX "IV"</u>   Tables and Charts

Types and shapes of turbomachines (adopted from Sayers)

CHAPTER (I)

BASIC THEORY
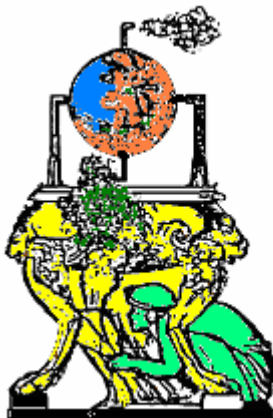
HISTORICAL REVIEW

Turbomachines by definition are those class of machines in which occurs a continuous energy transfer between a rigid body (Rotor) and a deformable media (fluid). A large number of machinery is characterized by this energy transfer process.
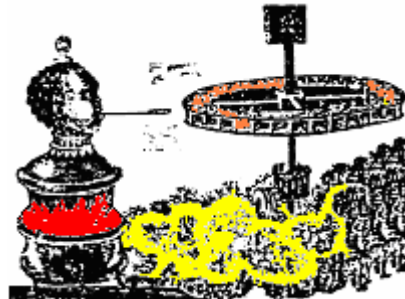
Historically, the first turbomachines can be traced back to hero of Alexandria who lived since 2000 years ago, (Fig. A.1). The machine was simply consists of a closed spherical vessel. The steam leaves the vessel through two pipes facing tangentially at the vessel's periphery. The vessel is then driven by the reaction of the steam jets.

The Romans introduced paddle-type water wheels, pure "impulse" wheels in around 70 BC for grinding grain, it seems that they were the true initiators, because Chinese writings set the first use of water wheels there at several decades later (26). In the succeeding centuries, water wheels of impulse type and windmills have been used.

In the 17th century Giovanni de Branca has suggested the idea of impulse steam turbine, (Fig. A.2).

**Fig. A.1 Hero's rotating sphere
of 120 B.C.**

**Fig. A.2 Giovanni de Branca's
turbine of 1629**

Through the eighteenth century, the mankind has acquired a suitable knowledge in hydrodynamics and thermodynamics to permit a real movement toward modern turbomachinery. In this time, the Swiss mathematician Leonard Euler (1707-1783), has published his application of Newton's law to turbomachinery which is known now as Euler's equation, since that time the development of turbomachinery has not ceased.

Now, the utilization of turbomachines is in all engineering applications. It is difficult to find any engineering construction without having a turbomachine element. The wide application of turbomachines has justified its important space in engineering curriculum.

1.1 General Introduction:

Every common turbomachine contains a rotor upon which blades are mounted, only the detailed physical arrangements differ. Fluid flows through the rotor from an entrance to an exit submit a change in momentum during the process because of the torque exerted on or by rotor blades.
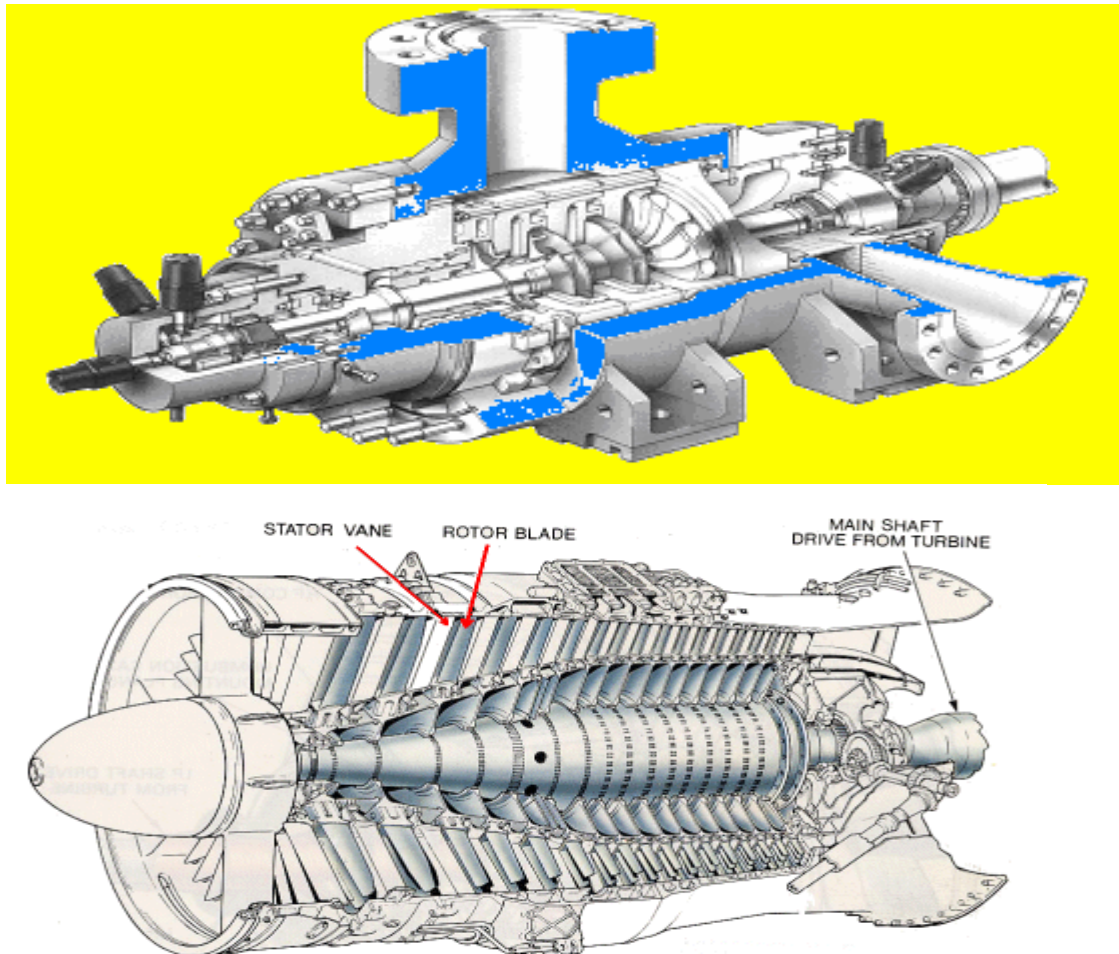
Fig. A.3 Modern turbomachinery rotor

Throughout this text, the emphasize has put on the practical aspects of the machines without going deep inside the mathematical formulation. Some important applications are treated separately as; cavitation

phenomena, pressure recovery devices and maintenance of turbomachines.

The turbomachines can be classified by the energy transfer principle, Figure 1.1:
    1. Turbines, energy transfers from the fluid to the rotor.
       2. Pumps, energy transfers from the wheel to the
  fluid.

The rotors also can be classified by the direction of flow in the wheel:
      - Radial Wheel,
      - Axial Wheel,
      - Mixed Wheel.
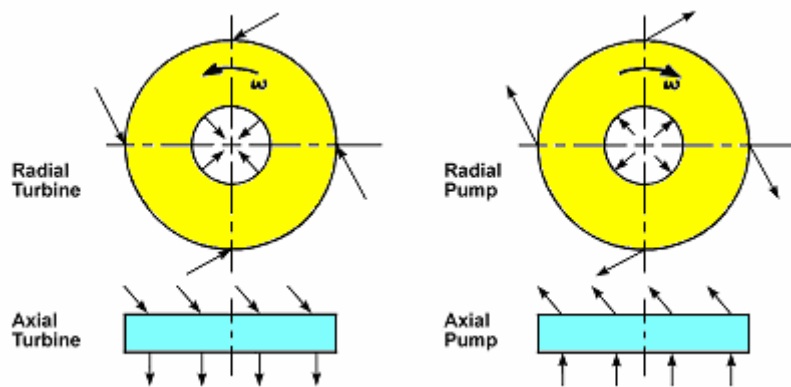
Fig. 1.1 Flow direction in turbines and pumps

Hydraulic Turbomachinery Classification

Energy Conversion Principle	Impulse	Reaction			
Energy transfer direction	+ ve	+ ve	- ve	+ ve	- ve
Flow Direction		Radial	Radial	Axial	Axial
Turbomachine	Pelton Wheel	Francis Turbine	Centrifugal Pump	Kaplan Turbine	Propeller Pump

    + ve   means energy transfer from fluid to wheel.
    - ve   means energy transfer from wheel to fluid.

1.2 Velocity Diagram:

Considering a fluid particle passing through the wheel, by definition C is the absolute velocity tangential to the absolute path, W is the relative velocity tangential to the blade or the relative path and U is the blade velocity.

Every instant during the particle movement through the wheel we have the following vectorial relationship:

$$\vec{C} = \vec{U} + \vec{W}$$

$U = \omega D / 2$

D : wheel diameter

α = angle between $\vec{U}, \vec{C}$

β = angle between $\vec{U}, \vec{W}$

$C_u = C \cos \alpha$

$C_r = C \sin \alpha$

1 - 2 relative path
1' - 2' absolute path
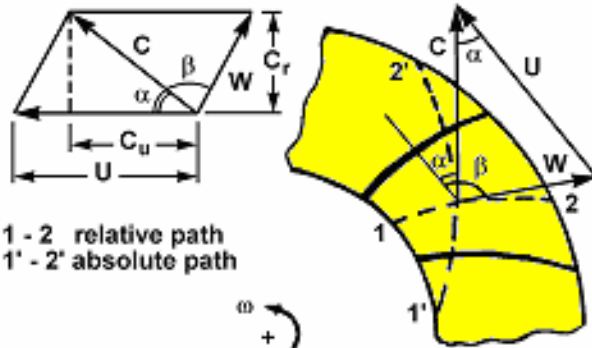
Fig. 1.2 Velocity triangle

C_u : tangential component of $\vec{C}$

C_r : radial component of $\vec{C}$

The velocity symbols in this text follow the European system. However, many authors used the American system wherein:

C designated by V, W designated by V,

C_r designated by V_r, C_u designated by V_u,

and sometimes $\beta = 180° - \beta$.

1.3 Momentum Transfer Principles:

Consider an open system with a volume V, if this volume is subjected to external forces, the contained fluid will move inward (contraction) or outward (expansion), the momentum at time t:

$$J = \iiint_V C . \rho . \delta V \quad \dots\dots\dots\dots\dots\dots\dots\dots\dots\dots\dots\dots\dots\dots\dots (1.1)$$

At time $t + dt$ the momentum in a unit volume could generally be written as follows:

$$\rho C + \frac{\partial (\rho C)}{\partial t} dt \quad \text{.................................…………...................... (1.2)}$$

Denoting the contracting volume by $\partial V'$, and the expanding volume by $\partial V''$. Considering the (+ve) sign for the outward flow and the (−ve) sign for the inward flow, thus the total momentum at the instant $t + dt$ equal:
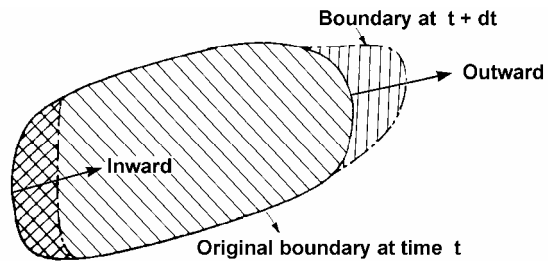
Fig. 1.3 The considered control volume

$$J + d J = \iiint_V \rho C \partial V + \iiint_V \frac{\partial (\rho C)}{\partial t} dt. \partial V$$

$$+ \iiint_{\delta V''} \rho C \partial V'' + \iiint_{\delta V''} \frac{\partial (\rho C)}{\partial t} dt. \partial V''$$

$$- \iiint_{\delta V'} \rho C \partial V' - \iiint_{\delta V'} \frac{\partial (\rho C)}{\partial t} dt. \partial V' \quad \text{...........………................. (1.3)}$$

We can convert the volume integral to a surface integral if we consider the surface Σ.

The flow across an element of the surface dS will be:

$$\delta V = dS. C_n. dt$$

Taking the (+ve) sign for the outward flow and the (−ve) sign for the inward flow in such a way the last four volume integrals of equation (1.3) could be converted to two surface integrals as following:
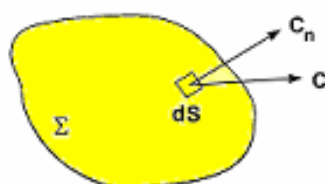
Fig. 1.4 The surface element

$$\iint_{\Sigma} C.\rho.dS.C_n.dt + \iint_{\Sigma} C_n.\frac{\partial(\rho C)}{\partial t}.dt^2.dS \quad \text{...................} \quad (1.4)$$

The second term of relation (1.4) contains a second order integral in t, thus we can neglect the second term compared to the first.

Now substitute in equation (1.3) to calculate dJ only (The change in momentum between the instant t and the instant $t + dt$)

i.e.
$$dJ = \iiint_{V} \frac{\partial(\rho C)}{\partial t}.dt.dV + \iint_{\Sigma} C.\rho.dS.C_n.dt$$

$$= dt \left[\iiint_{V} \frac{\partial(\rho C)}{dt}.dV + \iint_{\Sigma} C.\rho.C_n.dS \right] \quad \text{...................} \quad (1.5)$$

The above equation contains two terms, the first refers to the local change in the control volume and the second refers to the connective change through the boundary of the control volume. The mass flow rate element is given by:

$$dQ_m = \rho.C_n.dS \quad \text{...................} \quad (1.6)$$

Differentiating equation (1.1):

$$\frac{\partial J}{\partial t} = \iiint_{V} \frac{\partial(\rho C)}{\partial t}dV \quad \text{...................} \quad (1.7)$$

From equations (1.5), (1.6), and (1.7):

$$\frac{dJ}{dt} = \frac{\partial J}{\partial t} + \iint_{\Sigma} C \, dQ_m \quad \text{...................} \quad (1.8)$$

Now we can apply Newton momentum theory:

Force = rate of change of momentum

$F = d$ (mass x speed) $/ dt$

$\quad = dJ/dt$

The torque equals the rate of change of angular momentum:

$$T = F.r = \frac{d\,J.r}{d\,t} = \frac{\partial\,J.r}{\partial\,t} + \iint_{\Sigma} C.r.dQ_m \quad \text{................................} \quad (1.9)$$

The above equation is the general equation of angular momentum.

Taking the time average of the above equation i.e. $\partial J.r/\partial t = 0$, the mean value of the local change of momentum vanishes and we have only the average value

i.e. $\quad T = \iint_{\Sigma} \overline{C}.\overline{r}.dQ_m \quad \text{..}$ (1.10)

1.4 Energy Equation:

In the previous paragraph, the principles of the conservation of momentum were applied to study the transfer process between the fluid and the rotor. In fact, in applying the momentum principles the internal energy is canceled in pairs, this energy becomes important in some cases, as in the explosion of a shell while the momentum is constant, the internal energy transferred into kinetic energy. So, to present a more generalized approach, the principles of conservation of energy shall be used, which is a form of the first law of thermodynamics.

Consider a control volume V, the heat transfer through the system during time dt :

$$d\,Q = d\,E + d\,W \quad \text{..} \quad (1.11)$$

where $d\,E$ is the change in energy per unit mass, this term includes internal, kinetic and potential energy.

$$d\,E = d\left(E_n + C^2/2 + gZ\right) \quad \text{..}$$ (1.12)

Similarly to the previous paragraph, consider the change in energy consists of two parts, a local change and convective change:

$$dE = dt \iiint_V \frac{\partial\left(E_n + C^2/2 + gZ\right)}{\partial\,t}\rho.dV +$$

$$dt \iint_S \left(E_n + C^2/2 + gZ\right)\rho.C_n.dS$$

$$\text{..........................} \quad (1.13)$$

The work done dW through the boundary:

$$dW = dt \iint_S C.\sigma.dS \quad \text{..............……..} (1.14)$$

where σ denotes a stress and $C.dt$ denotes a displacement, the stress σ consists of two parts, a shear stress τ parallel to the wall, and a hydrostatic pressure P normal to the wall, using the (+ve) sign for outward and (–ve) sign for inward:

i.e. $\qquad dW = dt \iint_S \tau.C_\tau.dS - dt \iint_S P.C_n.dS \quad \text{........……….......} (1.15)$

In fact, one has to distinguish between three kinds of boundaries:
a) an open boundary where the flow occurs across the boundary,
b) a closed and stationary boundary,
c) a closed and moving boundary as a moving wing.

In the case of an open boundary, the term $\iint_S \tau.C_\tau.dS$ denotes a friction energy E_f which is sometimes can be neglected compared to the other stresses involved, despite in the case of a closed but moving boundary as a turbine rotor, this tangential stress delivers power E_s.

$$E_s = \iint_S \tau.C_\tau.dS \quad \text{........….....................................…....…........} (1.16)$$

One can combine the convective part of energy with the hydrostatic pressure to give;

$$\iint_S \left[P.C_n + \left(E_n + C^2/2 + gZ\right)\rho.C_n\right]dS = \iint_S i_o.dQ_m \quad \text{..........} (1.17)$$

where $dQ_m = \rho.C_n.dS$ and denotes the mass flow rate,
$\qquad i_o$ denotes the stagnation enthalpy,
$\qquad i_o = P/\rho + E_n + C^2/2 + gZ = i + C^2/2 + gZ \quad \text{.....................} (1.18)$

Usually in turbomachines, one can consider the heat transfer from or to the working medium is negligible, i.e.
$\qquad dQ = 0$
From equations (1.11) to (1.18), one can write:

$$\frac{dE}{dt} + E_s + \iint_S i_o . dQ_m = 0 \quad ....………..........………...…....... \text{(1.19)}$$

In many cases the change in energy E with time is constant, thus we can write the energy equation as follows:

$$E_s = -\iint_S i_o . d Q_m \quad ....………....................…….... \text{(1.20)}$$

The above equations are for steady flow, the dimensions of E_s is length per unit mass. From equations (1.14) and (1.20):

$$\left(i_1 + gZ_1 + C_1^2/2\right) - \left(i_2 + gZ_2 + C_2^2/2\right) = \frac{C_1^2 - C_2^2}{2} + \frac{W_2^2 - W_1^2}{2} + \frac{U_1^2 - U_2^2}{2}$$
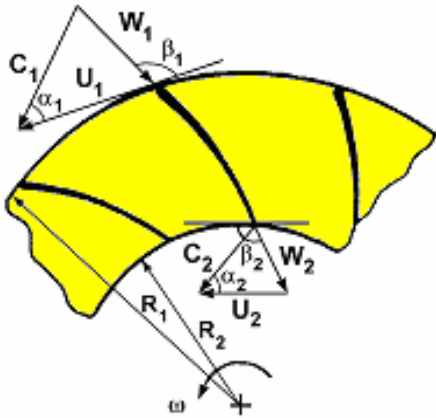
$$................ \text{(1.21)}$$

1.5 Theories of Turbomachines:
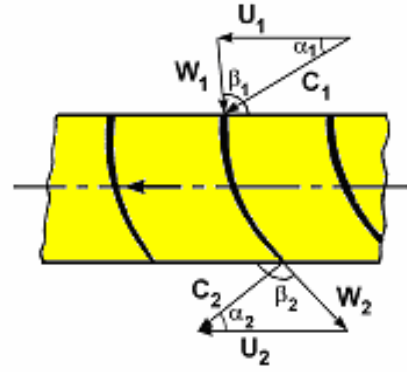
1.5.1 Euler Theory (Elementary)

The simplified theory is based on the following assumptions:

- The impeller has an infinite number of blades, which signifies a perfect guidance of fluid, neglecting separation, circulation and turbulence.
- The fluid leaves the impeller tangentially to the blades.
- In the impeller passages, the fluid velocities at similar points on all the flow lines are the same.

a) radial rotor   **b) axial rotor**

Fig. 1.5 Inlet and exit velocity triangles

Applying the general equation of momentum on the flow inside a turbine, change the vector value of $\vec{C}$ by $C \cos \alpha$ and by integration we find:

Torque $T = Q_m \left(R_1 C_1 \cos \alpha_1 - R_2 C_2 \cos \alpha_2 \right)$ ….…........................ (1.22)

where T torque
  Q_m mass flow rate $= W / g$
  W weight flow rate $= \gamma Q$ with Q the volume flow rate

we have:

$$C_{u1} = C_1 \cos \alpha_1, \quad C_{u2} = C_2 \cos \alpha_2,$$
$$U = \omega.R, \qquad Power = T.\omega$$

Substituting those values in equation (1.22) we find:

$$Power = Q_m.\omega.\left(R_1.C_{u1} - R_2.C_{u2} \right)$$

or

$$P = Q_m \left(U_1.C_{u1} - U_2.C_{u2} \right)$$ ......………........................…….... (1.23)

and virtual head or theoretical head H_o

$$H_o = U_1.C_{u1} - U_2.C_{u2} \qquad \text{per unit mass} \qquad \text{or}$$

$$= \left(U_1.C_{u1} - U_2.C_{u2}\right)/g \qquad \text{per unit weight} \dots\dots\dots\dots (1.24)$$

Remarks:

- From equation (1.22) we can see that the maximum power generated by the turbine occurs when $\cos\alpha_2 = 0$, i.e. when $\alpha_2 = 90°$, radial exit.
- Also, from equation (1.22) we see that Euler theory does not take into consideration the geometric form of the blades, it considers the inlet and outlet angles only.
- Applying the triangle relations to equation (1.24) we find another form of equation (1.24):

$$W^2 = U^2 + C^2 - 2U\,C.\cos\alpha$$

or:

$$H_o = \frac{\left(C_1^2 - C_2^2\right) + \left(W_2^2 - W_1^2\right) + \left(U_1^2 + U_2^2\right)}{2g} \quad \dots\dots\dots\dots (1.25)$$

- It may be noted that equations (1.24) and (1.25) do not contain the specific weight of the fluid handled, an impeller operating at a given speed will develop the same head for any fluid handled.

- Analysis of the energy transferred, Degree of Reaction:

The change of head due to the fluid flow through the wheel can be written as following:

$$H_o = H_1 - H_2 = \left[\frac{P*}{\rho g} + \frac{C^2}{2g}\right]_1 - \left[\frac{P*}{\rho g} + \frac{C^2}{2g}\right]_2 \quad \dots\dots\dots\dots (1.26)$$

where

$$P* = P + \rho g h \quad \dots\dots\dots\dots\dots\dots (1.27)$$

After equations (1.25), (1.26) and (1.27), we have:

$$\frac{P_1^* - P_2^*}{\rho g} + \frac{C_1^2 - C_2^2}{2g} = \frac{C_1^2 - C_2^2}{2g} + \frac{W_2^2 - W_1^2}{2g} + \frac{U_1^2 - U_2^2}{2g}$$

From the above equation the total change in head can be divided into the following three terms:

a. $\dfrac{C_1^2 - C_2^2}{2g}$ represents the change in kinetic energy.

b. $\dfrac{U_1^2 - U_2^2}{2g}$ represents the change in energy due to centrifugal force.

c. $\dfrac{W_1^2 - W_2^2}{2g}$ represents the change in relative kinetic energy.

The degree of reaction σ is the ratio of the change in static pressure to the change in total pressure.

$$\sigma = \left. \frac{P_1^* - P_2^*}{\rho g} \right/ H_o$$

$$= \frac{\left(U_1^2 - U_2^2\right) + \left(W_2^2 - W_1^2\right)}{\left(C_1^2 - C_2^2\right) + \left(U_1^2 - U_2^2\right) + \left(W_2^2 - W_1^2\right)} \quad \dots\dots\dots\dots\dots\dots\dots \text{ (1.28)}$$

$\sigma = 0.0$ designate an impulse machine.
$\sigma \neq 0.0$ designate a reaction machine.

1.5.2 Modern Theory

The basic equations just developed are based upon a certain assumptions namely frictionless, non-turbulent flow in a plane and complete guidance of the fluid.

To explain the actual flow inside the impeller we may consider the case of a centrifugal pump impeller as follows:
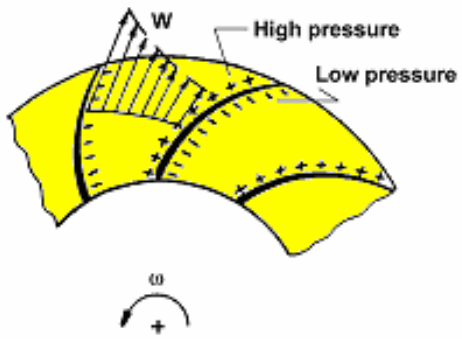
**Fig. 1.6 Pressure distribution
between two blades**
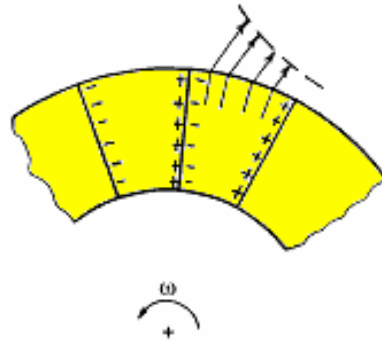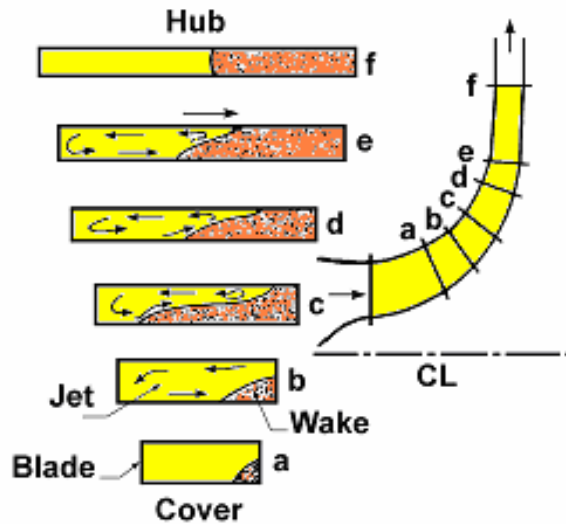
**Fig. 1.7 Exit flow shape in
radial blades**

a. During the energy transfer process between the blades and the fluid, a
    positive pressure acting on the driving face of blade and negative
    pressure on the trilling face, (See Figures 1.6 and 1.7). If one consider
    the total energy is constant, the increment of the static pressure energy
    from the trailing edge to the driving edge is made on the dispense of
    the dynamic pressure energy. The relative velocity magnitude, which is
    a form of dynamic pressure energy, is inversely proportional to the
    pressure difference. The relative velocity exit direction is tangential to
    the high pressure side of the blade, and inclined opposite to the rotating
    speed in the low pressure side of the blade. This fact has been observed
    early in the 60's by Dean et al., after a measurement of flow pattern at
    the impeller exit, this flow pattern is known as jet-wake flow pattern.

Fig. 1.8 Development of the wake, secondary flow pattern
(obtained by Dean, Jr.)

Figure 1.8 shows the development of the Jet-Wake flow pattern inside an impeller; the jet is corresponding to the driving edge with a high static pressure energy. Consequently, the wake region corresponds to the low static pressure region; extensive measurements show clearly the existence of this deformed flow pattern.

b. Another secondary effect studied by Stodola is the inertia effect (See Figures 1.9 and 1.10). The fluid particles tend to keep its primary direction relative to absolute axis; this effect produces a relative circular eddy adding another distortion to the relative velocity distribution.
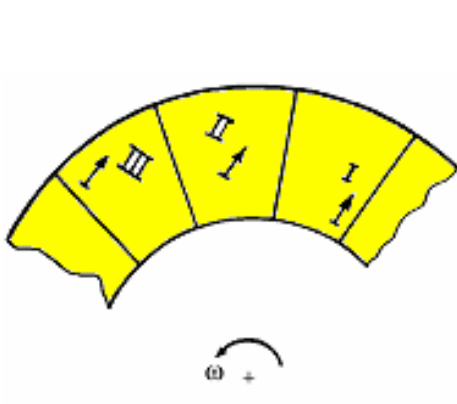
Fig. 1.9 Inertial effect   **Fig. 1.10 The flow pattern inside the impeller**
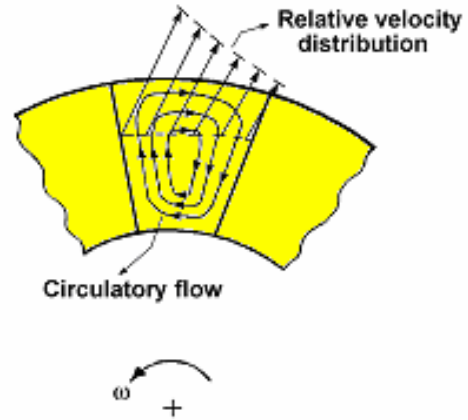
From a, b we can see that for actual machine the relative velocity mean exit angle does not equal to the ideal exit angle suggested by Euler theory, usually this deviation is about 5 - 10°.

In practice the designer used empirical correction factor based on test results and experiments, Figure 1.11.
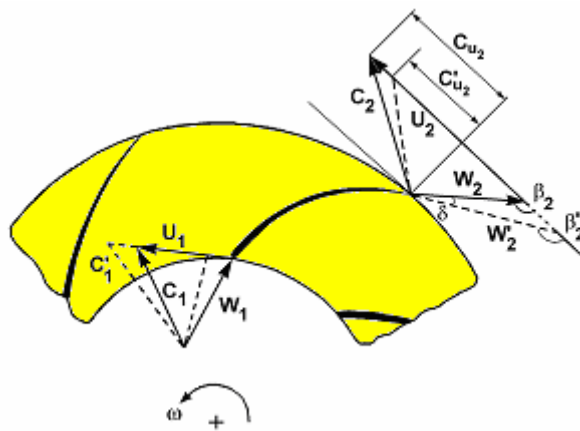
Fig. 1.11 The velocity triangles after the modern theory

1.5.3 Necessity for flow unsteadiness

The energy transfer process between fluid and rotor will occur only if E_s not equals zero.

Thus, one can write the following substantial derivative:

$$\frac{D i_o}{D t} = \frac{\partial i_o}{\partial t} + C \frac{\partial i_o}{\partial \ell} \quad \text{..} \quad (1.29)$$

(Where C is the velocity and ℓ is in the direction of the velocity). The above substantial derivative must be different than zero.

Apply Euler's equation as following:

$$\frac{\partial C}{\partial t} + C \frac{\partial C}{\partial \ell} = -\frac{1}{\rho} \frac{\partial P}{\partial \ell} - \frac{\partial (gZ)}{\partial \ell} \quad \text{...} \quad (1.30)$$

or

$$\frac{\partial C}{\partial t} = -\frac{\partial}{\partial \ell} \left(\frac{C^2}{2} + gZ + \frac{P}{\rho} \right)$$

Isentropic process $\left(di = \frac{dP}{\rho} \right)$, and after equation (1.18) the following relationship is reached:

$$\frac{\partial C}{\partial t} = -\frac{\partial}{\partial \ell} \left(\frac{C^2}{2} + gZ + i \right) = -\frac{\partial i_o}{\partial \ell} \quad \text{.................................} \quad (1.31)$$

Introducing equation (1.31) in equation (1.29), and noting that $\partial Z/\partial \ell = 0$.

$$\frac{D i_o}{D t} = \frac{\partial i_o}{\partial t} - C \frac{\partial C}{\partial t} = \frac{\partial i}{\partial t} \quad \text{...} \quad (1.32)$$

The above equation indicates clearly that i or H must not equal zero to extract or to supply energy from a turbomachine. In other words, the flow must be unsteady to permit energy transfer. The physical meaning of equation (1.32) is experimentally well presented by the jet-wake flow pattern; a pressure measurement impeller's exit at a fixed point will show the nature of the flow unsteadiness.

1.5.4 Approximate calculation of deviation after Stodola

Stodola assumes that the inertia effect and circulation can be simulated to a rotation cylinder in the impeller passage, Figure 1.12. The rotational speed of the cylinder about its axis equal to the angular velocity

of the impeller ω, and finally Stodola assumes that the deviation in the tangential component of the absolute velocity ΔC_u is proportional to the channel width and the rotating speed.

$$\Delta C_u \propto \frac{a}{2}\omega \quad\text{..} (1.33)$$

where a is the channel width and ω is the rotating speed.
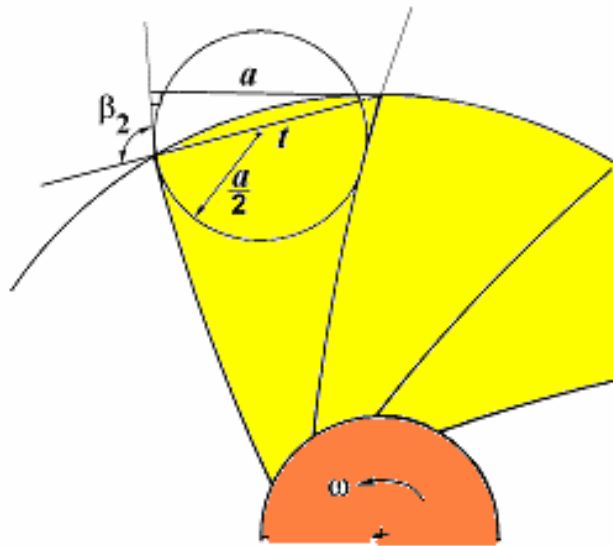
Fig. 1.12 Stodola's model

The space between two successive blades at the outer radius is given by:

$$t = \pi D_2 / Z_n$$

where Z_n is the number of blades, thus the deviation ΔC_u equal:

$$\Delta C_u = U_2\,\pi\,\sin\beta_2 / Z_n \quad\text{..} (1.34)$$

Certainly, equation (1.34) gives an approximate value of the deviation.

1.6 *Some Practical Considerations (Actual Machine Design):*

Many other factors influence the actual machine design as follow:

1.6.1 Friction:

The actual fluid flow (viscous flow) through a channel or closed conduit loses a part of its energy due to skin friction and turbulence eddies.
The loss increases with the roughness of the surface of the impeller, also the amount of losses are proportional to the turbulence level, a machine designed to operate at certain Reynolds number and certain ratio of revolution per minute, when operating at other flows or speed the losses will change, also the angles will not be correct.

1.6.2 Disk Friction:

The power required to rotate a disk in a fluid is known as the disk friction. The disk friction loss is due to two actions which occur simultaneously, namely (1) the actual friction of the fluid on the disk, which is relatively minor, (2) a pumping action, the fluid which is in contact with the disk or near it is thrown outward by the centrifugal action and circulates back toward the shaft to be pumped again as shown in Figure 1.13. The energy consumed by the disk friction depends upon the mass of fluid coming into contact with the disk per unit of time and the kinetic energy, which the fluid receives. Many formulas have been found experimentally for liquid and gases, these will be discussed later.
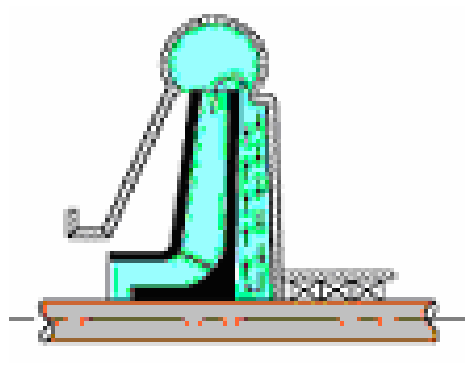
| **Fig. 1.13 Disk friction** | **Fig. 1.14 Circulation** |
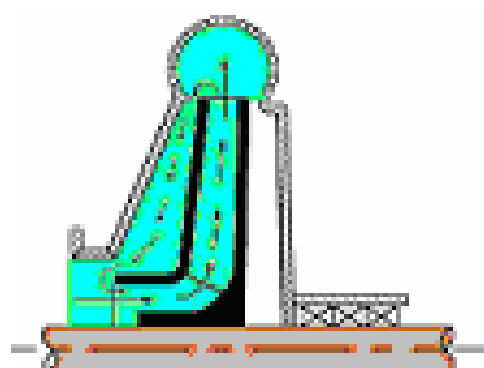
- ***Mechanical losses:*** the term mechanical losses includes the friction losses in bearing and seal, these losses are equal to 2 - 4 % of brake horsepower.

1.6.3 Leakage:

Leakage occurs as seen from Figure 1.14 because of the pressure difference between the fluid being compressed and the inlet pressure; this amount of leakage recirculates and enters with the inlet flow. The leakage has no effect on the theoretical head but it lowers the capacity and increases the brake horsepower required.

1.6.4 Pre-Rotation of the Fluid:

The usual assumption made in designing is that the fluid enters the impeller vanes radially so that $\alpha_1 = 90°$, as the fluid approaches the vane inlet it becomes into contact with the rotating shaft and impeller, this tends to cause it to rotate the wheel. Pre-rotation reduces the theoretical head, as may be seen from equation (1.24).
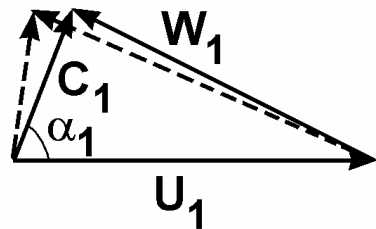
Fig. 1.15 Pre-rotation of the inlet velocity

1.7 Coefficients and Efficiencies:

1.7.1 Circulatory Flow Coefficient:

As shown previously in section 1.5.2, the effect of circulatory flow is to reduce C_2, this reduces the theoretical head H_o which the impeller is able to develop. If $\overline{C}_{u2}$ is the tangential component of C_2 based on a finite number of vanes and C_{u2} is the tangential component neglecting circulatory flow, then the circulatory flow coefficient:

$$\eta_\infty = \overline{C}_{u2} / C_{u2}$$

It is important to note that the reduction in the head due to the circulatory flow is not a loss. It is just an incompleteness, which has not been taken into consideration in Euler theory, so the theoretical head H_o now equal:

$$H_o = \frac{U_2 C_{u2}}{g} . \eta_\infty$$

21

for radial flow at inlet considering the case of a pump, in turbine case it will be $H_o = \eta_\infty . U_1 C_{u1} / g$ assuming radial flow at exit. The method of calculating this coefficient from tests will be explained latter.

1.7.2 Manometric Efficiency:

The actual head developed by the unit or energy generated in turbine case is less than the theoretical head, owing to the turbulence, friction and circulatory flow losses previously discussed. The ratio of the actual head developed to the theoretical head for a finite number of vanes is the hydraulic efficiency.

$$\eta_{man.} = \frac{Actual\ measured\ head}{Head\ imparted\ to\ fluid\ by\ impeller} = \frac{H_a}{H_o}$$

1.7.3 Mechanical Efficiency:

The mechanical efficiency is the ratio of power supplied to (or generated from) the shaft to the power supplied to the fluid by impeller (or delivered by the fluid to impeller).

$$\eta_{mech.} = P_o / B.H.P.$$

where $P_o = \gamma Q H_o / \text{Constant}$.

1.7.4 Volumetric Efficiency:

The volumetric efficiency is a measure of the amount of leakage.

$$\eta_{vol} = \frac{delivered\ weight}{delivered\ weight + internal\ leakage}$$
$$= \frac{Q}{Q + Q_L}$$

1.7.5 Hydraulic Efficiency (Turbine):

The hydraulic efficiency is the ratio of work done on the rotor to the available head of water or (energy actually supplied to the turbine).

$$\eta_{hyd.} = H_o / H_{av}$$

CHAPTER (II)

$$\boxed{\begin{array}{c} \textbf{DIMENSIONAL ~ ANALYSIS} \\ \textbf{AND} \\ \textbf{SIMILITUDE ~ OF ~ TURBOMACHINES} \end{array}}$$

2.1 Introduction:

The application of dimensional analysis and hydraulic similitude enables the engineer to organize and simplify the experiments. Since the beginning of the twentieth century the engineers involved in the design of hydraulic machines such as turbomachine, started their procedure by preparing a model and working backward by means of similitude to predict the actual machine performance.

2.2 Dimensional Analysis:

All physical relationships can be reduced to the fundamental quantities of force *F*, length *L*, and time *T*, (and temperature in case of heat).

One important procedure usually used in dimensional analysis is the Buckingham π theorem, any independent physical variable can be represented mathematically as follows:

$$f(q_1, q_2, q_3, \dots\dots, q_n) = 0 \quad \dots\dots\dots\dots\dots\dots\dots\dots (2.1)$$

This expression can be replaced by the equation:

$$\phi(\pi_1, \pi_2, \pi_3, \dots\dots, \pi_{n-k}) = 0 \quad \dots\dots\dots\dots\dots\dots\dots (2.2)$$

where *n* is the number of variables, *k* is the number of fundamental dimensions. The π theorem procedure can be explained in the following few steps:

a) Any equation could be reorganized by grouping the physical quantities assumed in dimensionless groups.

b) If the number of fundamental dimensions is k, the number of terms will be equal to $(n-k)$.

c) The first π term can be expressed as the product of the chosen quantities each to an unknown exponent and the other quantity to a known power (usually taken as one).

d) For each term, solve for the unknown exponent by dimensional analysis.

e) Any term can be replaced by any power of that term π_1 by π_1^2, or by $1/\pi_1$, also any term can be multiplied by a numerical constant.

2.3 Hydraulic Similarity:

The similarity is known as hydraulic similitude or hydraulic similarity. The main types of hydraulic similitude are:

a) <u>Geometric Similitude</u>, the geometric similitude exists between model and prototype if the ratios of corresponding dimensions are equal.

$$\frac{L_{model}}{L_{prototype}} = L_{ratio} \qquad , \qquad \frac{A_{model}}{A_{prototype}} = L_{ratio}^2$$

b) <u>Kinematic Similitude</u>, the kinematic similitude exists between model and prototype when the ratios of the corresponding velocities at corresponding points are equal.

Velocity $\qquad V_{model} / V_{prototype} = V_m / V_p = L_r / T_r$

Acceleration $a_m / a_p = \dfrac{L_m / T_m^2}{L_p / T_p^2} = L_r / T_r^2$

Discharge $\qquad Q_m / Q_p = \dfrac{L_m^3 / T_m}{L_p^3 / T_p} = L_r^3 / T_r$

c) <u>Dynamic Similitude</u>, the dynamic similitude exists between the model and the prototype if both of them have identical forces.

$$\frac{Forces_{model}}{Forces_{prototype}} = \frac{M_m.a_m}{M_p.a_p}$$

2.4 Application of Dimensional Analysis on Turbomachines:

Consider a series of geometrically similar pumps or turbines of different sizes but having similar flow patterns. The energy transferred E is a function of wheel diameter D, volumetric discharge Q_v, fluid density ρ, kinematic viscosity ν and the rotating speed N. These variables could be organized in mathematical form as following:

$$E = f(D, N, Q_v, \rho, \nu) \quad or$$
$$f(E, D, N, Q_v, \rho, \nu) = 0 \quad \text{... (2.3)}$$

where E represents pressure energy $= \rho g H_o$

Following π theorem, we have $(6-3) = 3\ \pi$ terms.

Select three independent variables, D, N, E.
$$\pi_1 = D, N, E, \rho$$
$$\pi_2 = D, N, E, Q_v \quad \text{... (2.4)}$$
$$\pi_3 = D, N, E, \nu$$

$$\pi_1 = D^x N^y E^z \rho = (L)^x (T)^{-y} (M^z L^{-z} T^{-2z}) M L^{-3}$$
$$x - z - 3 = 0$$
$$- y - 2z = 0$$
$$z + 1 = 0$$

i.e. $\quad \pi_1 = D^2 N^2 (gH_o)^{-1} = \dfrac{D^2 N^2}{gH_o}$

and $\quad \pi_1' = 1/\pi$

i.e. $\quad \pi_1' = \dfrac{gH_0}{N^2 D^2} \quad \text{... (2.5)}$

$$\pi_2 = D^x N^y E^z Q_v = L^x T^{-y} M^z T^{-2z} L_3 T^{-1} L^{-z}$$

$$x - z + 3 = 0$$

$$-y - 2z - 1 = 0$$

$$z = 0$$

$$\therefore \ z = 0, \ x = -3, \ y = -1$$

i.e. $$\pi_2 = \frac{Q}{ND^3} \ \dots \ (2.6)$$

$$\pi_3 = D^x N^y E^z v = L^x T^{-y} M^z L^{-z} T^{-2z} L^2 T^{-1}$$

$$x - z + 2 = 0$$

$$z = 0$$

$$-y - 2z - 1 = 0$$

$$\therefore \ z = 0, \ y = -1, \ x = -2$$

i.e. $$\pi_3' = 1/\pi_3 = ND^2 / v \ \dots \ (2.7)$$

2.4.1 Discussion

a) $\pi_1' = gH_o / D^2 N^2$ Manometric Coefficient

The head H_o is directly proportional to $(ND)^2$, thus for similar flows and the same efficiency, the proportionality factor for one machine equals that for other machine.

b) $\pi_2 = Q / ND^3$ analogue to Discharge Coefficient ψ

Similarity factor π_2 also must be equal for similar machines.

c) $\pi_3' = ND^2 / v$ Reynolds Number.

π_3' is the ratio of inertia force to viscous force.

For a true similitude between a pair of turbomachines π_1', π_2, π_3' should be equals for all operating points. This condition is hard to satisfy, because if we increase size and speed for a given machine handling the same fluids, π_1, π_2 remain constant but the Reynolds number will increase because the dominator will stay constant for the same fluid, so, we neglect Reynolds number effect, considering that its effect on power is minor. It is important to note the industrial practice of selecting some constant quantities from the non-dimensional coefficients. For example,

the well-known practice of reducing gH to H in the non-dimensional coefficients because it is constant, however, this practice leads to a diversity in the value of the performance parameters, this could be easily seen from the different dimensional specific speed used.

2.4.2 Performance Curves:

The performance curves usually correlate the relation between power, flow, and head for pump, for example the relation between π_1 and π_2 could be drawn as seen in Figure 2.1.
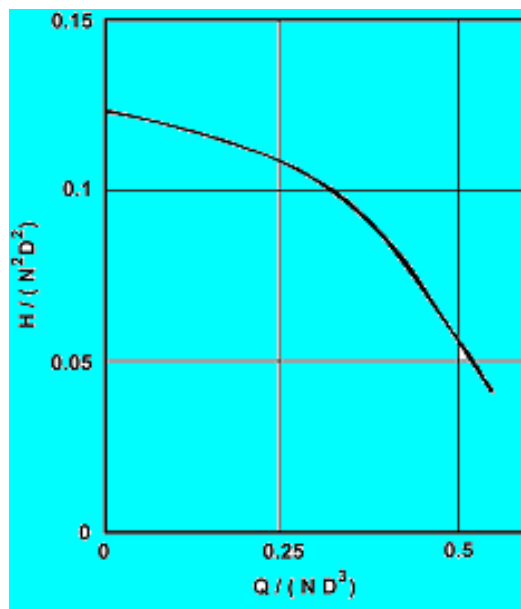
Fig. 2.1 Non-dimensional Head-Volume characteristics

For a geometrically similar pump of different sizes, the same curve could be obtained, (approximately).

In the same manner, the relation between power and flow could be obtained:

Power $P = \rho\, g\, H\, Q$

$g\, H \propto N^2 D^2$

$Q \propto N D^3$

i.e. $P \propto \rho N^3 D^5$

So, in non-dimensional form, the relation between the power and the flow will be a relation between $P/\rho N^3 D^5$ and Q/ND^3, Figure 2.2, also for a geometrically similar pump of different sizes, the same curve could be obtained.
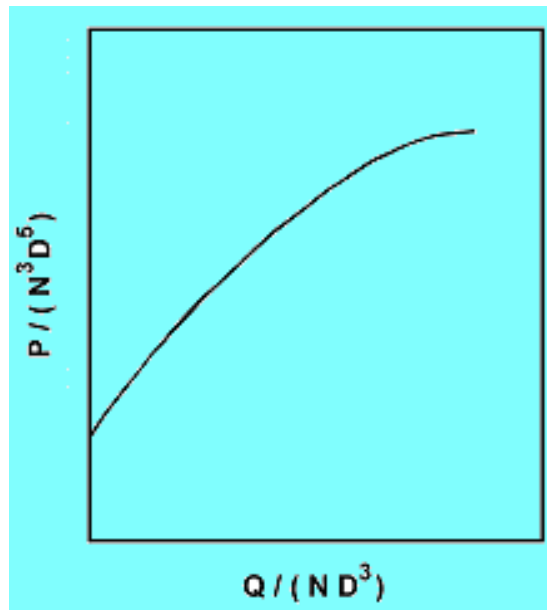
Fig 2.2 Non-dimensional Power-Flow characteristics

2.5 Scale Effect

a) Reynolds Number Effect:

The change in scale certainly implicates change in Reynolds number. As seen before, Reynolds Number is the ratio between the inertia force and the viscous force. In the study of viscous fluid flow, Reynolds Number is directly proportional to the mechanism of flow, consequently, the losses of fluid flow origin is a function of Reynolds number. If the variation in Reynolds number is small, its effect can be neglected assuming that the mechanism of flow is similar and consequently the losses. When there are a large variation in Reynolds number, its effect must be taken into consideration because large variation in Reynolds number may indicate a change in the flow regime as from laminar to transition or from transition to fully developed turbulent flow. Unfortunately, only experiences can provide available information about its effect.

Generally, from the physical point of view, we can expect that Reynolds number effect on the performance behaves similarly in all turbomachines.
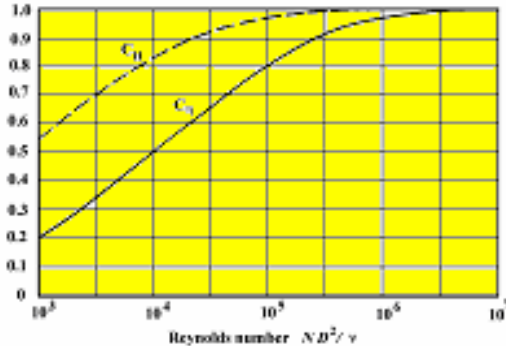
Fig 2.3 Reynolds Number factor for head C_H and efficiency C_η

As it could be seen from Figure 2.3 that over $Re > 10^7$ their is no required correction because the flow would be fully-developed turbulent flow and the effect of viscosity will be minor. With decreasing Reynolds number, the correction factor C_η increases to take into account the excess of losses.

b) Scale effects in hydraulic machines

The Reynolds number effect is clear particularly if there is a great change in its value.

The use of models for predicting full size water turbine performance is well established, but the same technique for pumps is relatively recent. Significant differences in efficiency between model and full size occur, suggesting departures from strict dynamic similarity. It is argued by both turbine and pump authorities that losses differ, and that work-capacity curves differ too. All are agreed that exact mathematical treatment is difficult. The discussion here is based on examples of a logical approach.

It may be suggested that departures from the scaling laws are due to:

Geometrical dissimilarities due to tolerances
Clearance variations
Surface finish
Hydrodynamic effects (skin friction)
Testing errors
Installation effects.

These were examined for the prototype and four models, three of which were in aluminum and the other in fiberglass, but being one-eighth scale for comparison with the aluminum surface produced. Figure 2.4 illustrates the variations observed from the prototype machine when the three aluminum models were tested.
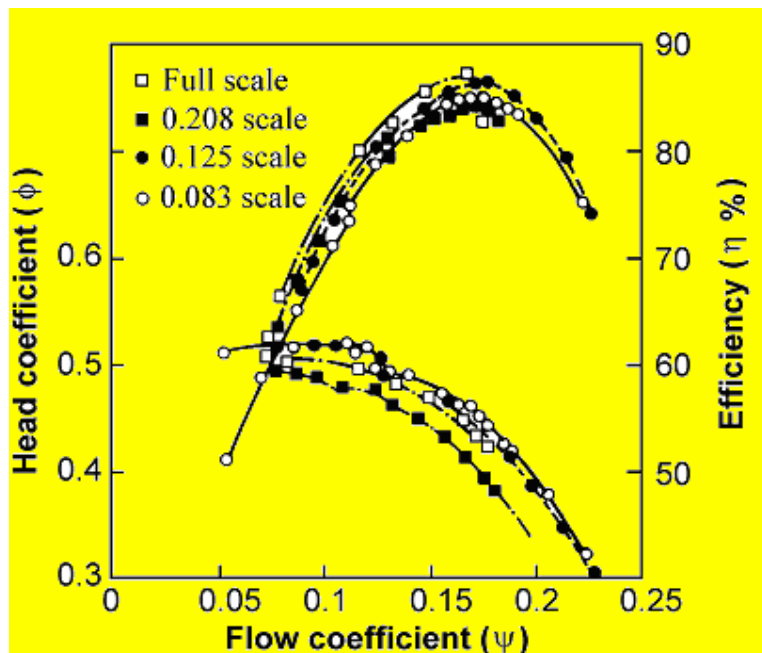
**Fig. 2.4 Non-dimensional presentation of model and full size performance
for the Eggborough pump (adapted from Nixon and Cairney, 1972)**

Geometrical dissimilarities and their effects were examined. For example blade shape, as determined by blade angle, was compared. A variation of $\pm 0.5°$ about a mean value which was $1.5°$ less than design was found for the full size machine, and in the models the scatter was of the same order, apart from the glass-fiber impeller in which it was much worse. It must be commented that much higher variations are quite common in commercial cast impellers. Since the small aluminum models were shell moldings the area variations were small, but the larger one was

floor molded, giving at least a 10% variation in area from passage to passage. Again, larger variations have been observed, particularly in cast impellers. The volute throat is a most important area, and correction is needed if variations occur.

__Clearances__ tend to be of the same order in models as on the prototype, so leakage losses tend to be larger, and model surface roughness cannot be super smooth in scale without large cost. This is therefore a significant problem because it affects boundary layers, as discussed in the following section.

__Hydrodynamic problems__, Nixon and Cairney (1972), Osterwalder (1978), and Osterwalder and Ettig (1977), suggest the following relation:

$$1 - \eta_Y = \delta_T = \delta_M + \delta_L + \delta_D + \delta_F + \delta_I$$

	Total	mechanical	leakage	disc	skin	inertia
	loss	loss	loss	friction	friction	loss

Here, δ_M and δ_I are unaffected by the Reynolds number and δ_I is usually assumed to remain the same. δ_M is considered to vary as speed, in contrast to the other hydrodynamic losses which tend to follow an N^3 law, and reduces with reducing speed at a lesser rate, thus being proportionally more important at low speeds. Nixon and Cairney (1972) present a method of finding δ_M, and suggest that prediction from low speed tests be limited to differential head readings.

The estimation of disc friction loss has been a subject for argument, as the classical work was done on plain thin discs rotating in a close fitting closed casing. Nixon used work by Necce and Daily (1960) and Watabe (1958) for "smooth" and "rough" discs, and showed an error from measured data of about 10%. Sutton (1968) studies this problem, particularly the effect of leakage flow through wear rings and its relation to disc friction. Osterwalder (1978) commented that there is little current data of general applicability, but Kurokawa and Toyokura (1976) and Wilson and Goulburn (1976) extended the database.

The same situation is attempting to correlate δ_F. Both Nixon and Osterwalder suggest the applicability of Nikuradse and Colebrook data with a limiting Reynolds number criterion for "transition". Nixon proposes a relatively simple approach, which is applicable and gives reasonable accuracy. Osterwalder surveys the published material and does

not propose a general correlation, but indicates that a computer-based in-house study is relevant.

Table 2.1 A selection of model scale formulae (as quoted for example by Nixon, 1965). Subscript m denotes 'model'

Moody (1942):

$$\frac{1-\eta}{1-\eta_m} = \left(\frac{D_m}{D}\right)^n \quad 0 \le n \le 0.26$$

or

$$\frac{1-\eta}{1-\eta_m} = \left(\frac{Re_m}{Re}\right)^n \quad 0 \le n \le 0.2$$

Moody:

$$\frac{1-\eta}{1-\eta_m} = \left(\frac{H_m}{H}\right)^{0.01}\left(\frac{D_m}{D}\right)^{0.25}$$

Anderson:

$$\frac{1-\eta}{1-\eta_m} = \frac{0.94 - Q^{-0.32}}{0.94 - Q_m^{-0.32}}$$

Pfleiderer:

$$\frac{1-\eta}{1-\eta_m} = \left(\frac{Re_m}{Re}\right)^{0.01}\left(\frac{D_m}{D}\right)^{0.25} \quad \text{valid between } 1/12 < Re_m / Re < 20$$

Hutton:

$$\frac{1-\eta}{1-\eta_m} = 0.3 + 0.7\left(\frac{Re_m}{Re}\right)^{0.2}$$

Ackeret:

$$\frac{1-\eta}{1-\eta_m} = 0.5\left[1+\left(\frac{Re_m}{Re}\right)^{0.2}\right]$$

Usually, most of turbomachines operate at high Reynolds number in the region of fully-developed turbulent flow, this problem arise when a machine is originally designed at certain Reynolds number and tested in the shop at different Reynolds numbers, so a correction must be taken into consideration. Generally, a common empirical relation is used as follow:

$$\frac{1-\eta_1}{1-\eta_2} = \left(\frac{Re_2}{Re_1}\right)^n \quad \text{.......................................………….....................} \quad (2.8)$$

when n varies from 0.1 to 0.25, the above relation is also used to take into account the seal effect.

Fans and blowers

The prediction of fan performance from models was studied at the National Engineering Laboratory (NEL), UK, resulting in a report by Dalgleish and Whitaker (1971) in which work on three small fans was used to predict the performance of fans at a scale of 1.5:1 and at a scale of about 2.5:1. The report underlined Nixon's comments on tolerancing and proposed a formula for η_A similar to the pump equations just discussed:

$$\frac{(1-\eta_A)_p}{(1-\eta_A)_m} = 0.3 + 0.7\left(\frac{\text{Re}_m}{\text{Re}_p}\right)^{0.2} \quad\quad\quad (2.9)$$

where η_A is the air efficiency and $Re = \rho\omega D^2/\mu$ for a range $0.8 \times 10^6 < Re < 6.5 \times 10^6$. They comment that clearances are important, and that the best efficiency moved to higher flow coefficients than suggested by scaling as size increased. It is of interest that improvement in surface roughness does not give better efficiency except for small high-speed fans.

c) Scale effects in compressible machines

The non-dimensional power given as $P/\rho N^3 D^5 = f\left(Q/ND^3, gH/N^2D^2, ND^2/v\right)$ was quoted as applying to compressible machines, but limits of application apply, as for incompressible machines. If single-stage machines are considered, the effect of compressibility may be neglected for low Mach numbers (below about 0.5); the divergence caused increases with Mach number. Work with compressors using refrigerant and other "heavy" gases indicates that the effect of the adiabatic exponent may be neglected for few stages. However, as the overall pressure ratio and hence the number of stages increase, density change particularly is important. As an example, if a pressure ratio of 8:1 is chosen, with air ($K = 1.4$) the density ratio is 4.41:1; if K is 1.05 this

becomes 7.23:1. This is clearly important in a multistage compressor where the stages are designed assuming a constant flow coefficient for air, but the machine used for a heavier gas ($K = 1.05$) even though use of the gas reduces power demand for dynamically similar conditions since acoustic velocity goes down. The only technique proved satisfactory is to blend gases to give the right K, as Csanady (1964) showed.

The scaling problems in pumps, discussed in the previous section, occur in compressors. For example, Henssler and Bhinder (1977) studied the influence of size on a family of small turbocharger compressors; these had 60 mm, 82 mm and 94 mm impeller diameters, and other dimensions were scaled, but surface finishes had the same surface roughness. They show how performance varied with flow coefficient and Reynolds number based on peripheral speed. The authors comment that these changes are not predicted by the similarity laws, but do not attempt to suggest the correlation that different laws apply to different families of machines.

A contribution by Miller (1977) surveyed earlier correlations of scaling predictions for axial compressors. His approach was based on the need to conserve rig power consumption by testing at reduced pressure levels and dealing with the associated problems of correcting efficiency pressure ratio and flow to normal operating level, and was also concerned with scaling model tests to full size performance. Miller examined a number of Reynolds number correction approaches and concluded that although careful testing would yield effective prediction for one compressor design, this could not be applied to another, and that pressure level effects appear to be more pronounced than scale effects.

Others have contributed to the discussion as part of their study; for example, McKenzie (1980) shows a scatter in his predictions. No completely satisfactory general prediction appears to be available at the moment, although individual companies and groups use their own approaches and satisfy their own needs.

Illustrative examples

Similarity laws applied to a water turbine

The turbines in a river barrage hydroelectric plant are designed to give 55 MW each when the level difference is 25 m and they are running

at 94.7 rpm. The designed overall efficiency is 93%, and the runner diameter is 6 m. A model with a runner diameter of 300 mm is to be tested under the same level difference. Suggest the probable rotational speed, flow rate, efficiency and power produced when the model is operating in dynamically similar conditions.

The full size flow rate is first calculated:

$$\frac{55 \times 10^6}{0.93} = 25 \times 9.81 \times 10^3 \times Q$$

Therefore

$$Q = 241 \text{ m}^3/\text{s}$$

Applying the scaling laws, equations (2.5) and (2.6),

$$\frac{Q}{ND^3} = \text{constant}$$

$$\frac{gH}{N^2 D^2} = \text{constant}$$

and substituting the known data, it is found that
$$Q_{\text{model}} = 0.602 \text{ m/s}$$
$$N_{\text{model}} = 1894 \text{ rpm}$$

The model efficiency must now be found using one of the equations in Table 2.1. The well-known turbine equation due to Hutton will be used:

$$\frac{1 - \eta}{1 - \eta_{\text{model}}} = 0.3 + 0.7 \left(\frac{1894 \times 0.3^2}{94.7 \times 6^2} \right)^{0.2}$$

from which the model efficiency is found to be:

$$\eta_{\text{model}} = 89.77\%$$

The model power developed, assuming the same mechanical efficiency, is therefore

$$P_{\text{model}} = 25 \times 9.81 \times 10^3 \times 0.602 \times 0.8977$$

= 132.54 kW

Compressor performance prediction problem

A compressor for hydrogen duty is to deliver 18 kg/s while increasing the pressure from 1.01×10^5 N/m^2 to 16.5×10^5 N/m^2. The inlet temperature is expected to be 300 K, and the rotational speed 2900 rpm.

For development purposes a half-scale machine is to be tested using air as the medium, with inlet conditions 10^5 N/m^2 and 288 K. Suggest the model mass flow rate, delivery pressure and rotational speed for dynamical similarity.

The full size pressure ratio is 16.5/1.01 = 16.34:1. The model outlet pressure will be 16.34×10^5 N/m^2. For dynamical similarity,

$$\frac{\dot{m}\sqrt{(RT_{01})}}{P_{01}D^2} = \text{constant}$$

and

$$\frac{ND}{\sqrt{(RT_{01})}} = \text{constant}$$

For hydrogen, R = 4.124 kJ/kg.K; for air, R = 0.287 kJ/kg.K. Thus:

$$\frac{18\sqrt{4.124 \times 10^3 \times 300}}{1.01 \times 10^5 \times D^2} = \frac{\dot{m}\sqrt{0.287 \times 10^3 \times 288}}{10^5 \times (0.5D)^2}$$

$$\dot{m} = 17.24 \ kg/s$$

and

$$\frac{2900D}{\sqrt{4.124 \times 10^3 \times 300}} = \frac{N \times 0.5D}{\sqrt{0.287 \times 10^3 \times 288}}$$

$$N = 1499.15 \ rpm$$

2.6 Affinity Laws:

Although the non-dimensional presentation is preferable from the scientific point of view, the dimensional presentation is also important for the practical use in a plant for example. The personnel need to know directly the variation of performance under different operating conditions.

Figure 2.5 represents the relation between H and Q. It is enough only to establish one curve and it is easy to predict the rest by the mean of affinity laws.

For the same machine operating at different speeds and flow:

from π_1 : $\left[\dfrac{gH_o}{N^2D^2}\right]_1 = \left[\dfrac{gH_o}{N^2D^2}\right]_2$

i.e. $H_1/H_2 = (N_1/N_2)^2$ .... (2.10)

from π_2 : $\left[\dfrac{Q}{ND^3}\right]_1 = \left[\dfrac{Q}{ND^3}\right]_2$

i.e. $Q_1/Q_2 = N_1/N_2$ .... (2.11)

and $Q_1/Q_2 = \sqrt{H_1/H_2}$

Remarks:

The above relations are applicable only if we neglect Re number effect, i.e. assuming small variation in Re number but if Re number changes, for example, if different fluids are considered as water and oil, the kinematic viscosity of oil is about 100 times that of water $\nu_{oil} = 100\ \nu_{water}$, in such case we have to take into consideration the third term and the above relation will be $Q_1/Q_2 = N_1/N_2 = \nu_1/\nu_2$.

38
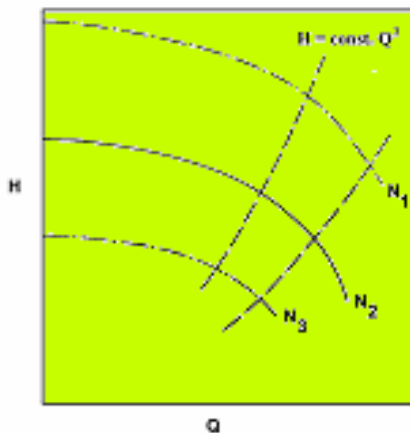
Fig 2.5 Head-capacity curve for a pump at different speeds

2.7 Specific Speed:

Various factors or parameters are used in practice in correlating data on performance and design, as we have seen before, but one of the more common terms is specific speed.

We can make another combination of non-dimensional numbers as $\left(\pi_2^2 / \pi_1^3\right)^{1/4}$ which leads us to the following expression:

$$N_s = \frac{N\sqrt{Q}}{(gH)^{\frac{3}{4}}} \quad \text{(rad)} \qquad \begin{array}{l} N \text{ in r.p.s.,} \\ Q \text{ in m}^3\text{/s,} \\ g \text{ in m/s}^2, \\ H \text{ in m.} \end{array} \quad \text{.................…..…..... (2.12)}$$

where H and Q are measured at the point of maximum efficiency. N_s is not dependent upon the speed as one may suggest from the equation, it's a parameter relates to the dimensions of the wheel, it provides an excellent tool to enable the engineer to suggest which kind of wheel to use to meet the required head and capacity.

Impellers for high total heads and low capacity usually have low specific speeds, whereas impellers for low heads and large capacity usually have high specific speeds.

As a general, radial machines have low specific speeds and axial machines have high specific speeds.

In the industrial practice, there are many forms of N_s equation depending upon the case of the machine considered if it's pump or turbine ..., etc.

2.7.1 Pumps:

In industrial practice, the following relation is usually used:

$$N_s = \frac{N\sqrt{Q}}{H^{\frac{3}{4}}} \quad (rpm)^* \qquad \begin{array}{l} N \text{ in r.p.m.,} \\ Q \text{ in G.P.M.,} \\ H \text{ in feet.} \end{array} \quad .... (2.13)$$

N_s for radial centrifugal impeller varies from 500 to 3000,
N_s for mixed impeller varies from 3000 to 7000,
N_s for axial impeller varies from 8000 to 15000.

[Hint: The conversion between the different units of the specific speed is as follows:

$$rpm \frac{\sqrt{gpm}}{(ft)^{3/4}} = 21.19\, rpm \frac{\sqrt{ft^3/s}}{(ft)^{3/4}} = 1.633\, rpm \frac{\sqrt{l/s}}{(m)^{3/4}} = 51.64\, rpm \frac{\sqrt{m^3/s}}{(m)^{3/4}} \quad]$$

---

* The dimensions of N_s is rpm.$((gpm)^{1/2}ft^{-3/4})$ in the English system or rpm.$((m^3/s)^{1/2}m^{-3/4})$ in the French system but it is common practice to omit the units in brackets
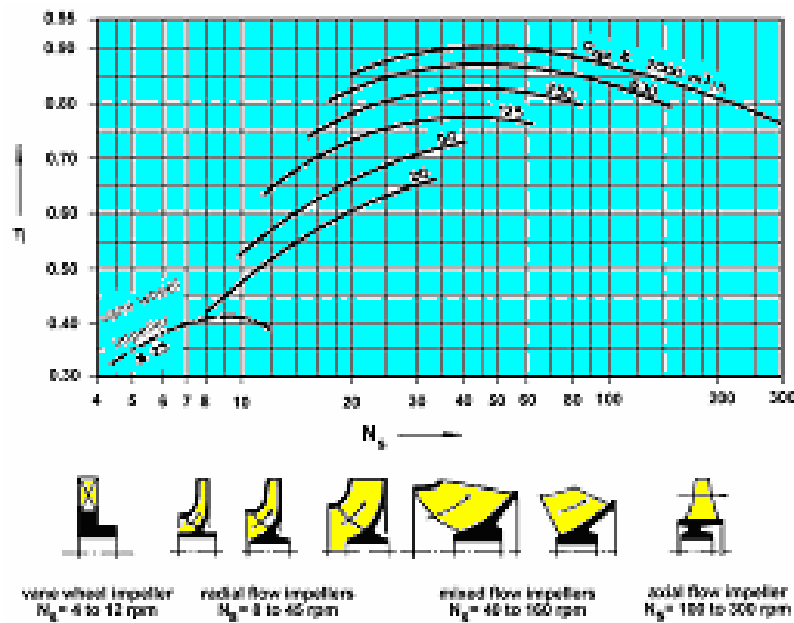
Fig. 2.6 Approximate relative impeller shapes and good average efficiencies obtained for commercial pump as a function of specific speed,

$$N_s = \frac{N}{60}\frac{\sqrt{Q}}{H^{3/4}}$$ **where N in (rpm), Q in (m^3/h) and H in (m)**
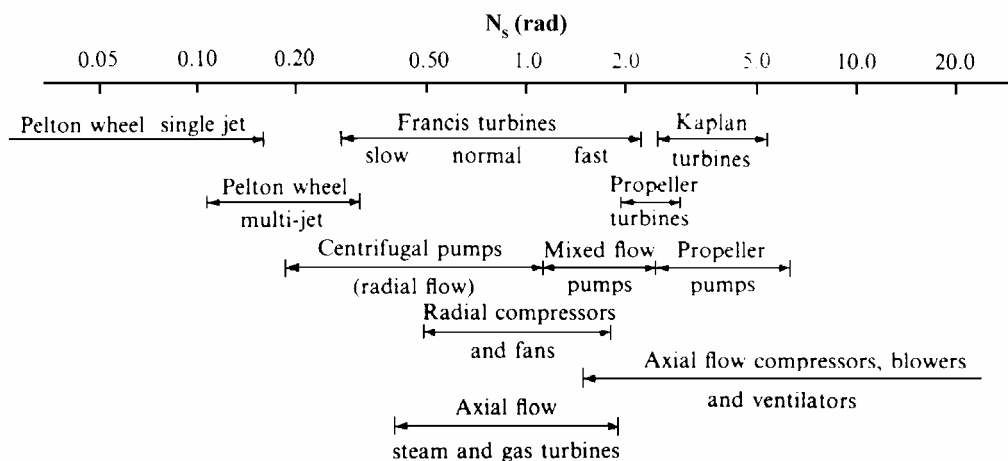
Fig. 2.7 Approximate specific speed and turbomachine type

Table 2.2 Conversion factors for specific speed

$N_s = N\sqrt{Q}\big/H^{3/4}$	N	Q	H	To obtain $N_s = N\sqrt{Q}\big/(gH)^{3/4}$ (rad), divide by:
Pumps, Compressors, Blowers, Ventilators	rpm	G.P.M.	ft	2730
	rpm	cfs (ft^3/s)	ft	129
	rpm	m^3/s	m	53
	rpm	lit/s	m	1675
$N_s = N\sqrt{B.H.P.}\big/H^{5/4}$	N	B.H.P.	H	To obtain $N_s = N\sqrt{B.H.P.}\big/[\rho^{1/2}(gH)^{5/4}]$ (rad), divide by:
Turbines	rpm	hp	ft	42
	rpm	Metric hp	m	187
	rpm	kW	m	218

N_s (rad) for centrifugal impellers varies from 0.0025 to 0.3 and reaches 1 for some axial impellers.

2.7.2 Compressors and Blowers:

$$N_s = \frac{N\sqrt{Q}}{H^{\frac{3}{4}}} \quad \text{(rpm)} \qquad\qquad \begin{array}{l} N \text{ in r.p.m.,} \\ Q \text{ in C. F. M. (ft}^3\text{/min),} \\ H \text{ in feet.} \end{array} \quad \text{..........……..….... (2.14)}$$

N_s for centrifugal impellers varies from 140 to 3000,
N_s for axial machines varies from 4000 to 8000.

2.7.3 Hydraulic Turbines:

For turbines, it's more convenient to use power instead of Q. i.e.

$$N_s = \frac{N\sqrt{B.H.P.}}{H^{5/4}} \quad \text{(rpm)} \quad \text{………….…...........…..…….... (2.15)}$$

N in r.p.m., H in (feet) in English system or in (m) in French. For radial and mixed flow runners, N_s varies from 10 to 100 in English system and 40 to 400 in French system. For axial flow turbines, N_s varies from about 80 to 200 in English system and from 300 to 800 in French system.

2.8 Pressure and Flow Coefficients:

[*] Pressure coefficient $\phi = H/(U_2^2/g)$ …...…..............…...……..... (2.16)

Flow coefficient $\psi = (Q/A)/U$ …...……..............…...…….... (2.17)

Each kind of machine has design values of ψ and ϕ those fall in a somewhat range and thus those coefficients are characteristics of machine's type. For example, considering axial flow compressors ϕ values are from 0.2 to 0.6 and ψ from 0.3 to 0.9, for radial flow compressors ϕ values are from 0.03 to 0.1 and ψ from 1.1 to 1.5.

2.9 Specific Diameter:

Another useful combination of non-dimensional groups is the specific diameter, which is defined as follow:

$$D_{sp} = \frac{D(gH)^{\frac{1}{4}}}{\sqrt{Q}}$$ …………….………….............…...…….... (2.18)

D_{sp} and N_s are important to the designer to predict the efficiency. Many diagrams exist, the presented data in these diagrams are collected from the field for the machines which they have been already build. For the convenience of the application, a distinction is made between water turbines, compressors and pumps. Figure 2.9 represents N_s, D_{sp} diagram for single stage pumps at Reynolds number in the range of 10^8 with constant geometric parameters. The left position of the curve with high pressure coefficient more than unity is corresponding to volumetric machines. It is evident that for dynamic machines ϕ does not exceed one.

---

[*] Sometimes ϕ is known as speed factor $1/\sqrt{\phi} = U/\sqrt{2gH}$. It's important to notice that there are many other definitions to those coefficients so, every coefficient will be redefined for every type of turbine.
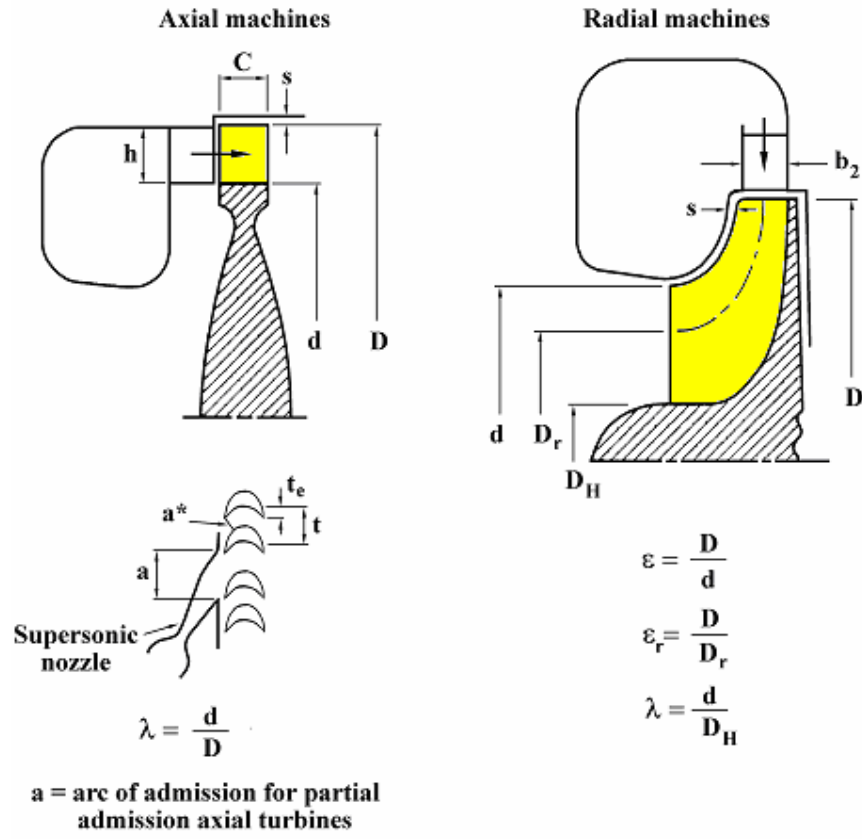
Fig. 2.8 Notation for Fig. 2.9

A comparison of test data is shown in Fig. 2.9 where the solid line shows the location of efficient turbomachine designs (optimum D_{sp} values), this line is frequently referred to as the "Cordier" line and the diagram is known as the Cordier diagram. The diagram indicates that axial machines dominate the high specific speed region, whereas radial machines are more efficient in the low specific speed region. From the diagram also it is clear that N_s and D_{sp} values of efficient turbomachines are close to the Cordier line, thus Cordier diagram is a good tool to permit the designer to reach the optimum efficiency. Certainly, the performance of turbomachines depends to a large extent on the compromises made by the designer regarding the various parameters involved.
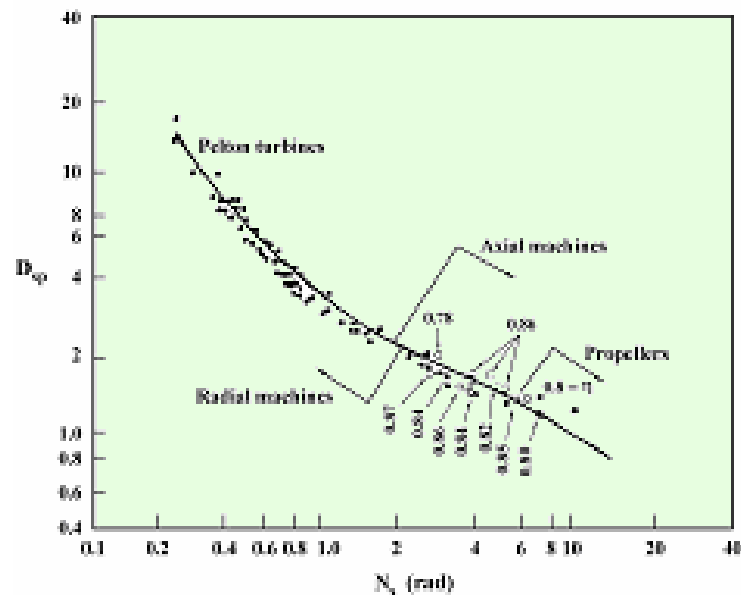
Fig. 2.9 "Cordier" line in N_s, D_{sp} diagram

CHAPTER (III)

<div style="border:2px solid black; padding:1em;">

CASCADE MECHANICS

"TWO-DIMENSIONAL APPROACH"

</div>

3.1 Introduction:

In the previous chapters, the momentum transfer in turbomachines was treated, considering the problem in one dimension. To go more deeper insight, we may consider the details of the fluid motion inside the rotor.

The study of the flow in the surfaces generated by the rotation of a streamline about the machine axis is called cascade mechanics or two-dimensional approach. The study of flow in three dimensions is beyond the scope of these notes.

The cascade consists of a number of identical blades equally spaced, the flow submit a change in angular momentum due to its passage through it.

There are two kinds of cascade:

a. *Straight cascade:* produced after the development of cylindrical surface generated by the rotation of streamlines (case of axial machines).

b. *Radial cascade*: is the stream surface in the cross sectional planes, this may be considered as plane flow from source or to a sink.

3.2 Cascade Nomenclature:

The profile of cascade consists of a curved line (camber line) upon which a profile thickness is superimposed.
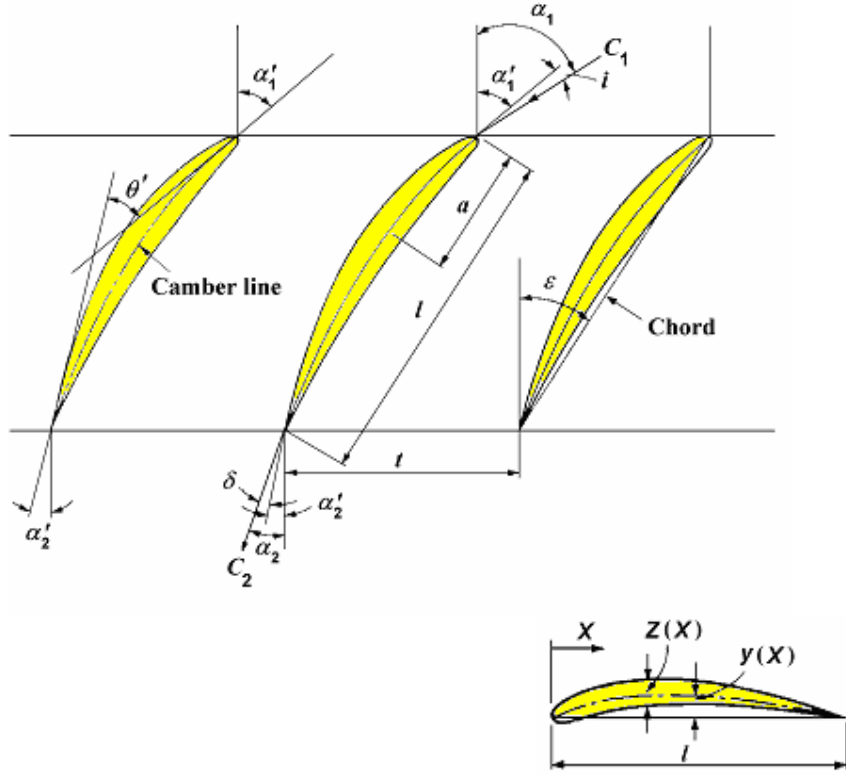
Fig. 3.1 Straight cascade

Blade inlet angle	α_1'	Position of	
Blade outlet angle	α_2'	maximum camber	a
Fluid inlet angle	$\alpha_1 = \alpha_1' + i$	Chord	l
Fluid outlet angle	$\alpha_2 = \alpha_2' + \delta$	Spacing	t
Blade camber angle	$\theta' = \alpha_1' - \alpha_2'$	Space-chord ratio	t/l
Stagger angle	ε	Solidity	l/t
Deflection	$\theta = \alpha_1 - \alpha_2$		
Incidence angle	$i = \alpha_1 - \alpha_1'$		
Deviation angle	$\delta = \alpha_2 - \alpha_2'$		

The line connecting the two points of the intersection of the camber line with the inlet and exit of the cascade is known as the chord, the stagger angle ε is the angle which the chord forms with the perpendicular to the cascade.

The camber line y and the profile thickness Z are expressed as a function of the distance along the blade (X). t is the spacing between two

48

blades. α'_1 and α'_2 are the blade angles at inlet and exit from the cascade, and $\theta' = \alpha'_1 - \alpha'_2$.

Usually, the performance of the cascade is given in tables as a function of y/l, Z/l and X/l. Also useful parameters used to define the cascade are the maximum thickness to chord ratio, Z_{max}/l, maximum camber to chord ratio, y_{max}/l, and the space-chord ratio t/l, (l/t is known as solidity).

3.3 Analysis of Cascade Forces:
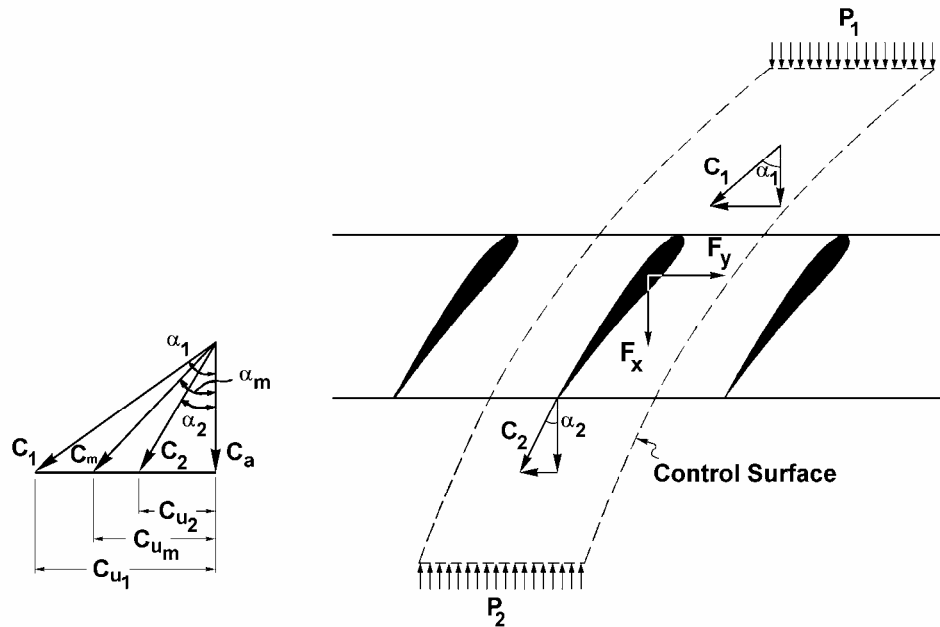
Fig. 3.2 Forces on cascade

Consider a row of a cascade, the fluid reaches the cascade front with a velocity C_1, pressure P_1, and leaves with a velocity C_2, pressure P_2. Assume the flow is steady which is only true in the case of an isolated row of cascade. Also assume incompressible flow.

The flow in turbomachines is usually incompressible; the effect of Mach number will be considered where compressibility becomes important.

Applying the principles of continuity on the control volume of a unit blade depth, yields:

$$C_1.\cos\alpha_1 = C_2\cos\alpha_2 = C_a \text{ ....…................................…............. (3.1)}$$

Applying the momentum equation in X, and y directions gives:

$$F_x = t(P_2 - P_1) \text{ ....……................. (3.2)}$$

$$F_y = \rho t C_a(C_1\sin\alpha_1 - C_2\sin\alpha_2)$$
$$= \rho t C_a^2(\tan\alpha_1 - \tan\alpha_2) \text{ ……….….......................…............. (3.3)}$$

The forces in the above equation are forces per unit depth exerted by the blade on the fluid.

To consider the energy losses due to skin friction and other losses of fluid mechanics, Bernoulli's equation will be applied neglecting potential energy.

$$P_1/\rho + C_1^2/2 = P_2/\rho + C_2^2/2 + E_L \text{ ....….….................. (3.4)}$$

where E_L presents the energy dissipation due to friction, $E_L = g\,h_L$. Noting that:
$$C_1^2 - C_2^2 = (C_a^2 + C_{u1}^2) - (C_a^2 + C_{u2}^2) = (C_{u1} + C_{u2})(C_{u1} - C_{u2})$$
and $\quad \tan\alpha_m = \dfrac{1}{2}(\tan\alpha_1 + \tan\alpha_2)$

we find; $\Delta P_o/\rho = E_L = -F_x/\rho t + (F_y/\rho t)\tan\alpha_m$ ……...........…....... (3.5)

The energy loss is usually expressed in a non-dimensional form. A frequent quantity usually used is the through flow dynamic pressure $0.5\rho C_a^{\,2}$. Now, the total pressure loss coefficient is defined as follows:

$$\zeta = \frac{\Delta P_o}{\dfrac{1}{2}\rho C_a^2} \text{ ....…………...…………….......... (3.6)}$$

Also similarly, one can define the pressure rise coefficient and the tangential force coefficient as follows:

$$C_p = \frac{\Delta P}{\frac{1}{2}\rho C_a^2} = \frac{F_x}{\frac{1}{2}t\rho C_a^2} \quad \text{.................} \quad (3.7)$$

$$C_f = \frac{F_y}{\frac{1}{2}\rho t C_a^2} = 2(\tan\alpha_1 - \tan\alpha_2) \quad \text{.................} \quad (3.8)$$

After some manipulations, one can write the following relation between C_f, C_p, and ζ:

$$\zeta = C_f \tan\alpha_m - C_p \quad \text{.................} \quad (3.9)$$

3.4 Lift and Drag:

The resultant force acting on the fluid, *F*, can be resolved into two components: one perpendicular to the blade *Lift*, *L*, and the other parallel to the blade *Drag*, *D*, Figure 3.3. The lift and drag forces may be then written in terms of tangential and axial forces as follows:
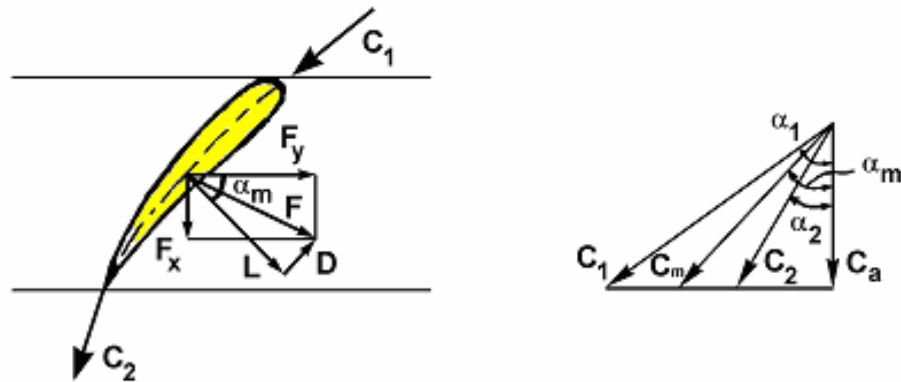
Fig. 3.3 Lift and Drag on cascade blade

$$L = F_x.\sin\alpha_m + F_y.\cos\alpha_m \quad \text{.................} \quad (3.10)$$

$$D = F_y.\sin\alpha_m - F_x.\cos\alpha_m \quad \text{.................} \quad (3.11)$$

From equation (3.5):

$$D = \cos\alpha_m\left(F_y.\tan\alpha_m - F_x\right) = t\,\Delta P_o.\cos\alpha_m \quad\text{................…........ (3.12)}$$

From equations (3.10) and (3.5):

$$
\begin{aligned}
L &= \left(F_y.\tan\alpha_m - t\,\Delta P_o\right)\sin\alpha_m + F_y.\cos\alpha_m \\
&= F_y.\sec\alpha_m - t\,\Delta P_o\sin\alpha_m \\
&= \rho t\,C_a^2\left(\tan\alpha_1 - \tan\alpha_2\right)\sec\alpha_m - t\,\Delta P_o\sin\alpha_m \quad\text{.....…......... (3.13)}
\end{aligned}
$$

The mean velocity is defined as follows:

$$C_m = C_a\,/\cos\alpha_m$$

Lift and drag coefficients may then be introduced:

$$C_L = \frac{L}{\rho\ell C_m^2\,/2} \quad , \quad C_D = \frac{D}{\rho\ell C_m^2\,/2} \quad\text{............…….. (3.14)}$$

From equations (3.12) and (3.6):

$$C_D = \frac{t\,\Delta P_o\cos\alpha_m}{\rho\ell C_m^2\,/2} = \zeta\,\frac{t}{\ell}\cos^3\alpha_m \quad\text{.....…................................ (3.15)}$$

From equation (3.13):

$$C_L = 2\frac{t}{\ell}\cos\alpha_m\left(\tan\alpha_1 - \tan\alpha_2\right) - C_D\tan\alpha_m \quad\text{…...…….......... (3.16)}$$

From equations (3.15) and (3.8):

$$C_L = \frac{t}{\ell}\cos\alpha_m\left(C_f - 0.5\zeta\sin 2\alpha_m\right) \quad\text{.............……................. (3.17)}$$

From equation (3.16), the quantity $C_D\tan\alpha_m$ is usually small. It may be dropped to give the following equation:

$$\frac{L}{D} = \frac{C_L}{C_D} \cong \frac{2\sec^2\alpha_m}{\zeta}\left(\tan\alpha_1 - \tan\alpha_2\right)$$

$$= \frac{C_f}{\zeta}\sec^2\alpha_m \quad \text{…………………………….......................... (3.18)}$$

Usually in turbomachines, D must be small and much less than lift. Also, the lift may be expressed in terms of circulation. After Kutta-Joukowski theorem:

$$L = \rho\Gamma C \quad \text{...………................. (3.19)}$$

After equation (3.13) neglecting the total pressure loss and after some manipulations, one can obtain the following relation:

$$L = \rho t C_m\left(C_{u1} - C_{u2}\right) \quad \text{.......................….....................……........ (3.20)}$$

From equations (3.19) and (3.20):

$$\Gamma = t\left(C_{u1} - C_{u2}\right)$$

and $\quad L = \rho\Gamma C_m \quad \text{.........................….................…………....... (3.21)}$

3.5 Cascades in Motion:
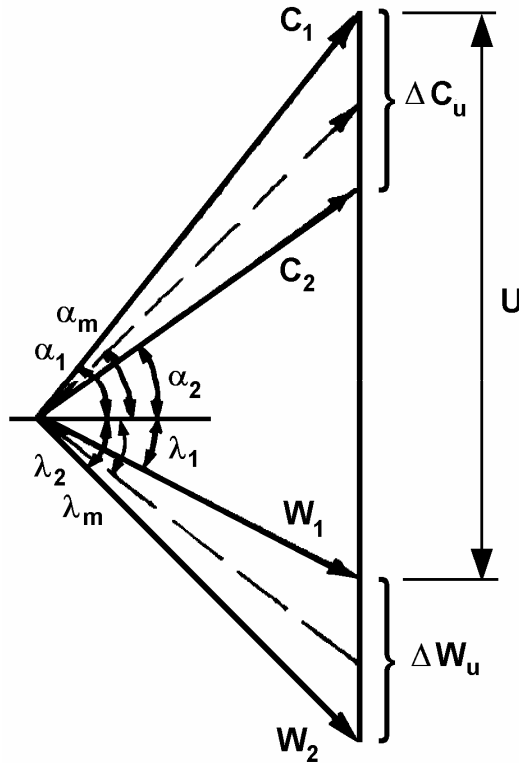
Fig. 3.4 Velocity triangle

Consider a cascade row in motion, λ is the angle included between the relative velocities and the cascade front. It is easy to show that the change in the tangential absolute velocity and tangential relative velocity is the same, hence $\Delta C_u = \Delta W_u$ and consequently, the tangential coefficient is written as follows:

$$C_f = 2(\tan\alpha_1 - \tan\alpha_2) = 2(\tan\lambda_2 - \tan\lambda_1)$$

The shaft energy transferred per unit mass of fluid:

$$E = \frac{F_y.U}{\rho t C_a} = \frac{C_a.U}{2}.C_f \quad ....\ldots\ldots............................ (3.22)$$

From the definition of work coefficient ϕ which is analogue to $\pi_1 = gH/N^2D^2$ (see Chapter II, 2.4.1) and the discharge coefficient ψ .

$$\phi = \frac{E}{N^2 D^2} = \frac{E}{4U^2} \quad \text{.................………...............................} \quad (3.23)$$

$$\psi = C_a / U$$

Note that E has the dimension of energy per unit mass or $= gH$, from equations (3.22) and (3.23):

$$\phi = \psi C_f / 8 \quad \text{...………...…….......} \quad (3.24)$$

Now, it becomes easy to present the efficiency of a moving pump cascade, which is similar to the hydraulic efficiency:

$$\eta = 1 - E_L / E \quad \text{….......................................……...........................} \quad (3.25)$$

where E_L is the energy loss per unit mass and equals $gH_L = \dfrac{\Delta P_o}{\rho}$. From equations (3.6) and (3.22) we may write:

$$\eta = 1 - \frac{\zeta}{C_f} \psi \quad \text{...…..............} \quad (3.26)$$

3.6 Cascade Performance:

3.6.1 General Approach:

As it may be noticed from the previous paragraphs, the cascade performance may be determined by knowing the inlet, outlet flow angles and the loss coefficient. For example, tangential force coefficient is a function of flow angles, for a given cascade one of these variables is usually known, the other two being fixed by the cascade geometry or more precisely by the Mach number and Reynolds number of the flow. The forgoing statements may be written mathematically on the following form:

$$\zeta, \alpha_2 = f\left[\alpha_1, (\ell C_m / v), (C_m / a)\right] \quad \text{…...................................} \quad (3.27)$$

where a being the sound velocity, and v the kinematic viscosity.

Actually, the performance of a cascade can not be completely determined theoretically. Recourse to experiment is necessarily, there are many data published in this field mainly extensive research undertaken by the NACA.

Figure 3.5 shows the experimental results between lift and drag coefficients, the deflection θ, and the lift-drag ratio as a function of the stagger angle at constant fluid angle.

65 (27) 10 means a 65 series foil,
design lift coefficient = 2.7,
Z_{max}/l = 10%
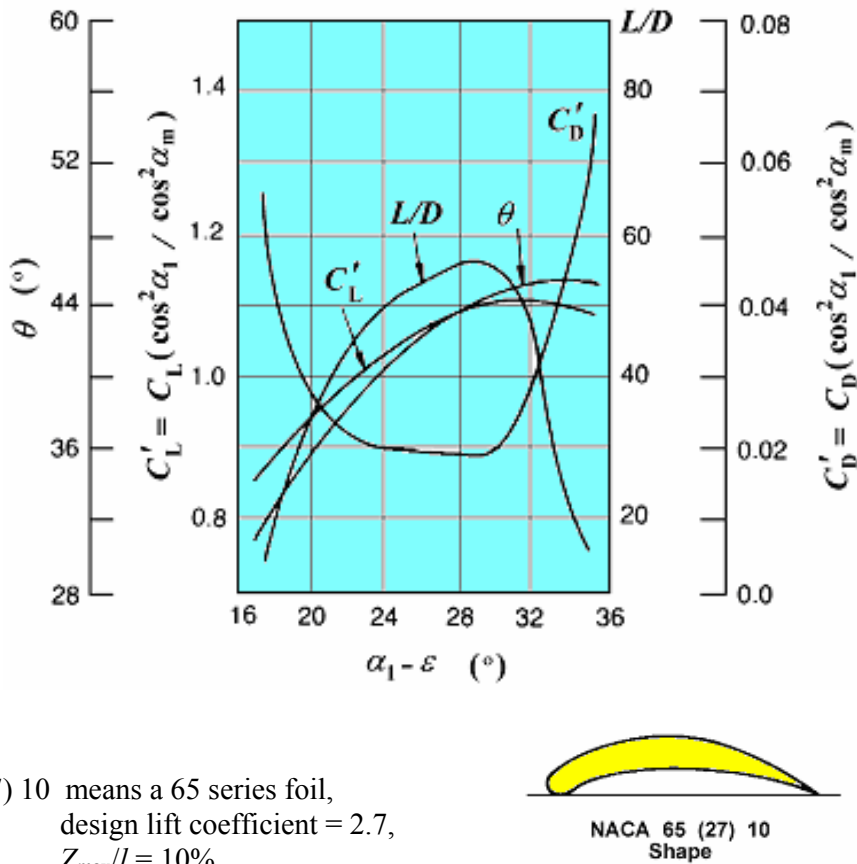
NACA 65 (27) 10
Shape

Fig 3.5 NACA cascade data, $\theta = \alpha_1 - \alpha_2$, $t/l = 1$,
$\alpha_1 = 45°$, Section NACA 65 (27) 10,
(adapted from Csanady)

From equation (3.26) the smallest ζ / C_f the highest the efficiency, hence another useful correlation ζ and C_f with the space-chord as

parameter which enable the designer to select the best ζ / C_f ratio and consequently the corresponding space-chord ratio, Figure 3.6.
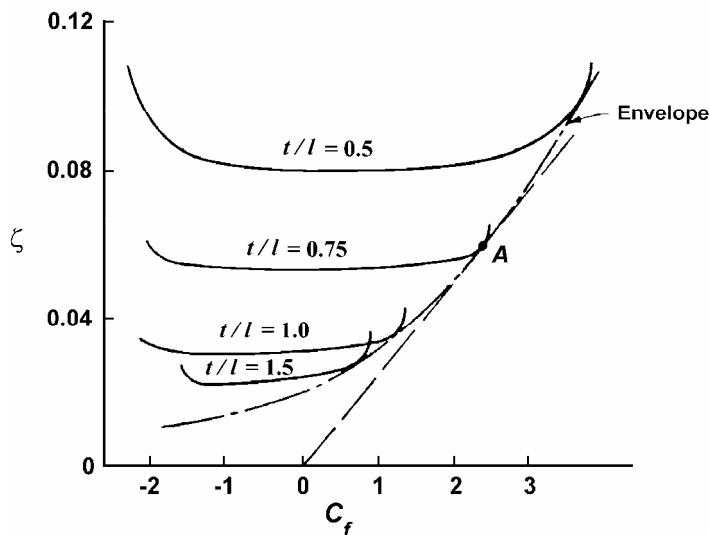
Fig 3.6 Loss-coefficient versus tangential force coefficient curves of cascades (adapted from Csanady)

Another important feature in the performance is to define a range of operation where the losses are minimum. The optimum operation will correspond to minimum loss coefficient ζ and drag coefficient C_D. Usually, this operating condition corresponds to an optimum inlet flow angle α_1, increasing α_1 increases losses and reduces the flow until the stall point is reached and separation occur. On the other hand, decreasing α_1 increases losses and also flow, in practice the working range is laying between those two values of α_1 at which the losses equal twice the minimum loss.

3.6.2 Fluid Deviation:

The difference between fluid and blade angles at exit is called the deviation $\delta = \alpha_2 - \alpha_2'$ where α_2 is the deviated flow angle at exit. The deviation is usually positive.

The experimental results of Howell correlate the deflection to the outlet angle α_2, using the t / ℓ as parameter, Figure 3.7.
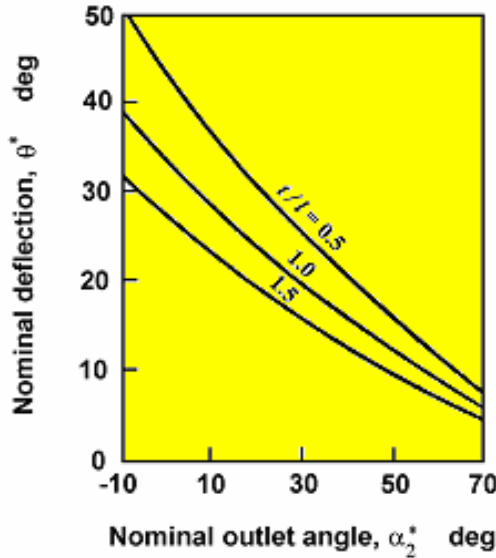
**Fig. 3.7 Variation of nominal deflection with nominal outlet angle
for several space-chord ratios (after Howell)**

Howell used an empirical formula to relate the nominal deviation δ^* to the camber angle and the space-chord ratio:

$$\delta^* = m\theta'(t/\ell)^n \quad\text{............................…..................…...........…... (3.28)}$$

where *n* depends on the kind of turbomachine, and equal 1/2 for compressor cascades, l for compressor inlet guide vanes. The value of *m* depends upon the shape of the camber line and the blade setting. For a compressor cascade:

$$m = 0.23\,(2a/\ell)^2 + \alpha_2^*/500 \quad\text{.....…..................................…....... (3.29)}$$

where *a* is the distance of maximum camber from the leading edge, Figure 3.1.

3.6.3 Off-Design Performance:

Also exists a kind of correlation between the design point and the off-design operating points. The off-design performance of a compressor cascade is published by Howell and is shown in Figure 3.8.
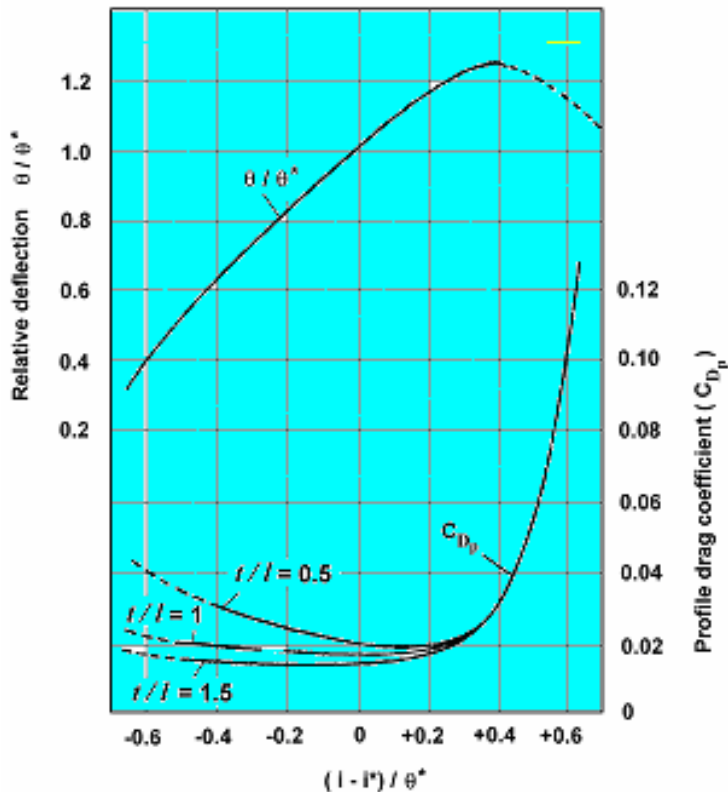
Fig. 3.8 The off-design performance of a compressor cascade
(after Howell)

3.6.4 Turbine Cascade Performance:

Figure 3.9 shows some performances of turbine cascade obtained by Ainley. The process of energy transfer in reaction and impulse turbines has been explained in Chapter I, so in impulse blade row there is no pressure change, despite in reaction blade row there are pressure and velocity changes.

The performance as presented by Ainley is expressed in the form of profile loss coefficient $\Delta P_o /(P_o - P_2)$ and α_2 against incidence i.

From Figure 3.9, we can remark that:

- The fluid outlet angle remains relatively constant over the whole range of incidence.
- The reaction blades have a much wider range of low loss performance than the impulse blades.
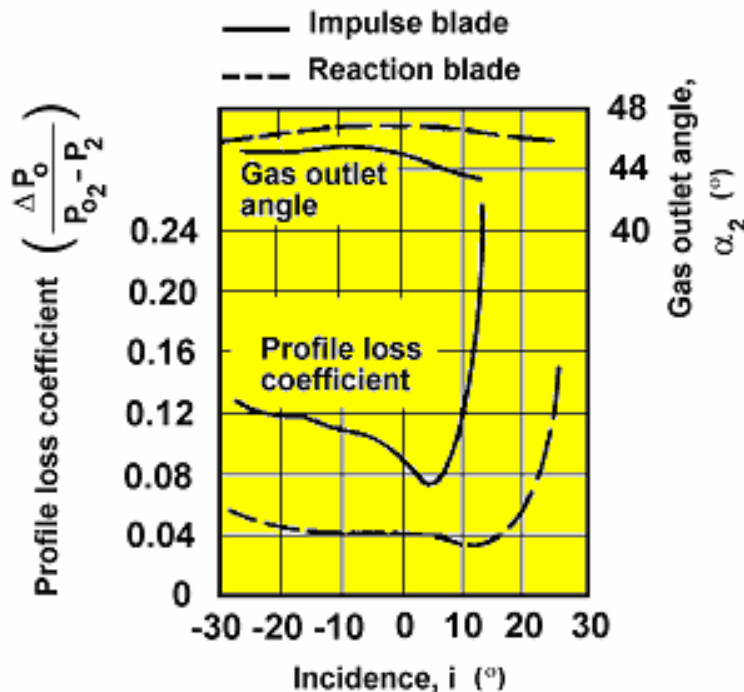
Fig. 3.9 Variation in profile loss with incidence for typical turbine blades after Ainley (adapted from Dixon)

3.7 Mach Number Effect:

The performance of cascade described in section (3.6) has been obtained with low speed neglecting the compressibility. When the Mach number reaches 0.4, compressibility becomes important and consequently the performance is altered. Usually in design, care should be paid to avoid reaching sonic speed and exception is made for supersonic compressor. When compressibility becomes important, we have to consider a so-called an *equivalent cascade*. The dimensions of an equivalent cascade in incompressible flow are changed by a factor $B = 1/\sqrt{1-M^2}$ to the real cascade, in which compressible flow is investigated.
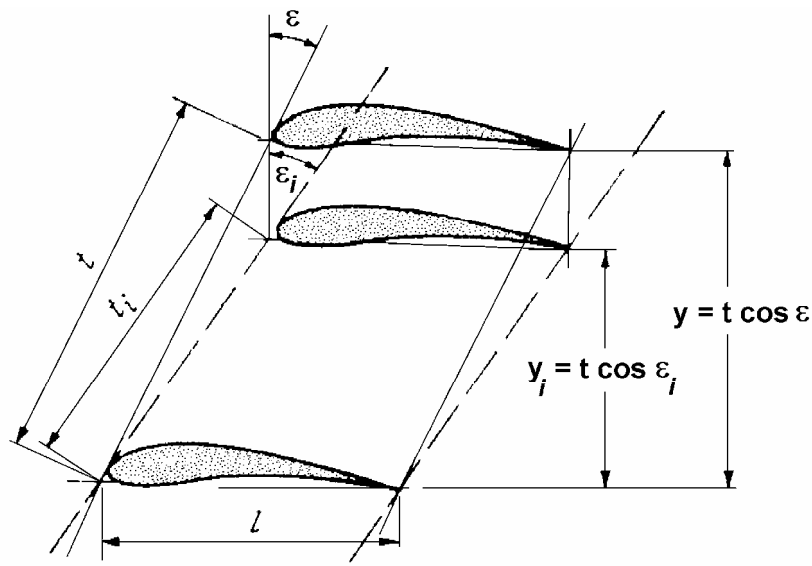
**Fig. 3.10 Geometry of the real and the equivalent cascade, *i* denotes parameters
referring to equivalent cascade in incompressible flow**

Hence, stagger angles become;

$$\tan \varepsilon / \tan \varepsilon_i = y_i / y = \sqrt{1 - M^2} \quad \text{.....……............................ (3.30)}$$

$$t_i / t = \sqrt{1 - M^2 . \cos^2 \varepsilon} \quad \text{.................................…................. (3.31)}$$

The Mach number at which the performance starts to change is
known as the *critical Mach number*.
Howell shows clearly the dependence of Mach number on the angle of
incidence, which can be characterized by the factor:

$$(M - M_c) / (M_m - M_c) \quad \text{.. (3.32)}$$

where M_m denotes the maximum Mach number which can reach unity.

3.8 Ideal Characteristics:

The cascade performance laws are generally determined after the
perfect fluid theory, i.e. assuming inviscid flow, at least this will help the
calculation of pressure field, but the perfect fluid theory breaks down

when calculating velocity field. In real case, fluid particles adhere to the walls resulting in zero velocity on the walls.

Consider equation (3.27) and neglect the effect of Mach number and viscosity, thus;

$$\alpha_2 = f(\alpha_1) \quad \text{...………. (3.33)}$$

With linearized Laplace's differential equations, using the superposition principle after Ruden, the two extreme conditions exist with:

a. Zero-Lift Angle δ ;   where the flow does not exert any force on the blade. The inlet flow angle will be, Figure 3.11;

$$\alpha_1 = \delta = \alpha_2$$
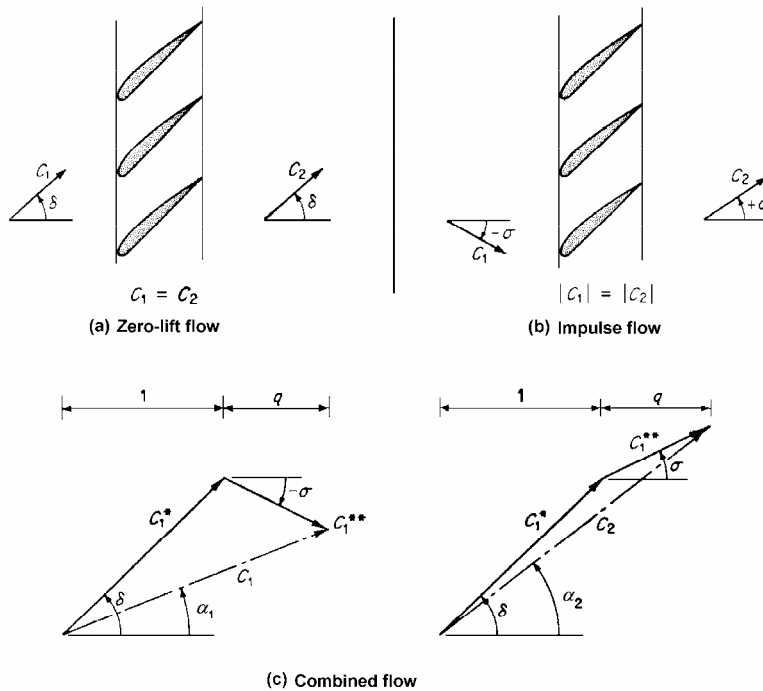
Fig. 3.11 Zero-lift and impulse flow angles

b. Impulse Flow Angle σ ;   in this case, pressure will remain constant, velocity magnitude remains unchanged while the outlet angle $= +\sigma$ if the inlet angle $= -\sigma$.

62

Now, superpose the two flow patterns giving the unity value to the zero-lift inlet velocity and q to the impulse flow. New values of C_1, C_2, α_1, and α_2 will be produced and expressed as follows;

$$\tan \alpha_1 = \frac{\tan \delta - q.\tan \sigma}{1+q} \quad \text{...} \quad (3.34)$$

$$\tan \alpha_2 = \frac{\tan \delta + q.\tan \sigma}{1+q} \quad \text{...} \quad (3.35)$$

Eliminate q from equations (3.34) and (3.35) to obtain:

$$\frac{\tan \alpha_2 - \tan \delta}{\tan \alpha_1 - \tan \delta} = \frac{\sin(\delta - \sigma)}{\sin(\delta + \sigma)} \quad \text{...} \quad (3.36)$$

Put equation (3.36) on the form of performance equation (3.27) as follows;

$$\tan \alpha_2 = A_o + A_1 \tan \alpha_1 \quad \text{...} \quad (3.37)$$

with;

$$\tan \delta = \frac{A_o}{1 - A_1} \qquad , \qquad \tan \sigma = \frac{A_o}{1 + A_1}$$

In Euler approximation where $t \approx 0$ (infinite number of blades) $\sigma \rightarrow \delta$ and $\tan \alpha_2 = \tan \delta$. In most cases where $t/\ell \approx 1$ the constant A_o is small and hence α_2 differs a little from the zero-lift angle δ. This means that Euler approximation is acceptable in preliminary calculations.

3.9 The Head-Capacity Curve of a Straight Cascade:

| a. Through Flow | b. Circulatory Flow | c. Displacement Flow |
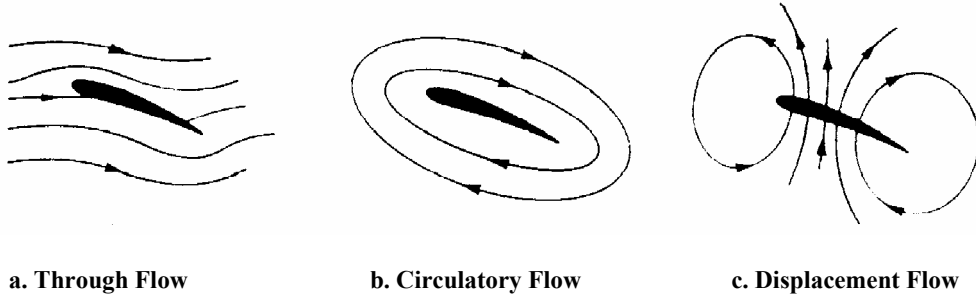
Fig. 3.12 Flow around a moving blade profile

Considering the flow around an isolate airfoil, the superimposed velocity field is referred to the displacement flow, as shown in Figure 3.12. This velocity field satisfies Kutta Condition, namely that the velocity at the trailing edge is zero which requires a certain circulation. This will lead to consider the circulatory flow field; the foregoing three fields can describe any actual flow pattern at the trailing edge where the velocity is zero.

$$a.\Gamma - b.Q + c.U = 0 \quad \text{....................................…….……. (3.38)}$$

where a, b, and c are constants determined from cascade geometry. Introducing the definition of the tangential force;

$$F_y = \frac{\rho}{t} Q.\Gamma \quad \text{...……..... (3.39)}$$

Substituting in equation (3.39)

$$F_y = \frac{\rho}{t} \left(\frac{b}{a} Q^2 - \frac{c}{a} Q.U \right) \quad \text{..................…….................. (3.40)}$$

Consider the input head $E = F_y U /(\rho Q)$, [Equation (3.22)], yields;

$$E = B.U^2 - A.U.Q \quad \text{.........................……....……........ (3.41)}$$

or a straight line head-capacity curve at constant speed, Figure 3.13.
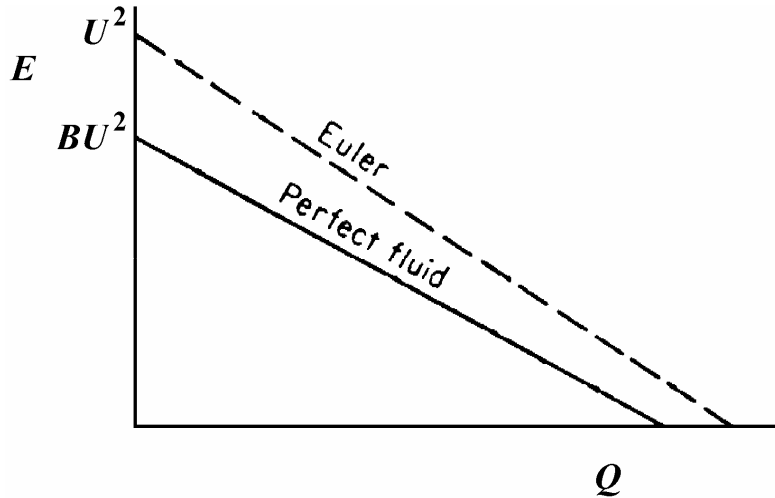
Fig. 3.13 Head-capacity curve for straight and radial cascades

For a straight cascade, the Euler approximation $\lambda_2 = \alpha_2$, (outlet fluid angle equals blade angle). For a pump straight cascades, the relative inlet angle, from Figure 3.4: $-\tan \lambda_1 = \dfrac{U}{C_a} - \tan \alpha_1$. The tangential force coefficient, C_f

$$C_f = 2(\tan \lambda_1 - \tan \lambda_2) = \frac{F_y}{\rho.t.C_a^2 / 2}$$

and $\quad Q = t.C_a$

The constants in the equation (3.41) can easily be determined:

$$A = \frac{1}{t}(\tan \alpha_1 - \tan \alpha_2) \qquad , \qquad B = 1$$

3.10 Radial Cascade:

The plane flow in an impeller may be presented by a cascade, if a straight cascade is wrapped it will form a radial cascade. The transfer of the straight cascade to radial cascade is made using the conformal mapping. From the geometry of the mapping, the connection between the variables in straight cascade and radial cascade may be deduced. For example ℓ/t ratio is equivalent to r_2/r_1 ratio and for a log spiral blade:

65

$$\frac{\ell}{t} = \frac{Z_n}{2\pi \cos \varepsilon} \ln \frac{r_2}{r_1} \quad \text{.......................................………...... (3.42)}$$

where Z_n is the number of blades.
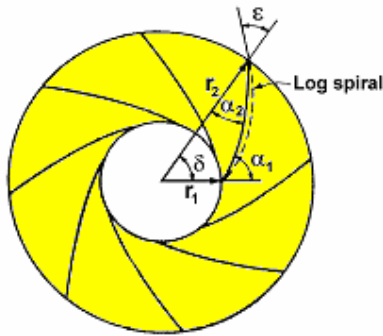
Fig. 3.14 Radial cascade

The evaluation of the constants A and B in equation (3.41) is difficult. Considering the fact that the effects of the radius ratio become negligible for l/t ratio about unity, i.e. equation (3.42), the following simplification can be used:

$$\frac{r_2}{r_1} \geq e^{(2\pi/Z_n)\cos \varepsilon}$$

The details of radial cascade are lying beyond the scope of these notes. For further reading, the reader is invited to refer to Csanady.

3.11 Cascade Characteristics Analysis:

As described before, the perfect fluid theory can supply useful information on the pressure field. If there is no separation, we have to classify two kinds of problems:

1. Direct problem; the geometry of cascade is known, find the corresponding pressure field.
2. Inverse problem; for a given velocity and pressure distribution, find the required blade angle.

Two methods exist, the first is the singularity method and the second is the conformal mapping method.

3.12 Singularity Method:
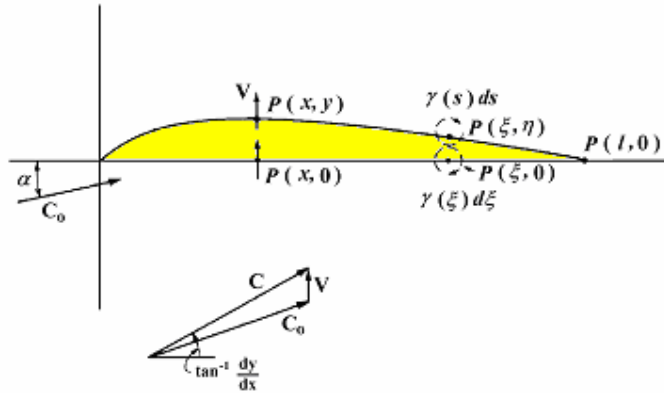
Fig. 3.15 An isolated thin airfoil

In this method, the airfoil is considered to be formed from a line of a bound vortex (or a sheet in 3-directions). The velocity induced by the vortex at any point is perpendicular to the radius vector drawn from the vortex center (x_o, y_o) to the point considered (x, y) and is given by:

$$U = \frac{\Gamma}{2\pi} \frac{y - y_o}{r^2} \quad \text{..} \quad (3.43)$$

$$V = -\frac{\Gamma}{2\pi} \frac{x - x_o}{r^2} \quad \text{..} \quad (3.44)$$

If the local strength of the vorticity (circulation per unit length) is $\gamma(s)$, the circulation in an airfoil of chord l, as shown in Figure 3.15;

$$\Gamma = \int_0^l \gamma(s)\,ds \quad \text{..} \quad (3.45)$$

If the airfoil is subjected to a wind speed of C_o arriving at an incidence of α, and if the camber is small, the velocity induced at a point $P(x, y)$ on

the mean camber line by a vortex at another point $P(\xi, \eta)$ on this line is approximately that which would be induced at the point on the X-axis $P(x,0)$ by the same vortex $\gamma(s) ds = \gamma(\xi) d\xi$ at the point $P(\xi, 0)$.

The total induced velocity at $P(x, y)$ from equation (3.43) with $r \approx x - \xi$,

$$V = \frac{1}{2\pi} \int_0^l \frac{\gamma(\xi)}{\xi - x} d\xi \quad \text{..} \quad (3.46)$$

and the resultant velocity C tangential to the camber will be at an inclination;

$$\frac{dy}{dx} = \frac{V}{C_o} + \alpha \quad \text{..} \quad (3.47)$$

Equations (3.46) and (3.47) describe the complete solution of velocity distribution for a given camber, or vice versa.

It should be pointed that the integral [Equation (3.46)] is improper, since it tends to infinity. Practical profiles cannot be thin sheets because sharp edges produce separation at almost all flow conditions.
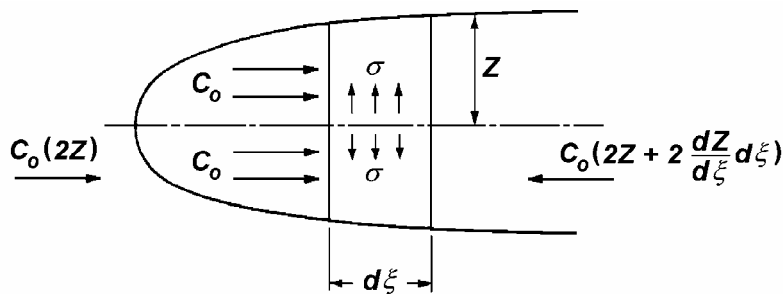

Fig. 3.16 Allowance for profile thickness

The thickness is achieved by arranging sources and sinks in the fluid in such a manner that the total strength of sources is equal to that of sinks. The fluid coming from the sources displaces the main flow in such a manner creating a closed contour, which of course is the shape of the airfoil.

68

Arranging a source $\sigma(\xi).d\xi$ on the chord, the induced velocity will be;

$$dU = \frac{1}{2\pi} \frac{\sigma(\xi).d\xi}{x - \xi}$$ .... (3.48)

and the total induced velocity at $P(x,0)$ by all the source and sink elements is,

$$U(x) = \frac{1}{2\pi} \int_0^l \frac{\sigma(\xi)}{x - \xi} d\xi$$ .... (3.49)

For a mass balance of element $d\xi$, height Z and unit depth;

$$U = \frac{C_o}{\pi} \int_0^l \frac{dZ}{d\xi} \frac{d\xi}{x - \xi}$$ .... (3.50)

3.12.1 *Method of Solution for Single Airfoil:*

The solution consists of introducing auxiliary variables as follows:

$$\xi = \frac{l}{2}(1 - \cos\theta)$$
$$x = \frac{l}{2}(1 - \cos\tau)$$ .... (3.51)

Substituting equation (3.51) into equation (3.47) and simplify using trigonometry identities, one can reach;

$$\frac{dy}{dx} = \alpha + \frac{1}{2\pi.C_o} \int_0^\pi \gamma(\theta) \frac{\sin\theta}{\cos\tau - \cos\theta} d\theta$$ .... (3.52)

The evaluation of the integral in equation (3.52) is presented by Glauert; as follows;

$$\int_0^\pi \frac{\cos(n\theta)}{\cos\theta - \cos\tau} d\theta = \pi \frac{\sin(n\tau)}{\sin\tau}$$ .... (3.53)

Then the lift coefficient is defined:

$$C_L = \frac{2\Gamma}{lC_o} = \frac{2}{lC_o} \int_0^l \gamma(x).dx \quad \text{.. (3.54)}$$

and the loading coefficient;

$$\frac{P_2 - P_1}{(\rho/2).C_o^2} = 4\frac{\gamma}{2.C_o} \quad \text{.. (3.55)}$$

and finally the inclination equation can be written on the following form;

$$\frac{d\,y}{d\,x} = \alpha - A + \sum_1^\infty A_n.\cos(n\tau) \quad \text{.. (3.56)}$$

The coefficients of the Fourrier series A_1 to A_n clearly depend on the shape of the camber line and the infinite sums are referred to as the basic vorticity and camber distributions.

$$\frac{\gamma_b}{2.C_o} = \sum_1^\infty A_n.\sin(n\theta)$$

$$\frac{dy_b}{dx} = \sum_1^\infty A_n.\cos(n\tau) \quad \text{.. (3.57)}$$

The details of the solution could be found in Csanady.

3.12.2 Conformal Transformation Method:

Consider the continuity equation applied on a flat plate with reference to Figure 3.17. The following relation is obtained for the difference in the stream functions;

$$\Delta\psi = tc_\infty \cos\varepsilon \quad \text{.. (3.58)}$$

From Z-plane, the equipotential lines (ϕ = Const.) are perpendicular to the streamline $\psi = 0$, thus the following relation can be written;

$$\Delta\phi = tc_\infty \sin\varepsilon \quad \text{.. (3.59)}$$

70

For the produced mass flow rate per spacing, a source of strength $q = \Delta\psi$ should be placed at a point -*R*, i.e. $q = \Delta\psi$. Similarly, the potential difference could be established by introducing the circulation at the point -*R*, we have;

$$\Gamma = |\Delta\phi| \quad \text{... (3.60)}$$
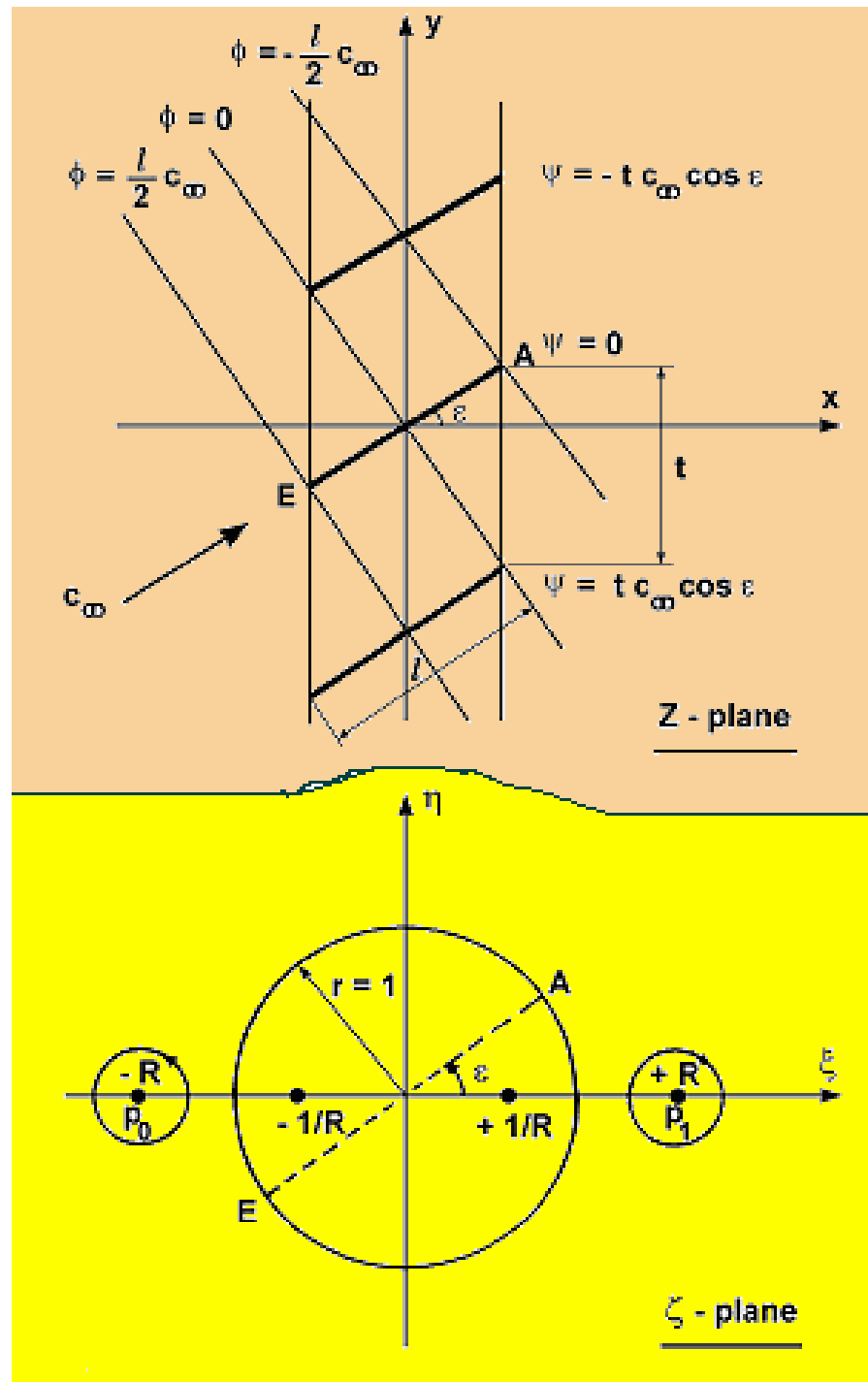
Fig. 3.17 Conformal transformation of a flat plate cascade

Since the flow far upstream and downstream are parallel, a sink of the same strength $-q$ and circulation of the same magnitude but of opposite sign of rotation should be introduced at a point $+R$ as shown in Figure 3.17.

Since for transformation, the flat plate should be transformed to a unit circle, it is necessary to put at the reflection point $\pm 1/R$ a sink and source vortex of the same strength as before. The total potential at any point in the ξ-η plane of the system of sink-source is then given by:

$$\phi_q = \frac{q}{2\pi}\ln(\xi + R) + \frac{q}{2\pi}\ln(\xi + 1/R) - \frac{q}{2\pi}\ln(\xi - 1/R) - \frac{q}{2\pi}\ln(R - \xi)$$

$$\downarrow \qquad\qquad \downarrow \qquad\qquad \downarrow \qquad\qquad \downarrow$$

source at	source at	sink at	sink at
$\xi = -R$	$\xi = -1/R$	$\xi = +1/R$	$\xi = +R$

Similarly, the total potential due to the system of vortex is given by;

$$\phi_\Gamma = -i\frac{\Gamma}{2\pi}\ln(\xi + R) + i\frac{\Gamma}{2\pi}\ln(\xi + 1/R)$$

$$- i\frac{\Gamma}{2\pi}\ln(\xi - 1/R) + i\frac{\Gamma}{2\pi}\ln(R - \xi) \quad \text{...............................} \quad (3.61)$$

The total complex potential of the flow is then given by;

$$W = \phi_q + \phi_\Gamma = \phi + i\psi = c_\infty Z e^{-i\varepsilon}$$

which leads to the following equation;

$$W = \frac{t.c_\infty}{2\pi} e^{-i\varepsilon}\left[\ln\frac{R+\xi}{R-\xi} + e^{2i\varepsilon}.\ln\frac{\xi+1/R}{\xi-1/R}\right] \quad \text{.....................} \quad (3.62)$$

For x-y plane, the complex velocity may be written as;

$$\frac{dW}{dZ} = c_x - ic_y = c_\infty\left(\cos\varepsilon - i\sin\varepsilon\right)$$

Putting $c_\infty = 1$, we get;

$$W(Z) = Z.e^{-i\varepsilon} \quad \text{..} \quad (3.63)$$

Comparing equation (3.62) with (3.63), we can get the transformation function:

$$Z = \frac{t}{2\pi}\left[\ln\frac{R+\xi}{R-\xi} + e^{2i\varepsilon}\ln\frac{\xi+1/R}{\xi-1/R}\right] \quad ....\text{ (3.64)}$$

The stagnation points E and A are located on the circle and the difference in potential $\phi_E - \phi_A$ gives a relation between t/ℓ and R.

An actual flow plates (with circulation) is made of:
  i. A uniform flow at zero incidence.
  ii. A flow perpendicular to plates.
  iii. A circulatory flow.

Weinig (1935) transforms three flows in $\zeta(\xi,\eta)$ plane into three flows in $Z(x,y)$ plane using transformation previously found. The magnitude of the circulation is found by ensuring that the flow leaves the trailing edge of the plane at the plate angle in the Z-plane. Weinig expresses his results as the ratio:

$$\lambda = \frac{\text{Lift on plate in cascade}}{\text{Lift on isolated plate}} = \frac{C_L}{C_{L\infty}}$$

Two simple approximations for λ may be obtained; for $t/\ell \to \infty$, where $\lambda = 1$ and for $t/\ell \to 0$ (for small t/ℓ), the deviation is nearly zero and $\lambda = 0$, (Figure 3.18).
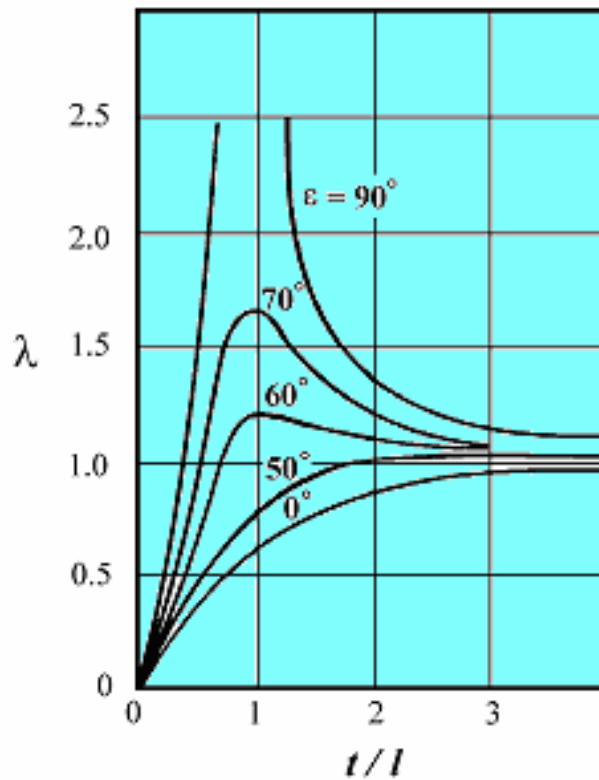
Fig. 3.18 Theoretical lift ratio for flat plate cascade versus pitch chord ratio for different stagger angles

For flat plate cascade, using Eq. (3.16) with $C_D = 0$, it may be shown that:

$$C_L = \frac{2}{\sigma} \cos \alpha_m \left(\tan \alpha_1 - \tan \alpha_2 \right) = \frac{4}{\sigma} \frac{\sin i}{\cos \varepsilon}$$

where σ is the solidity ($\sigma = l/t$), and i is the angle of attack. Since

$$C_{L\infty} = 2\pi . \sin i$$

then:

$$\lambda = \frac{C_L}{C_{L\infty}} = \frac{2}{\pi} \frac{1}{\sigma \cos \varepsilon} \quad \text{..} \quad (3.65)$$

Introducing the coefficient C_t where

$$C_t = \frac{2.m.\sigma.\sin \beta_v}{4 + m.\sigma.\sin \beta_v} \quad \text{.....….................................} (3.66)$$

C_t is the ratio of the change in the tangential velocity by the cascade to the change which would correspond to turning the inlet velocity vector into the direction β_v. In Eq. (3.66), m is a constant depending on the airfoil shape and cascade geometry. For a general cascade, m and β_v must be found from experiments or estimated with the aid of a suitable theory. However, when the solidity is less than about 0.35, m and β_v are well approximated by the values of the isolated airfoil. For a flat plate, for example, $m = 2\pi$ and $\beta_v = 90°$ - ε. Theoretical results can be shown in Figure 3.19 which gives the coefficient C_t as a function of σ and ε.
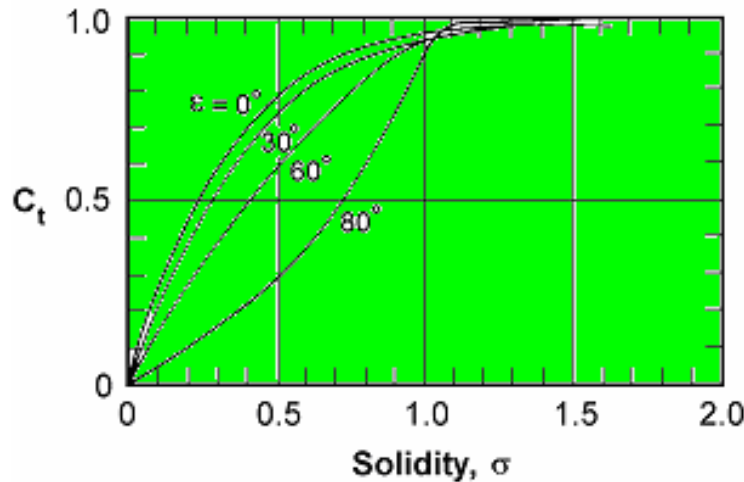

Fig. 3.19 Coefficient C$_t$ versus solidity for various stagger angles of a cascade of flat plates

This analysis has been extended to find the potential flow through logarithmic spiral blades of radial cascade. The analysis of the rotor in this case differs from that of the stator. Considering, first, the stationary radial cascade as shown in Figure 3.10, the equation of a logarithmic spiral is $\theta = A.\log r$, from which it can be seen that the angle β_v between the normal to the radius and the tangent to the curve is a constant all along the curve. In this respect, the spiral blade in the radial cascade is similar to the flat plate blade of a linear cascade and that the potential flow through a cascade of flat plates can be transformed by conformal

transformation into that through a stationary radial cascade of logarithmic spiral blades. The solidity σ for the radial cascade becomes; Eq. (3.42):

$$\sigma = Z_n \frac{\ln(r_2/r_1)}{2\pi . \sin \beta_v}$$

with this definition of σ, the coefficient C_t is equal to the one for linear cascade of flat plates and these values of C_t are applicable directly to the stationary radial cascade. As for rotating cascade, neglecting friction, the absolute flow may be still considered irrotational, in spite of the fact that the cascade is rotating. This unsteady potential flow problem has been solved by Busemann and the total pressure rise through a rotor of this type may be written as;

$$\psi = \psi_o - C_t \, \phi (\cot \beta_v + \cot \alpha_1) \quad \ldots\ldots\ldots\ldots\ldots\ldots\ldots\ldots\ldots\ldots\ldots \text{(3.67)}$$

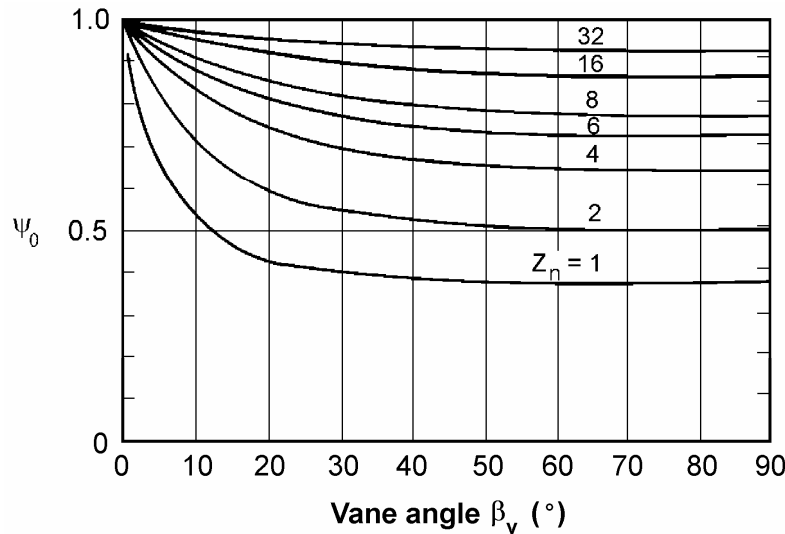ψ_o is given in Figure 3.20 in terms of β_v and the number of blades Z_n.

Fig. 3.20 Values of shut-off head coefficient ψ_0 for various vane angles β_v and number of vanes for a radial cascade of logarithmic spiral blades

CHAPTER (IV)

INCOMPRESSIBLE FLOW TURBOMACHINES (PUMPS)

4.1 Introduction:

Pumps present a part of turbomachines in which the energy transfer process occurs from the rotor to the fluid, in other words, in pump the mechanical energy is converted to a fluid energy (head). Pumps are classified according to their impeller type to radial, mixed, and axial.

4.2 Centrifugal Pumps (Radial):
4.2.1 General Considerations:

Centrifugal pumps, Figure 4.1, are used in a wide variety of applications. These machines operate at high speeds and usually direct connected to the driver so that the transmission losses are small. These types of pumps are usually used when relatively high pressure and large capacity are desired.

There are minimum of moving parts which reduces the maintenance and increase the working time, other advantages of centrifugal pumps are:

1. its smaller size,
2. its low installation costs.

As discussed before the total energy gained by the fluid $H = P*/\rho g + C^2/2g$, a part of it comes from pressure energy $P*/\rho g$ and the other is a kinetic energy $C^2/2g$. To increase the total pressure energy at the pump exit, kinetic energy should be converted to pressure energy. Volute casing and diffuser ring are usually used to convert kinetic energy to pressure energy.
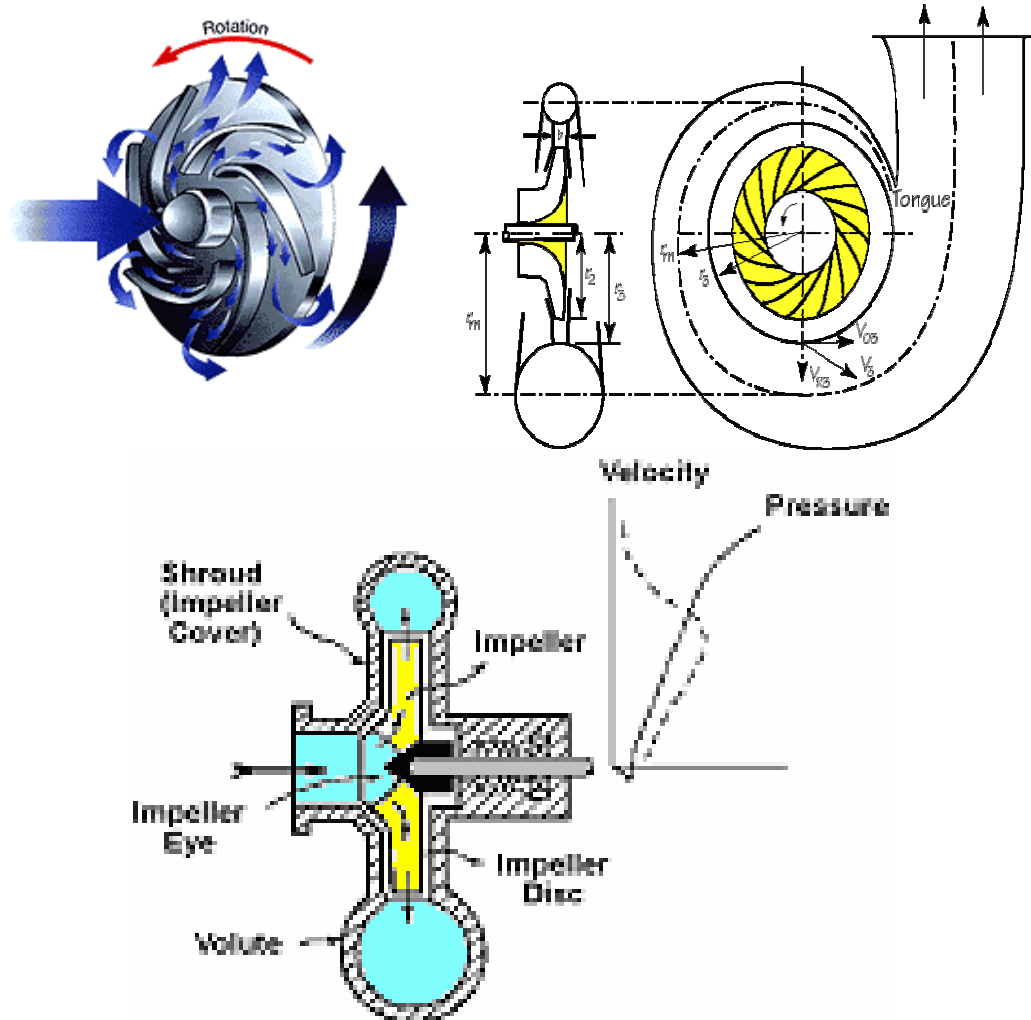
Fig. 4.1 Section at centrifugal pump

a. _Volute type pump:_ (Figure 4.2.a) In this kind of pumps a volute type diffuser is used. The volute diffuser is a spiral, which surround the periphery of wheel having increasing cross-sectional area as it approaches the discharge. The volute type is commonly used for single stage pumps, and for the last stage of multistage pumps.

b. _Diffuser type pump:_ (Figure 4.2.b) In this kind of pumps the diffuser consists of a number of relatively short expanding passages surrounding the periphery of the wheel. The diffuser is used usually in multistage pumps and also in stages developing high heads.
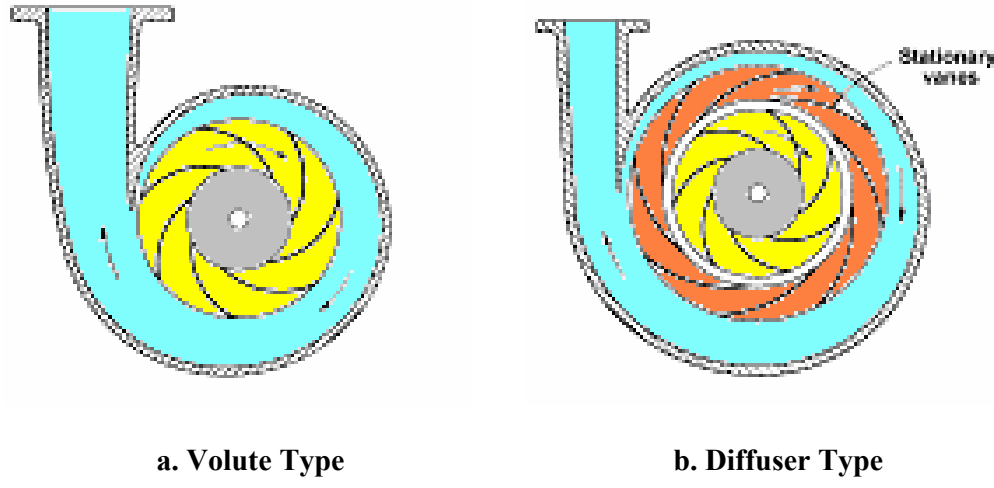
| a. Volute Type | b. Diffuser Type |

Fig. 4.2 Centrifugal pump types

To reduce the cost of making and storing patterns, manufacturers generally adopt a "standard line" or set of casings which cover the usual field of operating conditions. If a volute type diffuser is used, a new design should be prepared for every new conditions but if diffuser ring type is used, a standard design could be prepared and only vanes can change to meet the required new conditions, keeping the same casing dimensions.

4.2.2 Effect of Impeller Exit Angle β_2 :

As shown from Figure 4.3 for forward blades impeller, the fluid leaves the impeller with relatively high speed which means that the major part of the energy gained is kinetic energy, this type of impeller requires a very good diffuser to convert this kinetic energy to pressure energy. In practice, it is difficult to construct this kind of diffuser, also it is usually more efficient to convert pressure energy to kinetic energy rather than converting kinetic energy to pressure energy.

In backward curved impeller the exit velocity is relatively low. There is a small amount of kinetic energy to be converted through the diffuser which does not require any special design of diffuser, but this kind of impeller supplies a lower head than the forward impeller type.
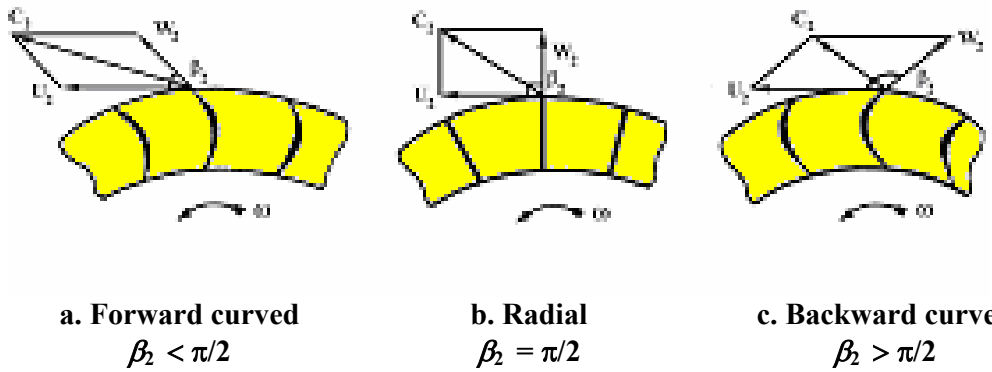
a. Forward curved
$\beta_2 < \pi/2$

b. Radial
$\beta_2 = \pi/2$

c. Backward curved
$\beta_2 > \pi/2$

Fig. 4.3 Impeller exit angles

As a result, the more efficient impeller could be the radial type. In practice, for pumps $\beta_2 = 90°$ to $170°$.

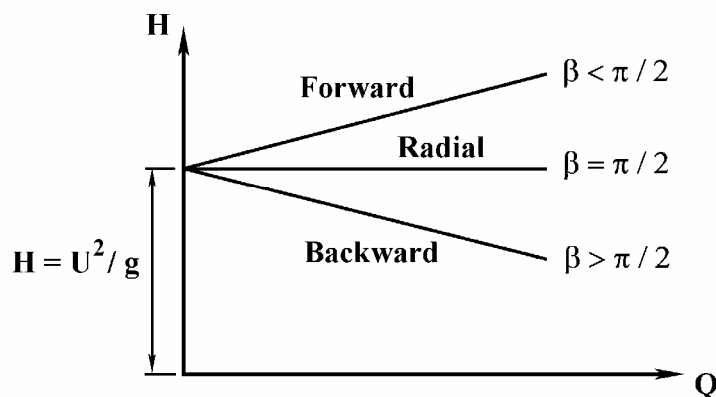To study the effect of exit angle on performance, we have to draw the *H-Q* curve as follows;

Fig. 4.4 Theoretical performance curve

From equation (1.24) we have;

$$H_o = (U_1.C_1.\cos\alpha_1 - U_2.C_2.\cos\alpha_2)/g$$

Assuming radial inlet and substitute $C_2.\cos\alpha_2$ by $U_2 + C_{r2}/\tan\beta_2$,

i.e. $\qquad H_o = \dfrac{U_2^2}{g} + \dfrac{U_2.C_{r2}}{g.\tan\beta_2}$

and $\qquad Q = \pi.D_2.b_2.C_{r2}$

81

i.e. $\quad H_o = \dfrac{U_2^2}{g} + \dfrac{U_2 . Q}{g . \pi . D_2 . b_2 . \tan \beta_2}$ $\qquad\qquad$ (4.1)

For a constant speed N, Figure 4.4 represents the above relationship.

4.2.3 Efficiencies and Coefficients of Centrifugal Pumps:

i. Efficiencies:

The efficiency of a centrifugal pump depends upon a number of factors, the more important of which are;

  a. Hydraulic losses:
   1- Friction and turbulence.
   2- Disk friction.

  b. Mechanical losses in bearings and packings, and the leakage losses.

All these efficiencies have been discussed. Here is a summary:

η_m = Manometric efficiency (sometimes called hydraulic efficiency)
$\quad = H_a \,(\text{measured head}) / H_o$

$\eta_{mech.}$ = Mechanical efficiency
$\quad$ = the ratio of the power supplied to the fluid by the impeller to the power supplied to the machine

$$\eta_{mech.} = \frac{\gamma \, Q \, H_o}{const . BHP}$$

η = Overall efficiency or Gross efficiency
$\quad$ = Water horsepower / Brake horsepower
$\quad$ = W.H.P. / B.H.P.

B.H.P. = W.H.P. + H.P. to overcome disk friction + Hydraulic losses (turbulence & friction) + Leakage losses + Mechanical losses.

i.e. $\quad \eta = \eta_m . \eta_{mech}$

The overall efficiency equal the hydraulic efficiency when $\eta_{mech} = 1.0$.

ϕ = Speed coefficient or speed factor = $U_2 / \sqrt{2gH_o}$ and sometimes called head factor.

ψ = Flow coefficient or discharge coefficient $Q / \left(D^2 . \sqrt{2gH} \right)$

iii. Affinity Laws:

For the same machine operating at variable speeds;

$$\frac{Q_1}{Q_2} = \frac{N_1}{N_2} \qquad \& \qquad \frac{H_1}{H_2} = \left(\frac{N_1}{N_2} \right)^2$$

Generally speaking, it is important to note that the overall pump efficiency depends mainly upon capacity and specific speed.

iv. Specific Speed:

$$N_s = N\sqrt{Q} / H^{3/4} \qquad Q \text{ in gpm, } H \text{ in ft.}$$

or $\quad N_s = N\sqrt{Q} / (gH)^{3/4} \qquad Q \text{ in m}^3\text{/s, } H \text{ in m.}$

See section 2.7.1 for details.

4.2.4 Centrifugal Pump Actual Performance:

4.2.4.1 Actual Head Capacity Curve:

As seen in section 4.2.2, the theoretical head capacity curve is a straight line, H decreases when Q increases for $\beta_2 > 90°$, and H increases when Q increases for $\beta_2 < 90°$.

To study the actual head capacity curve, Figure 4.5, we may consider a backward curved impeller, for the actual flow of the fluid in the impeller the circulation (discussed in section 1.5.2) will reduce the theoretical head, this reduction is practically constant. It should be remembered that this effect is not a loss but a discrepancy not accounted for by the basic assumptions.

The friction losses are proportional to the capacity Q and it will be minimum at no discharge.

The third type of losses is turbulence losses. The losses due to turbulence will be a minimum at design flow, for reduced or increased capacity the turbulence losses increase.

The actual head at no flow condition will be:
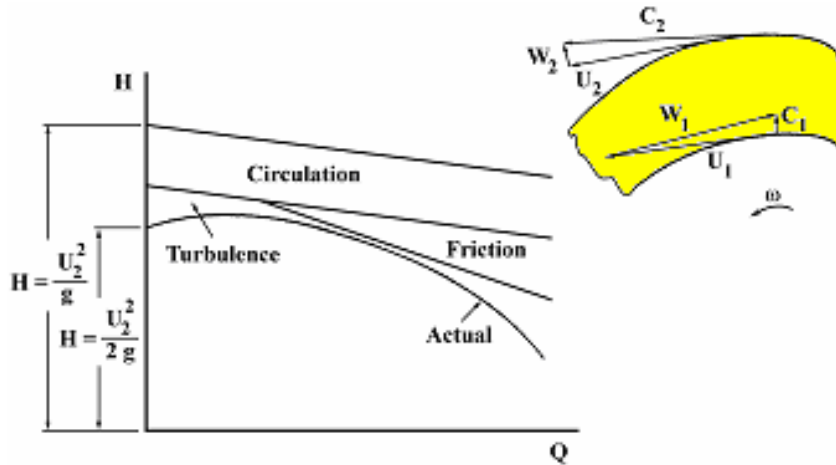
$$H_a = U_2^2 / 2g$$

Fig. 4.5 Actual head-capacity curve

Remark: to obtain the value of the actual head we may consider that even at no flow conditions exists a small amount of fluid in the impeller, and it will rotate with the impeller creating a forced vortex.

Applying Bernoulli's equation on the flow we have;

$$\left(\frac{P_2^*}{\gamma} + \frac{C_2^2}{2g} \right) - \left(\frac{P_1^*}{\gamma} + \frac{C_1^2}{2g} \right) = \frac{U_2^2}{g}$$

i.e. $\dfrac{P_2^* - P_1^*}{\gamma} + \dfrac{U_2^2}{2g} = \dfrac{U_2^2}{g}$ 　　　　　　　　(4.2)

From the above equation we can see that the gained energy consists of two equal parts of energy;

    i. Pressure energy,
    ii. Kinetic energy.

The kinetic energy could not be converted to pressure energy because there is no flow through the diffuser, this energy will dissipate and the

84

actual head $H_a = U_2^2 / 2g$. This equation is a convenient mean to calculate the approximate impeller diameter required for specific conditions of operation.

4.2.4.2 Brake Horsepower and Efficiency Curves:

In similar manner to the head capacity curve, we can draw the brake horsepower curve and efficiency.

The leakage, disk friction, and bearing losses for a machine operating at constant speed are all practically independent of the capacity and remain approximately constant for all flows as shown in Figure 4.6. The efficiency will be maximum at design flow.

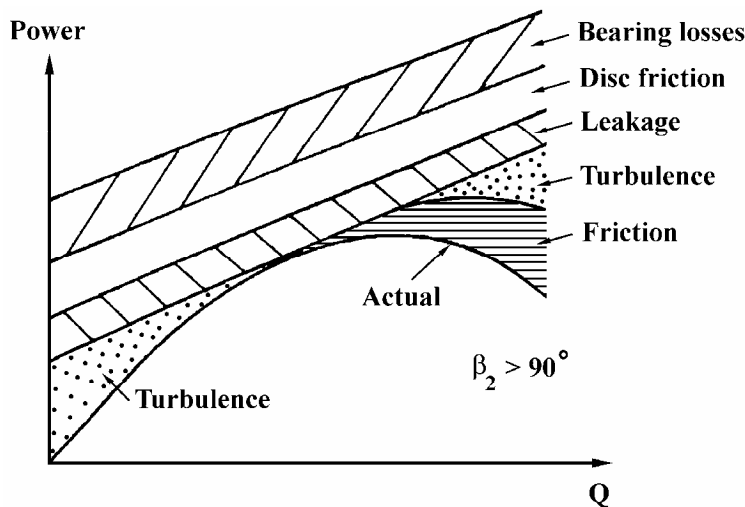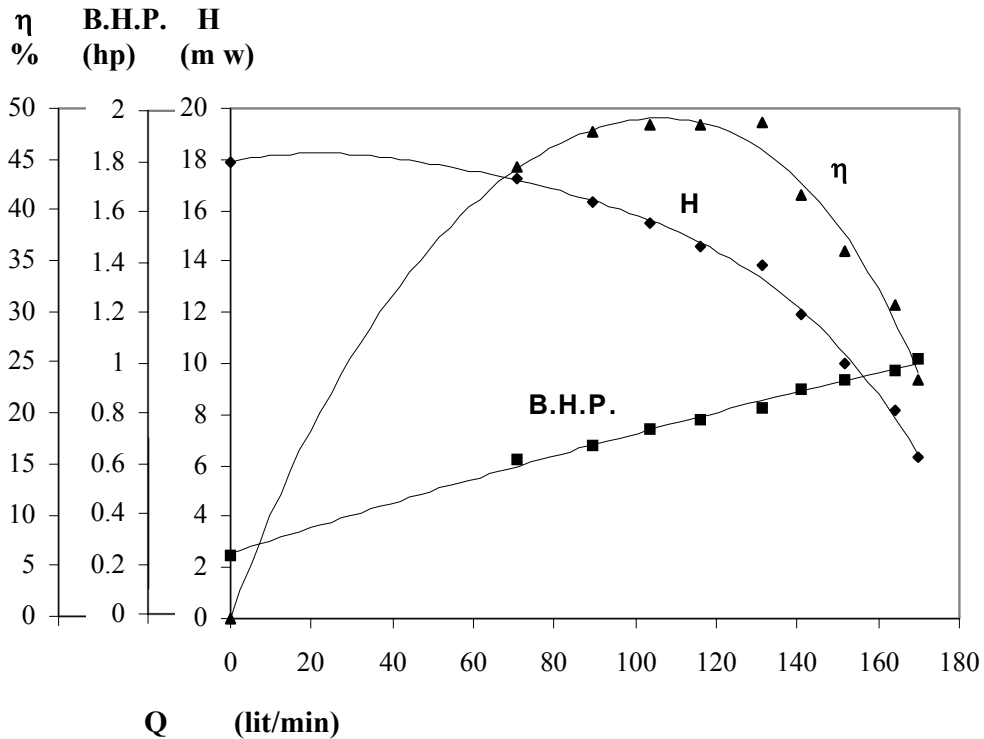Fig. 4.6 Actual power-capacity curve

4.2.4.3 Analysis of Characteristic Curves:

The characteristic curves shown in Figure 4.7 were obtained for a constant speed, to deduce the general characteristic curve for a pump we may use the affinity laws discussed in Chapter II.

$$H_1 / H_2 = N_1^2 / N_2^2 \qquad , \qquad Q_1 / Q_2 = N_1 / N_2$$

and thus we can deduce H and Q for different speeds.

(Mansoura University, Hydraulic Laboratory)

Fig 4.7 Pump characteristic curve for a constant speed (N = 2920 rpm)

To obtain the iso-efficiency curves, Figure 4.8, Q/N must be constant for every constant efficiency line. The similarity ratio means that the viscous friction losses are constant, as discussed in section 1.5.1. As it could be seen from dimensional analysis:

$$Q \propto N$$
$$H \propto N^2$$
$$Power \propto H.Q \propto N^3$$

It could be said that if, instead of plotting values of H, Q and power P for various speeds we may plot values of Q/N, H/N^2 and P/N^3, Figure 4.9, then all the points would fall on a single set of curves representing the performance of the pump at a speed of 1 rpm.
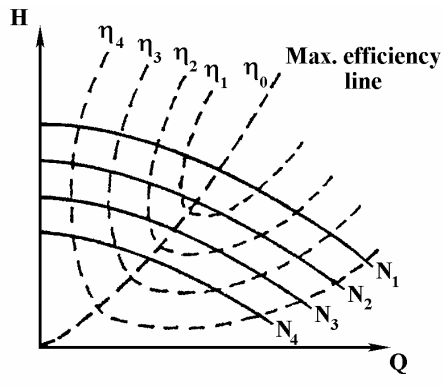
Fig. 4.8 Iso-efficiency curves
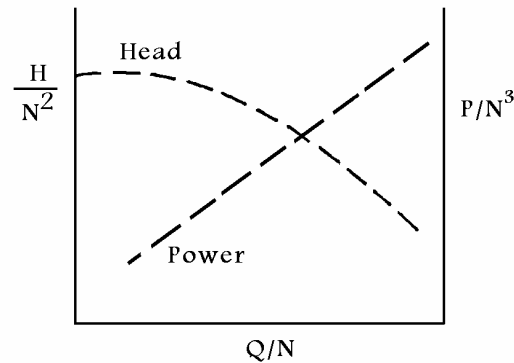
Fig. 4.9 Non-dimensional performance curves

4.2.4.4 Influence of Physical Properties on Performance:

i. Viscosity Effect:

The great majority of pumps handle water, however in chemical industries many pumps handle oil which is more viscous than water, the increase in viscosity increases friction losses and hence decreases the generated head and increases the consumed horsepower, Figure 4.10.
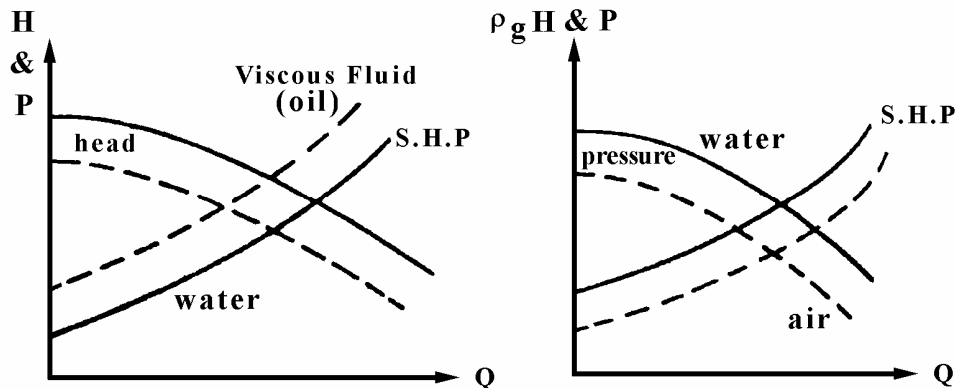
Fig. 4.10 Effect of viscosity and density on pump performance

ii. Density:

Changes in the density of the liquid will not affect the head discharge characteristics but they will affect the pressure generated ($P = \rho g H$), Figure 4.10. In steam power stations, centrifugal pump may have to handle water at higher temperatures, which mean low density, as for feed pump, which required to deliver a specified weight of water per

hour against a stipulated boiler pressure. The power input to the pump increases as the temperature rises, for this reason it is more economical to place the feed heaters on the delivery rather than on the suction side of feed pump.

4.2.5 Some Design Features of Centrifugal Pumps:

There are many design procedures used by the pump manufactures. In practice, every pump manufacturer has his own design procedure. All of them contain the same outlines, here only the general outlines will be considered.

4.2.5.1 Leakage Calculation:

As seen before in section 1.6.3, leakage depends on clearance area and pressure difference between inlet and exit, labyrinth may be used on the impeller hub to reduce leakage.

To calculate the amount of leakage, consider the flow through an orifice;

$$Q = V.A = C_v.A\sqrt{2gh_1} \qquad (4.3)$$

where:
    C_v = velocity coefficient
    A = clearance area
    h_1 = head across the orifice = $0.75 \dfrac{U_2^2 - U_1^2}{2g}$

Leakage will cause efficiency drop and increase the required B.H.P.

4.2.5.2 Disk Friction:

Also as seen in section 1.6.2, the energy dissipated in disk friction depends on speed, disk area, and specific density. The value of losses could be written as following:

$$\text{Disk friction losses} = K.D^2.U^2.\rho \qquad (4.4)$$

where K is a constant.

4.2.5.3 Diffuser Losses:

The kinetic energy of the fluid leaving the impeller should be converted to pressure energy; diffusers are used to achieve this conversion, which is called *static regain*. The loss mechanism and the design of pressure recovery will be treated more in details in Appendix I. Providing the enlargement of the guide channel is small, so that separation of flow does not occur, the pressure losses can be given by:

$$\frac{\Delta P}{\gamma} = \frac{1}{2g}\left(C_3^2 - C_4^2\right) \qquad (0.2 \text{ to } 0.3) \qquad (4.5)$$

where C_3 is the velocity at the inlet of the diffuser and C_4 is the velocity at the exit of the diffuser. C_4 is related to C_3 by continuity equation. The last equation may be written as a function of C_3 only:

$$\frac{\Delta P}{\gamma} = \frac{C_3^2}{2g} \qquad (0.15 \text{ to } 0.25) \qquad (4.6)$$

Now if we introduce the pressure coefficient and consider that $C_3 = C_a$ because α is generally small 15° to 20°; so the ratio of the losses in the diffuser to the total losses could be written:

$$\frac{\Delta H_{loss}}{H} = \frac{1}{2\phi}\left(\frac{C_{3u}}{U}\right)^2 \qquad (0.15 \text{ to } 0.25) \qquad (4.7)$$

C_{3u}/U is proportional to η, so the losses is directly proportional to the pressure coefficient, with the large values of ϕ generally met in engineering applications, it is important to ensure the correct shape of the diffuser.

4.2.5.4 Mechanical Seals:

Mechanical seals are used for shaft sealing in centrifugal pumps. The types employed are mainly standardized according to DIN 24 960. The standard distinguishes two types: type U (unbalanced) for sealing pressures up to 10 bar, and type B (requires a shaft sleeve with balancing step) for sealing pressures up to 50 bar.
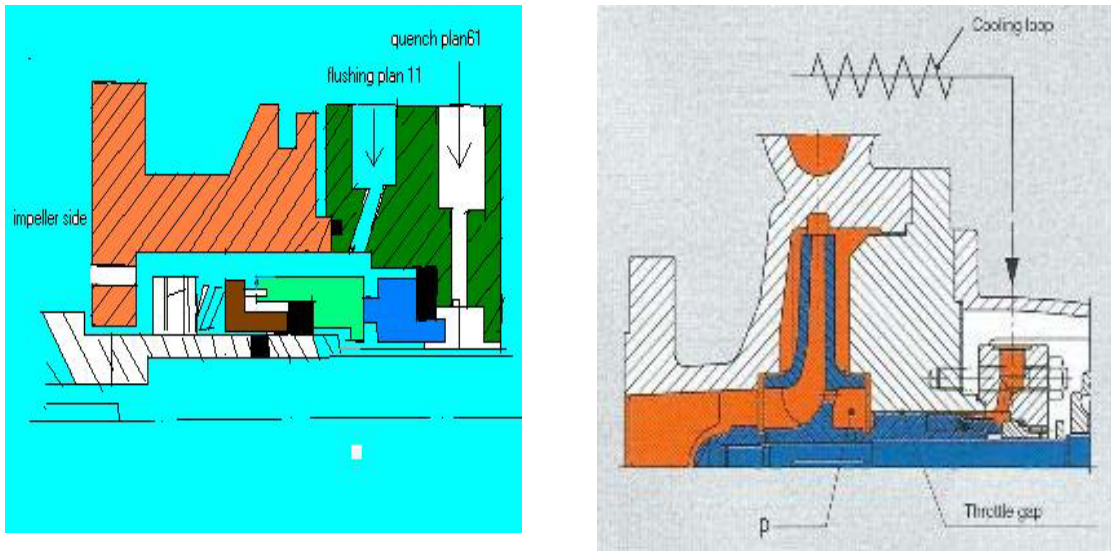
a. Single Seals

For centrifugal pumps with overhung impeller, preference is given to the short standard mechanical seal shown in Figure 4.11 at the top. In
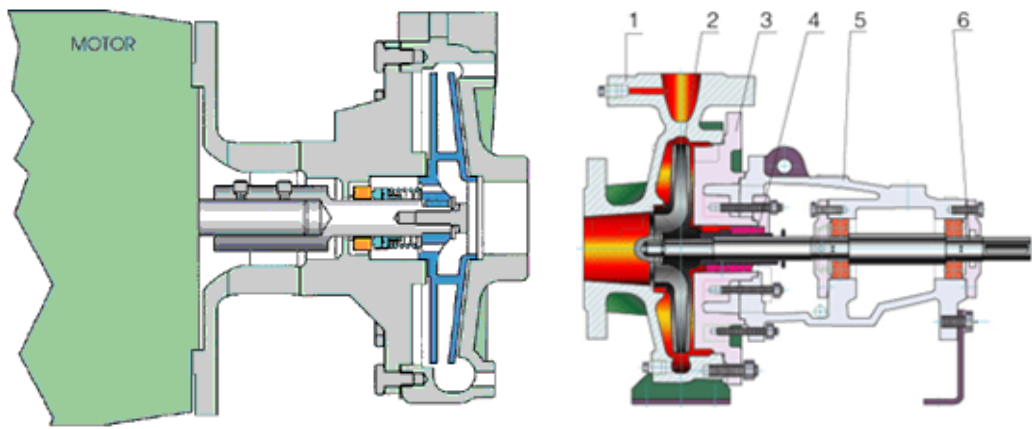
this way the unavoidable combination of multiple seal, stuffing box and pump ring can be achieved without problems, and the disadvantage of short spring displacements entailing narrow fitting tolerances is less important.

Where the impeller is supported at both sides, however, the long standard mechanical seal (Figure 4.11, bottom) finds favor, because bigger spring displacements allow longitudinal tolerances up to + 4 mm, while combinations are less common. If combinations are necessary none the less, then resort must be had to short seals. Adoption of the cartridge type is then advisable, because all pump tolerances can thus be eliminated (Figure 4.12).

Fig. 4.11 Single mechanical seals, type B:
      (top) short variant with flow-inducing ring and stuffing box;
      (bottom) standard variant with stuffing box

Fig. 4.12 Bellows seal, type U, cartridge variant. The seal is located exactly with the assembly washer

In cases where high-viscosity liquids (from about 120 mm^2/s have to be pumped, a large spring or metal bellows must always be employed and the elbows must be relieved of torque transmission by suitable design. Auxiliary measures are often necessary with single seals too (Figure 4.13, Table 4.1).
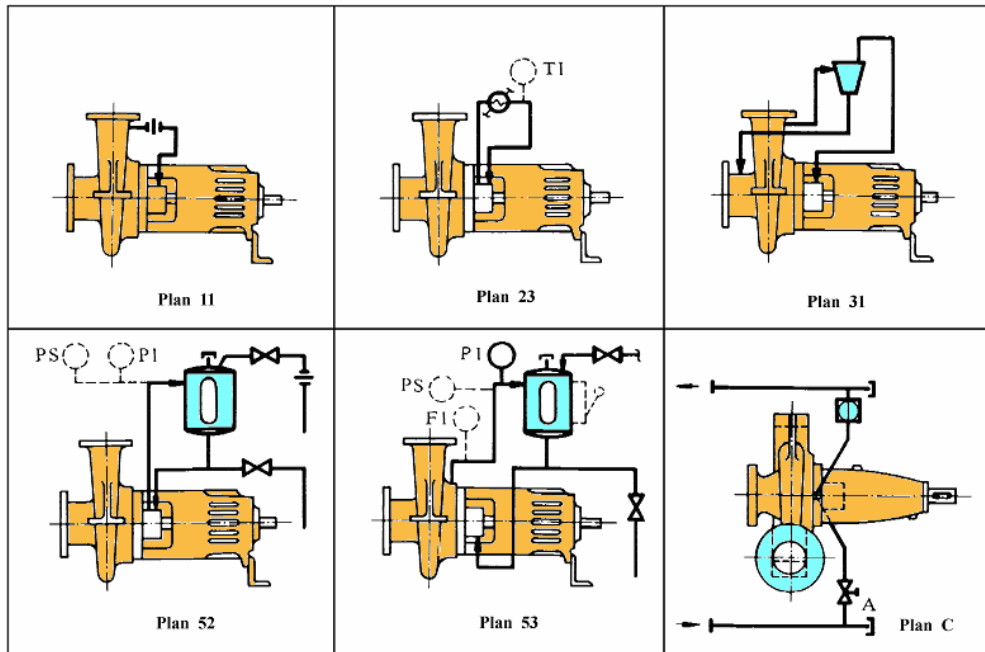
Fig. 4.13 Pipe work for auxiliary circuits to mechanical seals

Table 4.1 Auxiliary measures with single seals

Measure	Purpose
Pumping liquid circulation to *Plan 11*	Leading off frictional heat and flushing out impurities
Cyclone separator to *Plan 31*	Separating solid particles up to 10% Requirement: solids heavier than fluid fluid viscosity $\leq$ 20 mm^2/s
Cooling jacket round shaft seal (neck bush between pump and seal chamber) to *Plan C* Pumping liquid circulation via flow-inducing ring and water/air cooler to *Plan 23*	Lowering the product temperature in the seal chamber to improve the lubricant film on the contact faces, increasing Δt

b. Tandem Seals

The tandem seal, functioning analogously to the single type, is employed where the pumped liquid must be isolated from the atmosphere on account of safety or environmental considerations. In the principal application area, the secondary seal should be able to take over the sealing function in full if the primary seal fails. In subordinate cases, however, the secondary seal serves merely to contain a sealing fluid. As a general rule the secondary seal ought to have a flow-inducing ring to initiate and boost the thermosiphon system usually employed. For pumping liquefied petroleum gas (LPG), intermediate degassing is often provided as well (Figure 4.14). More recent investigations have shown that this can be omitted if a liquid seal at about 35% of the shaft sealing pressure is provided instead of the pressureless seal. It is necessary to establish in situ the exact pressure at which no leakage takes place on the primary seal. In this way, the flaring-off of liquefied petroleum gases with its attendant environmental offence is eliminated. Nevertheless the pressureless seal will remain the commonest method by far, because providing overpressure always entails higher investments and ongoing costs. At all events the seal containers must be tested and satisfy the regulations governing pressure vessels. Non-pressurized sealing fluids do not have to meet any special requirements except good lubricity (low viscosity, wide margin to boiling point and explosion-proof). In principle the sealing fluids described under double seals are applicable.
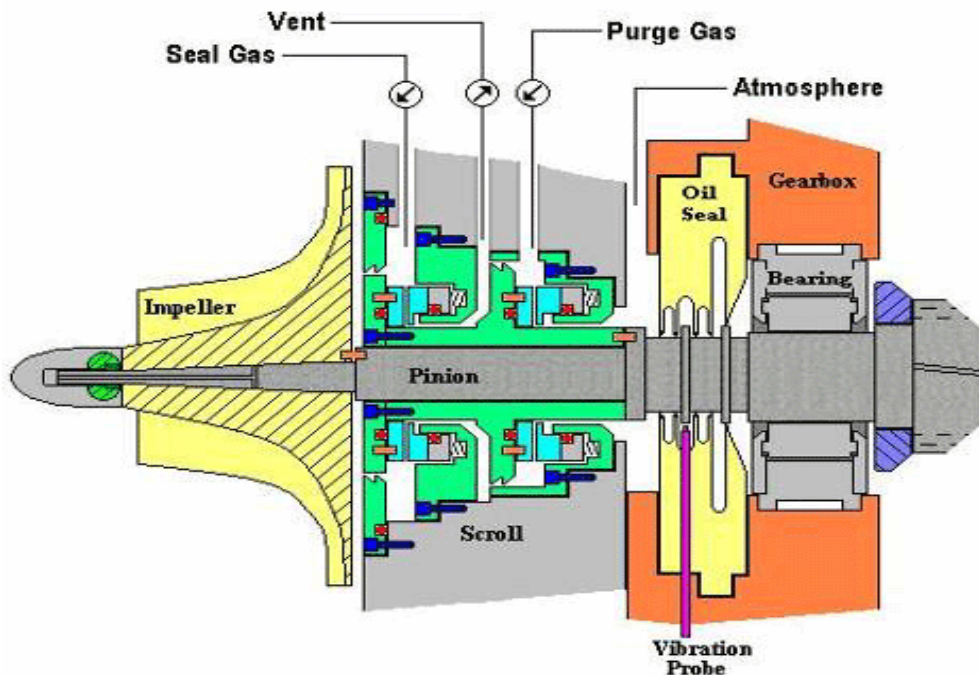

94

Fig. 4.14 Tandem mechanical seal, type B, with degassing chamber and flow-inducing ring at the secondary seal

The auxiliary facilities for the primary seal are largely analogous to those described for single seals. Prime consideration is given to self-circulation in accordance with Plan 11, or to outside jacket cooling as in Plan C (Figure 4.13).

Principle auxiliary systems for the secondary seal are:
External non-pressurized sealing tank as in Plan 52, with and without cooling jacket, or pressurized in accordance with Plan 53 (Figure 4.13).

A half-way solution between single and tandem seals is the single seal with stuffing box, which normally consists of two packing rings and an adjustable gland and is supplied with quenching liquid at a minimum rate of 40 1/h. Gland leakage is adjusted to 0.25 1/h. With this provision the leakage can be led off for certain, and there is an assurance that the function of the main seal can be taken over for a short time in the event of failure, until the installation has run down to a stop.

A special variant repeatedly specified is the dry-running stuffing box, likewise with two packing rings and a non-adjustable gland. To prevent heating at the running point, a diametrical clearance of 0.5 mm must be maintained between packing and shaft sleeve, and the packing rings must be of asbestos-free material like Teflon silk with graphite. Because this kind of auxiliary stuffing box cannot take over the sealing function even for a short time in the event of failure, it must be rejected for technical reasons (Figure 4.11).

c. Double Seals

This term denotes the previously usual combination of two single seals arranged back-to-back. In order to save space, the flexible and moving parts of the single seals may also be combined into one assembly, though this no longer conforms to DIN 24 960 (Figure 4.15).

**Fig. 4.15 Double mechanical seal comprising two single seals, type B
(axially-located seat ring on product side and seal with
flow-inducing ring on atmosphere side)**

In any case recourse is had to double sealing only if all other possibilities are ruled out, as for example where the viscosity of the pumped liquid is too low to assure a stable lubricant film in the sealing clearance, where there is a negative overpressure less than -0.5 bar, where the minimum temperature is not assured or where toxic or otherwise hazardous fluids are to be sealed.

What makes the operation of a double seal so costly is the sealing pressure system demanding constant attention and the need for a suitable sealing liquid. Often though is given to this sealing product, which must be pumpable as well as compatible with the mechanical seal, only when it is too late. Minor problems arise only where process water can be used for sealing, which occurs at the most in wastewater, paper and sugar plants. For chemical, petrochemical and refrigerating plants what matters is that the sealing liquid should have a viscosity between 1 and 12 mm^2/s, with limits of 0.5 to 20 mm^2/s still acceptable. It must not be prone to carbonization and must stand up well to high or low temperatures depending on the duty. Typical products are:

Heat transfer oils (like Mobiltherm 603) for high temperatures.

Refrigeration oil or methyl alcohol for cryogenic pumps.

Sealing pressure systems may be divided roughly into two classes:

Sealing pressure vessel pressurized with nitrogen (up to 10 bar) or pressure transmitter with pulse line from discharge branch to

thermosiphon circuit and refilling arrangements under sealing pressure;

Sealing pressure systems with forced circulation by gear or plunger pump and pressureless refilling.

For the first class, the mechanical seals should be equipped with a pumping system to assist the thermosiphon action. Flow-inducing rings give satisfactory delivery only at a speed of $N = 2900$ rev/min and seal sizes of 40 mm.

4.2.5.5 Bearing Losses:

Bearing losses are calculated after the following formula:

Losses in $HP = \mu\,GU\,/\,75$

where G is the weight of the rotor, U its peripheral velocity at the shaft journal μ is the coefficient of friction (0.0015 for ball bearing, 0.005 for sleeve or plain bearing, and 0.003 for Michell self-aligning bearing).

4.2.5.6 Axial Thrust:

Due to leakage from the impeller tip, Figure 4.16, the fluid with a pressure P_2 will act on the disk, the same pressure will act on the cover. As the disk area is larger than the cover, the resultant will be an axial thrust opposite to the inlet.
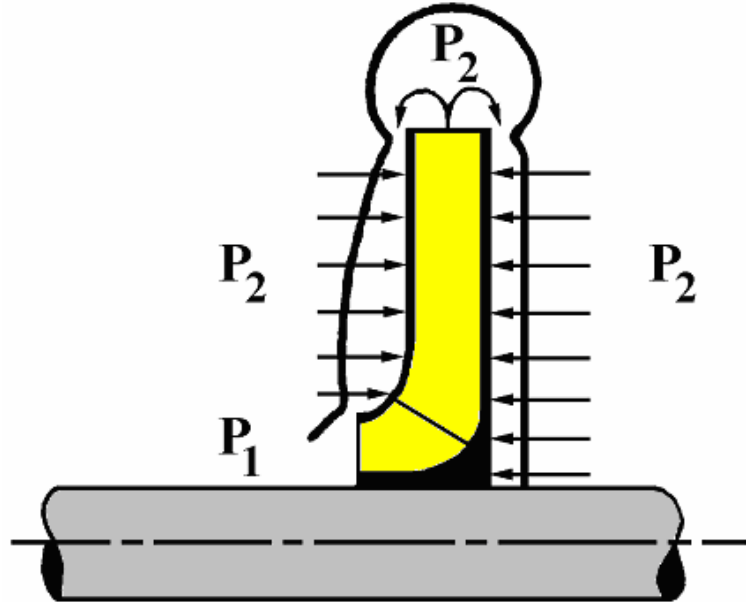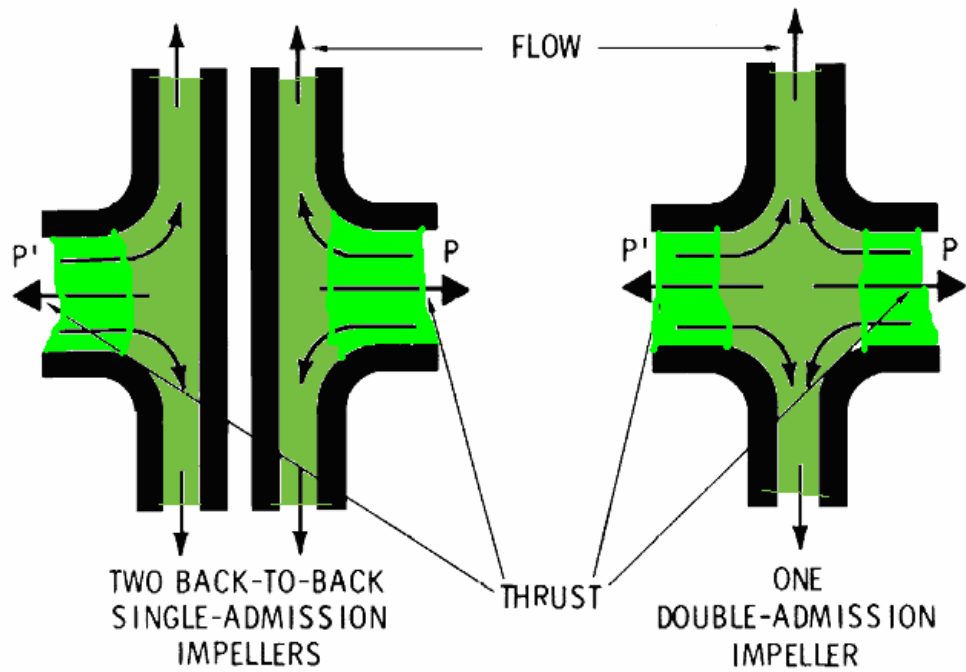
Fig. 4.16 Hydrodynamic pressures

$$\text{Axial Thrust} = \left(P_2 - P_1\right).\frac{\pi}{4}\left(D_1^2 - D_s^2\right) \qquad (4.8)$$
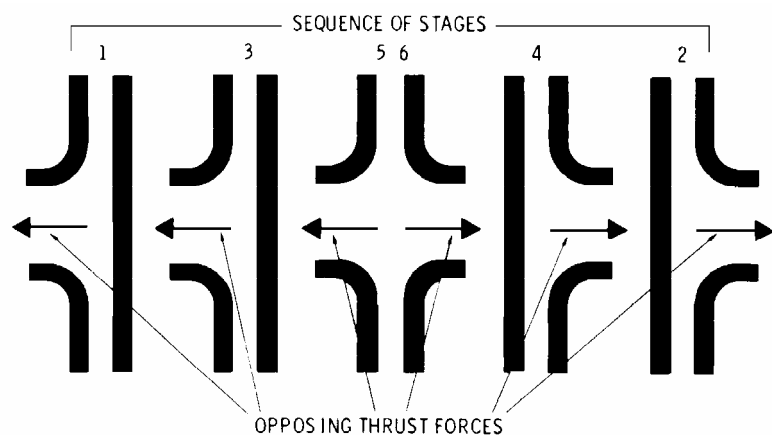
In multistage machines, thrust is very important and should be kept into consideration in the machine design.

Figure 4.17 shows the different methods to eliminate the axial thrust:
a. A double suction impeller type.
b. Balance holes on the disk, but this method may increase the leakage.
c. Balance disk connected to the suction pressure, the disk area depends on the amount of the axial thrust and the pressure difference.
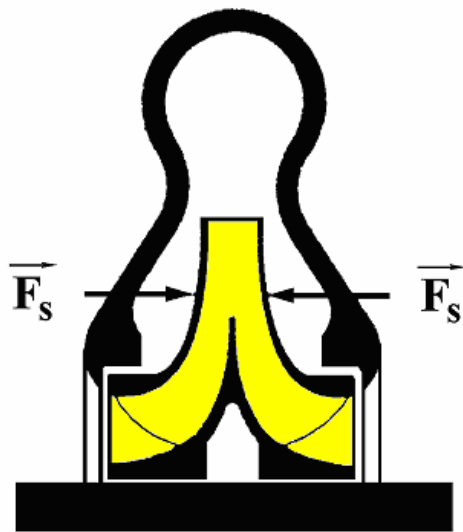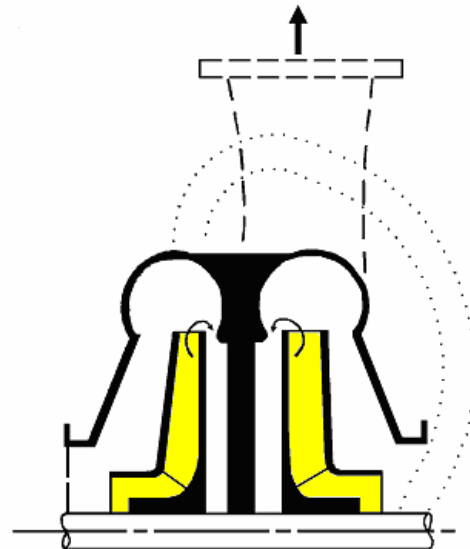
a.1 Natural balancing achievement in single-stage pumps by means of two-back-to-back single-admission types of impellers (left) and one double-admission type of impeller (right)
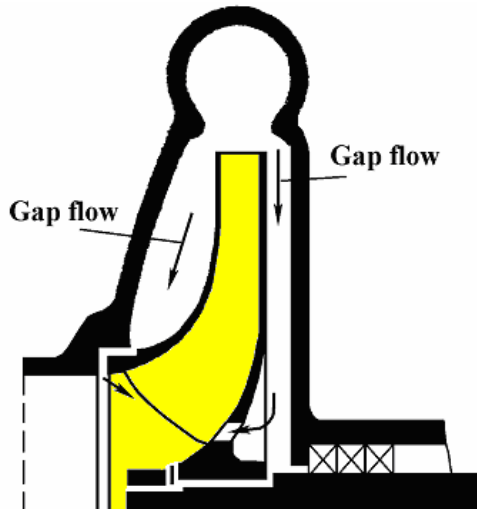
a.2 Natural balancing achievement in a six-stage centrifugal pump, four impellers back-to-back and one double suction
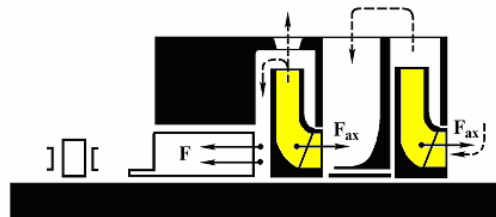
a.3. **Double Suction Impeller Arrangement**

a.4. **Two-Stage Back-to-Back Impeller Arrangement**

b. **Single Stage Centrifugal Pump with Balance Holes**

c. **Balance Device with Balance Piston and Thrust Bearing**

Fig. 4.17 Different ways to eliminate axial thrust

4.2.5.7 Impeller Design:

The first step in designing the impeller is the selection of the speed; the speed relation depends on the driver type mainly; specially for small units. In large units, the speed should be calculated to meet the optimum hydraulic efficiency.

Once the speed is selected, the design procedure could be started.

100

a. Impeller Inlet Dimensions and Angles:

The shaft approximate diameter should be calculated first to calculate the hub diameter, Figure 4.18. The calculation is related to machine design and strength of material science, here a short review will be presented.
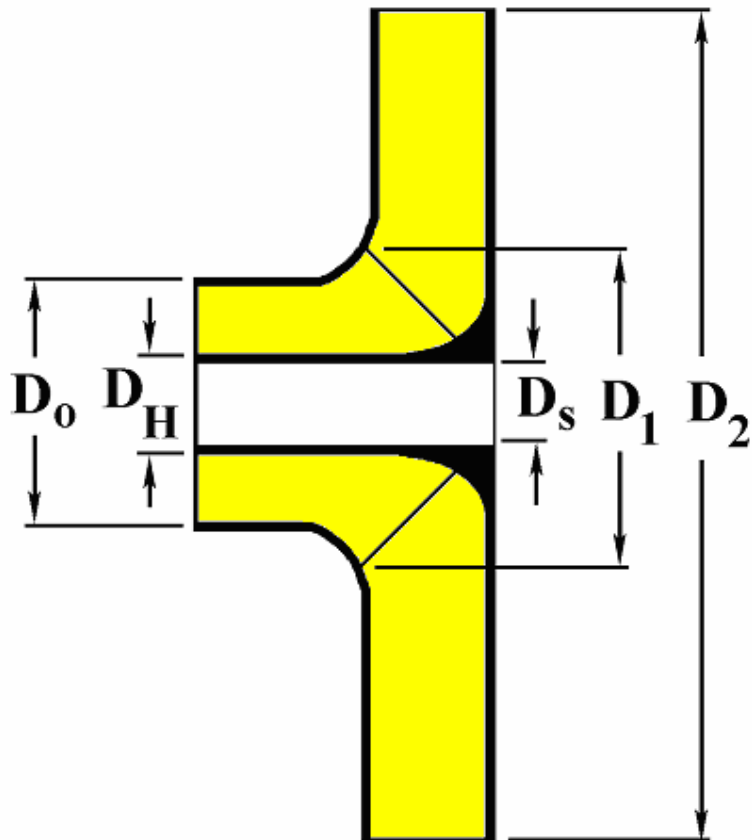
Fig. 4.18 Impeller dimensions

Shaft diameter depends on power transmitted, the calculation of the shear stress, torsional stress should be done, the bending moment is difficult to determine, so an adequate safety margin should be handled after completing the design to be sure that the machine is running at about 15 % away from its critical speeds. As a first approximation shaft diameter could be found by using the following formula:

$$D_s = \sqrt[3]{\frac{16\, T}{\pi S_s}}$$

(4.9)

where T is the torque, S_s is the allowable shear stress. The hub diameter is usually larger than the shaft diameter by 0.8 to 1.5 cm. The inlet velocity to the impeller eye V_o should be kept as low as possible, and slightly higher than that of the suction flange. V_o varies between 3 - 5 m/s.

To obtain the eye diameter D_o the continuity equation may be used,

$$Q/V_o = \frac{\pi}{4}\left(D_o^2 - D_H^2\right) \tag{4.10}$$

where D_H = hub diameter,
Q = total discharge including leakage.

The inlet blade diameter D_1 is usually made about the same as the eye diameter D_o to ensure smooth flow. C_{r1} is usually 10 - 15 % higher than V_o.

$$b_1 = \frac{Q}{\pi D_1 \varepsilon_1 C_{r1}} \tag{4.11}$$

where ε_1 is the contraction ratio which takes into consideration the blade thickness, for preliminary calculations this could be taken equal to 0.8 - 0.9.

α_1 assumed always equal 90° to increase the head
i.e. $\tan(180 - \beta_1) = C_{r1}/U_1$,
$U_1 = \pi.D_1.N/60$

In case of electric motor drive, speeds are constant; 1700 rpm or 3600 rpm.
β_1 usually equals 155° - 170°.

b. Impeller Exit Dimensions and Angles:

As seen before, there is no uniform idea about how to predict the actual velocity diagram due to actual flow inside the impeller channel. Many investigations have been carried on all results show that even (in some cases) the fluid flow does not fill the entire impeller channels. Many formulas had been introduced, all of them are based mainly on factors calculated from tests.

102

A useful formula to calculate the dimensions is the speed factor formula using the following relationship,

$$\phi = U_2 / \sqrt{2gH_{act}} \tag{4.12}$$

where the value of ϕ could include all necessary corrections. ϕ usually varies between 0.9 - 1.2 and taken unity for preliminary calculations.

The outlet vane angle β_2 may be selected within fairly wide limits. The relationship between it and the characteristic curve was discussed in section 4.2.2. Usually backward impeller is used and $\beta_2 = 140° - 170°$ (slightly lower than β_1). C_{r2} is ordinarily made equal or slightly less than C_{r1}, thus b_2 (impeller tip width) could be found by the following relationship:

$$b_2 = \frac{Q}{\pi D_2 . C_{r2} . \varepsilon_2} \tag{4.13}$$

ε_2 is the contraction ratio and taken for preliminary calculations from 0.9 to 0.95.

Blade Shape:

There is no published information concerning the effect of the vane curvature on the flow, this is usually determined by every pump manufacturer according to test results. Generally, there are two methods; the first consists of drawing series of tangential circular arcs, the second uses polar coordinates. The number of blades Z_n is based upon experience, large number of blades provides a complete guidance of the fluid, but friction losses will increase. Many empirical formulas exist to calculate Z_n one of them is Pfleiderer formula;

$$Z_n = 6.5 \frac{D_2 + D_1}{D_2 - D_1} \sin(180 - \beta_n) \tag{4.14}$$

where $\beta_n = (\beta_1 + \beta_2)/2$

Hence, the contraction ratio could be calculated:

$$\varepsilon = \frac{\pi D - t.Z_n}{\pi D} \tag{4.15}$$

where t is the thickness.

NUMERICAL EXAMPLE FOR IMPELLER DESIGN:

It is required to design a pump impeller to develop a head of 50 m and discharge of 10000 lit/min of water. The pump will be direct connected to an electric motor at a speed of 1700 rpm.

SOLUTION:

Water horsepower $= \dfrac{\gamma.Q.H}{75} = \dfrac{1000 \times 10 \times 50}{60 \times 75} = 111 \quad hp$

$$N_s = \frac{1700 \sqrt{10/60}}{(9.81 * 50)^{3/4}} = 6.658 \quad \text{French system}$$

or $\hspace{4cm} = 2245 \quad$ English system

The corresponding overall efficiency $\eta = 0.75$
$\hspace{1cm}$ BHP $= 111/0.75 = 148$ hp
Power = Torque x ω
i.e. Torque $= 148*75*60/(2\pi *1700) = 62$ kp.m

1. Impeller inlet diameter and angles:

Assuming a maximum allowable shear stress of 280 kp/cm^2
i.e. Shaft diameter $= \sqrt[3]{16 \times 62 \times 100 /(\pi \times 280)}$
$\hspace{3cm} = 4.8$ cm

It's difficult to predict the bending moment at this time but to care of it and to keep the critical speed above the running speed, a safety factor of 1.25 will be introduced.
$\hspace{1.5cm}$ i.e. $\quad D_s = 1.25 * 4.8 = 6$ cm
The hub diameter D_H could be 1 cm larger, i.e. $D_H = 7$ cm. V_o, the suction velocity (inlet velocity to the impeller eye) will be taken equal to 4 m/s.

$$Q/V_o = \frac{\pi}{4}\left(D_o^2 - D_H^2\right)$$

i.e. $\quad D_o = \sqrt{\dfrac{4.Q}{\pi.V_o} + D_H^2} = \sqrt{\dfrac{4 \times 10}{\pi \times 4 \times 60} + (0.07)^2} = 24 \quad$ cm

Assume $D_o = D_1$

i.e. $U_1 = \pi.D_1.N/60 = 21.1 \quad$ m/s

C_{r1} should be slightly higher than V_o

$C_{r1} = 4.3$ m/s

** Inlet blade width b_1

$$b_1 = \frac{Q}{\pi.D_1.\varepsilon_1.C_{r1}} = \frac{10}{60 * \pi * 0.9 * 0.24 * 4.3}$$

$$= 0.057 \text{ m}$$

where ε_1 is taken $= 0.9$

** Inlet blade angle β_1

$$\tan^{-1}(180 - \beta_1) = C_{r1}/U_1 \qquad \therefore 180° - \beta_1 = 11°30'$$

i.e. $\qquad\qquad \beta_1 = 168° \ 30'$

2. Impeller exit diameter and angles:

** Outlet diameter D_2

$$U_2 = \pi.D_2.N/60 = \phi.\sqrt{2.g.H} \qquad , \qquad \phi = 1.0$$

then,

$$D_2 = \sqrt{2 \times 9.81 \times 50}.60/(\pi \times 1700)$$

$$= 35.2 \quad \text{cm}$$

$$U_2 = \pi.D_2.N/60 = 31.33 \quad \text{m/s}$$

** Outlet blade width b_2

Assume $C_{r2} = C_{r1}$

$$b_2 = \frac{Q}{\pi.D_2.\varepsilon_2.C_{r2}} = \frac{10}{60 * \pi * 0.351 * 0.9 * 4.3}$$

$$= 0.039 \quad \text{m}$$

$$= 3.9 \quad \text{cm}$$

Assume $\beta_2 = 160°$

$$C_{u2} = U_2 + C_{r2}/\tan \beta_2 = 19.5 \quad \text{m/s}$$

$$H_o = U_2.C_{u2}/g = (31.33)(19.5)/9.81 = 62.28 \quad \text{m}$$

η_{hyd} or $\eta_{overall} = 50/62.28 = 0.8$ (which is not equal to the assumed efficiency and seems to be relatively high).

To reach the assumed efficiency, the theoretical head must be increased. The theoretical head could be increased by means of the following methods:

i. Increasing U_2, assuming higher value of ϕ and hence larger diameter.
ii. Decreasing C_{r2}.
iii. Decreasing β_2.

As first approximation, assume $\beta_2 = 158°$

i.e. $C_{u2} = 20.7$ m/s

        $H_o = 66$ m   and $\eta_{hyd} = 0.756$ (which is suitable)

$$Z_n = 6.5 \frac{D_2 + D_1}{D_2 - D_1} \sin \beta_n = 6.5 \frac{35.2 + 24}{35.2 - 24} \sin 163° = 10$$

i.e. Number of blades = 10 blades.

4.2.6 Centrifugal Pump Types:

4.2.6.1 Fire Pumps:

Usually, single stage type or two stages with double suction. They develop a pressure of 100 psia, and have standard capacities of 500, 750, 1000, and 1500 G.P.M. The efficiency is not particularly important as they are used only occasionally and the flows are not large.

4.2.6.2 Dredge Pumps:

These kind of pumps are usually used to handle fluids containing sand and gravel, so they are made very rugged and simple with large clearances, this generally results in sacrifice in efficiency. Care must be paid to packing box design to prevent sand from getting in it.

4.2.6.3 Slurry Pumps:

These pumps handle liquids containing solid suspended materials, as sand. These solid materials can attack the packing box and cause rapid wear, so they are continuously flushed with clean water. The back shroud

has series of radial ribs to prevent the slurry from packing in back on the impeller.

4.2.6.4 Deep Well Pumps:

Deep well pumps are used in pumping water from deep wells, Figure 4.19. The pump impellers are close to the water surface in the well, and motor is connected through a long transmission shaft. Bearings are spaced along the shaft to prevent excessive vibrations. The outside diameter of the pump must be small to reduce the size of the well. This necessitates the use of small diameter impellers and multi-staging.

Fig. 4.19 Deep-well pump

4.2.6.5 Circulating Pumps:

These pumps operate at particularly constant head and capacity, Figure 4.20. The flow required could be calculated by the following expression:

$$\text{Flow (GPM)} = \frac{W\left(xL + t_1 - t_2\right)}{500\left(T_1 - T_2\right)}$$

where:

W = pounds of steam per hour
t_1 = temperature of steam entering condenser, °F
t_2 = temperature of steam leaving condenser, °F
L = latent heat at condenser pressure, B.T.U.
x = quality of steam entering condenser, percent.
T_1 = circulatory water temperature at inlet, °F
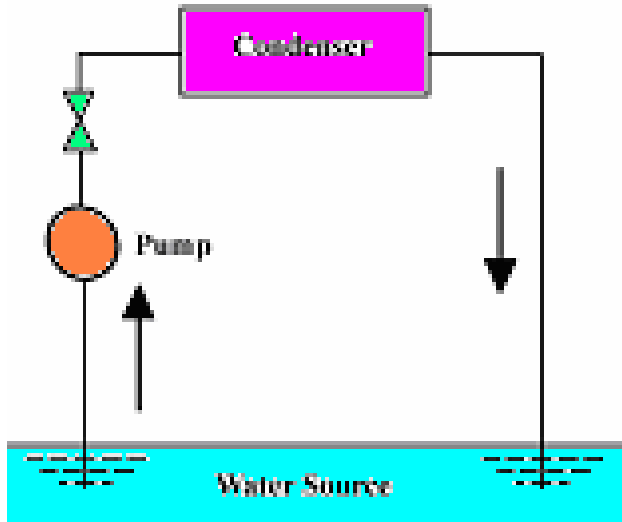T_2 = circulatory water temperature at outlet, °F

Fig. 4.20 Circulating pump arrangement

4.2.6.6 Boiler Feed Pumps:

These pumps are placed before the boiler. Special care must be paid to prevent cavitation hence water temperature could be increased. These pumps are usually driven at a speed of 5500 rpm; the flow through the pump is generally regulated by water level control that throttles the flow to the boiler. A check valve is placed in the discharge line to prevent back flow into the pump.

4.2.6.7 Pumping Liquid/Gas Mixtures:

Whilst centrifugal pumps are primarily used for pumping liquids, the pumping of undissolved gases and vapors cannot be excluded. Air entrainment can occur, for example, with inadequate bellmouth submergence when pumps draw from open chambers. Air can also be drawn in due to leakage between suction pipe flanges, down suction valve spindles and possibly through the pump stuffing box. This air generally cannot be controlled and it is undesirable. In special cases where pumps have to be operated in the cavitation range, the harmful effects of cavitation can sometimes be reduced by injecting air into the pump inlet pipe.

Different conditions apply in process plant. Here the pump is required, from time to time, to pump gases and vapors originating from the process in hand without interrupting operation. Special requirements are set by liquids which are being pumped close to the vapor pressure (condensate, liquid gases etc.). The generation and increase of gas or vapor bubbles from the liquid pumped are to be expected, when large

108

static suction lifts have to be overcome; when several fittings in the suction inlet pipe are arranged in series and cause a severe restriction, or when faulty insulation of the suction pipe allows the liquid pumped to become warmer.

It is therefore important to take into consideration the operational characteristics and the limits of application, of centrifugal pump types when liquid/gas mixtures are pumped. The influence of the mixture on the pump characteristics is a function of the percentage of gas q_{Gs} in the liquid:

$$q_{Gs} = \frac{Q_G}{Q_F} \qquad Q_G = \text{gas flowrate referred to suction conditions}$$

$$Q_F = \text{liquid flowrate}$$

4.3 Axial Pumps (Propeller Pumps):

In this type of pumps the flow is axial, Figure 4.21. The axial pumps are usually used in irrigation purposes. It develops relatively low head with large discharge. It has large specific speed.
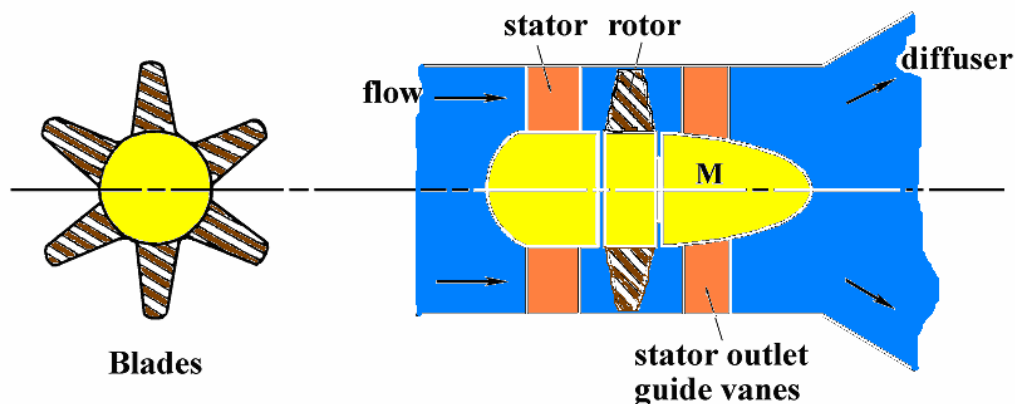

Fig. 4.21 Propeller pump
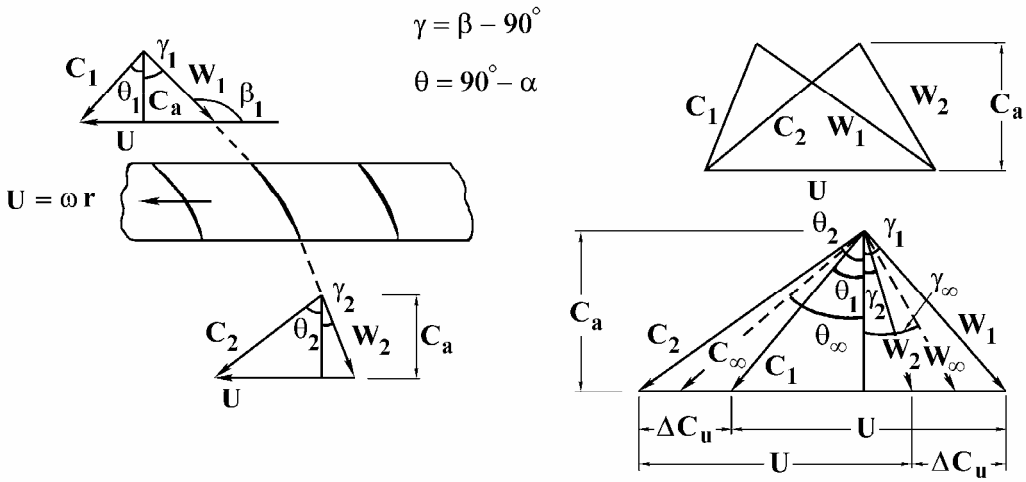
Fig. 4.22 Velocity triangles

From the velocity triangles, Figure 4.22:

$$H_o = \frac{U}{g}(C_2.\cos\alpha_2 - C_1.\cos\alpha_1) = \frac{U.\Delta C_u}{g}$$

$$= \frac{(C_2^2 - C_1^2) + (W_1^2 - W_2^2)}{2g}$$

It is important to note that H is a function of the radius r and to keep H_o constant along the same ratio, ΔC_u must vary as $1/r$.

4.3.1 Degree of Reaction:

As defined before, we shall use the following expression;

$$\sigma = (P_2^* - P_1^*)/(\rho.g.H_o) = (W_1^2 - W_2^2)/2.U.\Delta C_u \qquad (*)$$

From the velocity triangles, Figure 4.22; $W_1^2 - W_2^2 = 2.\Delta C_u.W_{\infty u}$ $^{(**)}$
i.e. $\sigma = W_{\infty u}/U$

(*) This relation could be found by applying Bernoulli's equation on the flow inside the rotor, and then between the inlet and exit as follows;

$$P_2^* - P_1^* = \rho/2(W_1^2 - W_2^2)$$
$$P_3^* - P_2^* = \rho/2(C_2^2 - C_3^2)$$
(**) $W_1^2 - W_2^2 = (C_a^2 + W_{u1}^2) - (C_a^2 + W_{u2}^2)$
$$= (W_{u1} + W_{u2})(W_{u1} - W_{u2}) = 2W_{\infty u}.\Delta C_u$$

110

4.3.2 Pressure and Flow Coefficients:

The definition is as section 2.8 and using the notations of Figure 4.23:

Pressure coefficient $\quad\quad \phi = \left(P_3^* - P_1^*\right)/\rho U^2$

Flow coefficient $\quad\quad\quad \psi = C_a/U$
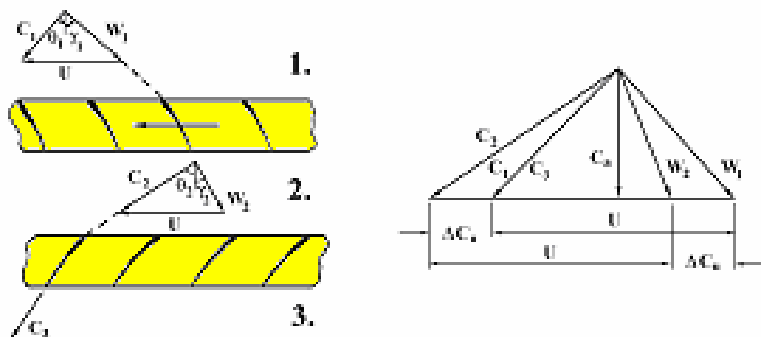
Fig. 4.23 Pressure and flow coefficients

Assume that: $\theta_1 = \theta_3$, $\quad C_1 = C_3$

i.e. $\quad P_3^* - P_1^* = \rho.U.\Delta C_u$

$$\phi = \frac{\Delta C_u}{U} = \frac{C_a}{U}\left(\tan\theta_2 - \tan\theta_1\right)$$

$$= 1 - \frac{C_a}{U}\left(\tan\theta_1 + \tan\gamma_2\right)$$

$$\boxed{\phi = 1 - \psi.\left(\tan\theta_1 + \tan\gamma_2\right)} \tag{4.16}$$

Figure 4.24 shows this relation.
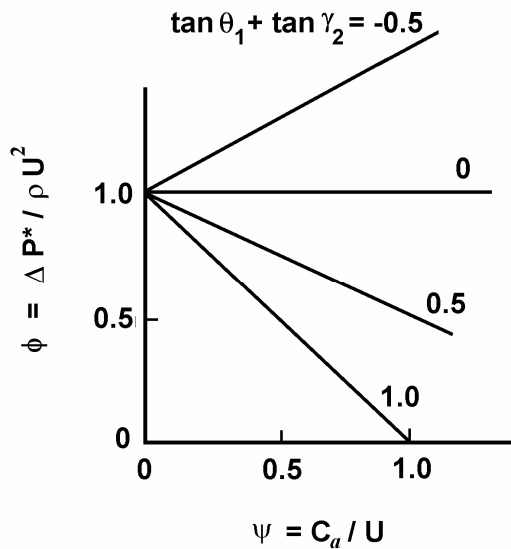
Fig. 4.24 ϕ - ψ **relation**

4.3.3 *Study of Flow Inside the Rotor* (*Radial Equilibrium*):

For the study of the particle motion inside the axial machine, we can consider the particle trajectory as a co-axial cylinder as shown in Figure 4.25. So we can write:

$$C^2 = C_a^2 + C_u^2 \tag{4.17}$$

Generally, when there is a curved trajectory a transversal pressure gradient is produced, and given by the following relation;

$$\frac{\partial P^*}{\partial r} = \rho \frac{C_u^2}{r} \tag{4.18}$$
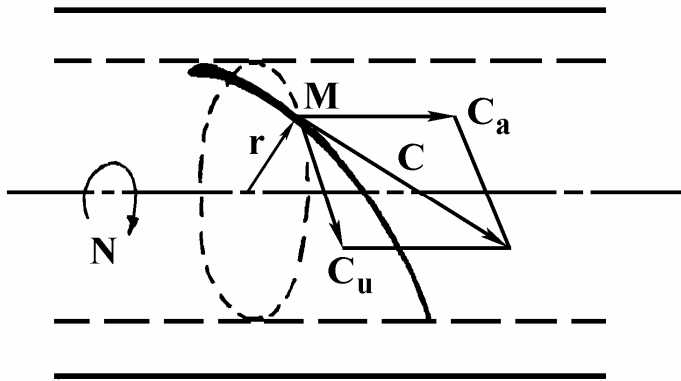
Fig. 4.25 The trajectory of fluid particles could be co-axial cylinder

Consider that H_o is constant for every particle and keep it constant along a plane perpendicular on the axis:

$$H_o = P^* / \gamma + C_a^2 / 2g + C_u^2 / 2g = \text{Constant} \qquad (4.19)$$

or $\quad \dfrac{\partial P^*}{\partial r} + \rho C_a \dfrac{\partial C_a}{\partial r} + \rho C_u \dfrac{\partial C_u}{\partial r} = 0 \qquad (4.20)$

From equations (4.18) and (4.20) we can write the following equation;

$$\dfrac{\partial C_a^2}{\partial r} + \dfrac{\partial C_u^2}{\partial r} + \dfrac{2 C_u^2}{r} = 0 \qquad (4.21)$$

The last equation could also be written on the following forms:

$$\dfrac{\partial C_a^2}{\partial r} + 2 \dfrac{C_u}{r} \cdot \dfrac{\partial}{\partial r} (r.C_u) = 0 \qquad (4.22)$$

$$\dfrac{\partial}{\partial r} (C_a^2) + \dfrac{1}{r^2} \cdot \dfrac{\partial}{\partial r} (r.C_u)^2 = 0 \qquad (4.23)$$

The equations (4.18), (4.20), and (4.21) are not sufficient to determine the flow, another relation could be written as following;

$$C_u = f(r) \qquad (4.24)$$

Integrating equation (4.21)

$$C_a^2 = \text{Constant} - C_u^2 - \int \frac{2 C_u^2}{r} dr \qquad (4.25)$$

In the case of free vortex flow, the last equation could be simplified;

$$C_u.r = \text{Constant}$$

or $\quad \dfrac{\partial C_a^2}{\partial r} = 0 \qquad$ i.e. $\quad C_a = \text{Constant}$

which gives that the axial velocity is constant along the axis.
From the last four equations the flow could be determined to keep $H_o = \text{Constant}$.

4.3.4 Performance of Axial Flow Propeller Pumps:

As seen from Figure 4.26, the head-discharge curve falls steeply with increasing discharge. The working head corresponding to maximum overall efficiency being hardly more than one third of the head corresponding to zero discharge.
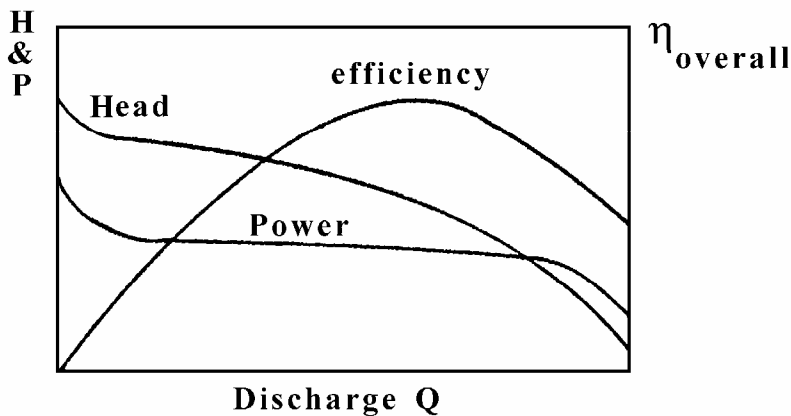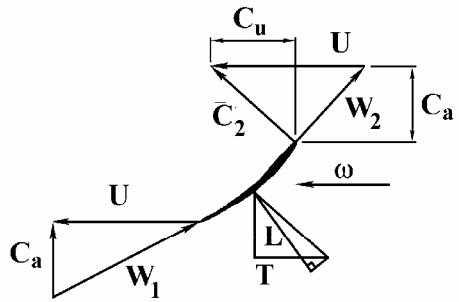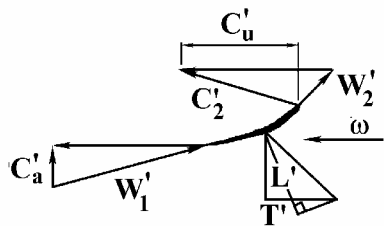
Fig. 4.26 Performance of axial pumps

Also from the power-discharge curve, Figure 4.26, it could be seen that P increases when decreasing Q, which means that the machine consumes more power at part load than at full load. The airfoil theory is particularly helpful in explaining the part load performance of propeller pump. When velocity and force diagrams are plotted both for normal discharge and reduced discharge, Figure 4.27, it's clearly to be seen that reducing the flow is equivalent to bringing the airfoil element into the stalled position.
114

Fig. 4.27 Velocity triangles for axial flow pumps;
 i. at full load,
ii. at part load.

As a consequence, the tangential component of the total dynamic thrust on the element increases from T to T' which helps to account for the trend of the power characteristics. At the same time, C_{u2} increases which result in increasing H. To overcome these tendencies a variable pitch propeller could be used, Figure 4.28.
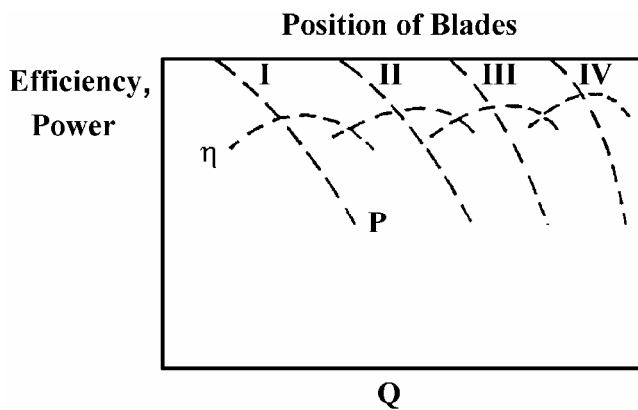
Fig. 4.28 Performance curves for variable pitch axial pump

4.4 Pump Selection and Applications:

For any application, selecting the proper pump type from the available different styles and sizes can be a difficult task.

A practical approach is to make preliminary calculations using the fundamental coefficients ϕ, ψ and N_s. For this preliminary decision, Figure 4.29 is useful in determining the range of size and type with the expected efficiency. Then the second step is to discuss the application with the pump supplier. The key to making the correct pump selection lies in understanding the system in which the pump must operate.

$$N_s = NQ^{1/2}/H^{3/4} \quad [\,N : rpm;\ Q : U.S.\ gpm;\ H : ft\,] \qquad D_{sp} = D\,H^{1/4}/Q^{1/2}\,[\,D : in.;\ H : ft;\ Q : U.S.\ gpm\,]$$
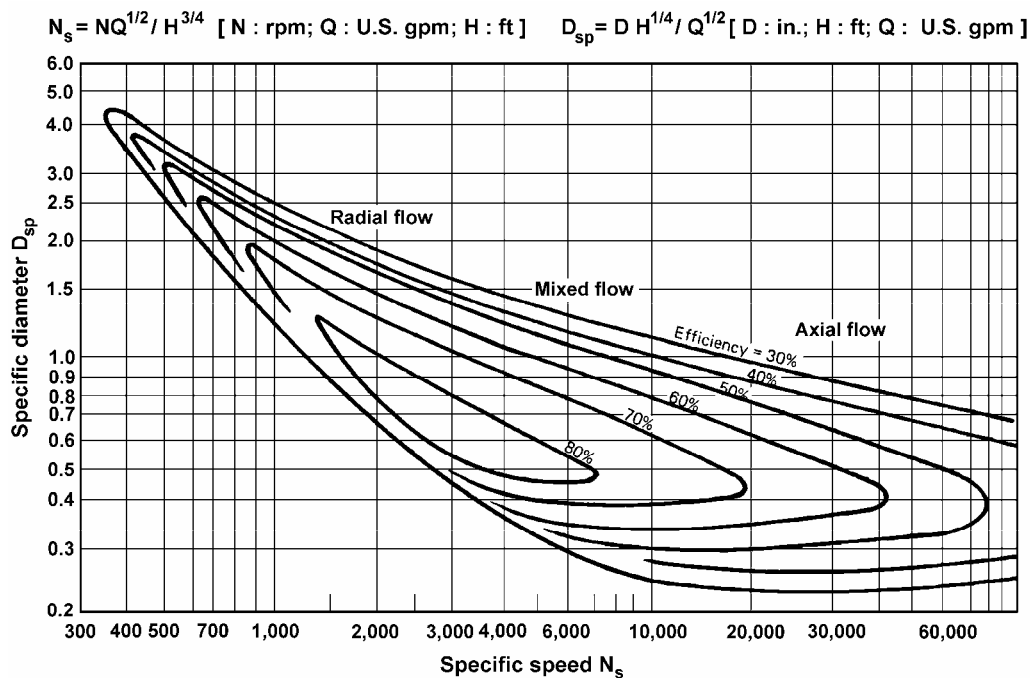
Fig. 4.29   Specific speed chart for the preliminary selection of single speed centrifugal pumps

If the flow is variable, it is better to select a number of individual units in parallel rather than a single unit. This will enable the inspection and maintenance of some units during the part load operation; also this prevents plant shutdowns which would be required with single unit.

4.4.1 Pumps in Parallel:

Usually used when large capacities are required in such the total capacity could be divided to two or more identical units. Figure 4.30 shows two pumps in parallel.

116

Fig. 4.30 Pumps in parallel

4.4.2 Pumps in Series:

When a high head is required, the required total head could be divided on two or more units. These arrangements are called pumps in series as shown in Figure 4.31.

Fig. 4.31 Pumps in series

117

4.4.3 Economic Considerations:

The final selection of the pumping arrangement depends upon an economic study of various alternatives available. Such a study may also dictate the replacement of an existing pump or pumping arrangement, which appears to be giving satisfactory service. An intelligent selection must be based on economic basis.

The unit total cost is made up of the initial purchase price plus the annual charges required to keep them in operation. The annual charges include; insurance, power cost, taxes, interest on the investment, depreciation, and maintenance. For comparison between different bids the initial purchase price should be divided by the expected lifetime in years. The running annual cost except the power cost could be taken as percentage of the initial purchase price.
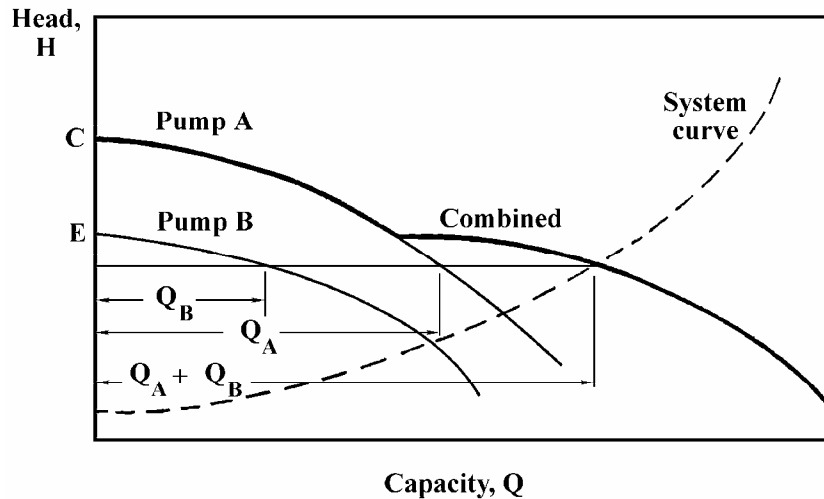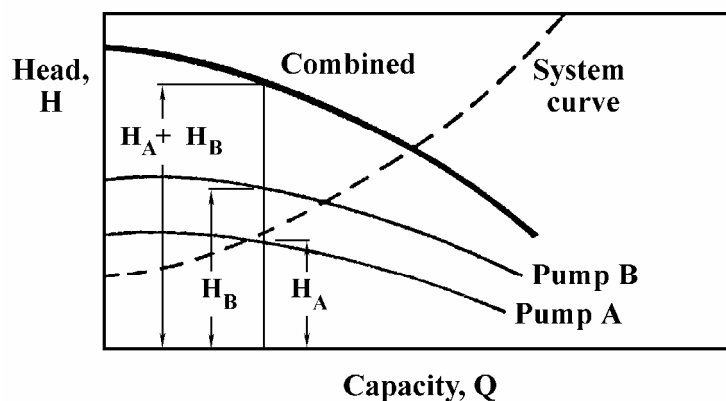
Usually in preparing proposal, a penalty should include this to be added to the bids price in case when the machine fall to operate with the guarantied efficiency.

The penalty values may be found by equating the increased annual power costs for each point to the annual percentage fixed charge times the penalty. This will make the annual charge the same as if the pump had the guarantied efficiency.

4.4.4 Design of the Intake Chamber of Vertical Pumps:

4.4.4.1 General

The intake chamber of a vertically installed pump should be designed so that undisturbed flow to the pump is ensured for each operating condition and for all inlet water levels. This is particularly important for pumps of high specific speed (mixed flow and axial flow pumps), as they are more sensitive to inlet flow conditions than centrifugal pumps.

Operation of the pump will be trouble-free if flow to the pump impeller inlet is swirl-free and if there is a uniform velocity profile across the entire impeller entry area. Additionally, the formation of air entraining vortices in the intake chamber must be prevented, when operating at minimum liquid levels. If these conditions are not met, the performance of the pump, in terms of flow rate and efficiency, will be impaired. In the worst cases, damage due to vibrations and cavitation could occur.

4.4.4.2 Open Intake Chambers

If a single pump is installed in an intake chamber, recommendations for the principal dimensions may be taken from Figure 4.32. A uniform channel cross-sectional area over a length of at least $5D$ upstream of the pump should be provided. The flow velocity in the intake channel should not exceed 0.5 m/s.

The reference dimension "D" corresponds to the outside diameter of the suction bellmouth of vertical SIHI-HAL-BERG pumps.
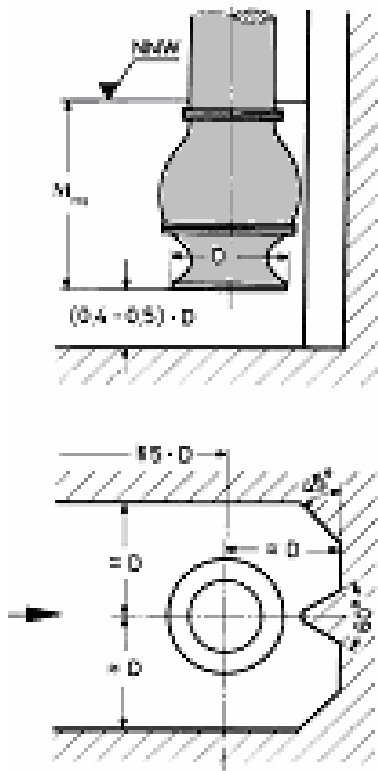
Fig. 4.32

The minimum submergence M_{req} is defined as the distance from the bottom edge of the suction bellmouth to the lowest inlet water level (NNW). For the installation of vertical pumps no general standard values can be given, but must be determined by the pump manufacturer in each individual case; see Figure 4.33.
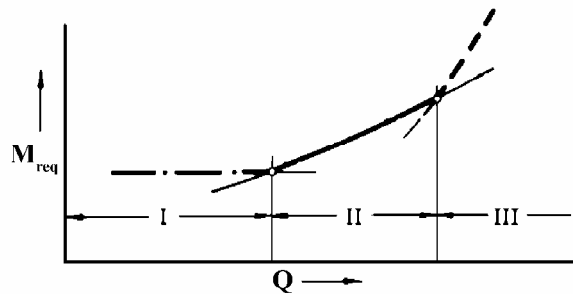
Fig. 4.33 Minimum submergence M$_{req}$ as a function of the flowrate

In the flow range I, the minimum submergence of pumps in wet installations, with bearings which are lubricated by the pumped liquid, ensures that the lowest bearing is lubricated during start-up. Here M_{req} is a function of the mechanical design of the pump.

In the flow range II, the minimum submergence must prevent the formation of air vortices, which could continue into the pump and be interrupted by the impeller vanes causing severe vibrations, which could damage the pump. Here M_{req} is a function of the flow velocity at the pump inlet.

In the flow range III, the pump NPSH (NPSH$_{req}$) is the determining parameter. The minimum submergence must ensure that cavitation does not occur at any point inside the pump. If several pumps have to be installed in one intake chamber, separate bays for the individual pumps provide the best solution, Figure 4.34.
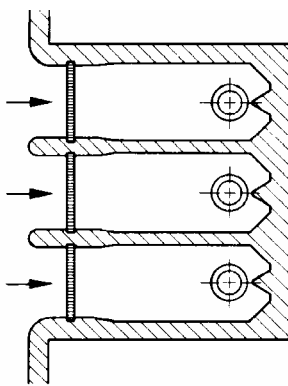
Fig. 4.34

If this solution is not possible, an arrangement similar to Figure 4.35 should be used. The distances quoted should be considered as nominal values. In very difficult cases guide walls (baffles) may have to

be provided (Figure 4.36), the siting of such walls should be agreed with the pump manufacturer.
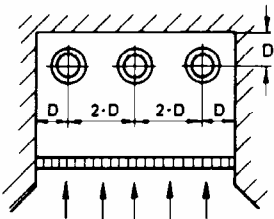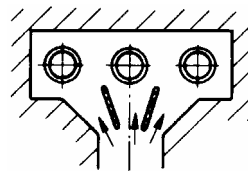
Fig. 4.35   **Fig. 4.36**

Avoidable mistakes in the design of intake chambers

In the arrangements shown in Figures 4.37 and 4.38, the liquid enters at one end of the intake chamber. The flow to the individual pumps is non-uniform and the pumps will affect each other.
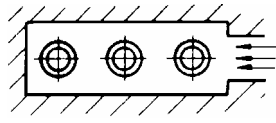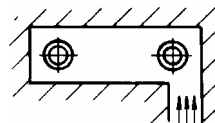
Fig. 4.37   **Fig. 4.38**

Several pumps arranged asymmetrically in one intake chamber.
Sudden expansion or contraction of the supply channel.
The length of supply channel with a uniform cross-sectional area is too short.
Beams, steps or pipes at the bottom of the intake chamber immediately before the pump.
Suction bellmouth too close to the bottom of the suction chamber.
The liquid supplied to the intake chamber is discharged above the level of the pumped liquid.

4.4.4.3 Covered Intake Chambers

If, for any reason, the extended supply channel length ($l \geq 5\,D$), which is required for trouble-free pump operation cannot be provided, an alternative consists in fitting a sloping cover to the intake chamber. These covers are very effective in reducing swirl. Approximate recommendations for the principal dimensions can be taken from Figure

4.38. However, in each case the dimensions should be determined by the pump manufacturer.
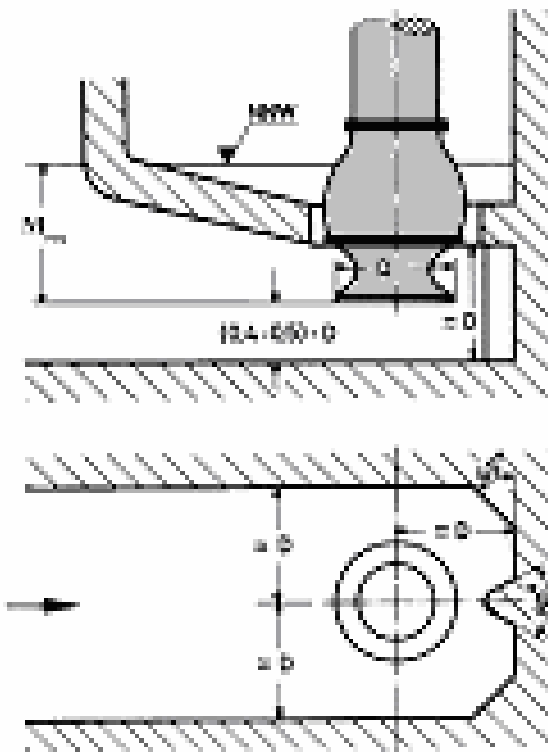
Fig. 4.39

If, due to the particular site conditions, widening of the intake chamber (oblique side walls, sloping bottom ending before the suction bellmouth) cannot be avoided, the use of a cover can provide the necessary acceleration of the inlet flow to achieve a more uniform velocity profile.

4.4.4.4 Inlet Elbows

Minimum dimensions are obtained with inlet elbows, which – similar to the well-known turbine elbows – are shaped as 'accelerating elbows' (Figures 4.40 and 4.41). If the flow velocity is accelerated by a factor of 4 or 5, the length of the elbow (= distance between the inlet area and the center of the pump), $l_{Kr} \approx 4$ x impeller inlet diameter, is sufficient to achieve a uniform velocity distribution at impeller entry.
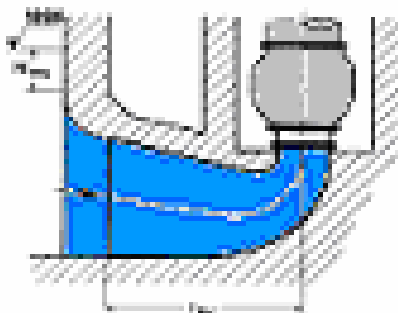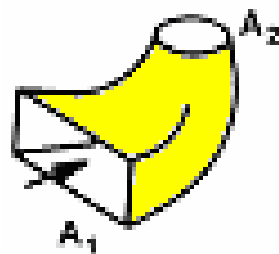
Fig. 4.40

$A_1 = (4 \text{ to } 5) \times A_2$

Fig. 4.41

The inlet cross-sectional area A_1 of the elbow should be large so that the velocity at entry to the elbow is insufficient to allow formation of air entraining vortices or to allow air to be drawn into the pump. In each individual case an economic assessment of the design has to be made to determine whether the higher construction costs of an inlet elbow are acceptable compared to the lower costs of a single intake chamber. The design and construction of an inlet elbow is more complex than that of an intake chamber, and in some cases deeper excavations may be necessary.

4.4.5 Pressure Surges (*Water Hammer*) in Piping Systems

If in systems with long discharge lines, (e.g. in industrial and municipal water supply systems, in refineries and power stations) the pumped fluid is accelerated or decelerated, pressure fluctuations occur owing to the changes in velocity. If these velocity changes occur rapidly, they propagate a pressure surge in the piping system, originating from the point of disturbance; propagation takes place in both directions (direct waves), and these waves are reflected (indirect waves) at points of discontinuity, e.g. changes of the cross-sectional area, pipe branches, control or isolating valves, pumps or reservoirs. The boundary conditions decide whether these reflections cause negative or positive surges. The summation of all direct and indirect waves at a given point at a given time produces the conditions present at this point.

These pressure surges, in addition to the normal working pressure, can lead to excessive pressure and stresses in components of the installation. In severe cases such pressure surges may lead to failure of pipework, of fittings or of the pump casings. The minimum pressure surge may, particularly at the highest point of the installation, reach the vapor pressure of the pumped liquid and cause vaporization leading to separation of the liquid column. The ensuing pressure increase and collision of the separated liquid columns can lead to considerable water

123

hammer. The pressure surges occurring under these conditions can also lead to the failure or collapse of components in the installation.

For the maximum pressure fluctuation, the Joukowski pressure surge formula can be used:

$$\Delta p = \rho . a . \Delta v$$

where
ρ = density of the pumped liquid
a = velocity of wave propagation
Δv = change of velocity of the flow in the pipe

The full pressure fluctuation corresponding to the change of velocity Δv occurs only if the change of velocity Δv takes place during the period:

$$t \le reflection\ time\ t_r = \frac{2l}{a}$$

where l = distance between the nearest discontinuity (point of reflection) and the point of disturbance.

The velocity of wave propagation is mainly a function of:
The density and the modulus of elasticity of the pumped liquid,
The dimensions (diameter, wall thickness) of the pipe and the pipe supports,
The modulus of elasticity of the pipe material.
As a mean value a = 1000 to 1200 m/s can be assumed for water as the liquid and for steel pipes.

An accurate knowledge of the rate of change of velocity Δv is also important in the evaluation of pressure changes, of the maximum surge pressure and of possible oscillations.

As an example, the closing of gate or throttle valves is interesting. It can be seen that the effective throttling process only takes place during the final 10 to 20% of the valve movement. This means that such valves can be closed up to 80 or 90% in an arbitrary time without any dangerous pressure increase occurring. However, the last part of the valve movement has to be effected more slowly depending upon the given parameters of the piping system.

Calculation of pressure surges can be very elaborate in complex networks. It is, however, essential, with long piping systems in particular, to carry out these calculations in order to determine if surge suppression

equipment is necessary. As an approximation the following formula can be used:

$$K = \frac{l\,v}{\sqrt{H}}$$

where l = length of the piping system in m between the point of
disturbance (pump, fittings) and the nearest discontinuity
v = flow velocity in m/s
H = total head in m
A detailed calculation for pressure surges is recommended for cases where $K > 70$.

In unfavorable piping systems, e.g. where there is a high point; the danger of pressure surge may be present at values of $K < 70$. In such cases it is therefore advisable to make a detailed calculation for pressure surges.

4.4.6 Pump Installation:

An actual pump installation is shown in Figure 4.42. The pump is motor driven, direct connected. Two pressure gauges are installed, the first on the pump suction, the second on the pump discharge.
A check valve and gate valve are usually placed on the discharge line, the check valve is used is used to prevent backflow into the pump which might cause it to operate like a turbine. Before the pump will operate, the eye of the impeller must be submerged and the suction line filled. The pump should never be started unless the impeller is filled with liquid because the wearing rings may rub. Some pumps are designed with a self-priming system.
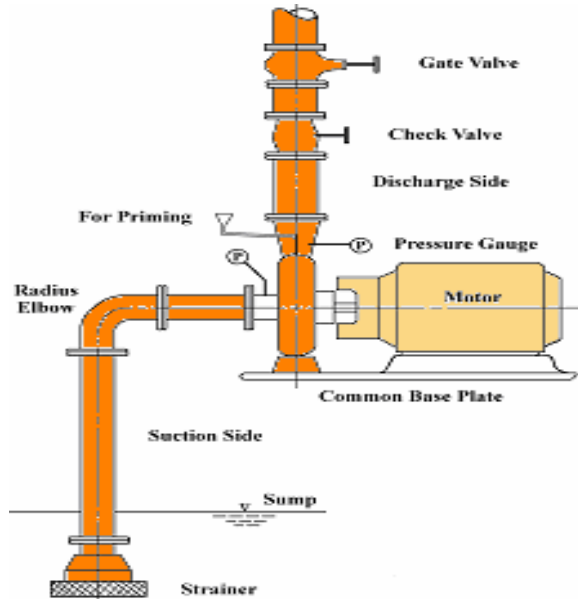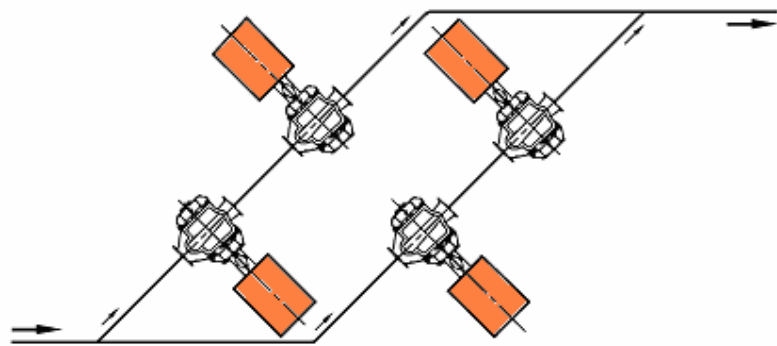
Fig. 4.42 Actual pump installation
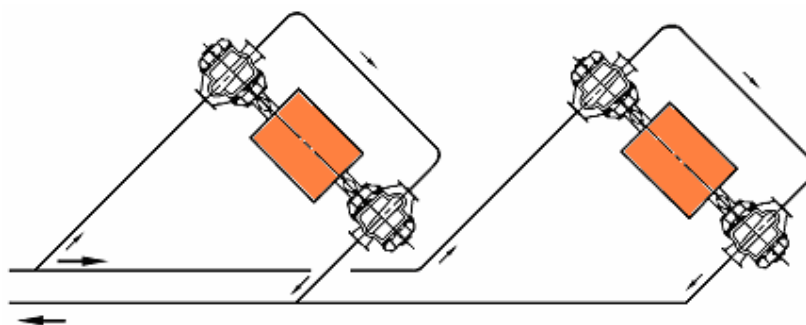
EXAMPLE: (*From Sulzer Technical Review 4/1985*)

Pipeline Layout in the Pumping Station
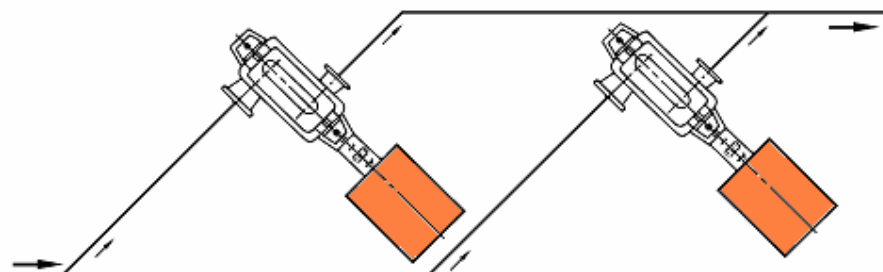
The disposition and the drive of the pumps can have a significant influence of the pipeline layout. Figure 4.43 shows a comparison between several arrangements using multi-stage, horizontal pumps to obtain the same delivery rate. Table 4.2 lists the advantages and disadvantages individually and balances them against each other.

a. Two standard pumps in series (each pump driven by its own individual motor)

b. Two standard pumps in series (each two pumps have one motor in common)

c. Instead of two standard pumps, one special pump per leg

Fig. 4.43 Various pump arrangements

Table 4.2 Advantages and disadvantages of various pipeline layouts (Fig. 4.43)

	Arrangement a	Arrangement b	Arrangement c
Required per pipe leg	4 seals	4 seals	2 seals
	4 bearings	4 bearings	2 bearings
	4 motors	2 motors	2 motors
	comprehensive instrumentation		usual instrumentation
Pipeline layout	good	poor	good
Efficiency	lower	lower	higher
Space requirement	greater	greater	less
Drive (e.g. 2 motors of 1500 kW are more expensive than 1 motor of 3000 kW for same speed (4 pole))	more expensive	less expensive	less expensive
Starting current	Half, when one motor switched on only when previous fully up to speed less expensive		full
Crane (where maximum load is weight of motor)	less expensive	more expensive	more expensive

Evaluation of the Pump Efficiency

The energy penalties for several large pumps are calculated below for the evaluation of the pump efficiency, or for the additional consumption of energy brought about by a lower efficiency. The following basic conditions/assumptions are used for this evaluation.

Efficiency:

Single- and multi-stage, double-flow water transport pumps with the same delivery head and nq = 30 (specific speed) approximately are used as basis. The efficiency rises with increasing impeller size. This is brought about by the fact that greater pumping capacity is achieved by increased impeller diameter, which in turn requires a greater flow cross section and reduce the effect of the boundary layer.

Number of Operation Hours:

It was assumed that the average operating time per year of the pumps amounted to 4000 h. The standby pump; which is not normally functioning was included in the calculation.

1% drop in efficiency:

When, for example, 84 % instead of 85 % efficiency is reached at 500 kW rating, the pump power consumption is 85/84 x 500 = 505.95 kW (i.e. the power loss, which is subject to a penalty, amounts to 5.95 kW).

The price per kWh is obtained from the following factors:

- Price of crude oil   27 US/barrel (June 1985)
- Calorific value of crude oil   43.6 MJ/kg
- Overall efficiency of steam power station   33%
- Crude oil density (Saudi Arabian Oil)   0.85 kg/dm^3
- Currency parity (June '85)   Sfr. 2.60 = 1 US$

Hence, the price is   0.13 Sfr./kWh

Price for 1% full in efficiency:

G = Increased power consumption x operating hours per year x operating life x price per kWh.

Value of penalty:
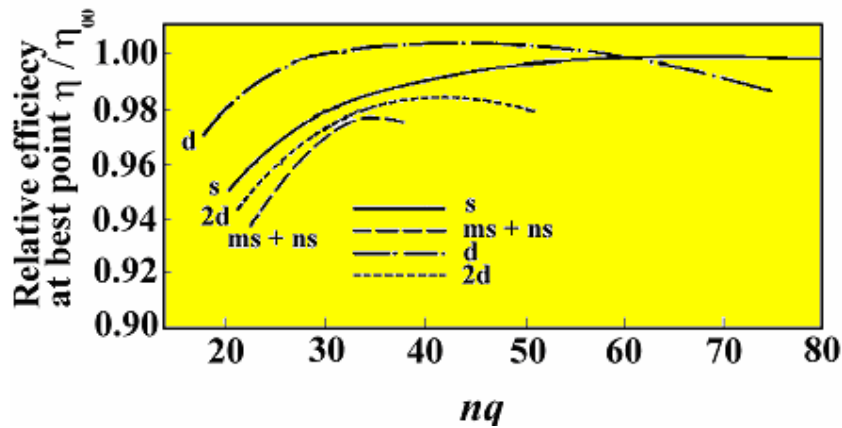
Where 1% efficiency drop occurs, higher operating costs have to be paid during the whole operating life of the pump (n). These costs have to be covered by a suitable financial provision at the time of commissioning. Assuming the rate of interest to be 10% per year (interest multiplication factor $R = 1.1$), a capital provision (C) has to be made at the time of pump commissioning in order to pay for the efficiency loss of the pump per year.

$$K = \frac{G\left(\text{Sfr.}\,/\,\text{pump}\right)}{n.R^n}\left(\frac{R^n - 1}{R - 1}\right)$$

Table 4.3 shows that the power penalty for larger pumps has to be set higher, since such pumps have a longer operating life. Statistics concerning power penalties assuming life. Statistics concerning power penalties assembled over a long period of time from international invitations to tender confirm that nowadays a mean value of Sfr. 3500/kW is assumed (Fig. 4.44). The pumping station designer can influence to some extent the type of pump required by distributing the total delivery flow over several pumps. The highest possible efficiency is to be obtained by suitable choice of specific speed; i.e. by variation of the number of stages, of the number of flows and of the speed of rotation. Figure 4.45 provides information regarding this. It is an illustration of the peak efficiencies for several types of water transport pumps as a function of the specific speed of rotation.

Table 4.3 Calculation of power penalties

Pump ratings, (kW)	500	1000	5000	10 000
Efficiency, (%)	85	86	89	90
Power loss at 1% drop in efficiency, (kW)	5.9	11.8	56.8	112.4
Operating life at 4000 h running per year, (years)	15	16	19	20
1% drop in efficiency equivalent to G (Sfr./pump), (Sfr.)	38 860	82 210	469 900	979 000
Value of penalty (Capital provision at time of commissioning), (Sfr.)	19 705	40 200	206 900	416 750
Price per additional kW consumption, (Sfr./kW)	3311	3400	3642	3700

$nq = n.Q^{1/2}/H^{3/4}$ where Q (m³/s), H (m), and n (min⁻¹)
η/η_{00} = for η = 90% (at nq = 70)
Drawn for H_{stage} = 100 m, impeller diameter 0.5 m
s   single-flow + single-stage + single-volute
ms + ns   single-flow + multi-stage back-to-back arrangement
d   double-flow + single-stage + single-volute
2d   double-flow + two-stage

Fig. 4.44 Hydraulic efficiency as a function of the specific speed and the pump design. Valid for cold water
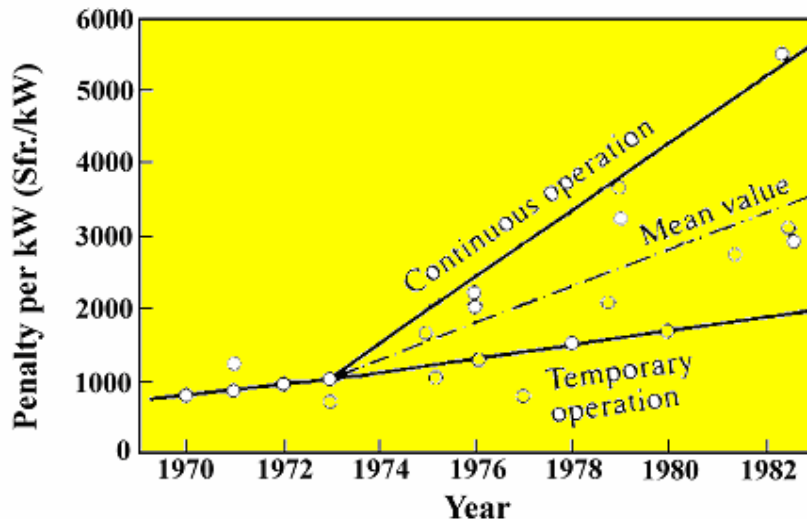
Fig. 4.45 Power penalties, summarized from some international invitations to tender

Polishing the impeller blades has an influence on the efficiency of pipeline pumps. The costs of improving the efficiency are low in comparison with those of the complete plant.

An example of the approximate make-up for a water transport system in Saudi Arabia is given here. It has to be noted that the specific energy requirement in kWh/m^3 is ten times the value applying for a normal European installation, since the pipeline lengths are greater in Saudi Arabia:

- Costs of pipeline	37.0%
- Costs of pumping station and connecting lines/valves	20.5%
- Operating costs of pump for 20 years, with capital provision made at time of commissioning	42.0%
- Costs of pumps and base plates	0.5%
100%	

Evaluation of the drive:

Variable speed drives are often used for water transport pumps, since the consumption of drinking water varies according to the season, month, day and time of day.

Notation:

G	Calculated capital value of power loss for 1 % drop in efficiency (Sfr. per pump)
H	Head (m)
P	Power (kW)
C	Capital (Sfr.)
n	Speed of rotation (min^{-1})
Q	Flow rate (m^3/h, m^3/s)
NPSH$_{plant}$	Total energy level present in front of the impeller
nq	Specific speed, where Q (m^3/s), H (m), and n (min^{-1})

	R	Interest multiplication factor (-)
	S	Suction specific speed, where Q (m^3/s), H (m), and n (min^{-1})
S_{wa}		Safety factor, dependent on the nature of the liquid pumped, circumferential speed, impeller material, size and design of machine
	η	Efficiency (%)
	Index 00	Value referred to pump best point
	Side	Flow rate per hydraulic channel.

4.4.7 Centrifugal Pump Trouble Shooting :

Trouble	Possible Causes	Trouble	Possible Causes
Liquid not delivered	* Pump not Primed. * Air or vapor pocket in suction line. * Pump not up to rated speed. * Wrong rotation. * Impeller or passages clogged.	Pump overloads driver	* Speed too high. * Sp. gravity or viscosity too high. * Packing too tight. * Misalignment. * Total head lower than rated head. * Low voltage or other electrical troubles. * Trouble with engine turbine, gear or other allied equipment.
Failure to deliver rated capacity & pressure	* Available NPSH not sufficient. * Pump not up to rated speed. * Wrong rotation. * Impeller or passages partially plugged. * Wear rings worn or impeller damaged. * Air or gasses in liquid. * Viscosity or sp. gravity not as specified. * Air or vapor pocket in suction line. * Air leak in stuffing box. * Total head greater than head for which pump designed. * Injection of low vapor pressure oil in lantern ring of hot pump.	Pump vibration	* Available NPSH not sufficient. * Air or gases in liquid. * Misalignment. * Wrong bearings. * Damaged rotating element. * Foundation not rigid. * Pump operating below minimum recommended capacity. * Impeller clogged.
Pump loses head after starting	* Air leak in suction line. * Air leak in stuffing box. * Air or gas in liquid.	Stuffing box overheat	* Packing too tight. * Packing not lubricated. * Gland packed. * Incorrect oil level. * Misalignment of piping strain. * Insufficient cooling water.
Bearings overheat or wear rapidly	* Bearings too tight or preload. * Oil rings not functioning. * Suction pressure appreciably different than specified. * Improper lubrication. * Vibration. * Dirties or water in bearings.		
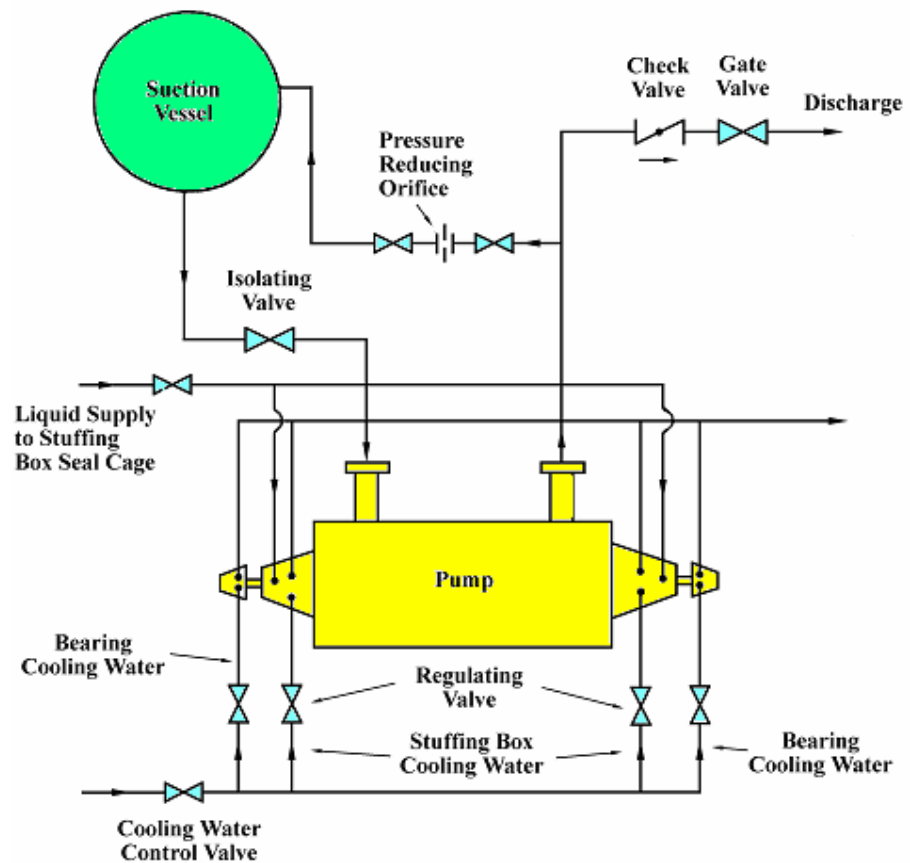
**Fig. 4.46 Example for auxiliary and main piping of a centrifugal pump
(Worthington Corp.)**

Fig. 4.47 Example of centrifugal pump installation in sewage service
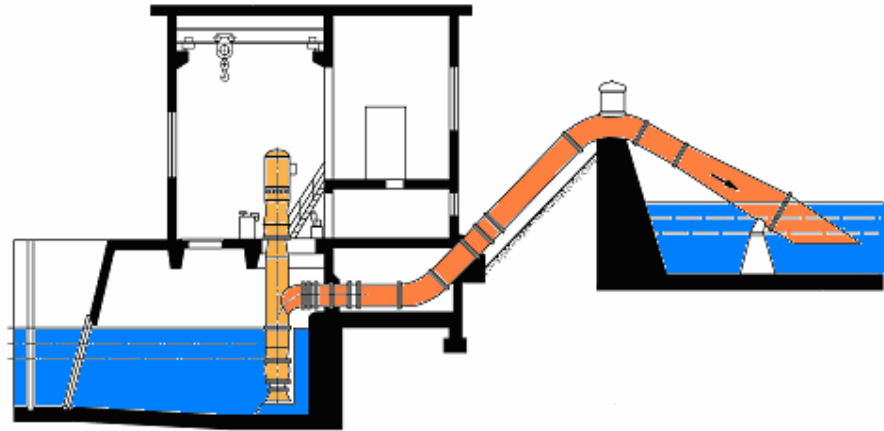
Fig. 4.48 Irrigation system using axial pumps (Courtesy of Sulzer Brothers)
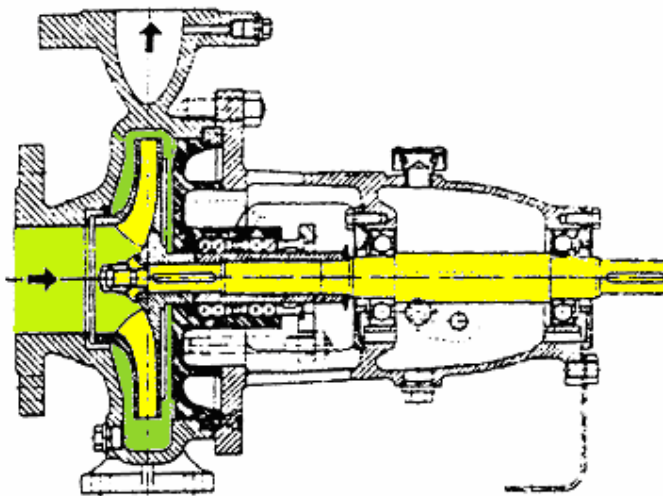
Fig. 4.49 A section in a radial centrifugal pump (Courtesy of Sulzer Brothers)
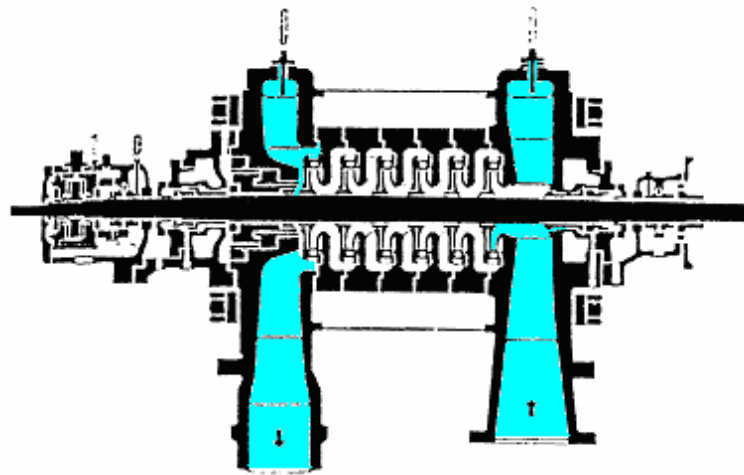
Fig. 4.50 Multistage boiler feed pump (Courtesy of Sulzer Brothers)
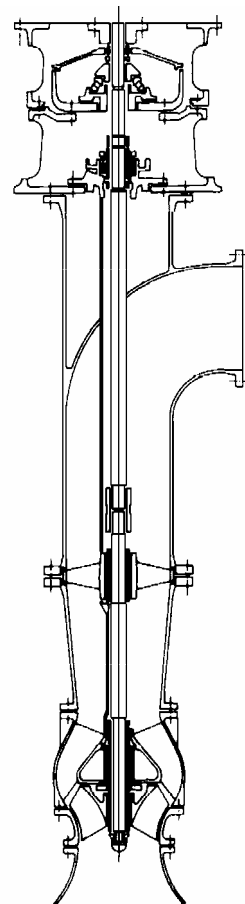
Fig. 4.51 Vertical axial pump (Courtesy of Sulzer Brothers)

Fig. 4.52 Vertical motor-mount type of a centrifugal pump
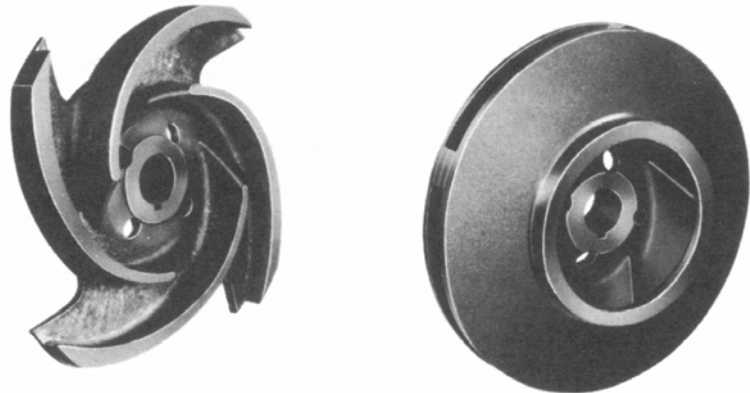
Fig. 4.53 Open–type (left) and enclosed-type (right) impellers
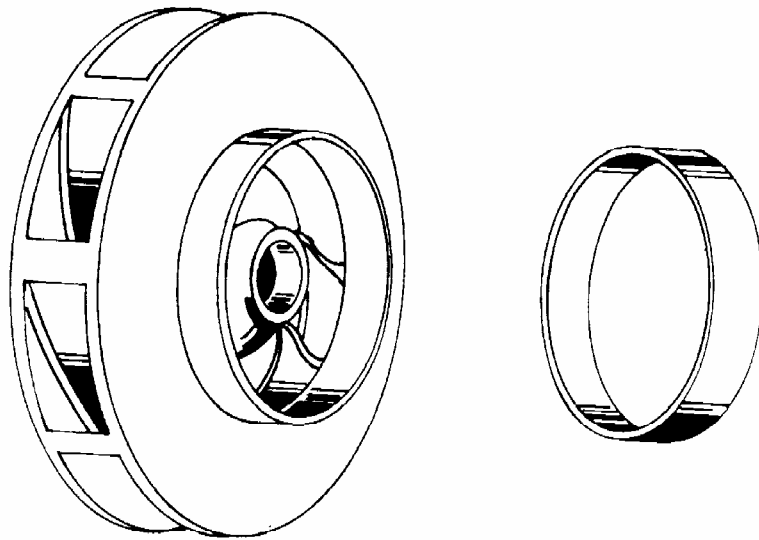
Fig. 4.54 Enclosed-type double-inlet impeller and wearing ring. Some liquids require the impeller be made of special metals, such as chrome, monel, nickel, or a suitable alloy

Fig. 4.55 An offset-volute design of casing (left) and cover (right). The casing is designed for top centerline discharge, self-venting, and back pull-out
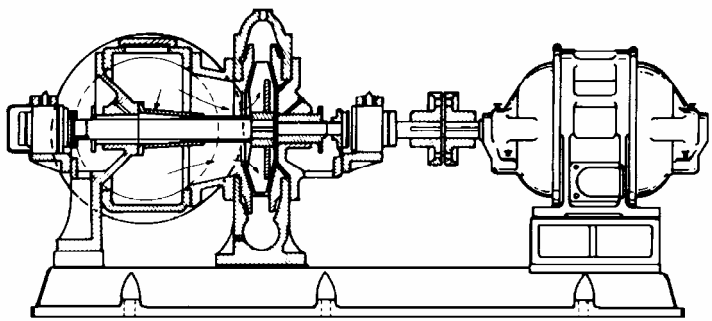
Fig. 4.56 Centrifugal pump and motor placed on a large sub-base and connected by a suitable coupling for direct-drive
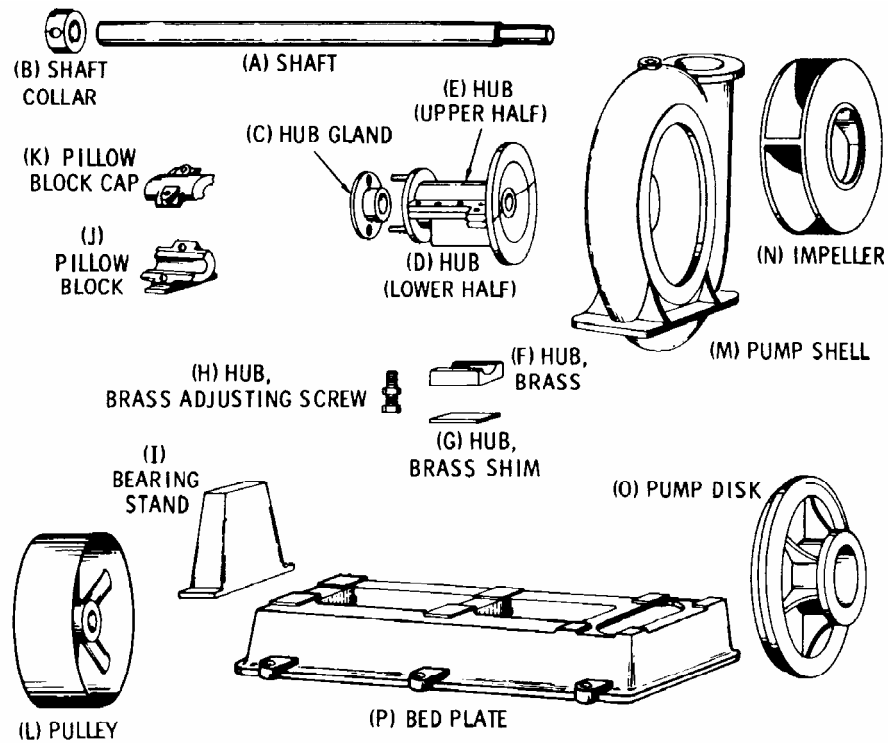
Fig. 4.57   Disassembly view showing parts of a belt-driven single-stage centrifugal pump. The parts shown are: (A) shaft; (B) shaft collar; (C) hub gland; (D) hub (lower half); (E) hub (upper half); (F) hub, brass; (G) hub, brass shim; (H) hub, brass adjusting screw; (I) bearing stand; (J) pillow block; (K) pillow-block cap; (L) pulley; (M) pump shell; (N) impeller; (O) pump disk; (P) bed plate

CHAPTER (V)

INCOMPRESSIBLE FLOW TURBINES

(Hydraulic Turbines)

General Introduction:

Turbines present a part of turbomachines in which the energy transfer process occurs from the fluid to the rotor, in other words, in turbines, the fluid energy is converted to a mechanical energy.

At the inlet of any hydraulic turbine the water speed is relatively small and its energy is essentially a pressure energy. This energy is totally transferred to kinetic energy (in case of impulse turbines) or partially transferred to kinetic energy (in case of reaction turbines).

5.1 Impulse Turbines (*Pelton Wheel*):

5.1.1 General Considerations:

By definition, the *impulse turbine* is a machine in which the total drop in pressure of the fluid takes place in one or more stationary nozzles and there is no change in the pressure of fluid as it flows through the rotating wheel.

Many designs has existed but only one has been currently used named by man who designed it first in California at 1810 Mr. A. Pelton. Usually, Pelton Wheel, Figure 5.1, is used for high head about more than 300 m.
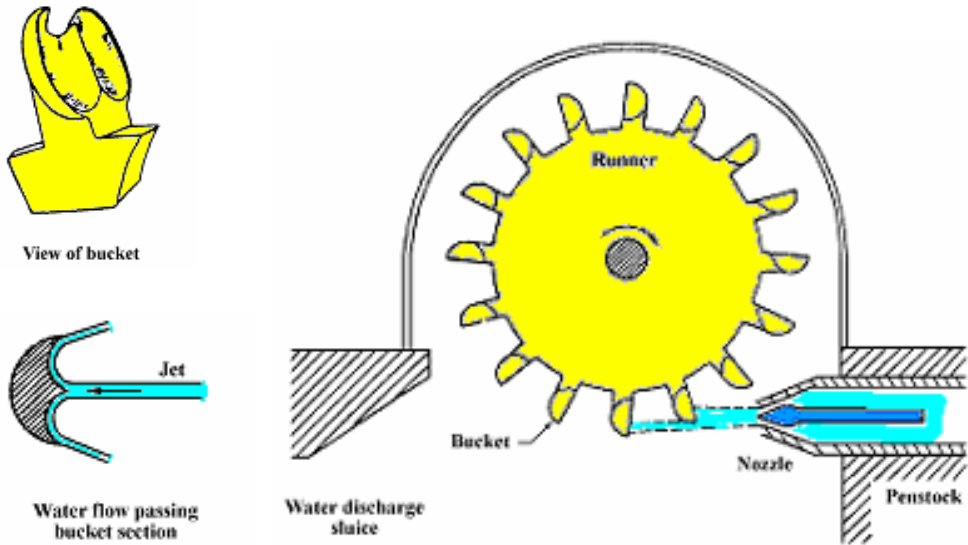
Fig. 5.1 Pelton wheel

Torque and Power Calculation:

From the velocity triangles, Figure 5.2, it can be seen that $W_1 = W_2$, this can be easily shown by applying Bernoulli's equation on relative path. The power as given by equation (1.23);
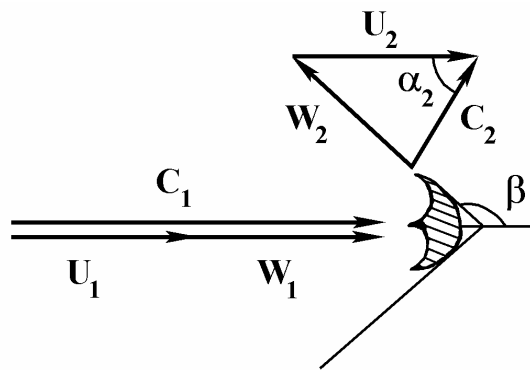
Fig. 5.2 Velocity diagrams

$$Power = \frac{\gamma\, Q}{g}(U_1.C_{u1} - U_2.C_{u2}) \qquad (5.1)$$

$$C_{u1} = C_1 . \cos \alpha_1 = C_1 \tag{5.2}$$

$$C_{u2} = C_2 . \cos \alpha_2 = U_2 - W_2 . \cos(180 - \beta) \tag{5.3}$$

and $\quad W_2 = W_1 = C_1 - U_1 \qquad$ and $\quad U_1 = U_2 = U$

i.e. $\quad C_{u2} = U_2 + (C_1 - U_1) \cos \beta \tag{5.4}$

Substitute the values of C_{u1} and C_{u2} in equation (5.1):

$$Power = \frac{\gamma Q}{g} \{ U [C_1 - (U + (C_1 - U).\cos \beta)] \} \tag{5.5}$$

$$= \frac{\gamma Q}{g} \{ U C_1 (1 - \cos \beta) - U^2 (1 - \cos \beta) \} \tag{5.6}$$

The expression (5.6) shows that the power equal zero when $U = 0$ or when $U = C_1$, the maximum value of the power occurs at some intermediate ratio of U to C_1 which can be found by differentiating and equating to zero;

$$\frac{d(Power)}{dU} = 0 = C_1 (1 - \cos \beta) - 2U (1 - \cos \beta)$$

then; $\qquad U = C_1 / 2$

Thus, the maximum power generated from the Pelton wheel equals:

$$P_{max} = \frac{\gamma Q}{g} (C_1^2 / 4).(1 - \cos \beta)$$

and the corresponding ideal efficiency

$$\eta_{ideal} = \frac{(\gamma Q / g).(C_1^2 / 4).(1 - \cos \beta)}{(\gamma Q / g).(C_1^2 / 2)}$$

$$= \frac{1}{2} (1 - \cos \beta)$$

which equals unity when $\beta = 180°$.

144

Figure 5.3 shows the theoretical efficiency as a function of velocity ratio.
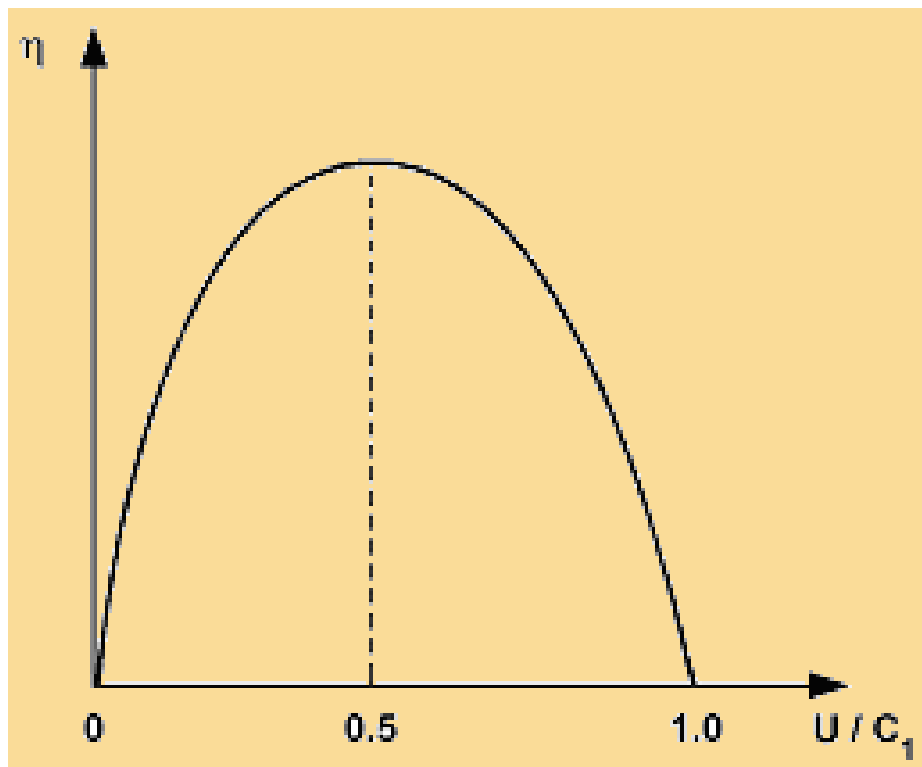
Fig. 5.3 Pelton wheel efficiency versus velocity ratio

Some Practical Considerations:

The ideal equations found previously need to be modified in practice to compensate the friction losses in the nozzle and in the buckets.

a. Nozzle Losses:

The flow rate must vary in proportion to the required power for impulse wheel. This is done by the size of the jet, with a little change in jet velocity as possible. This can be done by varying the position of the needle. The velocity of the jet could be given by the following relation: $C_1 = C_v \sqrt{2gh}$.

At full load, when the nozzle is fully opened, C_v is about 0.98 - 0.99, as the needle is moved to decrease the nozzle opening, the C_v coefficient decreases but it is still above 0.9, Figure 5.4.
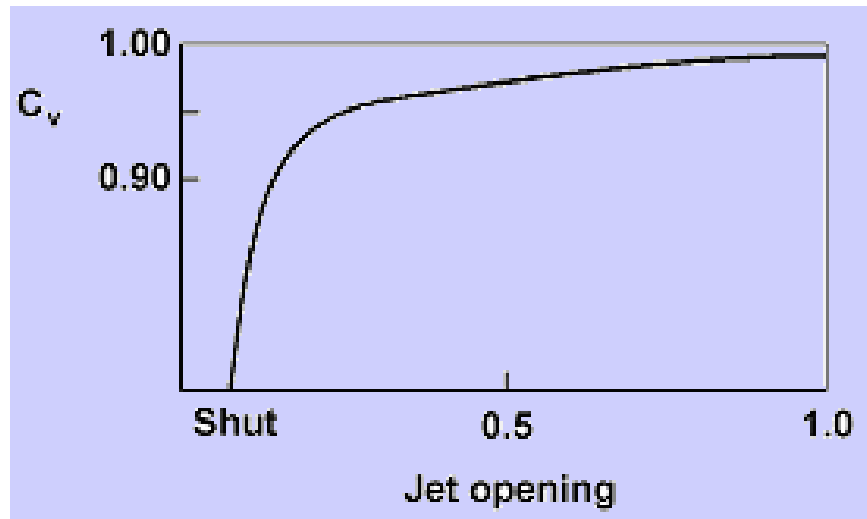
Fig. 5.4 Variation of C$_v$ with jet opening

b. Bucket Losses:

The losses in bucket due to friction could be given in a form of friction coefficient applying to the relative velocity W;

i.e. $W_2 = W_1$ x Constant

and this constant equals $1/\sqrt{1+k}$. Then, the power equation becomes:

$$Power = \frac{\gamma Q}{g}\left\{ U\,C_1(1-\frac{\cos\beta}{\sqrt{1+k}}) - U^2(1-\frac{\cos\beta}{\sqrt{1+k}}) \right\}$$
(5.7)

Usually β equals 165°.

The number of buckets could be determined approximately from the following equation;

$$\text{No. of buckets} = (\frac{D}{2d}+15)$$
(5.8)

where D = diameter of wheel,
               d = jet diameter.

c. Wheel Diameter:

The ratio D/d varies and there is no upper limit, but usually in practice the ratio is varying between 6-12.

146

Speed Regulation:

The speed regulation is done by the needle displacement, Figure 5.5. The speed regulation is necessary to protect the wheel from over speed, which could cause mechanical damage at part load operation. As impulse wheels are usually installed only in high head plants, there is necessary a long pipe and dangerous water hammer would result if there were a rapid reduction of velocity within it. To avoid this, a jet deflector is used, as seen in Figure 5.5. The deflector deviates the jet at part load within the necessary time to regulate the needle position to meet the new load requirement.

a. Full Load
(Normal operation)

b. Part Load
(The deflector deviates the flow)
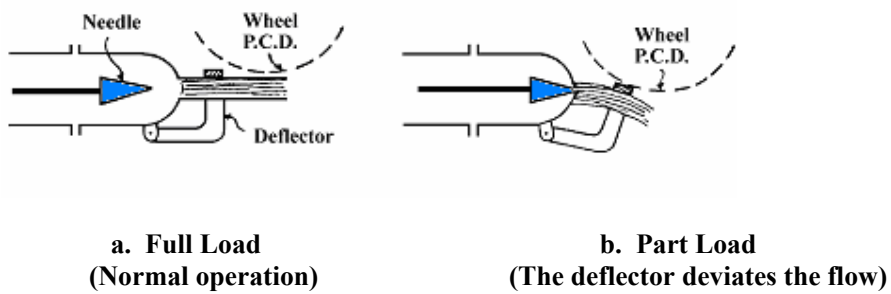
Fig. 5.5 Speed and power regulation

Efficiency and Coefficients:

a. Overall efficiency: $\qquad$ $\eta = B.H.P./W.H.P.$

b. Pressure coefficient: $\qquad$ $\phi = U/\sqrt{2gh}$

c. Specific speed: $\qquad$ $N_s = N\sqrt{B.H.P.}/H^{5/4}$

Performance of Pelton Wheel:

Figures 5.6 to 5.8 show the performance of Pelton wheel at different load operations.
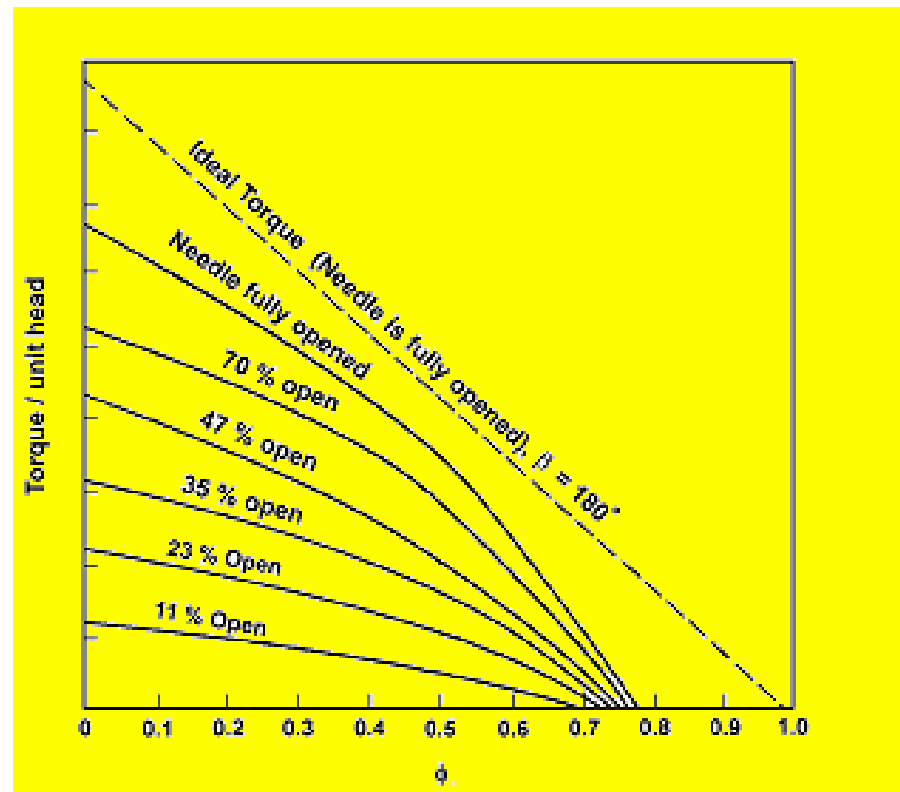
Fig. 5.6 Relation between torque and speed at constant head
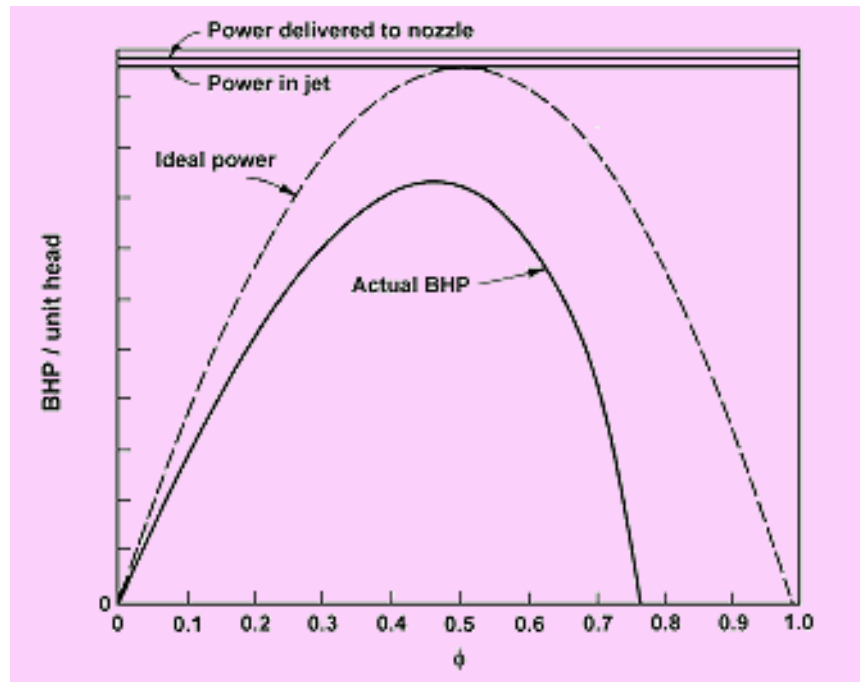
Fig. 5.7 Relation between power and speed at constant head

148
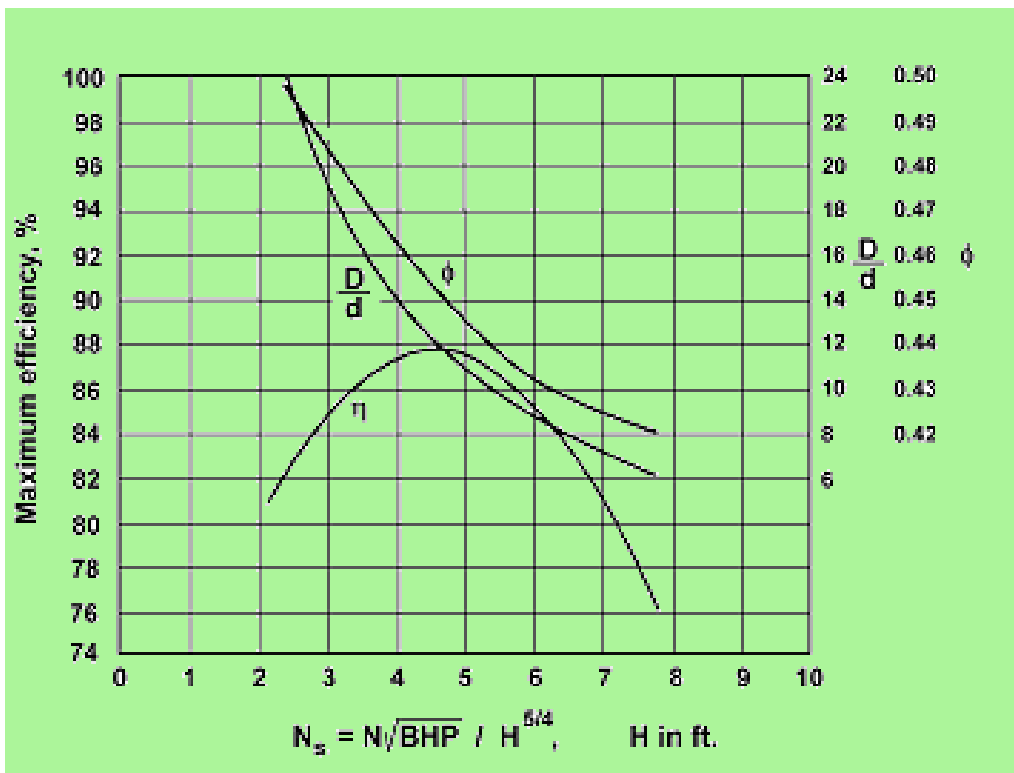
Fig. 5.8 Relation between ϕ, N_s and D/d

5.2 Reaction Turbines:

5.2.1 General:

Reaction turbines are those kind of turbines which the degree of reaction does not equal zero, and the major of pressure drop takes place in the rotating wheel (in impulse turbine, the pressure drop takes place in the nozzle).

The reaction turbines are classified into three types according to the flow direction, Figure 5.9:
  - Radial: (Francis), low specific speed, usually used for medium and high head installations.
  - Mixed: (Francis), medium specific speed, usually used for medium head installations.
  - Axial: high specific speed, usually used for low head installations (Aswan Dam).

a. Radial   b. Mixed   c. Axial
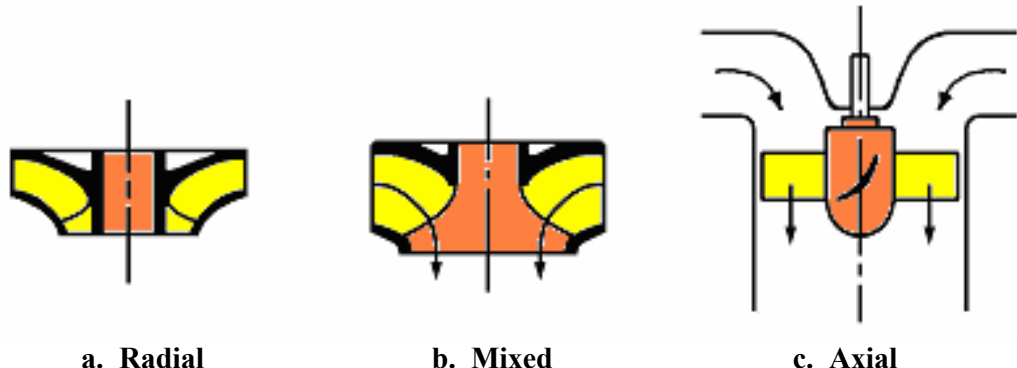
Fig. 5.9 Reaction turbine runners

5.2.2 *Francis Turbines* (*Radial and Mixed*):

5.2.2.1 General:

The Francis turbine original design was inward radial flow with high flow to make a more compact runner, Figures 5.10 - 5.12. The diameter was reduced and the water was discharged with a velocity having an axial component as well as a radial one. This type of runners is called a *mixed flow runner*.
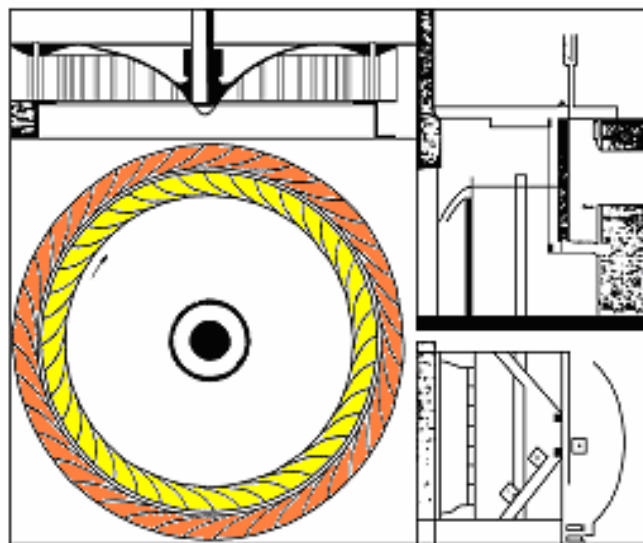
Fig. 5.10 Francis center vent (radial-inward flow) turbine
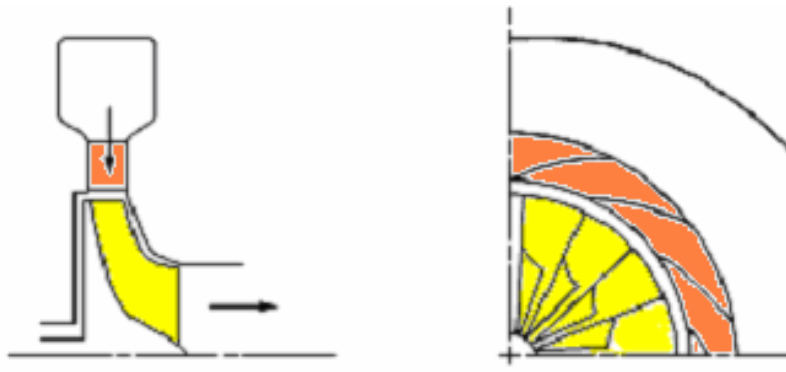
Fig. 5.11 Typical radial inward flow turbine profile
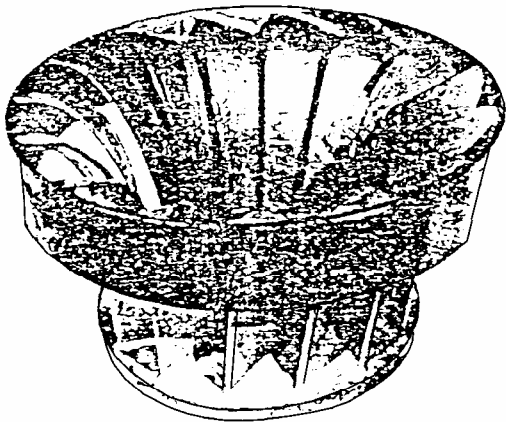
Fig. 5.12 Early Francis type turbine wheel

The inward flow turbine, Figure 5.13, permits a better mechanical construction since the rotor and shaft form a compact unit in the center while the stationary guide vanes are on the outside.

| a. Inward-Flow | b. Outward-Flow |
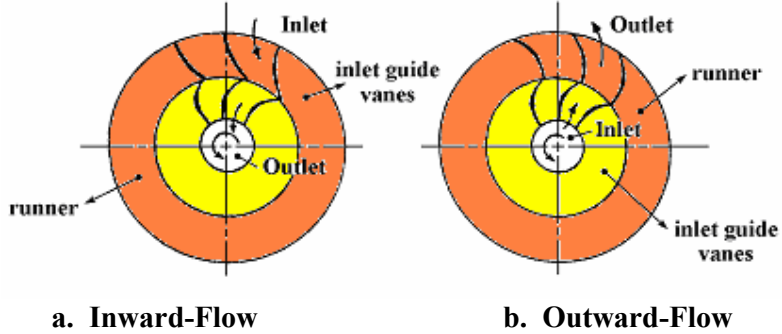
Fig. 5.13 Francis turbine types

5.2.2.2 Power, Efficiency and Coefficients:

Using the notations in Figures 5.14 and 5.15, the following expressions could be written:

$$Power = \frac{\gamma\, Q}{g}(U_1.C_{u1} - U_2.C_{u2})$$

$$\phi : \text{Pressure coefficient} = U_1 / \sqrt{2\,g\,h}$$

$$\psi : \text{Flow coefficient} \quad = C_{r1} / \sqrt{2\,g\,h}$$

$$N_s = N\sqrt{B.H.P.} / H^{5/4}$$

$$\eta_{hyd.} = H_o / H_{available}$$

$$\eta_{mech.} = B.H.P. / (\gamma\,Q\,H_o\,/\,Const.) = H / H_o$$

$$\eta_{over.} = \eta_{hyd.}.\eta_{mech.} = (H_o / H_{av.})(B.H.P. / (\gamma\,Q\,H_o\,/\,Const.))$$

$$\qquad = B.H.P. / (\gamma\,Q\,H_{av.}\,/\,Const.) = B.H.P. / W.H.P.$$

For ideal case where $\eta_{mech.} = 1$, the hydraulic efficiency equals the overall efficiency.

Discharge $Q = B_1 .\pi\, D_1 C_{r1}$
$$\qquad\qquad = B_2 .\pi\, D_2 C_{r2}$$

152
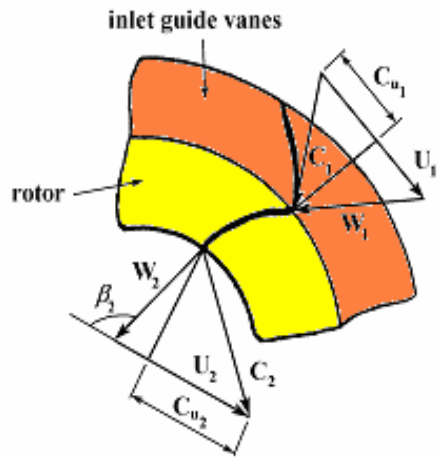
Fig. 5.14 Velocity triangles (inward turbine)
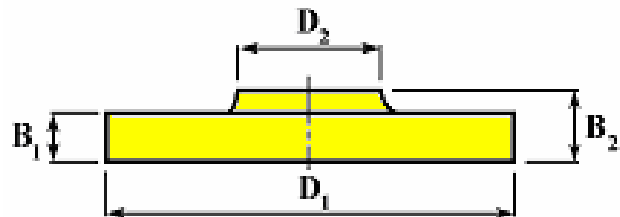
Fig. 5.15 Runner dimensions

5.2.2.3 Head Delivered by Turbine and Draft Tube:

To enable the turbine to be set above the water level, Figure 5.16, a kind of diffuser is provided and connected between the water exit and the tail race level. This is called a *draft tube*.

A partial vacuum is produced at the upper end of the draft tube, which compensates for the height at which the turbine runner is set within certain limits. The turbine rotor could be set at different elevations without altering the available head.

Another function to draft tube is to reduce the exit velocity from the turbine in such a way that the kinetic energy rejected in tail race could be reduced.
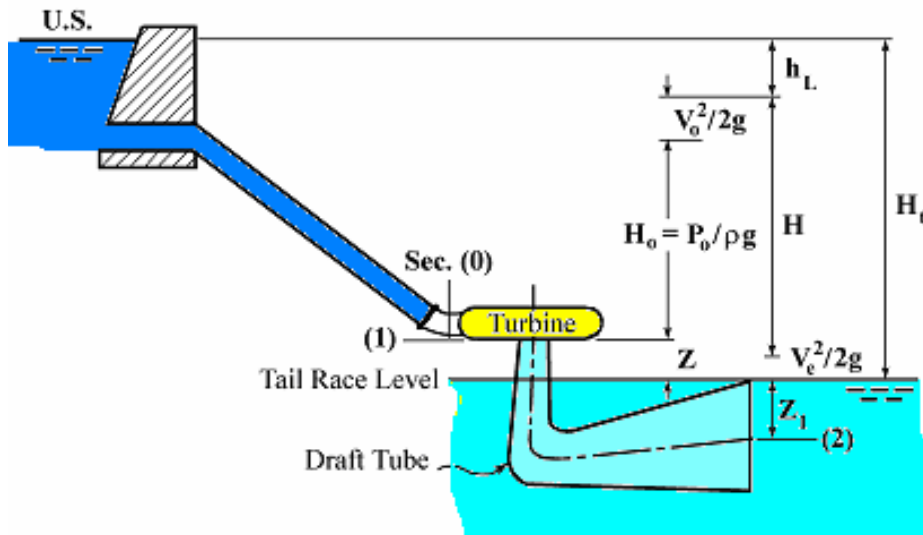
Fig. 5.16 Schematic diagram of reaction turbine installation

H_t = the geometric difference between the upstream and the downstream.

H_1 = the losses in the tunnel between the turbine and the U.S.

$V_e^2/2g$ = kinetic energy rejected in the tail race where V_e is the water exit velocity.

$V_o^2/2g$ = kinetic energy at inlet.

Applying energy equation (Bernoulli's) between points 1 and 2 (the turbine exit and the draft tube exit);

$$\frac{P_1}{\gamma} + \frac{V_1^2}{2g} + Z = \frac{P_2}{\gamma} + \frac{V_2^2}{2g} - Z_1 + h_L$$

but $\quad \dfrac{P_2}{\gamma} - Z_1 = \dfrac{P_a}{\gamma}$

i.e. $\quad \dfrac{P_1}{\gamma} = \dfrac{P_a}{\gamma} - Z - \dfrac{V_1^2}{2g} + (h_L + \dfrac{V_e^2}{2g})$

The term $(h_L + \dfrac{V_e^2}{2g})$ represents the tail losses; h_L represents the hydraulic losses due to friction and enlargement and $\dfrac{V_e^2}{2g}$ represents the losses due to the kinetic energy rejected in the tail race.

154

The losses could be presented as follows:

$$H_L = (h_L + \frac{V_e^2}{2g})$$

$$= K' \frac{(V_1 - V_e)^2}{2g} + \frac{V_e^2}{2g}$$

$$= K' \left(1 - \frac{A_1}{A_2}\right)^2 . \frac{V_1^2}{2g} + \frac{V_e^2}{2g}$$

$$= \left[K' \left(1 - \frac{A_1}{A_2}\right)^2 + \left(\frac{A_1}{A_2}\right)^2 \right] \frac{V_1^2}{2g}$$

$$= K . \frac{V_1^2}{2g}$$

i.e. $\quad H_L = K . \frac{V_1^2}{2g}$

The absolute pressure head at point 1 (turbine exit) could be presented as follows:

$$\frac{P_1}{\gamma} = \frac{P_a}{\gamma} - Z - (1 - K) . \frac{V_1^2}{2g}$$

When K equals zero, there will be no energy losses and hence the efficiency of the draft tube could be written as;

$$\eta_{D.T.} = 1 - K$$

The theoretical regain in head in draft tube due to kinetic energy h_g, Figure 5.17, is;

$$h_g = \left(V_1^2 - V_e^2\right)/2g$$

Introducing the draft tube efficiency $\eta_{D.T.}$, the above expression will be;

$$h_g = \frac{\left(V_1^2 - V_e^2\right)}{2g} \eta_{D.T.}$$

$$\eta_{D.T.} = h_g \left/ \frac{\left(V_1^2 - V_e^2\right)}{2g} \right. = 1 - K \qquad (5.9)$$
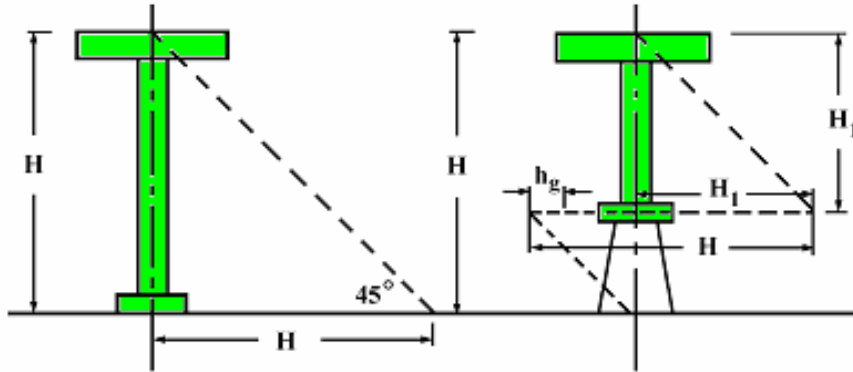
Fig. 5.17 Draft tube function

5.2.2.4 Types of Draft Tube:

Many different designs of the draft tube have been developed. Naturally, the most efficient type will be I and III in Figure 5.18. Both are straight which reduce losses. Type II has a bell-mouthed outlet and an internal conical core. In some cases, the control cone is extended up to meet the runner so as to form a solid core.
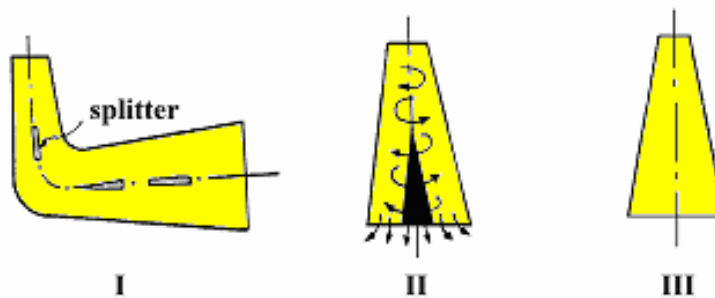
Fig. 5.18 Draft tube types

The water leaves the turbine with a whirl velocity forming a free vortex. According to physical laws when the radial velocity of vortex equals to zero, whirl approaches infinity, which is physically impossible. The

control core of a free vortex cannot follow the free vortex laws and this is conductive to eddy losses, which are avoided by the solid core. Unfortunately, for low head installations, the spaces between the turbine and the water tail race are rarely large enough to permit a draft tube of types II and III. In these cases, draft tube like type I is usually used. To assure a complete guidance of the water which help in reducing hydraulic losses a splitter is used.

5.2.2.5 Net Head:

By definition the *net head* is the difference in elevation between headwater and tail water levels minus the pipe friction losses and the velocity head in the tail race at the point of discharge from the draft tube (the rejected kinetic energy).

$$H_{net} = H_{av} - h_f - V_e^2 / 2g$$

5.2.2.6 Cavitation in Turbines:

The cavitation phenomenon occurs when, at any point, the water pressure drops below its corresponding vapour pressure. This will create bubbles and the fluid will rush into the cavities left by the bubbles causing a species of water hammer.

The resulting cavitation that occurs in the turbine not only impairs the turbine performance but it may also damage the machine itself.

The signs of cavitation are:
  i. Milky appearance of the water at the exit of draft tube.
  ii. Vibrations and noise.

It is convenient to define a dimensionless pressure coefficient that denotes the cavitation tendency of the flow. This expression could be written as the following form;

$$K = (P/\gamma - P_v/\gamma) / (V^2 / 2g)$$

where P and V are the pressure and velocity of flow at any point. The velocity and pressure of the flow are not easily measured and cannot be

computed. Another parameter could be easily used which is $\overline{K}$, similar to K, and is defined as;

$$\overline{K} = \frac{P_2/\gamma + V_2{}^2/2g - P_v/\gamma}{H}$$

This coefficient is applied on the turbine exit on the top of the draft tube or preferably to the highest point in the runner where cavitation might occur and where H is the net head on the turbine as defined before.

The above expression is also not practical because of difficulties of measuring the pressure and velocity at the top of the draft tube.

Applying energy equation between the section (2) and the tail race, Figure 5.16;

$$\frac{P_2}{\gamma} + \frac{V_2{}^2}{2g} + Z = \frac{P_a}{\gamma} + h_L$$

h_L is the head losses between section (2) and the water tail race level. These losses include the kinetic energy rejected to the water and the hydraulic losses.

However, the draft tube is considered an integral part of the turbine, hence the term head loss is omitted and the resulting parameter then covers the combination of runner and its draft tube.

This parameter is known by *Thoma cavitation factor*;

$$\sigma = \left(\frac{P_a}{\gamma} - \frac{P_v}{\gamma} - Z \right) \bigg/ H \tag{5.10}$$

The value of σ at which cavitation occurred is called the *critical value of Thoma cavitation factor* σ_c. This value could be determined by experiments. This can be done by varying Z_2 and noting the value of σ at which the power and efficiency are started to change, Figure 5.19.

158
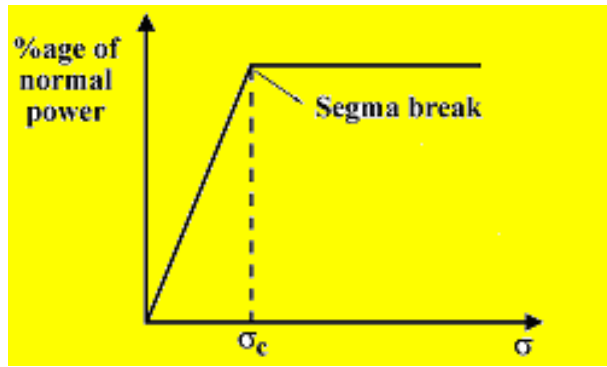
Fig. 5.19 Critical cavitation factor

The above expression is usually used to determine the maximum elevation above the tail water surface at which a turbine can be set without resultant cavitation as following;

$$Z = \frac{P_a}{\gamma} - \frac{P_v}{\gamma} - \sigma_c.H$$

A given turbine running at given N_s is to work under increased head, the turbine must be lowered, i.e. the greater the total head the less the suction head must be.

Some limiting safe values of σ_c are given by Moody for rated specific speeds;

	Francis Turbine					Propeller Turbine (Axial Flow)		
N_s	20	40	60	80	100	100	150	200
σ_c	0.025	0.1	0.23	0.4	0.64	0.43	0.73	1.5

$$N_s = \frac{N\sqrt{B.H.P.}}{H^{5/4}} \quad \text{English Units}$$

The critical cavitation number depends upon the type of turbine and is a function of the specific speed. For Francis turbine, it is given by:

$$\sigma_c = 0.625\left(\frac{N_s}{444}\right)^2, \qquad\qquad (N_s = \frac{N\sqrt{B.H.P.}}{H^{5/4}} \quad \text{metric units})$$

or $\qquad \sigma_c = 0.0317 \left(\dfrac{N_s}{100} \right)^2$, $\qquad\qquad$ ($N_s = \dfrac{N\sqrt{B.H.P.}}{H^{5/4}}$ metric units)

For propeller turbine, it is given by:

$$\sigma_c = 0.3 + 0.0024 \left(\dfrac{N_s}{100} \right)^{2.73} , \qquad\qquad (N_s = \dfrac{N\sqrt{B.H.P.}}{H^{5/4}} \text{ metric units})$$

For Kaplan turbine, σ_c is 10% higher than that for a similar propeller turbine.

5.2.2.7 Power and Speed Regulation:

The normal method of regulating the quantity of water admitted to the turbine is by controlling the guide vanes opening, Figure 5.20. This is done by pivoting the guide vanes about an axis parallel to the turbine axis so that by turning them, the water passage will change to admit the required flow and speed.

a. Opened Guide Vanes $\qquad\qquad$ **b. Closed Guide Vanes**
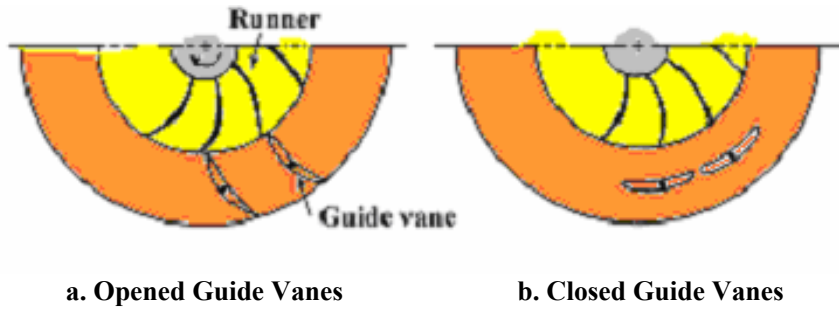
Fig. 5.20 Francis turbine speed and power regulation

5.2.2.8 Francis Turbine Performance:

Figure 5.21 shows the relation between the head and the specific speed for different types of turbines. The data has been taken from installations successfully at work.

160
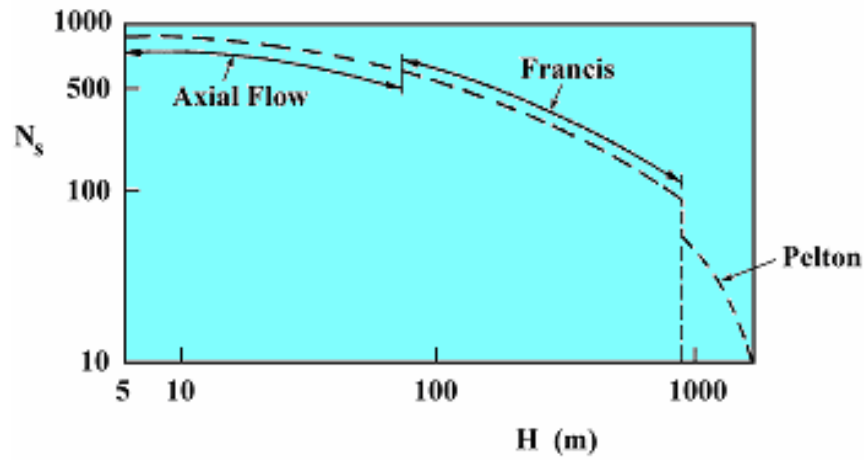
Fig. 5.21 Turbine classification according to specific speed and head
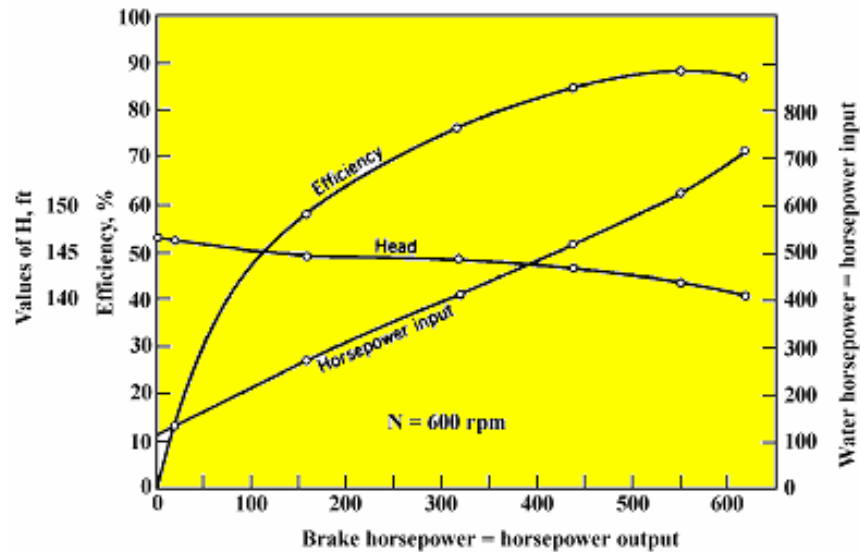
Fig. 5.22 Performance at constant speed and variable gate opening

Figure 5.22 shows the performance of a certain reaction turbine at constant speed.

Performance of Francis Turbine running at 1 m Head:

The flow is no longer independent of the runner speed as in Pelton wheel because of the unbroken flow from head water and any change within the runner will affect the flow, Figure 5.23.

The values of ϕ for maximum efficiency is in general ranges between 0.7 - 0.85.

Also, the maximum value ϕ is greater than one for the performance at constant speed. The efficiency curve is not as flat as that for impulse wheel. In the impulse wheel (turbine), the velocity triangles are independent of the quantity of the flow and so theoretically the hydraulic efficiency should be constant at all loads at constant speed.
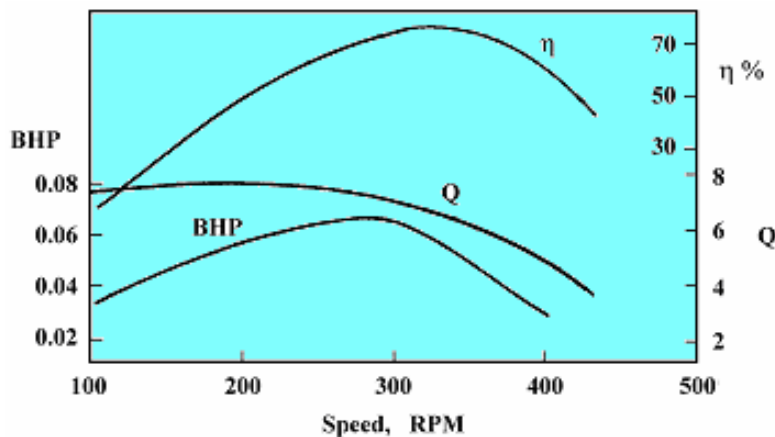
Fig. 5.23 Performance of Francis turbine running at 1 m head

5.2.3 Axial Flow Reaction Turbines:

The axial flow turbine is the development and the completion of the process began when once the radial flow was found to be inadequate for relating high flow and medium and low heads. Mixed flow turbine was found to meet these requirements for high flow and low head. The axial flow turbines are classified to:

A. Propeller Turbine:

The blades are fixed on the rotor and the number of the blades is from 3 to 8. In the simplest form of axial flow propeller turbine, the blades are cast integrally with the hub. The propeller turbine is used in the measurement of the flow, especially in petroleum industry to measure the flow rate.

B. Kaplan Turbine:

162

Although the propeller turbine is almost adequate for high flow and low head operation, it has one quite serious disadvantage is its part load efficiency is unsatisfactory. In Kaplan turbine, this problem is overcome by using movable blades, so that their angles of inclination may be adjusted while the turbine is in motion in such a way that the turbine can operate continuously at its maximum efficiency.

Normally, a kind of servo-motor is used to adequate the inclination of blades.

Efficiencies:

Figure 5.24 represents the relation between the maximum efficiency and specific speed for different types of turbines. It is important to note that these figures of efficiency are very high and applicable to large turbines. For small turbines, the efficiency is lower mainly because of leakage, which is more important in proportion to the flow in small turbine than larger turbine.
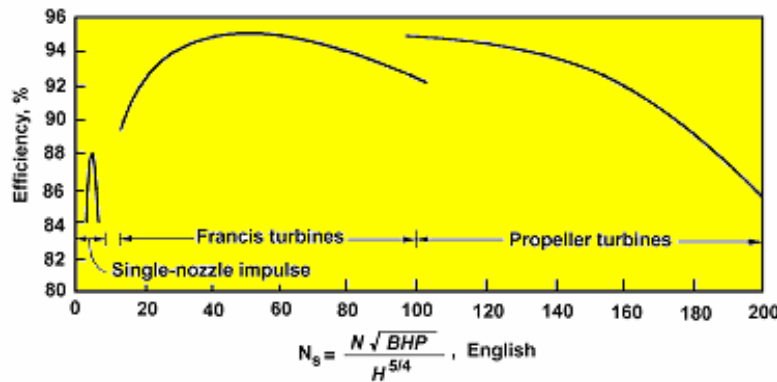
Fig. 5.24 Maximum efficiency versus specific speed for different types of turbines

The effect of size on turbine efficiency is of importance in transferring test results on small models to their prototypes. Moody has presented the following formula, Table 2.1;

$$\frac{1-\eta}{1-\eta_m}=\left(\frac{D_m}{D}\right)^{1/5}$$

5.2.4 Some Design Characteristics for Hydraulic Turbines:

For Francis and propeller turbines, Figure 5.25 shows the average values of the ratios ϕ, ψ and D/d suited for various specific speeds.
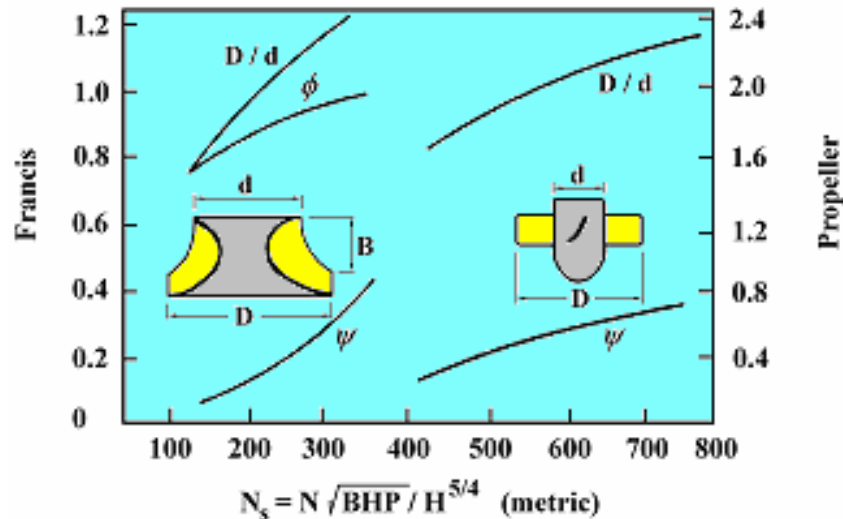
Fig. 5.25 Design characteristics for Francis and propeller turbines

5.3 Some Turbines Installations:

a. Impulse Turbine:

Specially designed for high head above 180 m. Among some interesting installations, Figure 5.26, are the following:

The fully plant in Valois Switzerland operates under a gross head of 5410 ft (1650 m) and a net head of 4830 ft (1473 m). There are four wheels of 3000 hp each running at 500 rpm. The jets are 1.5 inches in diameter and the wheels are 11.67 ft in diameter.
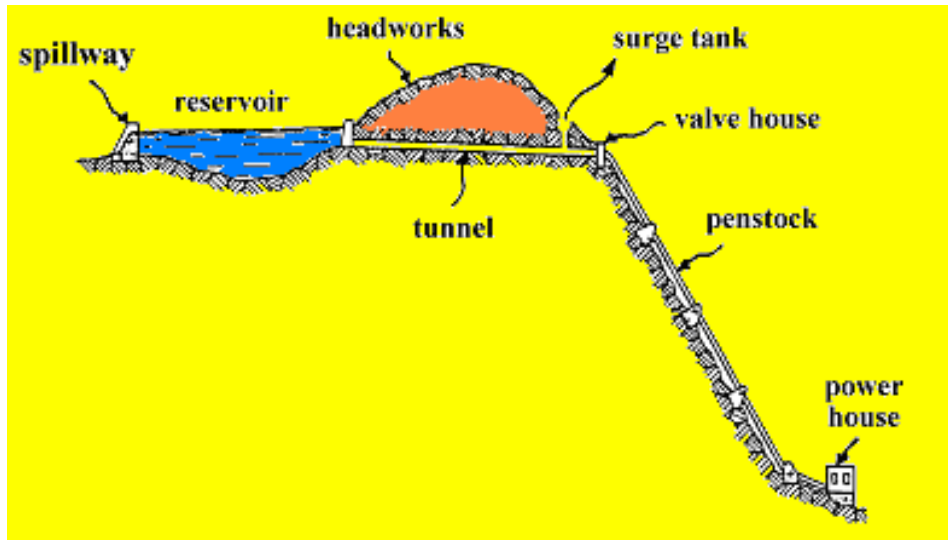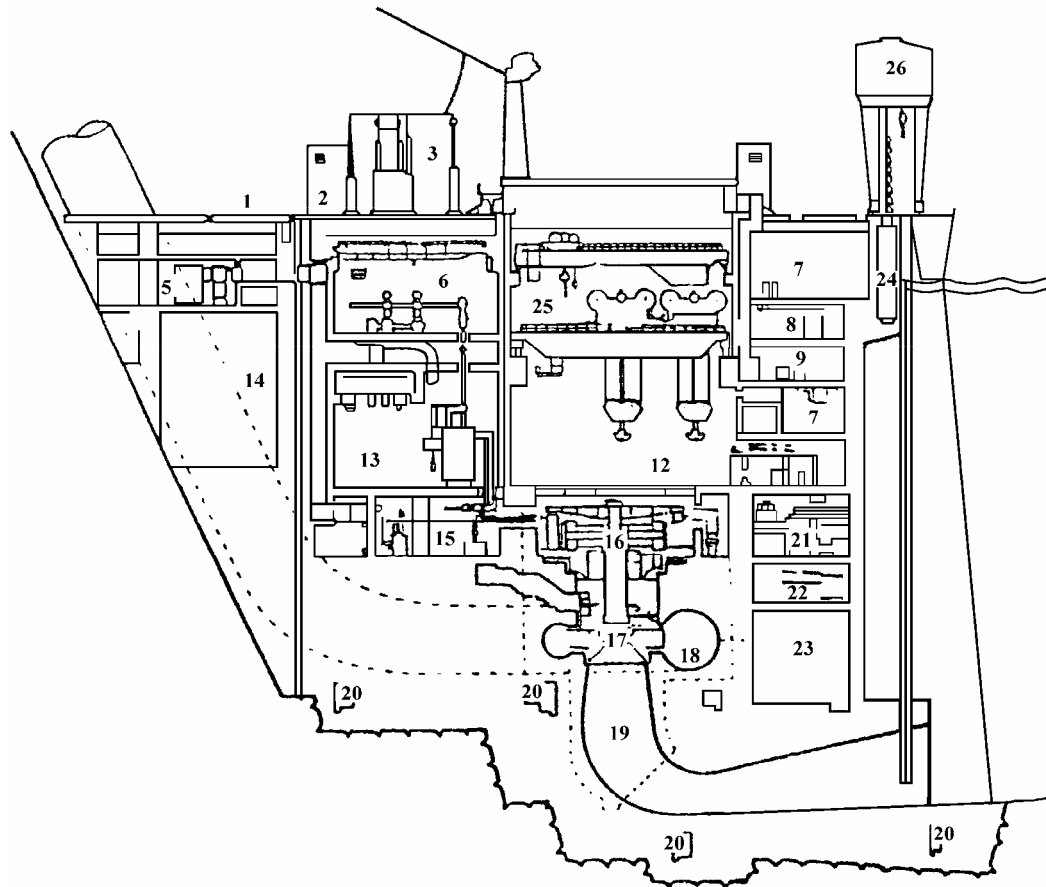
Fig. 5.26 Pelton wheel installation

b. Francis Turbine:

An example of Francis turbine installation is the High Dam of Aswan, The total power generated is 2.1×10^6 kW. The head varies from 57 to 35 m. The power is supplied by 12 units rotating at 100 rpm. The design discharge per unit equals 346 m^3/s. The runner outside diameter is 6.3 m. Another example of the Francis turbine installation is the Brazilian Itaipu Dam at Itaipu on the Parana River between Brazil and Paraguay, Figure 5.27. This is considered as the world's largest hydroelectric power generating complex. Itaipu dam is expected to have an installed capacity of 12,600 MW, delivered by eighteen turbine generators. The runner inlet diameter is 42.6 ft and height is 17 ft, the exit diameter is 28.2 ft and height is 14.7 ft.

1.	Upstream road	10.	Battery room	19.	Draft tube
2.	Vertical access	11.	Local unit control	20.	Drainage gallery
3.	Transmission line takeoffs	12.	Generator hall	21.	Mechanical equipment gallery
4.	Downstream road	13.	Transformer gallery	22.	Pump
5.	Upstream ventilation	14.	Penstock	23.	Antiflooding gallery
6.	Gas insulated (SF6) switch gear substation	15.	Upstream electro-mechanical equipment gallery	24.	Draft tube gates strong
7.	Electrical equipment gallery	16.	Generator	25.	Main powerhouse dam
8.	Cable gallery	17.	Turbine	26.	Gantry cranes
9.	Ventilation	18.	Spiral case		

Fig. 5.27 A sectional view of the powerhouse of Itaipu Dam

166

Cedillo, Spain: Kaplan turbines on the Tagus river

The Cedillo hydroelectric power station on the Tagus River is fitted with four ESCHER WYSS Kaplan turbines and governors, together with electricity generators supplied by General Electrica Espaňola, Figures 5.28 to 5.30. The main data of the turbine installation are:

Four vertical Kaplan turbines, runner diameter 7600 mm, six runner blades made from CrNi 13 4 steel, fixed to the blade disks by screws.
Runner blades can be dismantled via the draft tube doors without dismantling turbine and generator rotors.
Position of runner blades adjustable by means of servomotor in the runner hub.
Oil feed located above the generator.
Machine set carried by three self-lubricating radial bearings.
Axial bearing (maximum loading 28,000 kN) is supported directly on the turbine cover.
Turbine shaft forged from one piece of steel with a borehole for the oil pipes to the runner servomotor passing completely through the shaft.
Axial shaft sealing, hydraulically balanced.
Welded spiral casing, not machined, weight 408 t, inlet diameter 10 m.
Guide vanes adjustable by means of individual servomotors.
Governor fitted with electronic control and oil pressure reservoir.

Head	43 m
Output per turbine	110 MW
Speed	93.8 rev/min
Runner diameter	7600 mm

Fig. 5.28 Sit assembly of the spiral casing (inlet diameter 10000mm)
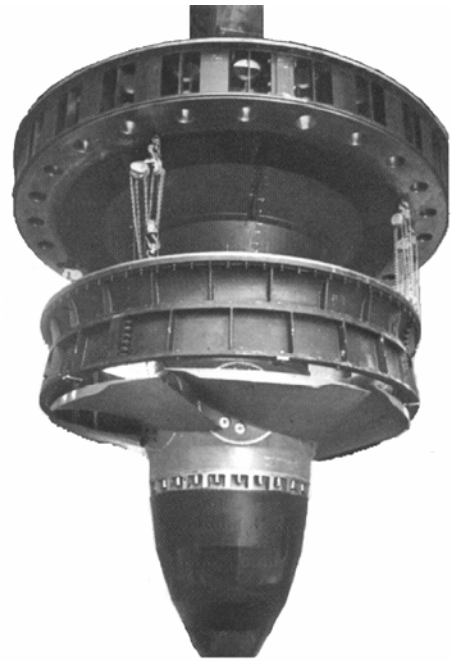
Fig. 5.29 Fitting of the turbine rotor with cover and half discharge ring (weight 570 t)
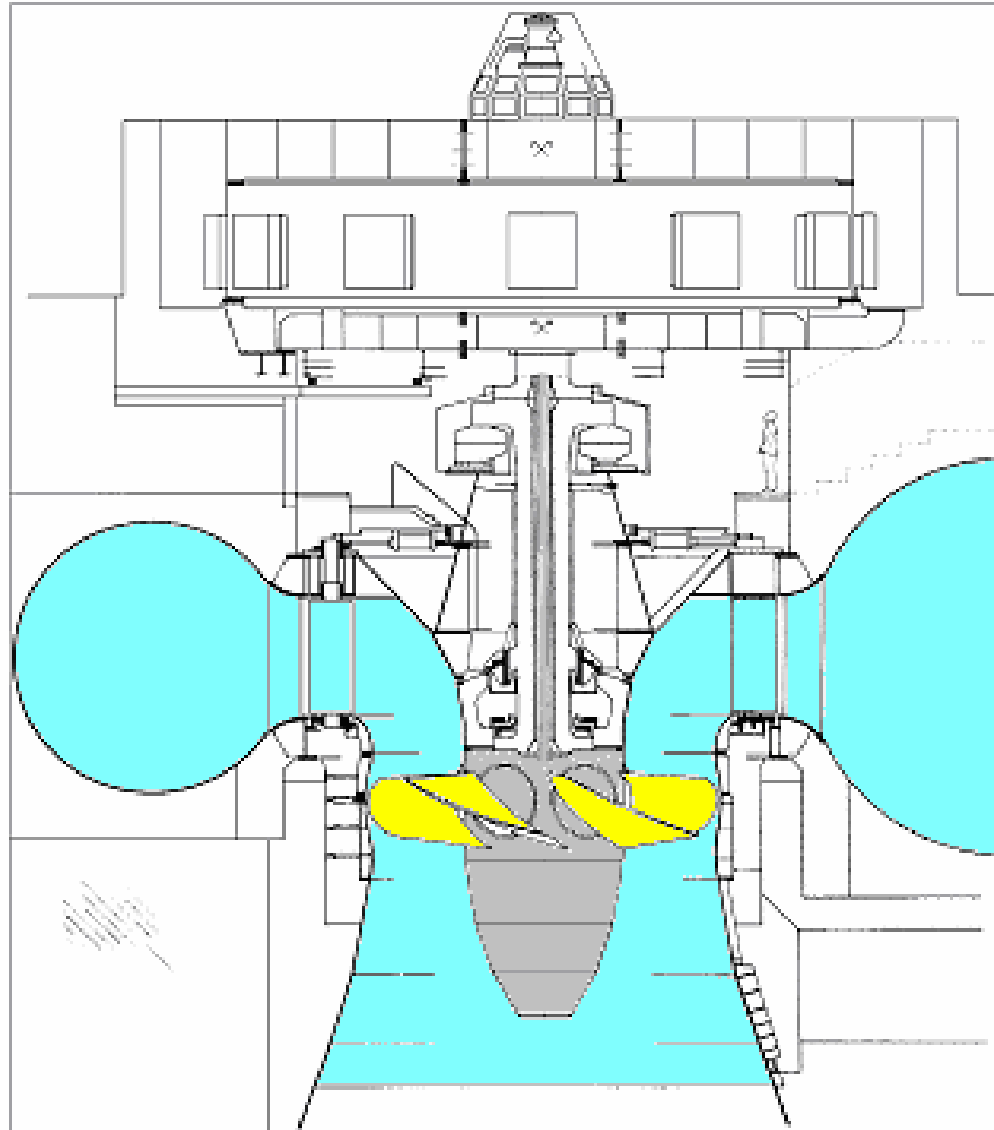
**Fig. 5.30 Turbine unit supported on three bearings.
The runner blades can be dismantled via a port in the draft tube**

Largest bulb turbine in the world: Racine, USA

The Racine installation on the Ohio River, near Charleston, USA, is equipped with two ESCHER WYSS bulb turbines, Woodward governors and ELIN generators, Figures 5.31 and 5.32. Particular design features are:

- Horizontal axis bulb turbines, runner diameter 7700 mm, runner blades made from cast stainless steel of grade CrNi 13 4 and located in a hub fabricated by welding.
- Welded, stainless, discharge ring.
- Guide vane system with adjustable blades, welded construction.
- Access shaft to the generator and access shaft to the turbine side both located in the bulb.
- Centralized lubrication system for turbine bearings as well as thrust and generator guide bearing.
- Oil head for the runner servomotor at the turbine bearing.
- Concreted-in turbine case reinforced with two tie bands round the turbine shaft.
- Bulb nose anchored into the concrete pier by means of tie rods and pegs.
- Generator stator screwed to the cooling support ring; closed cooling system.
- Thermal expansions and deformations caused by axial forces are taken up via two expansion connections, one located between the generator stator and cooling support ring and the other between the discharge ring and the draft tube flange.
- Governor fitted with compressed air tank and additional emergency shutdown system in case of governor failure.

Head	6.2 m
Output per turbine	24.6 MW
Speed	62.1 rev/min
Runner diameter	7700 mm
Weight per turbine	1130 t
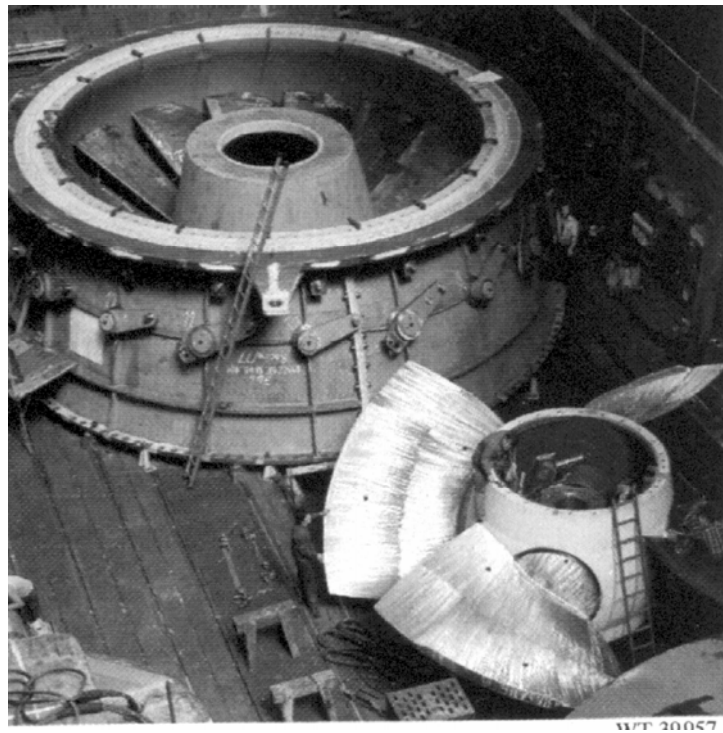
Fig. 5.31 Workshop assembly of complete guide vane apparatus (two-part guide vane casing, 18 adjustable guide vanes in closed position) and of the runner
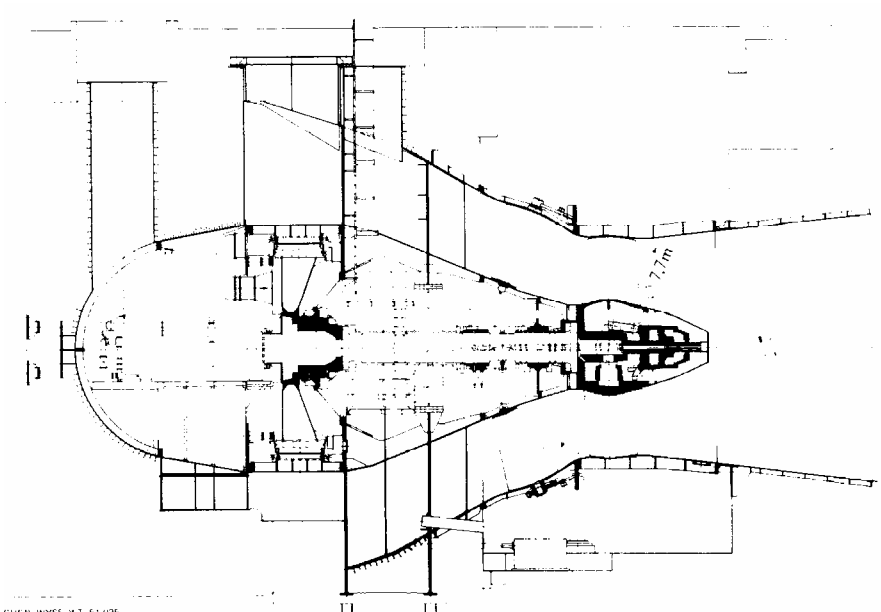
Fig. 5.32 Sectional drawing of the Racine bulb turbine, which has a runner diameter of 7700 mm. The bulb nose is fastened into the concrete pier of the inlet

c. Axial Turbine:

An example of the axial turbine installations, Figure 5.33, is the Aswan dam in which the turbines are of Kaplan type. The total generated power is 344,000 kW supplied by 9 turbines. The head varies from 8 to 24 m. The rotating speed is 100 rpm. The runner diameter is 5.6 m and the hub diameter is 2.8 m.
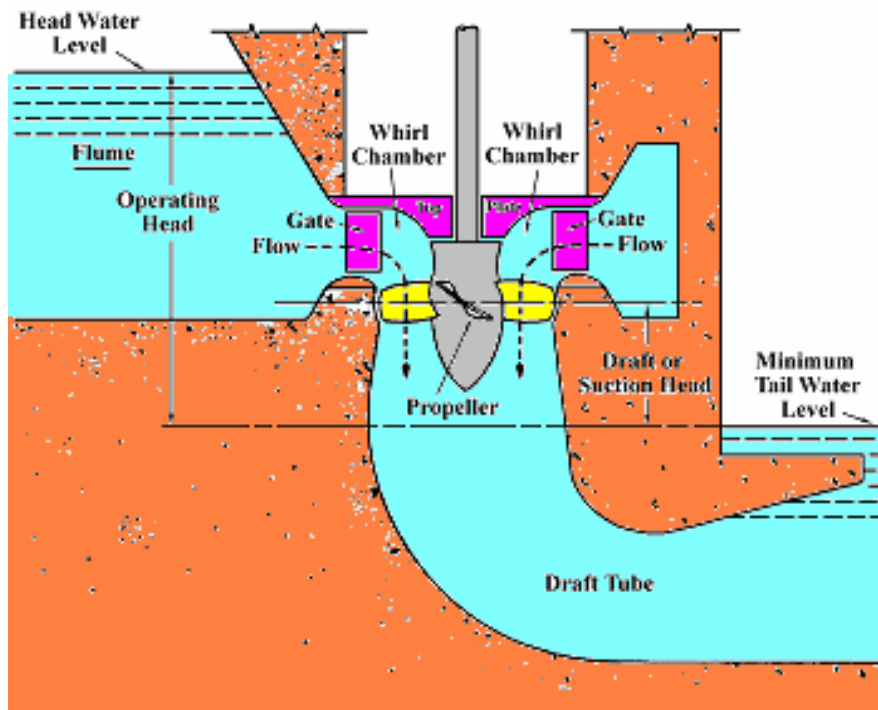
Fig. 5.33 Axial turbine installation

5.4 Fluid Coupling and Torque Converters:

Fluid coupling and torque converters are direct applications on the pump-turbine joint operation. In fluid coupling, for example, the energy transferred through the pump to the fluid is recuperated through the turbine. The principles of coupling and torque converter are the same as shown in Figure 5.34.
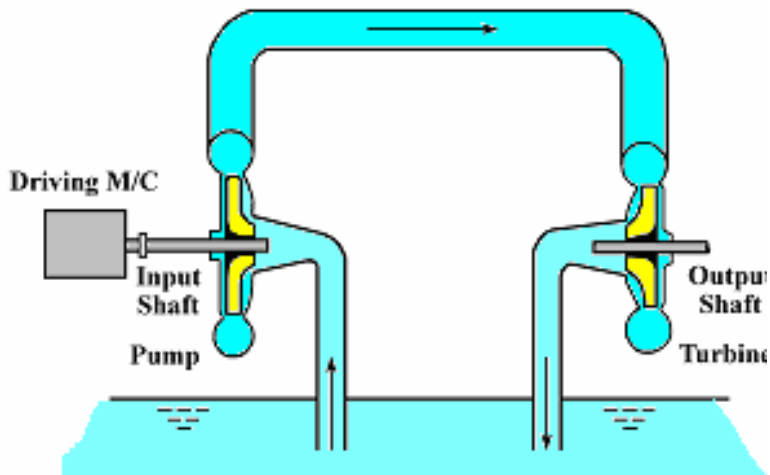
Fig. 5.34 The principles of hydraulic transmission

If the pump, which is connected to the driver, transmits a power P_1 to the fluid, the turbine recuperates a power P_2 on the output shaft. So, the hydraulic efficiency could be defined as:

$$\eta = \frac{P_2}{P_1} = \frac{T_2.N_2}{T_1.N_1}$$

5.4.1 Fluid Coupling:

The fluid coupling, Figure 5.35, transmits the power between the driver and the driven unit. The power transmission could be at the same speed but it permits also a variation in the speed. This is very practically in the starting of a large machine. Thus, it could be act as a slipping clutch.

1- Input Shaft,
2- Output shaft,
3- Pump Impeller,
4- Turbine Runner.
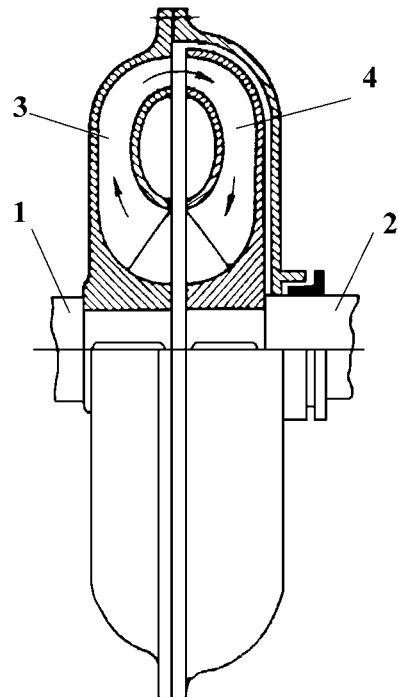
Fig. 5.35 Fluid coupling

The efficiency, as defined before, is;

$$\eta = \frac{P_2}{P_1} = \frac{T_2 . N_2}{T_1 . N_1}$$

The efficiency equals N_2 / N_1 if the torque is constant, Figure 5.36.
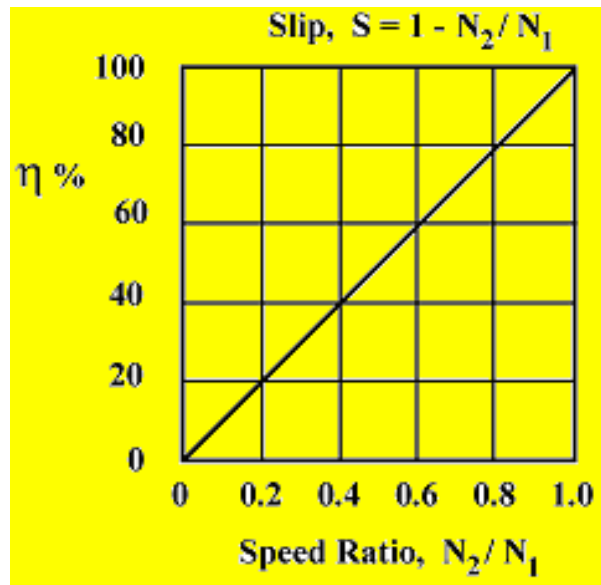
Fig. 5.36 Fluid coupling efficiency curve

The applications of fluid coupling are numerous. It has the advantage of damping out any torsional or lateral vibrations. This problem of vibrations arises usually in large machines operating at high speed such as large centrifugal compressors.

5.4.2 Torque Converter:

The difference between torque converter, Figure 5.37, and fluid coupling, Figure 5.35, is that in torque converter, the torque is multiplied and the change of the torque is obtained by fixed vane changing the direction of flow to the pump acting as an inlet guide vane.

1- Input Shaft,
2- Output shaft,
3- Pump Impeller,
4- Turbine Runner.
5- Inlet Guide Vanes.
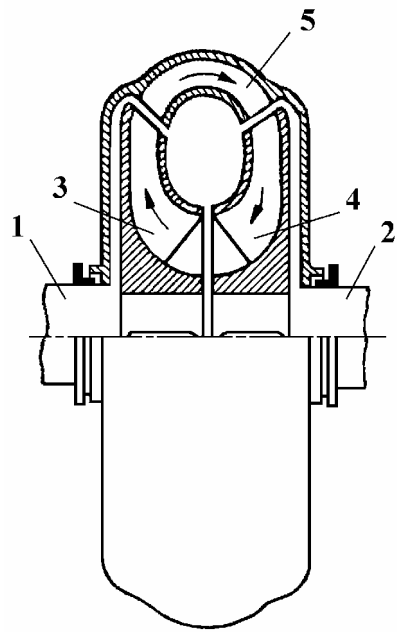
Fig. 5.37 Torque converter

The stator or guide vanes, Figure 5.38, are so shaped as to change the direction of flow and thus it could increase the angular momentum and the fluid flowing through the turbine given up an angular momentum equal to the sum of that from the stator and the pump. So, the torque of the turbine, which is delivered to the output shaft, is the sum of the pump torque and the stator torque. This could be easily seen from Figure 5.39.
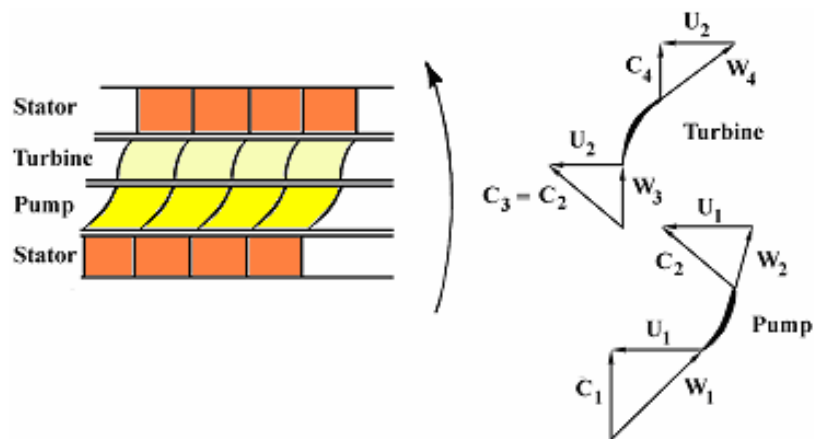
Fig. 5.38 Velocity triangles
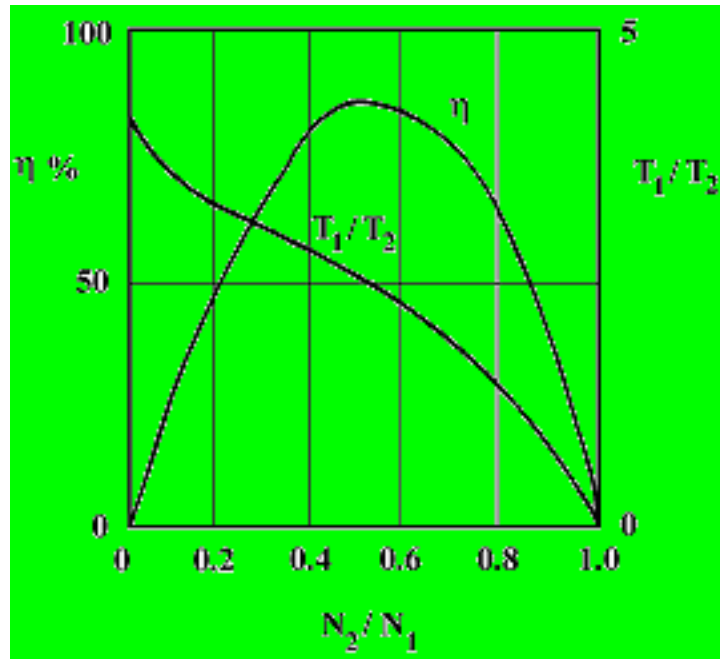
Fig. 5.39 Torque converter performance

5.5 *Pump-Turbine, Power Storage System:*

Usually, the electricity consumption is not constant through out the day. The consumption is minimum during the day time, this consumption is increased to reach its maximum level at night-time. This peak level is not continuous. In order to meet this peak load, the power station must use a power storage system. There are different types of power storage systems, the system which currently used is the Pump-Turbine power storage system. The system is consisted of pump working during the low power demand period (day time). The water is pumped to a reservoir at a high altitude. At night-time, the water in the reservoir will come back to rotate a turbine producing the additional power required for the utility during the peak hours. Figure 5.40 shows an example of this type.
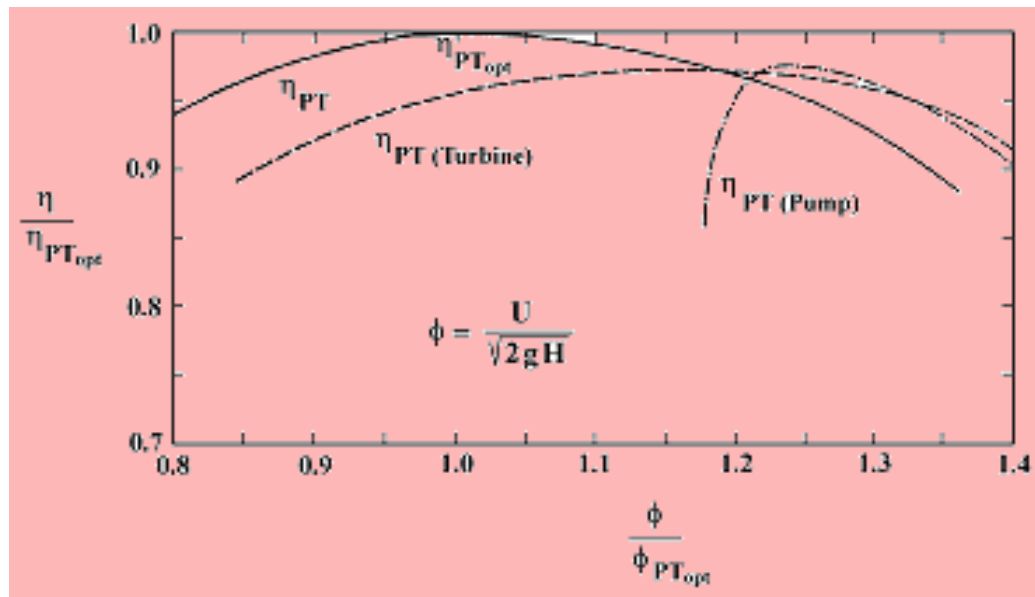
Fig. 5.40 Relative efficiency as a function of relative pressure coefficient. In the operating range, the turbine and the pump efficiencies are at approximately equally high levels. The optimum turbine efficiency of the system is however lower than that of a conventional Francis turbine (Courtesy of Escher Wyss)
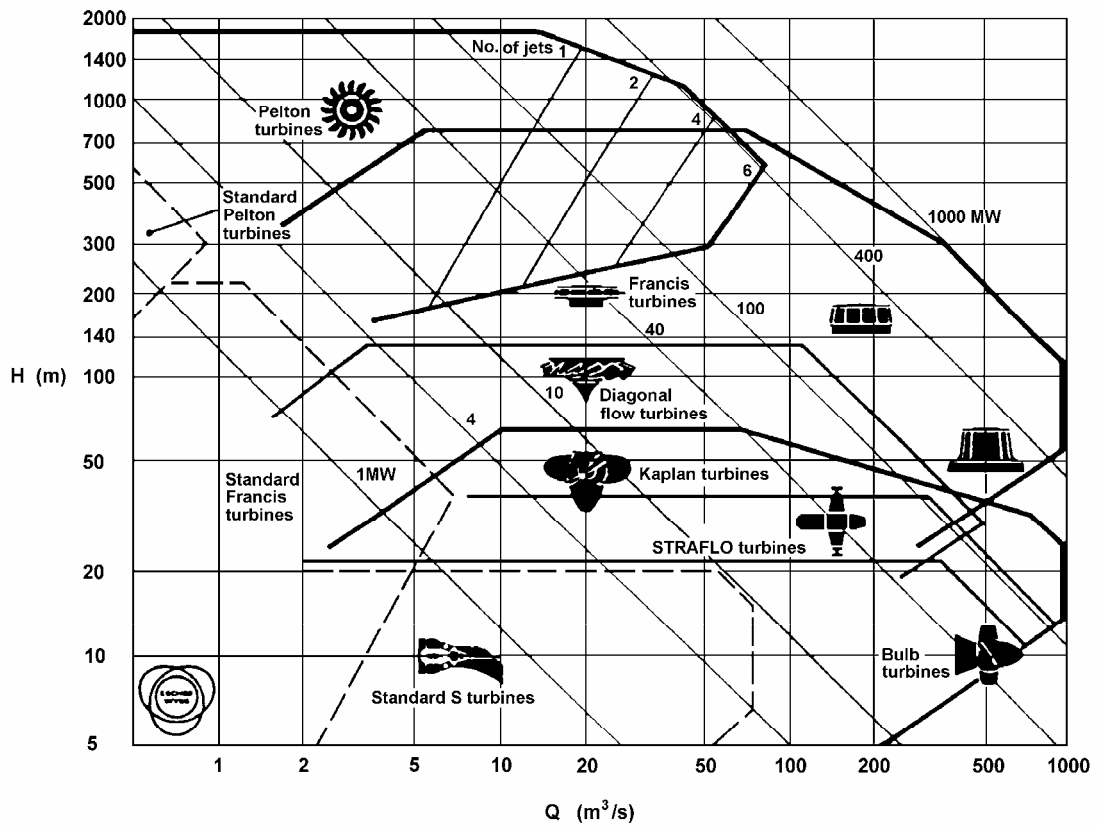
Fig. 5.41 Application ranges of different types of water turbines
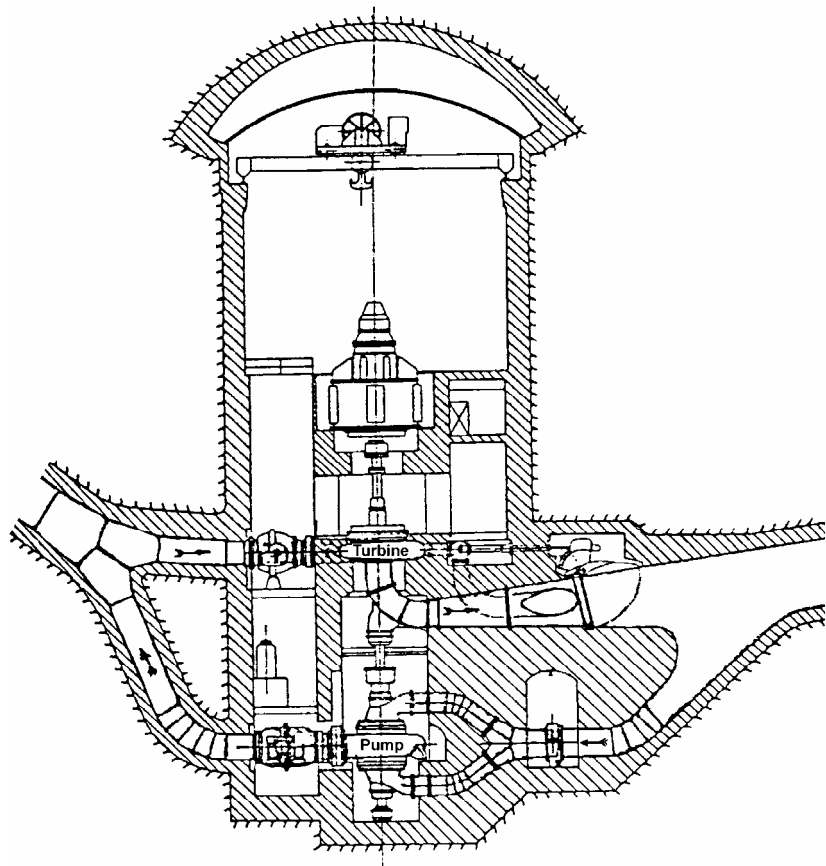
Fig. 5.42 Section through the 51 m high cavern of the pumped-storage power station at Villa Gargnano (Italy). The intake sections of the pumps and the outlet sections of the turbines are connected to the Lake of Garda. The delivery pipes of the individual pump are combined with the pressure pipe of the turbine into single pipeline after the closing devices. The schedule provides for 3000 hours of running time. (Courtesy of Escher Wyss)
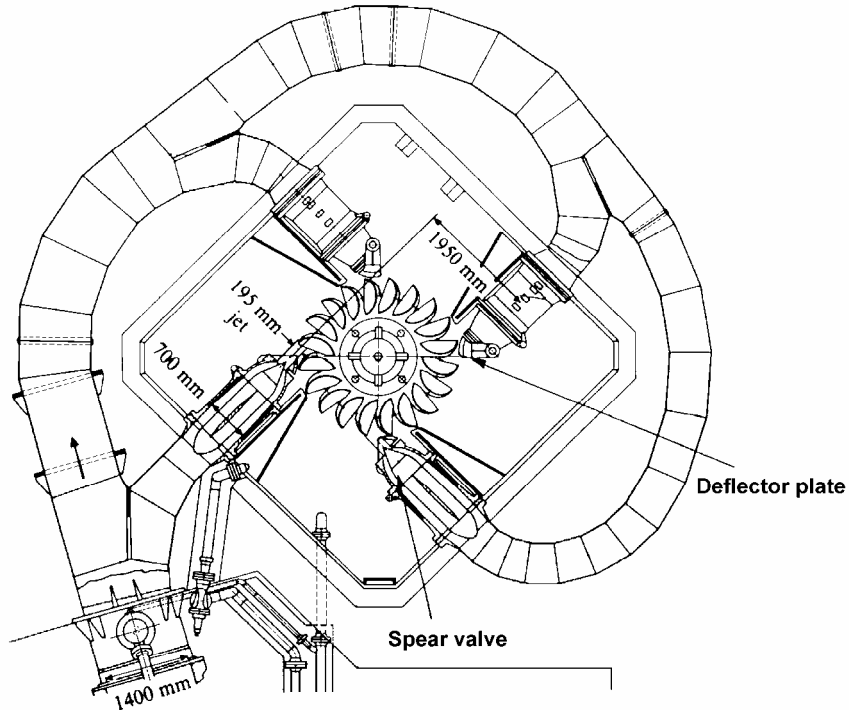
Fig. 5.43 Horizontal section in the plane of the annular duct, through one of the two vertical-shaft four-nozzle impulse turbines for the power station El-Salto II (Colombia). Short nozzles, in conjunction with a close-fitting turbine casing and internally situated servomotors, result in small machine dimensions and a correspondingly reduced distance between centres. The nozzles are bolted simultaneously to the pressure pipe and to the turbine casing by means of a common flanged section and can be removed, in the same way as the runner, through the discharge pit. P = 37,000 kW, H = 415.5 m, N = 400 rpm

182
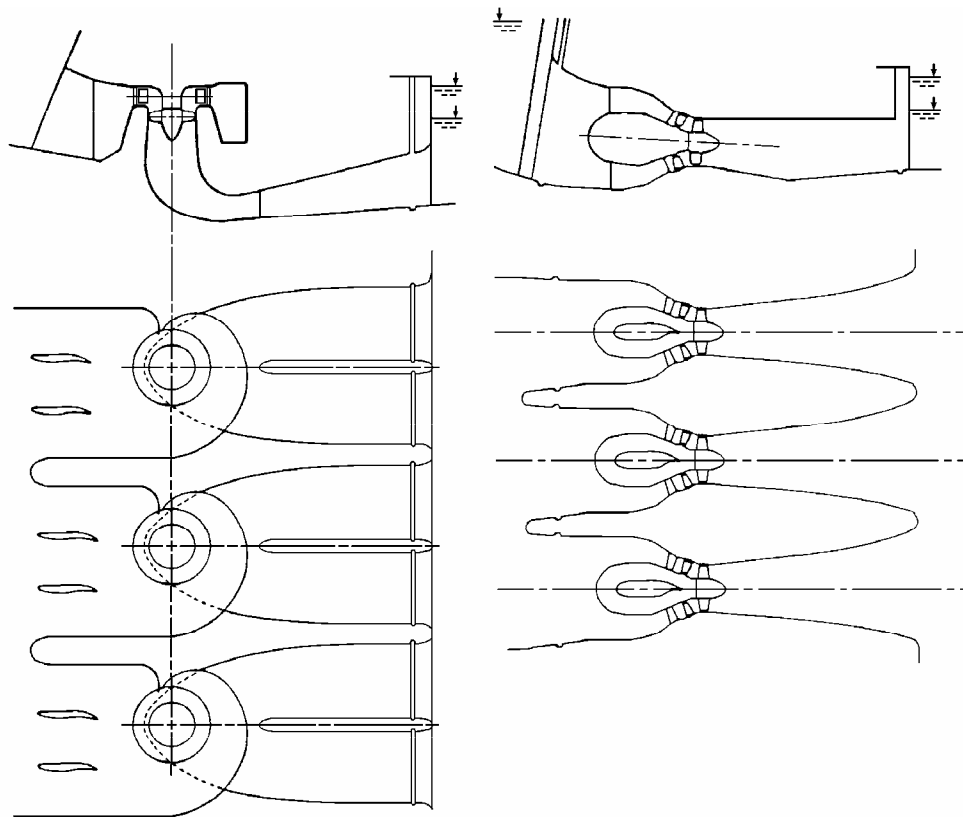
Fig. 5.44 Comparison of amounts of space required by conventionally arranged Kaplan turbines (left) and tubular turbines with the same output (right). Less excavation work is required with tubular turbines, and the powerhouse can be made much lower and shorter, in view of the smaller distances between centres. The saving in volume of building space is therefore considerable

Fig. 5.45 Francis turbine runner
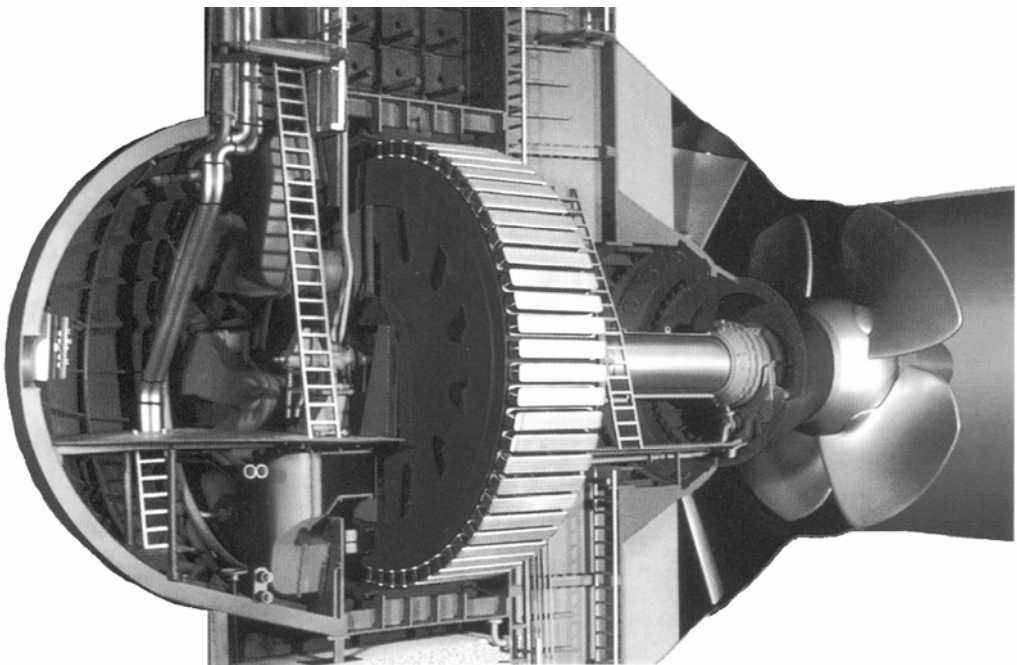
Fig. 5.46 The six bulb turbines at Vienna's Freudenau power plant belong to the largest one world-wide
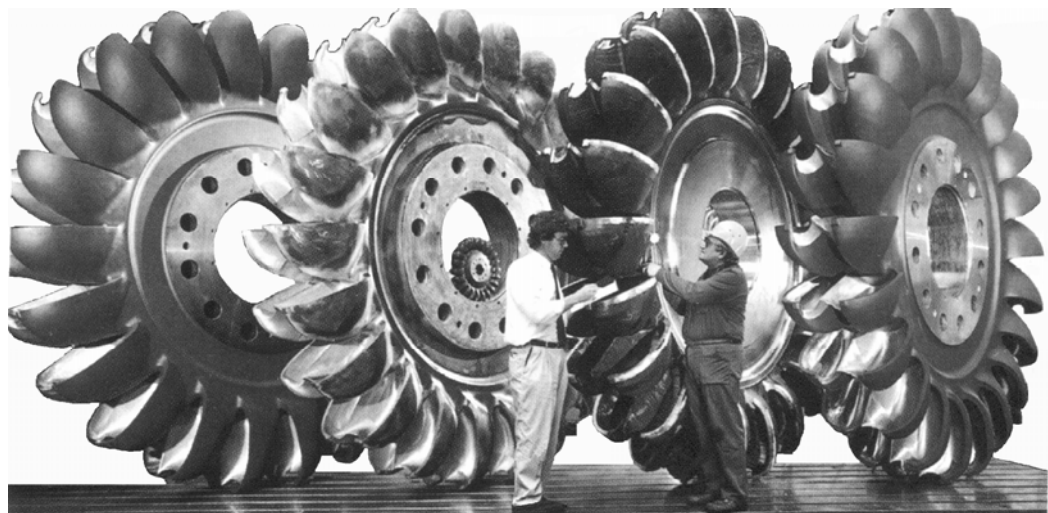
Fig. 5.47 Four 260 MW Pelton turbine runners under a head of 1140 m with the model runner inside one of them

**Fig. 5.48 Kaplan runner for a bulb turbine (diameter 3.8 m,
output 11.3 MW, head 14 m)**
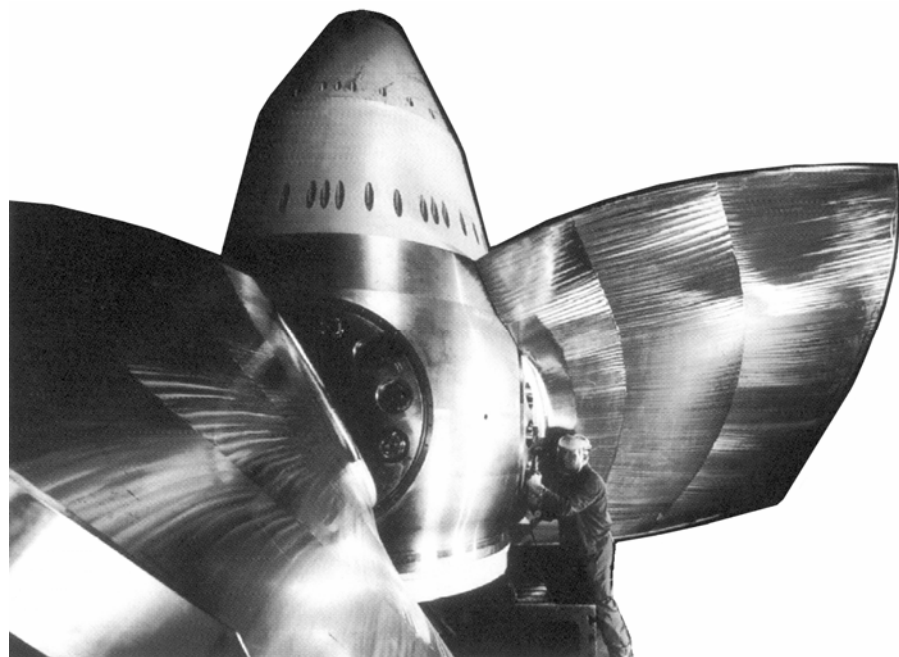
**Fig. 5.49 The Freudenau Kaplan bulb-turbine runners
have a diameter of 7500 mm**

**Fig. 5.50 Francis runner at Niagara Falls. Diameter = 176 in,
H = 214 ft, N = 107 rpm**
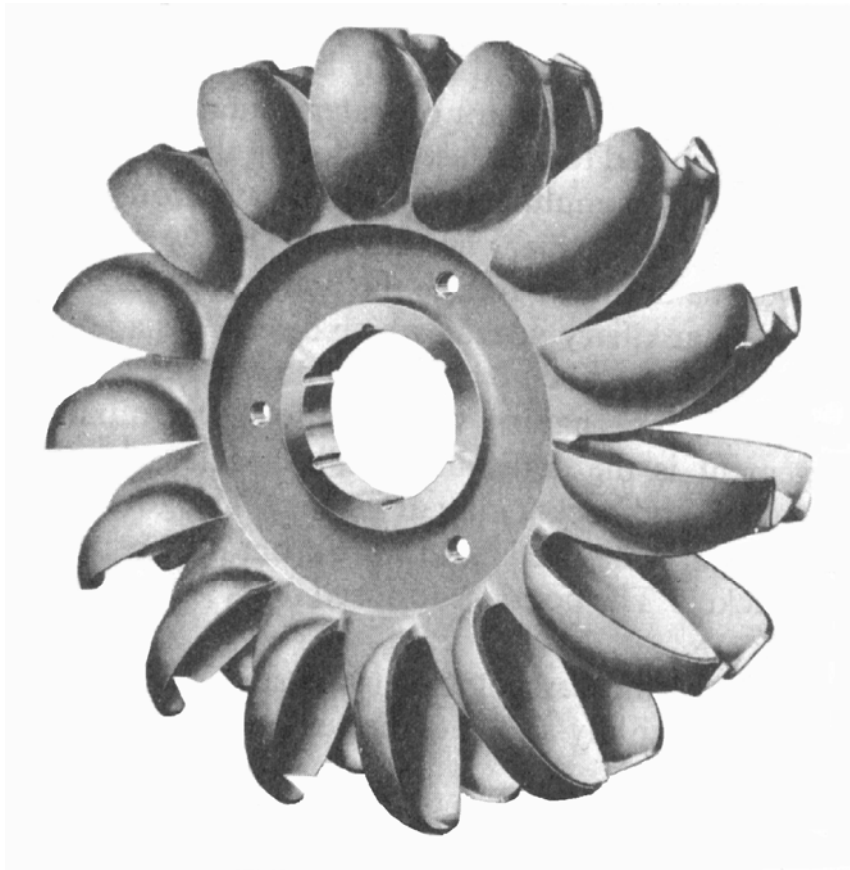
Fig. 5.51 Pelton wheel

CHAPTER (VI)

COMPRESSIBLE FLOW TURBOMACHINES
(Thermodynamic Principles)

Some thermodynamic principles, which apply to the compressors and blowers, will be reviewed briefly in this chapter.

6.1 Equation of state:

The equation of state is a mathematical relationship of the state variables; pressure, volume, density, and temperature as follows:

$$f(P,v,T) = 0$$

where

      P = the pressure,
      v = specific volume = V/M,
      T = absolute temperature.

If the function f could be calculated for a given substance, then any two of the variables P, v, or T will define the state.

The function f for a real gas is complicated, so it is more convenient to use ideal gas and in this case the equation of the state could be easily written as;

$$P.v = R.T \qquad\qquad\qquad (6.1)$$

where

      R = the gas constant = $\bar{R} / MW$ (6.2)
      $\bar{R}$ is the universal gas constant.

            $\bar{R}$ =1545 lb.ft/lb$_{mole}$.$^{\circ}$R   or

            $\bar{R}$ = 848 kp.m/kg$_{mole}$ .K

      or in thermal units:

$$\overline{R} = 1.9875 \text{ BTU/(lb}_{\text{mole}} .^{\circ}\text{R), kcal/ (kg}_{\text{mole}} .\text{K)}$$

The ideal gas obeys the above equation, for the real gases the above equation could be applied with good approximation at low pressures. There are other equations of state, which deal with real gases; this equation lay out of scope of this text. This could be easily found in any textbook on thermodynamics.

6.2 Specific Heat:

The *specific heat* is defined as the amount of heat required to raise the temperature of a unit weight of gas one degree. The value of the specific heat depends on the method by witch the heat is added. If it is added at constant pressure it is called C_p, and if it is added at constant volume it is called C_v.

The ratio of the specific heat at constant pressure C_p to the specific heat at constant volume C_v is denoted by K (*isentropic coefficient*).

$$K = C_p / C_v \tag{6.3}$$

The relation between C_p, C_v and R could be found easily;

$$C_p - C_v = R$$

where R is in thermal units, ($\overline{R} = 1.9875$)

$$\text{Also,} \quad C_v = \frac{R}{K-1} \quad , \qquad C_p = \frac{R.K}{K-1} \tag{6.4}$$

6.3 Enthalpy:

Applying the energy equation in the case of steady permanent flow we have:

$$\left(H_2 + gZ_2 + \frac{C_2^2}{2} \right) - \left(H_1 + gZ_1 + \frac{C_1^2}{2} \right) = W_T + Q_T \tag{6.5}$$

Q_T represents the heat added or removed.

$$H = E + P.dv \tag{6.6}$$

where E is the internal energy and H is the enthalpy per unit mass. The total enthalpy H_T is defined as

$$H_T = H + gZ + C^2/2 \qquad (6.7)$$

i.e.

$$H_{T2} - H_{T1} = W_T + Q_T \qquad (6.8)$$

From Joule's experiments, the change in internal energy of gas depends only on its temperature if the gas is subjected to a constant volume process. Thus,

$$\Delta H = \Delta E = C_v . \Delta T \qquad (6.9)$$

6.4 Entropy:

This important property of gas could not be measured like heat, it has no definite value. The change of entropy in a process is important and is given by:

$$ds = \int_1^2 \frac{dQ}{T} \qquad \text{kcal / K} \qquad (6.10)$$

6.5 Work:

Consider a system surrounded by arbitrary boundaries, Figure 6.1, if these boundaries are displaced due to energy transfer, the force: $F = P.A$ and the work done:

$$\Delta W.D = F.ds = P.A.ds = P.dv \qquad (6.11)$$

If the process is defined, the work done equation over boundary could be integrated;

$$W.D = \int_{v_1}^{v_2} P.dv \qquad (6.12)$$

191
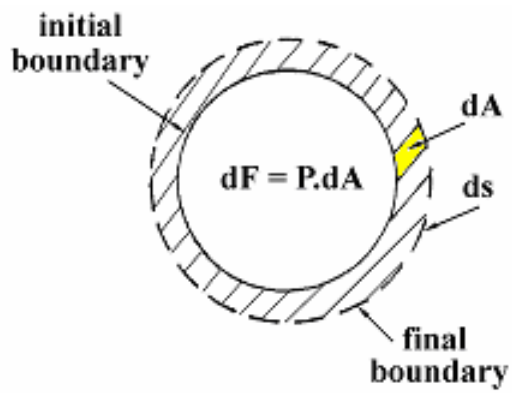
Fig. 6.1 System displacement

6.5.1 For a constant volume process,

$$W.D = P.dv = 0$$

6.5.2 For a constant pressure process,

$$W.D = P\int_{1}^{2} dv = P(V_2 - V_1) \tag{6.13}$$
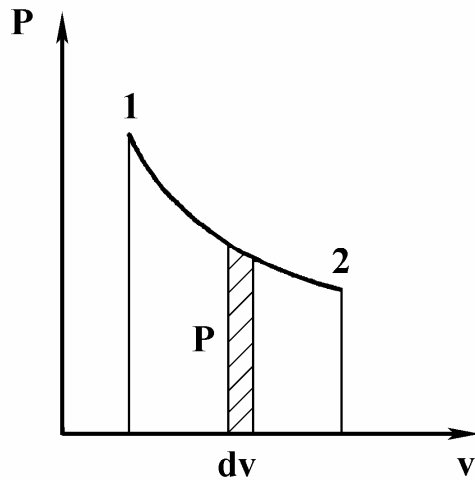
Fig. 6.2 Pressure volume diagram

6.5.3 For a constant temperature process (Isothermal process),

$$W.D = \int_{v_1}^{v_2} \frac{R.T}{v} dv = R.T.\ln(V_2/V_1) \tag{6.14}$$

6.5.4 For an adiabatic process,

No heat is added or removed from the system. During the process entropy remains constant so it is called *isentropic process*.

$$P.V^k = \text{Constant} \tag{6.15}$$

and

$$W.D = \int_{v_1}^{v_2} P \, dv$$

$$= \frac{k}{k-1} P_1.V_1 \left[\left(\frac{P_2}{P_1} \right)^{\frac{k-1}{k}} - 1 \right] \tag{6.16}$$

The classical alternative forms of the above equation could be written as follows;

$$W.D = \frac{k}{k-1} R.T_1 \left[\left(\frac{P_2}{P_1} \right)^{\frac{k-1}{k}} - 1 \right]$$

$$= \frac{k}{k-1}(P_2.V_2 - P_1.V_1)$$

6.5.5 For polytropic process,

For real gases, the adiabatic process exponent is greater than k because that the heat used in real gas is greater than that for ideal gas.

$$P.V^n = \text{Constant}$$

$$W.D = \frac{n}{n-1} P_1.V_1 \left[\left(\frac{P_2}{P_1} \right)^{\frac{n-1}{n}} - 1 \right] \tag{6.17}$$

and;

$$n = \frac{\ln(P_2 / P_1)}{\ln(V_1 / V_2)}$$

6.6 First Law of Thermodynamics:

This law states that the energy change in a system is exactly equal to the resultant energy transfer across its boundary. Resultant energy transfer means the difference in energy transfer in and out of the system.

i.e. $E_2 - E_1 = Q - W$ (6.18)

where E_1 = internal energy at start of process.
             E_2 = internal energy at end of process.
             Q = resultant heat transfer into the system.
             W = resultant work done by the system.

So, the first law could be expressed as follows;

$$dU = dQ - dW$$ (6.19)

Since dU is an exact differential, it is clear that for a cyclic change:
$$\int dU = U_2 - U_1 = 0$$
It follows that for a cycle: $dQ = dW$

This is very important result of the first law of thermodynamics and it is obvious for machine operating in a complete cycle. The machine could not supply more than the energy received.

6.7 Second Law of Thermodynamics:

The second law of thermodynamics is stated in many ways, the most fundamental and general definition is given in terms of the property known as *entropy*. The second law is stated in terms of entropy as follows:
The entropy of an isolated system cannot decrease but must increase to a maximum in all real processes. In other words, we can say that the

194

conversion of heat to work is limited by the temperature at which conversion occurs. It may be shown that:

1- No cycle can be more efficient than a reversible cycle operating between given limits.

2- The cycle efficiency of all reversible cycles absorbing heat only at a single constant higher temperature T_1 and rejecting heat only at a single constant lower temperature T_2 must be the same.

3- For all such cycles the efficiency is;

$$\eta = \frac{W}{Q} = \frac{T_1 - T_2}{T_1} \tag{6.20}$$

which is usually known as *Carnot efficiency*.

6.8 Compression of Gases:

6.8.1 Adiabatic Compression:

If there is no heat added or removed from the fluid during the compression, the compression is called *adiabatic*.

There are two possible cases of adiabatic process: reversible and irreversible. In reversible process, the entropy remains constant, and the process is called *isentropic process*. The *adiabatic efficiency* is defined as the ratio of isentropic work to real work, Figure 6.3.

$$\eta_{ad} = \frac{W.D_{isen}}{W.D_{real}} = \frac{H_2 - H_1}{H_2' - H_1} \tag{6.21}$$

and $H = C_p.\Delta T$, i.e.

$$\eta_{ad} = \frac{\Delta T_{isen}}{\Delta T_{real}'} \tag{6.22}$$
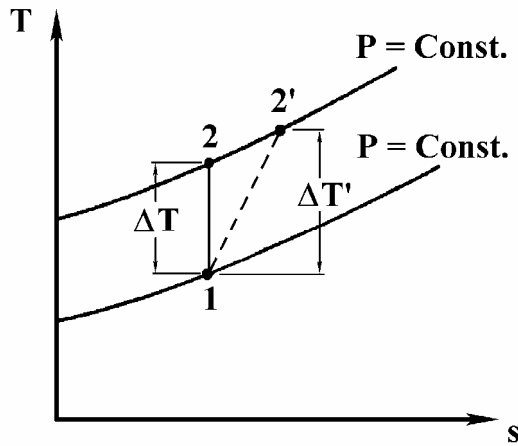
Fig. 6.3 Adiabatic compression

The process is defined by the equation $P.V^k = \text{Constant}$ and the work done,

$$W.D_{ad} = \frac{k}{k-1} P_1.V_1 \left[\left(\frac{P_2}{P_1} \right)^{\frac{k-1}{k}} - 1 \right]$$

6.8.2 Isothermal Compression:
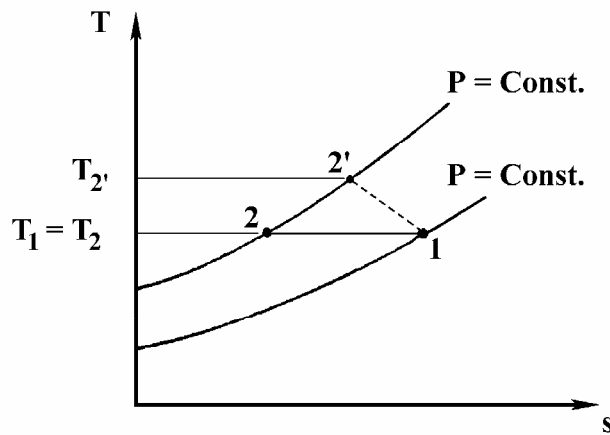
Fig. 6.4 Isothermal compression

Usually in cooled machine, the *isothermal efficiency* is the ratio of the isothermal reversible work to the real work, Figure 6.4.

$$\eta_{iso} = \frac{W.D_{iso}}{W.D_{real}}$$

$$W.D_{iso} = R.T_1.\ln\left(P_2 / P_1\right)$$

$$W.D_{real} = H_2 - H_1 - Q = C_p\left(T_2 - T_1\right) - Q$$

$$\eta_{iso} = \frac{R.T_1.\ln\left(P_2 / P_1\right)}{C_p\left(T_2 - T_1\right) - Q} \tag{6.23}$$

6.8.3 Polytropic Compression:

The *polytropic efficiency* is defined as the ratio of the reversible polytropic work done to the real work done, Figure 6.5.

$$\eta_{poly} = \frac{W.D_{poly}}{W.D_{real}} \qquad \text{or}$$

$$\eta_{poly} = \frac{(k-1)/k}{(n-1)/n} \tag{6.24}$$
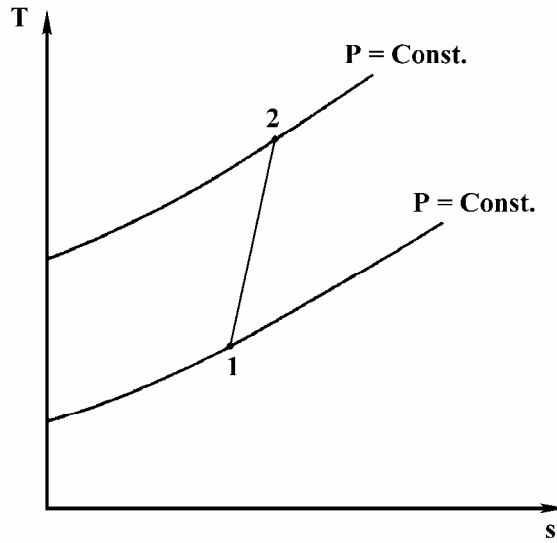
Fig. 6.5 Polytropic compression

6.9 Plane Compressible Flow:

197

To go deeper insight, we may consider the treatment of isentropic flow in two dimensions. Since this treatment is highly complicated, the so-called *linearised compressible flow theory* will be considered.

It is assumed that there are only small deviations in the flow field from an undisturbed parallel flow of high speed. For a stream of mean velocity C, with perturbation velocities u and v, the vorticity is everywhere zero.

$$\frac{\partial v}{\partial x} - \frac{\partial u}{\partial y} = 0 \tag{6.25}$$

Then, the equation of continuity;

$$\frac{\partial(\rho.C + \rho.u)}{\partial x} + \frac{(\rho.v)}{\partial y} = 0 \tag{6.26}$$

Introducing the velocity potential $\phi(x, y)$

$$u = \frac{\partial \phi}{\partial x} \quad , \quad v = \frac{\partial \phi}{\partial y} \tag{6.27}$$

Using the small perturbation hypothesis, the density and the speed of sound can be written as:

$$\rho = \bar{\rho} + \rho'$$
$$a = \bar{a} + a'$$

Substituting in equation (6.26), ignoring products of small quantities;

$$\bar{\rho}\frac{\partial u}{\partial x} + \bar{\rho}\frac{\partial v}{\partial y} + C\frac{\partial \rho'}{\partial x} = 0 \tag{6.28}$$

Introducing Euler's equation;

$$\frac{1}{2}dC^2 + \frac{dP}{\rho} = 0 \tag{6.29}$$

Then Euler's equation becomes;

$$C.du + \frac{dP}{\rho} = 0 \qquad (6.30)$$

Knowing that $a^2 = dP/d\rho$, equation (6.30) could be written as follows;

$$d\rho = \frac{-\bar{\rho}.C}{a^2}\, du \qquad (6.31)$$

After equations (6.28) and (6.31), one can obtain the following;

$$(1-M^2)\frac{\partial^2 \phi}{\partial x^2} + \frac{\partial^2 \phi}{\partial y^2} = 0 \qquad (6.32)$$

Equation (6.32) is similar to Laplace's equation. The quantity $(1-M^2)$ is important to describe the extent of the effect of Mach Number on the flow. For $M < 1$, the equation is of elliptic type and then reduced to Laplace's equation by the transformation;

$$\xi = x, \qquad \eta = y\sqrt{1-M^2}, \qquad \phi^* = K.\phi$$

K is an arbitrary constant and ϕ^* is the transformed potential. For $M > 1$, the solution is said to be *hyperbolic*.

6.10 Gothert's Rule:

Gothert's rule concerning the transformation between an incompressible flow field and the corresponding compressible flow field, Figure 6.6. This rule is useful since there are large information on the incompressible flow field. If u^* and v^* are the perturbation velocities in incompressible flow field, and u and v are the perturbation velocities in the compressible flow field, thus;

$$u^* = K\,u$$
$$v^* = \frac{K}{B}v \qquad (6.33)$$
$$\tan\theta^* = \frac{v^*}{C} = \frac{K}{B}.\tan\theta$$

with $\quad B = \sqrt{1 - M^2}$
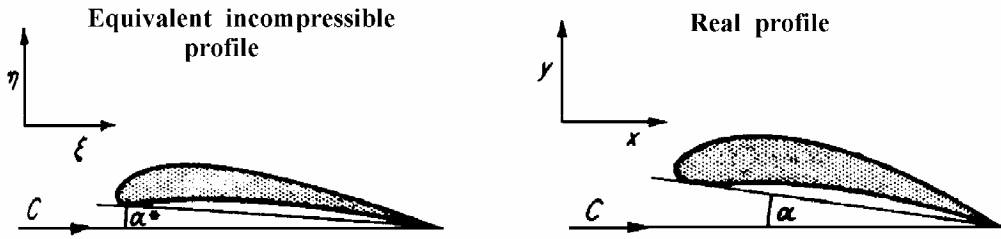
Fig. 6.6 Gothert's rule

Now transforming the coordinates,

$$\frac{dy}{dx} = \frac{v}{C + u} \approx \frac{v}{C} \approx \tan\theta \qquad (6.34)$$

$$\frac{d\eta}{d\xi} = \frac{v*}{C + u*} \approx \frac{v*}{C} \approx \tan\theta* \qquad (6.35)$$

$$\frac{d\eta}{d\xi} = B\frac{dy}{dx} \qquad (6.36)$$

and $\quad \tan\theta* = B\,\tan\theta \qquad (6.37)$

with $\quad K = B^2 \qquad$ resulting in:

$$\xi = x, \qquad \eta = B\,y, \qquad \phi* = B^2.\phi \qquad (6.38)$$

and for pressure:

$$P' = \overline{\rho}.C.u$$
$$P* = B^2.P' \qquad (6.39)$$

It arises from the above analysis that the lift is $1/B^2$ times greater for the profile in compressible flow than for the corresponding profile in incompressible flow.

6.11 Prandtl-Glauert Rule:

It is found that the pressure on an airfoil in compressible flow field increases in linear proportions to the coordinates by a factor $1/B$.

Surface pressures in compressible flow about an airfoil are greater by $1/B$ than in incompressible flow about the same airfoil, or $P = \dfrac{1}{B}P*$.

CHAPTER (VII)

FANS, BLOWERS, and
TURBO-COMPRESSORS

7.1 General:

The compressible flow turbomachines could be classified into three main types; fans, blowers, and compressors. As we have seen previously for pumps and turbines there are no definite differences between the utilization of the three types. There is a common region between every two types.

7.1.1 Fans:

Fans are usually used to circulate air and usually axial flow type. The pressure does not increase, one can assume it constant during the process. So, the problem could be simplified to an incompressible flow problem. The energy supplied by fan to fluid is mainly a kinetic energy.
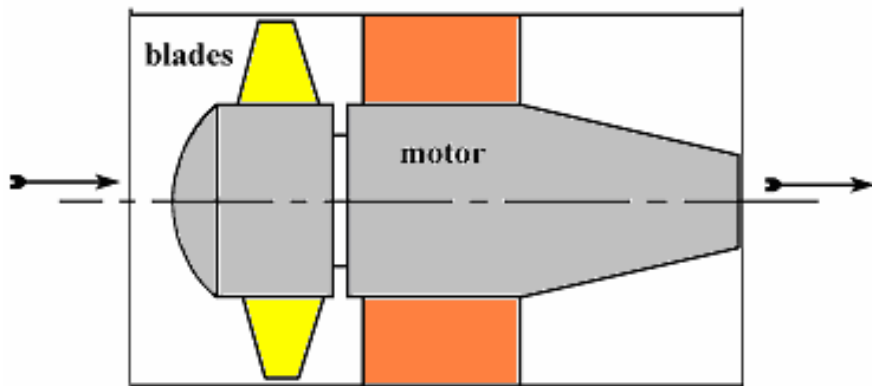
Fig.7.1 Fan with the driving motor

Figure 7.1 shows a schematic drawing for a duct type fan. The used head and capacity coefficients are $\phi' = 0.2$ to 0.3 and $\psi = 0.15$ with peripheral velocities up to 120 m/s. But at this velocity, the air velocity generates noise. To reduce the noise, peripheral velocity must be kept below 70 m/s.

7.1.2 Blowers:

Usually used when large capacity is required. It is also used to circulate gases. The pressure is slightly increased but not more than 2 kp/cm^2. The blowers could be axial or mixed flow. If the pressure increment is not sensible, the problem could be treated as incompressible flow problem. The blowers have other names according to the service in which it operates. For example, in gas service blower used to remove gasses from a coke oven is known as an exhauster.

7.1.3 Turbo-compressors:

Usually used when a compressed gas is required, the exhaust pressure is not less than 2 kp/cm^2. Centrifugal compressors, Figure 7.2, are used when high pressure is used and relatively low volumetric flow is required.

The axial flow compressors are used when large volumetric flow and low exhaust pressures are required. In this chapter, we shall deal with centrifugal compressors.
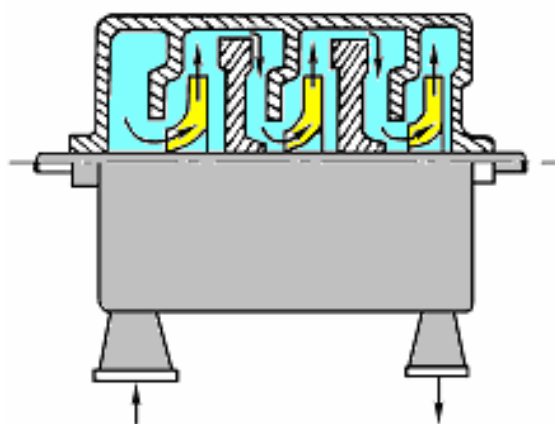
Fig. 7.2 Three-stages turbo-compressor

7.2 Head and Power:

From the work done equation, we can write the head equation if we divide by the weight flow rate.
i.e.

$$H = R.T_1 \frac{n}{n-1} \left\{ \left(\frac{P_2}{P_1} \right)^{\frac{n-1}{n}} - 1 \right\} \qquad \dots\dots\dots\dots\dots\dots(7.1)$$

Also, the head could be calculated by the classical turbomachines formula (see Chapter I and Figure 7.3).

$$H_O = \frac{U_2.C_{u2} - U_1.C_{u1}}{g}$$
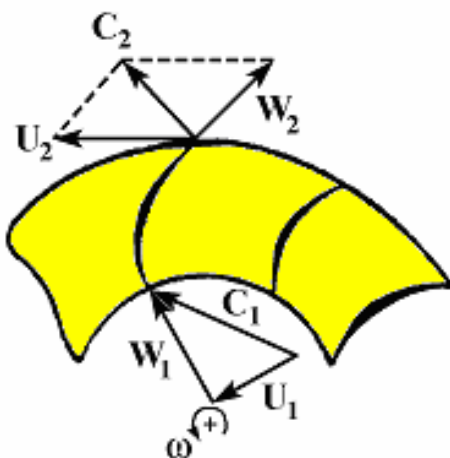
Fig. 7.3 Velocity triangles

Also, we can calculate the required head by the pressure coefficient formula:

$$\phi = U_2 / \sqrt{2g.H}$$

The pressure coefficient equation for compressors usually written on the following form;

$$\phi' = g.H / U^2 \qquad \dots\dots\dots\dots\dots\dots(7.2)$$

i.e. $H = \phi'.U^2 / g = U^2 /(2g.\phi^2)$ ....(7.3)

$\phi' = 1/(2\phi^2)$ or $\phi = 1/\sqrt{2.\phi'}$

ϕ' varies from 0.5 to 0.7

Power $P = \dfrac{\gamma Q H}{Const.\eta_{pol}}$ which usually called the gas h.p.

η_{pol} : the polytropic efficiency, sometimes called the hydraulic efficiency.

7.3 Coefficients and Specific Speed:

7.3.1. Pressure Coefficient ϕ' :

The pressure coefficient generally is a ratio between the kinetic energy and the head developed. For compressible flow machine, this definition could also be used. The pressure coefficient is the isentropic work required to raise the static pressure of the fluid to the actual level achieved in the compressor divided by the isentropic work required to raise the static pressure of the fluid to the maximum level prescribed by the impeller tip speed.

$$\phi' = \frac{H}{U^2/g} = \frac{\text{Isentropic work to reach } P_2}{\text{Theoretical work } \left(U^2/g\right)}$$

$$W.D. = C_p.T_1\left[\left(\frac{P_2}{P_1}\right)^{\frac{k-1}{k}} - 1\right]$$

$$\phi' = \frac{C_p.T_1\left\{\left(P_2/P_1\right)^{\frac{k-1}{k}} - 1\right\}}{U^2}$$ …….................... (7.4)

7.3.2 Slip Factor:

A quantitative evaluation of the influence of secondary flow is difficult to make and predicted results are rarely substantiated on test. It is customary therefore to assess this aspect of the flow problem in terms of a slip factor defined as follows:

$$\phi_s = C_{u2} / U_2 \qquad \dots\dots\dots\dots\dots\dots\dots\dots\dots\dots\dots(7.5)$$

7.3.3 Standard Air:

This expression is usually used in calculating the compressible fluid flow. The standard volume is a kind of weight flow rate because it is measured at a constant temperature and pressure. The standard cubic feet per minute SCFM is the volume of a gas at 60°F (520 °R) and 14.7 PSIA. The nominal meter cube (NM^3) is the volume of a gas at 0°C and 760 mm Hg.

7.4 Performance Characteristics:

The ideal (theoretical) performance of compressor is the same as shown before in Chapter (IV) for pump; the theoretical relation is a straight line between the head and capacity also, the same procedure as in Chapter (IV) could be used to deduce the theoretical power capacity curve.

As discussed before, the actual performance curve will change due to losses. The internal losses in a compressor are manifested by an increase in the enthalpy of the fluid with an increase in entropy. Thus, the required pressure is achieved by doing more work on the fluid to offset the effect of the irreversibilities and it is clear that the temperature of the fluid leaving the compressor must be higher than if an isentropic compression is occurred.

The performance curve of compressor could be presented on many ways; in dimensional form as head-capacity, Figure 7.4, and power-capacity, Figure 7.5, or in dimensionless forms as relative head, Figure 7.6, power, and capacity. In constructing the performance curves one must take into consideration that the volume flow rate is not constant through the machine, thus it must be specified where the volume is measured (normally at the entrance of the 1st stage) and the accompanying temperature and pressure.
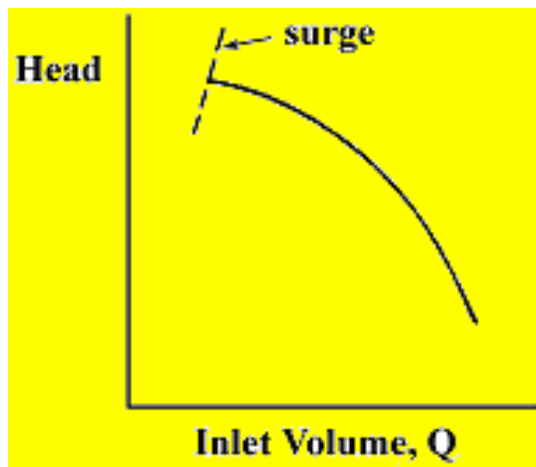
Fig. 7.4 Typical H-Q curve for a centrifugal compressor
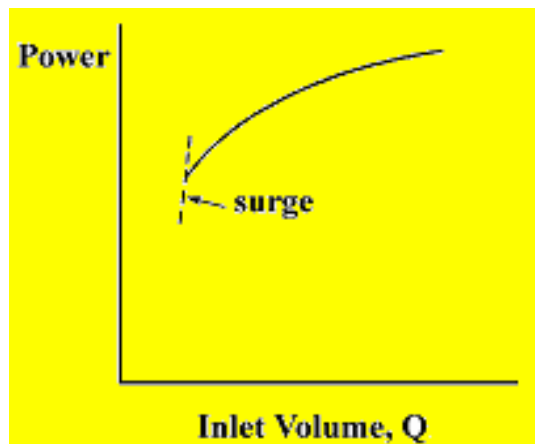
Fig. 7.5 Typical power-capacity curve for a centrifugal compressor

Another practice usually used also is the substitution of actual flow rate by the standard flow rate, which has been defined latter (NM^3, SCFM).

The Polytropic head is given by:

$$H_{poly} = R.T_1 \frac{n}{n-1} \left\{ \left(P_2 / P_1 \right)^{\frac{n-1}{n}} - 1 \right\} \qquad ....(7.6)$$

The Polytropic head H_{poly} is an imaginary head corresponding to the effective head H in the case of incompressible fluids but has no measurable physical counterpart.

Figure 7.7 shows a typical centrifugal compressor performance curve with its related terminology.
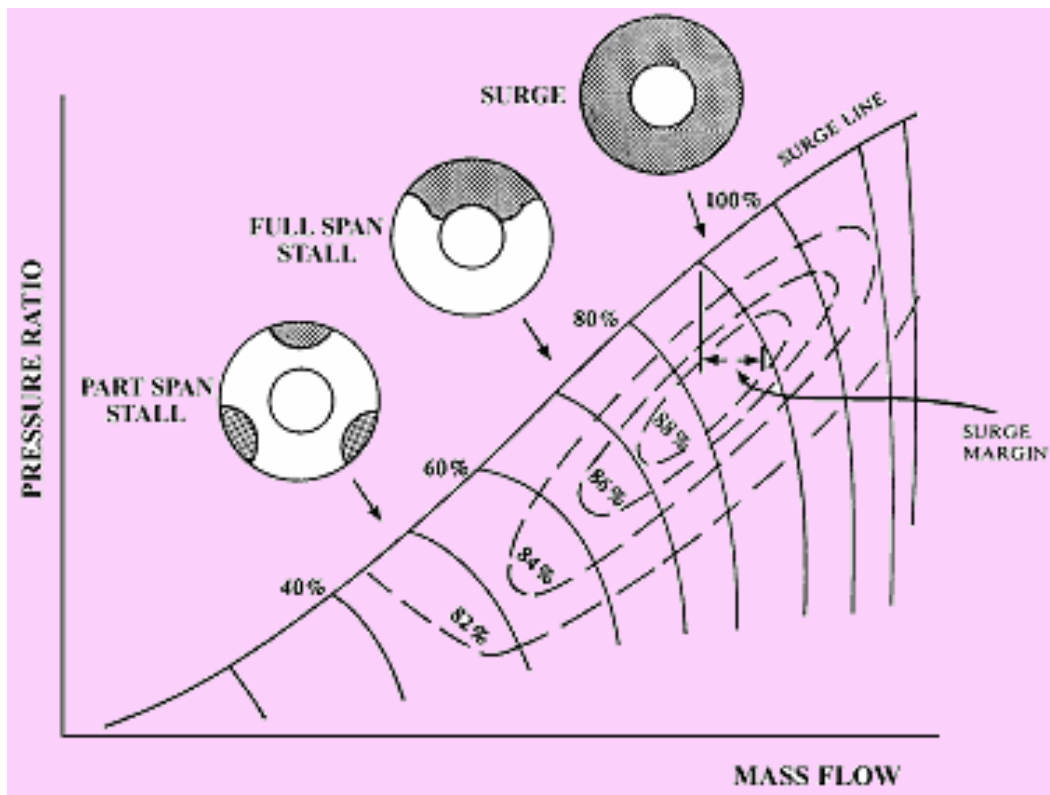
Fig. 7.6 Performance curve for centrifugal compressor. Solid lines are characteristics at various speeds; dotted lines are corresponding efficiencies

In the general sense, the shape of the head-capacity curve, Figure 7.7, refers to the extent of its stable flow rise as flow decreases. The full extent is defined at the low end by the flow rate at which surge begins, "surge flow" and at the high end by the maximum amount of flow in machine can pass and still be a contributor of positive head, "stone wall". The high flow region of the curve for compressor designed for air and lighter gases tends to fall smoothly and continuously to the zero head line. The high flow region of the head curve for compressors handling heavier gases than air tends to decrease more sharply because sonic velocity shock disrupts head generation at flow rates not far above rated.

208
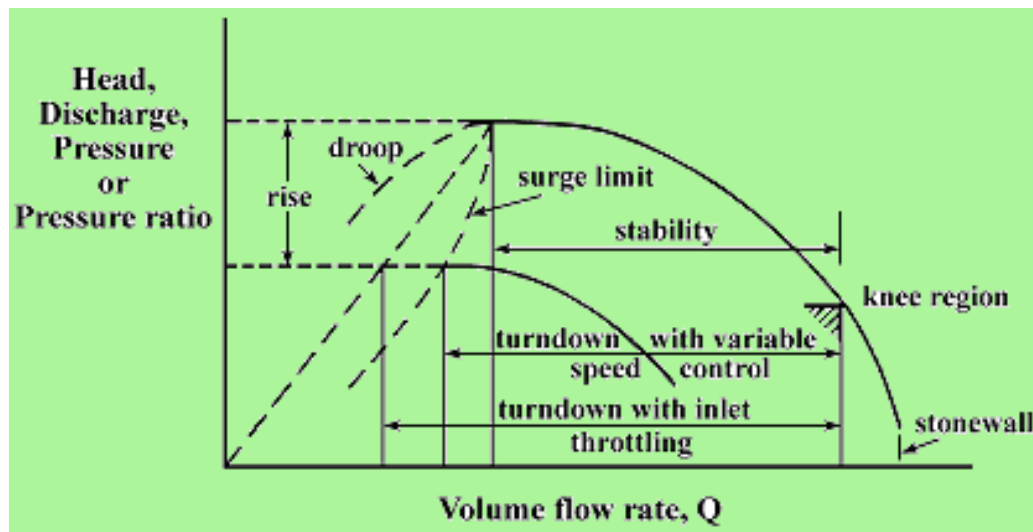
Fig. 7.7 Centrifugal compressor performance curve

The surge flow and maximum flow rates for multistage machine reflect the surge flow and maximum flow rates of the particular stages in the series which reach unstable flow (as flow decreases) and maximum flow (as flow increases) first.

The "*steepness*" of the head-capacity curve refers to the rise in head or pressure ratio or discharge pressure from a designated operating point to the point at which surge begins, since the location of the particular operating point on the overall curve is arbitrary.

The "steepness" tends to be influenced as much by the location of the operating point as it is by the absolute shape of the curve. If the operating point of interest is very close to the surge point the steepness is very low. If the operating point is beyond the peak efficiency flow rate near the stone wall region, the useful position of the curve tends to be very steep.

The form of the compressor characteristic, which best describes how "steepness" affects surge sensitivity in a practical system, is the pressure ratio versus capacity curve, rather than head versus capacity curve. The pressure ratio curve gives a quick indication of the magnitude of change in either suction or discharge pressure will send the compressor into surge. The pressure ratio curve differs from the head-capacity curve from which it is derived by virtue that it is directly affected by the gas molecular weight. Those gases with high molecular weight tend to make

the pressure ratio-capacity curve steep while the low molecular weight gases tend to flatten the curve.
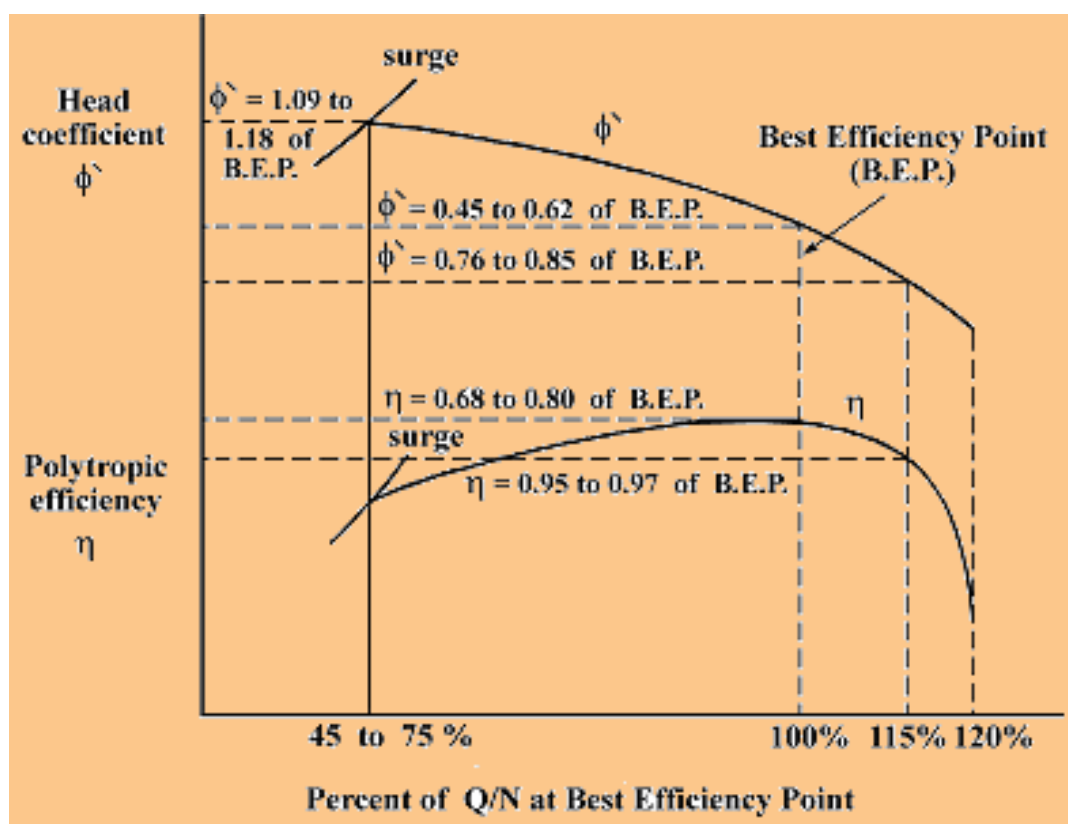
Fig. 7.8 Performance curves w. r. t. B.E.P.

The term *stability* means the stable flow range between surge and normal flow. Stability with respect to normal flow is defined as the percent of change in capacity between normal and surge point at normal speed; this equals 100 % minus the percent ratio of the actual volume flow rate of which surge begins (at normal speed) to the normal volume flow rate. The term "*turndown*" means the mass flow reduction, which is possible before encountering surge, recognizing the effects of the control method. "Turndown" with respect to normal flow is defined as the percent of change in capacity between normal and the surge point at rated head when operating at design inlet temperature and gas composition; it equal 100 % minus the percent ratio of the surge point mass flow at normal head to normal mass flow.

7.5 Mach Number Consideration:

Shock and flow separation are distinct possibilities even when the Mach number is less than unity.

Consider now the problem at the impeller eye;

i.e. $\quad M_1 = \dfrac{W_1}{\sqrt{g.K.R.T_1}}$ ....(7.7)

It could be seen that the maximum Mach number occurs at the outer radius of the eye at which W has its maximum value. To avoid shock and separation, Mach number at inlet must be about 0.85. Thus even if it reaches unity at impeller tip, diffuser will decelerate the flow.

7.6 Pre-Whirl:

When the absolute velocity of approach is high enough or the static absolute temperature is low, this will increase the Mach number as discussed before. The pre-whirl offers an opportunity to reduce the Mach number at eye entrance. The pre-whirl is obtained by bending the inlet guide vane in such a way as seen in Figure 7.9 to reduce the relative velocity.

i. No pre-whirl   ii. Pre-whirl
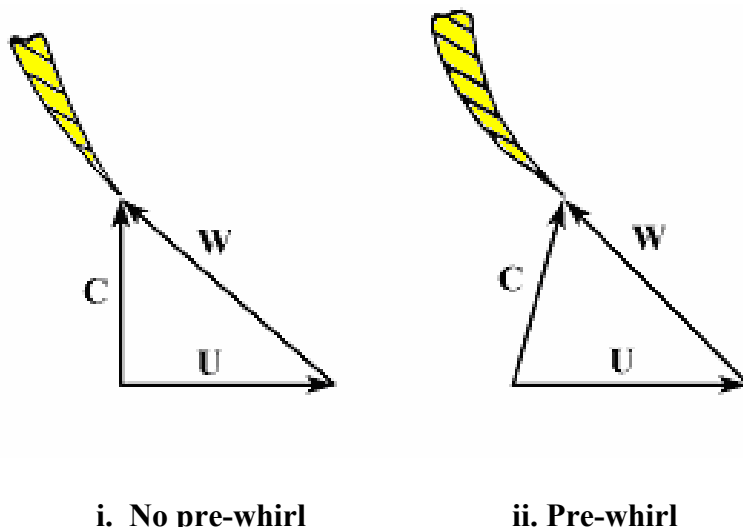
Fig. 7.9 The pre-whirl tends to reduce the relative velocity W

7.7 Surging:

Surging occurs when the losses are equal to the energy gained, this will cause the flow to stagnate causing backward pressure waves and will then move backward. This will cause the damaging of the machine.

It is difficult to predict the surge point, only experience could determine exactly the surge point. Usually, any operating point should lay 10 to 15 % away from the surge point.

7.8 Radial Type Impeller Design:

As stated in Chapter (IV), there is no standard procedure but every manufacturer has his own design procedure. All of them contain the same outlines. Here, only the general outline will be considered.

The design procedure used before in Chapter (IV) could be applied except that we take into consideration the compressibility effect. Many of design aspects have been discussed in Chapter (IV). This will not be regarded here. It should be referred to Chapter (IV) for details.

The speed is usually specified by the purchaser and depends on the kind of the driver, if it is a gas turbine or steam turbine or motor. This machine operates at high speed and thus the stress problem is very important.

As a first approximation, shaft diameter, Figure 7.10, could be found by using the following formula:

$$D_s = \sqrt[3]{\frac{16.T}{\pi.S_s}} \qquad \text{…..(7.8)}$$

The hub diameter D_H is varied from 2 to 5 cm greater than the shaft diameter. The eye diameter D_o is obtained from the continuity equation:

$$Q_1/V = \frac{\pi}{4}\left(D_o^2 - D_H^2\right) \qquad \text{...(7.9)}$$

The inlet diameter D_1 is equal or slightly larger than the eye diameter.

The impeller inlet width b_1 is found from the expression;

$$b_1 = Q_1 / (\pi.D_1.C_{r1}.\varepsilon_1)$$ ....(7.10)

Then $\tan \beta_1 = C_{r1} / U_1$, $U_1 = \pi.D_1.N / 60$
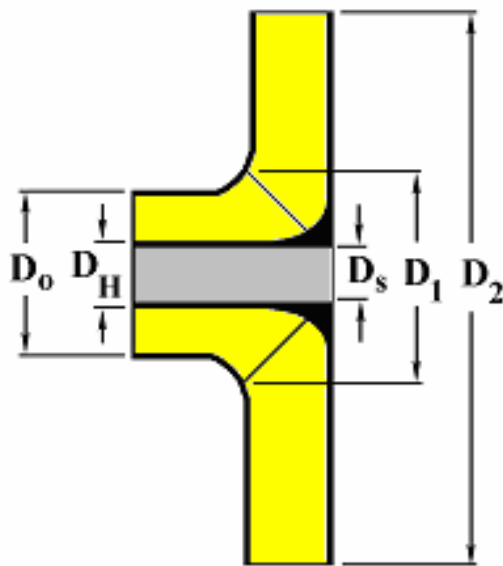
Fig. 7.10 Impeller Dimensions

To calculate the outlet dimensions, assume ϕ' varies from 0.4 to 0.65.

$$H = \phi'.U_2^2 / g$$

and $$H = R.T_1 \frac{k}{(k-1)\,\eta_p} \left[(P_2 / P_1)^{\frac{k-1}{k.\eta_p}} - 1 \right]$$ ....…..................(7.11)

The polytropic efficiency varies from 0.65 to 0.75 and

$$U_2 = \pi.D_2.N / 60$$

β_2 could be assumed between 90 to 135°. From stress standpoint a 90° angle is more satisfactory because the bending stresses are then eliminated. C_{r2} is slightly less than C_{r1}. The outlet width: $b_2 = Q_2 / (\pi.D_2.C_{r2}.\varepsilon_2)$.

Now, the outlet velocity triangle could be drawn. The circulatory flow effect reduces the tangential component C_{u2} by an amount equal to X, which could be calculated by the following formula;

$$X = \frac{\pi.\sin(180 - \beta_2)}{Z} \quad\quad\quad ....(7.12)$$
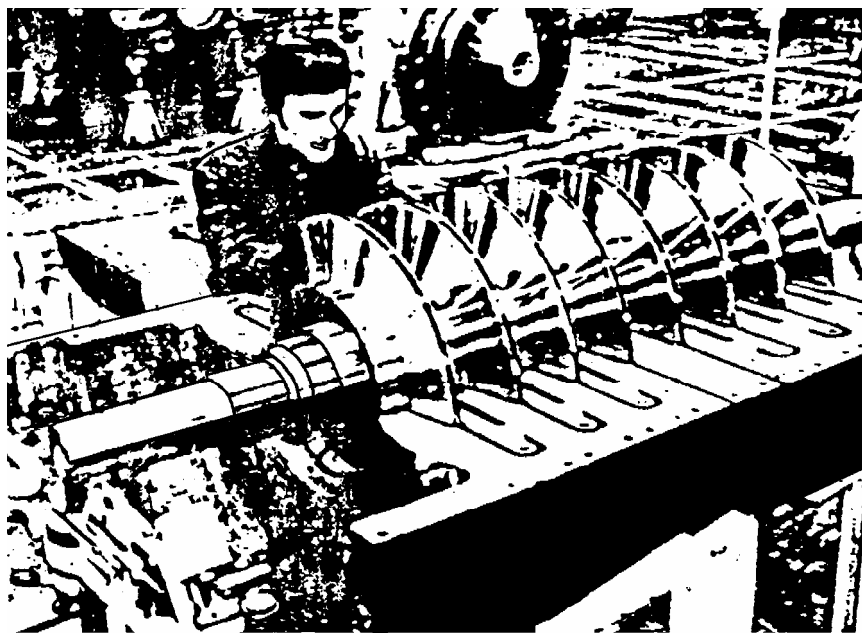
Fig. 7.11 Typical multistage process centrifugal compressor showing the flow-path layout (courtesy of Nuovo Pignone)
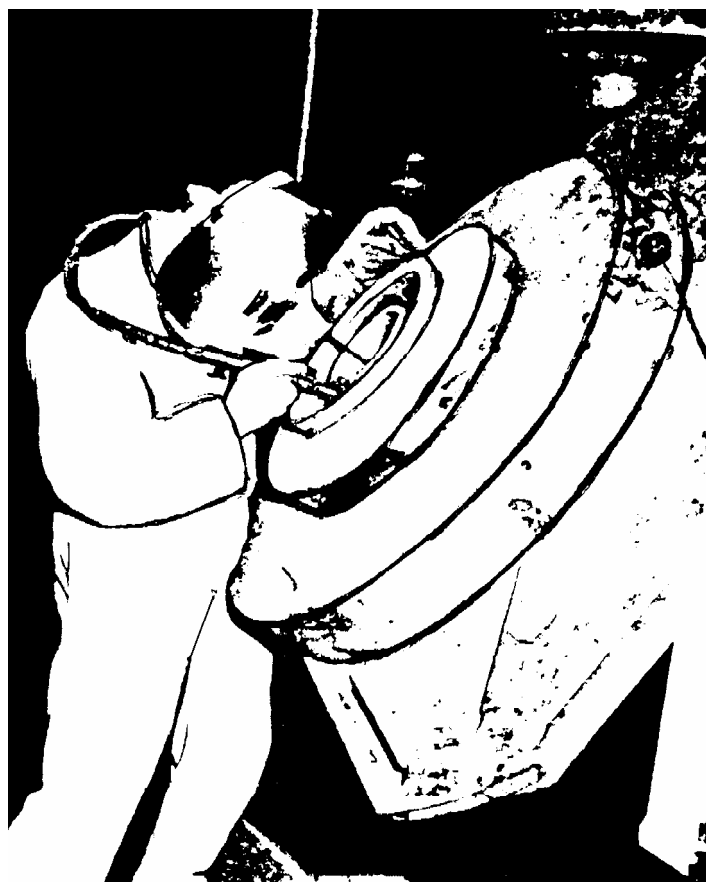
Fig. 7.12 Welding of an impeller for centrifugal compressor (courtesy Dresser Industries, Clark Division)
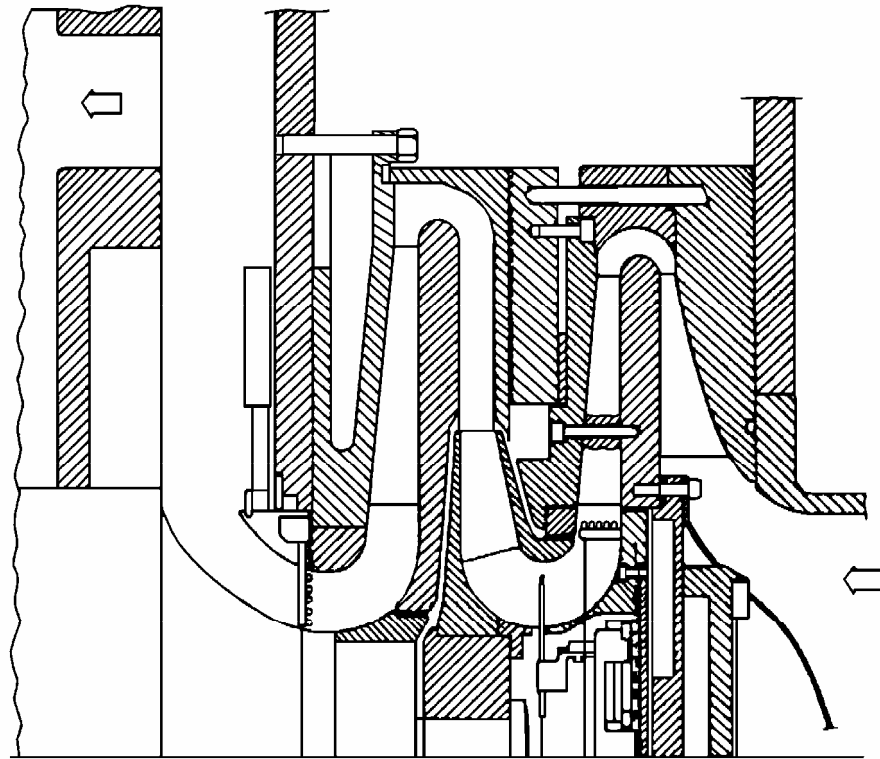
Fig. 7.13 Sectional view in a centrifugal compressor showing one stage for test purposes (courtesy Nuovo Pignone)
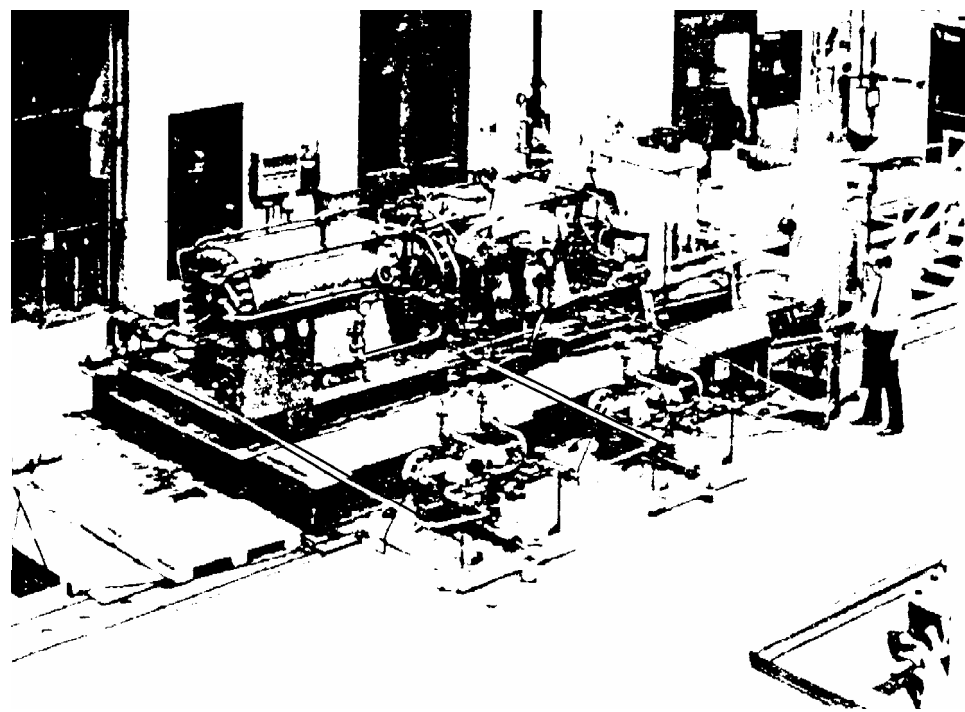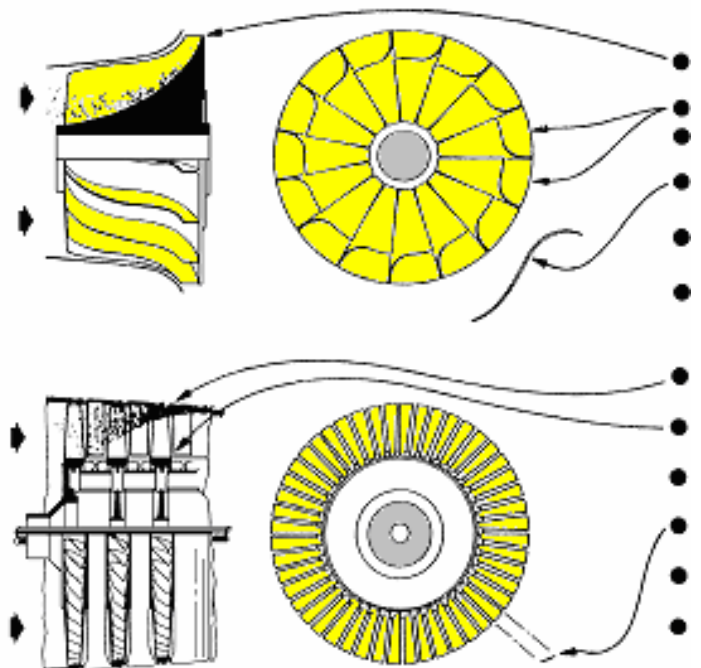
Fig. 7.14 Two vertically split centrifugal compressors on performance test (courtesy Dresser Industries, Clark Division)

COMPRESSOR AIR FLOW PATTERNS

Centrifugal

- Foreign objects centrifuge toward heavy blade root

- No blade clearance problem
- High pressure ratio provided with 2 stage compressor
- Blade fineness ratio-low (Higher relative strength and greater shock resistance)
- Efficiency not materially affected by film build-up or coating of foreign material
- Large foreign objects rejected at compressor face without significant performance degradation

Axial

- Foreign objects centrifuge and mass toward and against delicate blade tips

- Minute clearances between blades and stators increases sensitivity to fod

- Exposure to fod is high due to number of stages required for a given pressure ratio
- Blade fineness ratio-high (lower relative strength and shock resistance)

- Significant performance degradation due to foreign material filming

- Rotating clearances and design geometry will not accept ingestion of large foreign objects without possibility of total compressor failure

Fig. 7.15 Compressor air flow patterns
(courtesy Dresser Industries, Clark Division)

CHAPTER (VIII)

VOLUMETRIC MACHINES

Volumetric machines are those kind of machines which the energy transfer occurs due to the displacement of a certain volume which is alternately filled with the fluid and then emptied again.

This displacement could be linear as in the case of the reciprocating pump and compressors, or angular displacement as in the case of the rotary pumps.

The discharge of this kind of machines depends almost wholly on the speed of rotation and hardly at all upon the working pressure.

8.1 Reciprocating Pumps:

8.1.1 Piston Pumps:
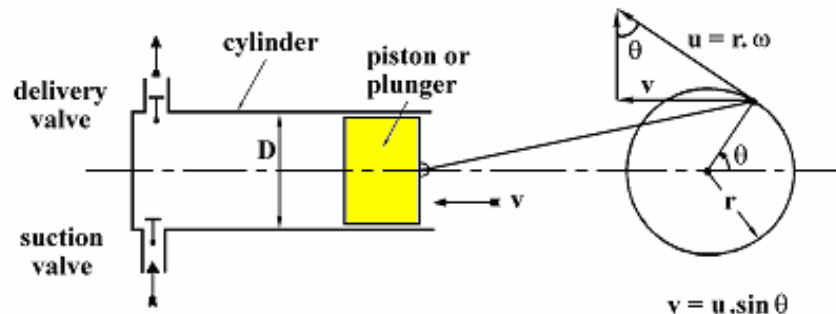
Fig. 8.1 Piston pump

The reciprocating pump, Figure 8.1, consists of a hollow cylinder and a moving piston or ram, the rotary motion of the shaft is converted to linear motion by means of the classical method of crankshaft and

connecting rod. This is the classical method used in petrol engines to convert linear motion to angular one.

The volumetric rate could be easily calculated from the following formula:

$$Q = \frac{\pi}{4} D^2 \frac{2rn}{60}$$

(8.1)

where: D = diameter of ram
r = crank radius
n = speed in r.p.m.

The swept volume $= \frac{\pi}{4} D^2 .2r$

The actual volumetric flow rate is lower than the theoretical because of leakage.

The volumetric efficiency is the ratio of the actual discharge to the theoretical discharge.

$$\eta_v = Q_a / Q$$

(8.2)

The volumetric efficiency could be written on the following form, $(Q - Q_a)/Q$ which is called the *slip*.

8.1.2 Instantaneous Rate of Flow:

The calculated discharge is the mean discharge but normally due to the ram motion, the discharge is varied with the time. This variation which occurs in a time interval (the revolution) repeats itself every revolution as simple harmonic motion.

Figure 8.2 shows the discharge fluctuation. The discharge reaches a maximum value at the middle of the stroke, then discharge becomes zero during the suction stroke.
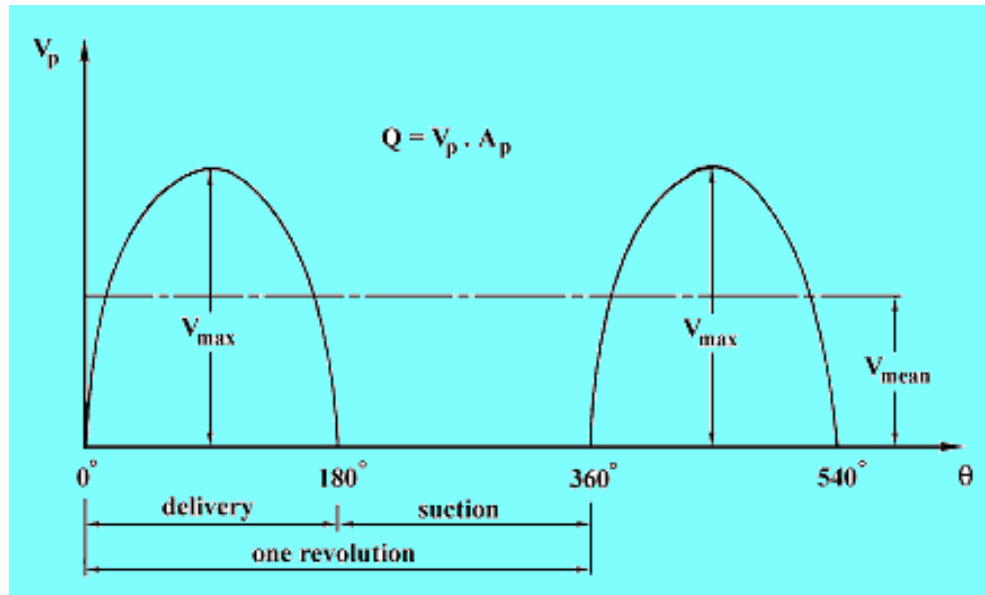
Fig. 8.2 The instantaneous velocity in delivery pipe

To find the shape of the relation between V_P and θ (or time), assume that the volume displaced by the piston at time t equal to that passing through the delivery pipe at the same time.
Thus:

$$V_P \frac{\pi}{4} d^2 = v \frac{\pi}{4} D^2$$

where: d = the delivery pipe diameter
v = the piston velocity

$$v = u \sin \theta = \frac{2 \pi n r}{60} \sin \theta \qquad (8.3)$$

where u is the crank pin velocity.
Thus:

$$V_P = \frac{2\pi.n.r}{60} \cdot \frac{D^2}{d^2} \sin \theta \qquad (8.4)$$

So, the relation between V_P and θ is a kind of a sinusoidal curve.

To overcome this fluctuation in the flow, air vessel is used, Figure 8.3. The air vessel is a container filled with compressed air at a certain pressure. The container is placed on the delivery pipe, during the delivery stroke all fluid in excess of the mean discharge will be stored in the air vessel, this will be replaced during the suction stroke.

220
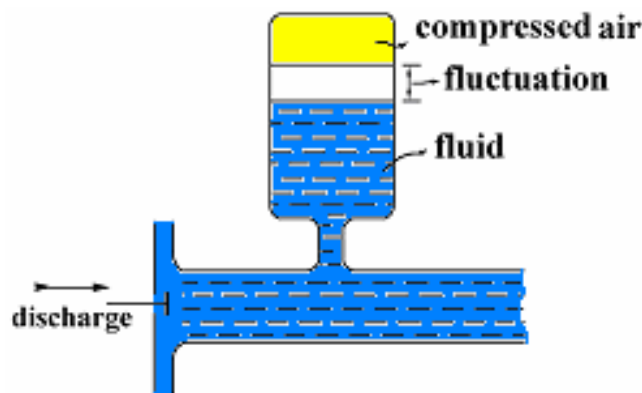
Fig. 8.3 Air vessel

Some slight change in the air pressure must naturally take place as the fluid surface in the vessel rises and falls. At high pressure, air is slowly dissolved in liquid, the dissolved air must be replaced in large units and air compressor is used.

Another way to overcome the fluctuations in the discharge is the use of multi-cylinder pump. It is preferably to use two or more cylinders of smaller sizes to supply the required discharge. As much as the cylinders number increased the fluctuation decreased. This fact will be noticed from Figure 8.4.
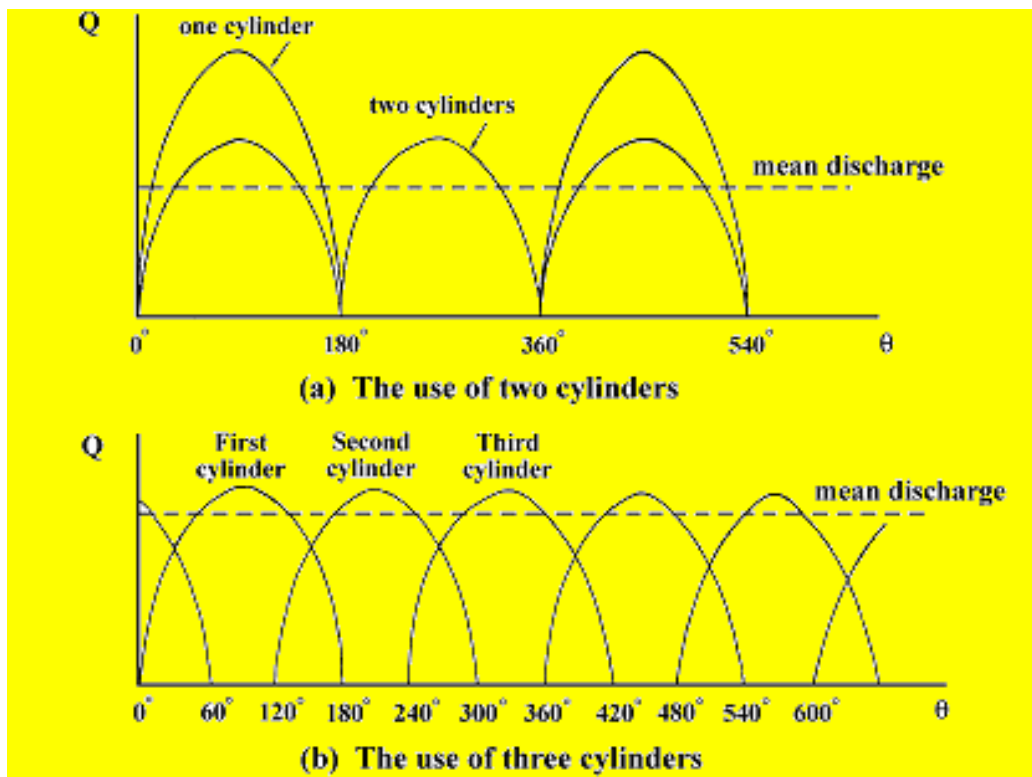
Fig. 8.4 The damping of fluctuation

8.1.3 Diaphragm Pumps:

It is a kind of reciprocating pumps provided by flexible diaphragm instead of the piston. The motion of the diaphragm is provided by means of a lever adjacent to a cam as seen in Figure 8.5.

Diaphragm pumps are particularly advantageous in handling dirty or corrosive fluid. Also, this kind of pumps is usually used in petrol engines as fuel pump.
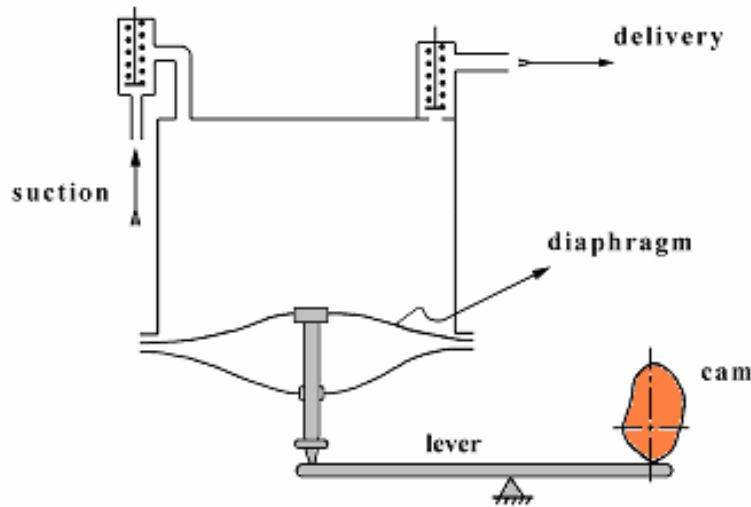
Fig. 8.5 Diaphragm pump

** Pressure and Discharge Regulation of Reciprocating Pump:

The reciprocating pump could deliver an infinite pressure. It depends on the power supply and system design. So usually a control valve could be used to control the pressure and recirculating the excess fluid again into the sump, Figure 8.6.

The discharge regulation is also provided by means of a by-pass system, which could be opened during the starting until we reach the normal operation.
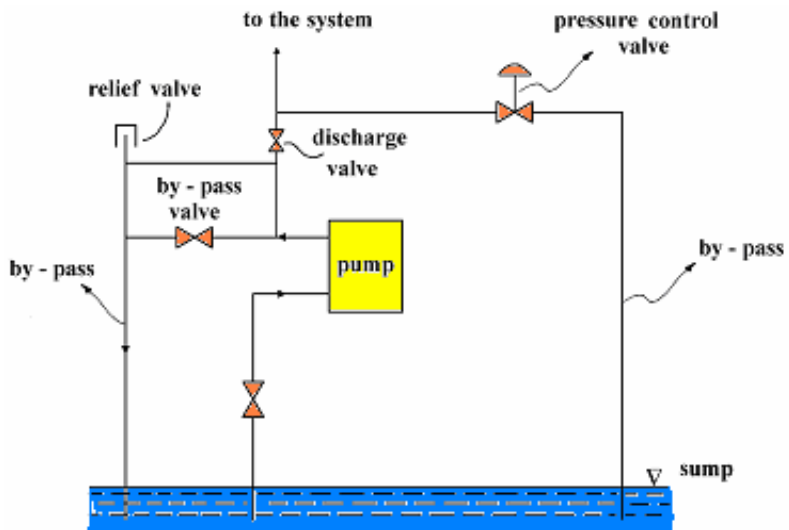
Fig. 8.6 Typical positive pump installation

8.1.4 Reciprocating Pump Trouble Shooting:

Trouble	Possible Reasons	Trouble	Possible Reasons
Pump does not discharge	* Suction lift too high. * Pump not primed. * Suction air-bound. * Suction line vapor bound. * Obstructions in suction line. * Worn parts.	Discharge pressure fluctuates	* Speed higher than rated. * Tight packing. * Pump not primed. * Pump not aligned. * Suction lift too high. * Suction air bound.
Pump short strokes	* Wrong lubricant. * Packing too tight. * Gas or air in liquid. * Incorrectly set valves	Low discharge pressure	* Packing tight. * Back pressure high. * Valves or rings worn.
Piston hits head	* Excess in last motion. * Piston rings worn. * Leaky liquid valves.	Pump runs too fast	* Suction-line troubles. * Liquid-piston packing worn.
Pump stops	* Valve trouble.	Excess in packing wear	* Piston-rod defects * Rod lift.

8.2 Rotary Pumps:

There are many types of rotary pumps, as rotary cylinder pumps, gear pumps.... etc.

224

8.2.1 Rotating Cylinder Pump:

The radial rotary pump consists of the illustrated mechanism in Figure 8.7. The rotation of the shaft makes the ram moves in and out of the cylinder, compressing the liquid in between. The suction and delivery holes are located longitudinally on the outer cylinder.
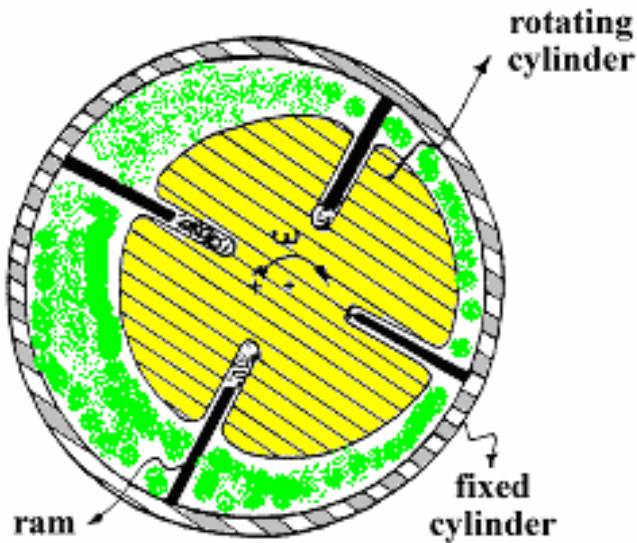
Fig. 8.7 Radial cylinder rotary pump

The parallel cylinder rotary pump consists of a rotating cylinder block and a fixed plate. The pistons are connected to a ring mounted on the rotating shaft, Figure 8.8. The ring is inclined with a certain angle to the shaft. Due to this inclination the pump operates.
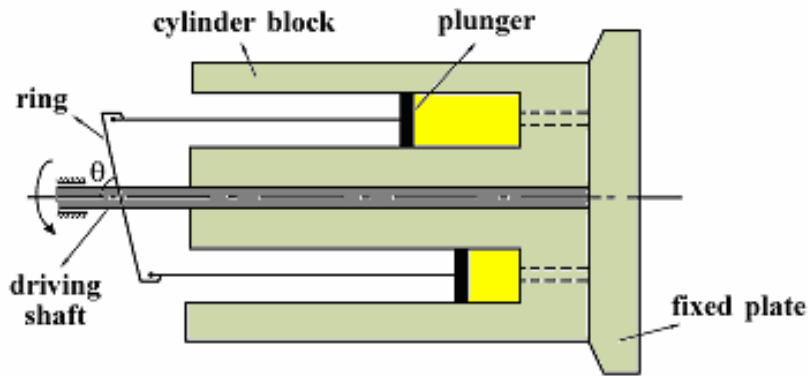
Fig. 8.8 Parallel cylinder rotary pump

8.2.2 Gear Wheel Pump:

The gear pump consists of two identical intermeshing gears, Figure 8.9. For a small pump, only one gear is connected to the driver and the other is turning idly.
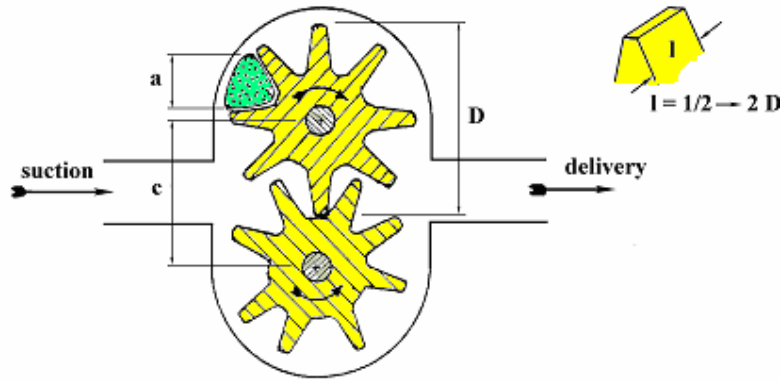
Fig. 8.9 Gear wheel pump

The discharge could be calculated by the following formula;

$$Q = \frac{2.a.l.n.N}{60}$$ (8.5)

where:

a = area enclosed between any two adjacent teeth and the casing.
l = axial length of teeth.

n = number of teeth in each gear.

N = speed in rpm.

The last formula is not of great practical use because of the difficulty of measuring the area between two teeth. An approximate formula could be used, easily, as follows:

$$Q = K C (D - C) l \qquad\qquad (8.6)$$

where:

K is a constant = 2.983

D is the gear diameter.

C is the distance between the two gear centers.

The gear pump is usually used in the lubrication of petrol engines, as lube oil pump.

8.2.3. Rotary Pump Trouble Shooting:

Trouble	Possible Reasons	Trouble	Possible Reasons
Pump does not discharge	* Suction line troubles. * Pump not primed. * Pump worn excessively. * Driver troubles. * Open or leaking relief valve or by-pass. * Excessive suction lift.	Reduced capacity	* Suction line troubles. * Air in pump casing. * Driver troubles. * Excessive wear. * Discharge misdirected.
Excessive noise	* Liquid troubles. * Misalignment. * Discharge pressure too high.	Excessive power consumption	* Excessive discharge pressure. * Shaft troubles. * Liquid too thick. * Pump speed higher than rated.
Excessive wear	* Liquid troubles. * Discharge pressure too high.	Pump loses its suction	* Suction line troubles.

8.3 Performance of Positive Pumps:

The performances of positive pumps are generally the same for all kinds of this pump, Figures 8.10 and 8.11. This kind of pumps discharge

a definite quantity of liquid for each revolution, provided their suction is flooded and the discharge head is zero.

(a) constant speed   (b) constant pressure   (c) constant speed
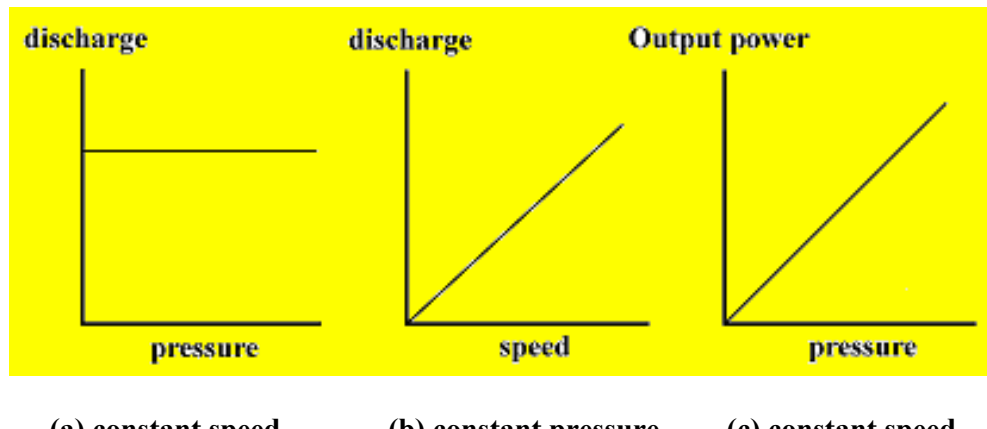
Fig. 8.10 Ideal performance of positive pumps
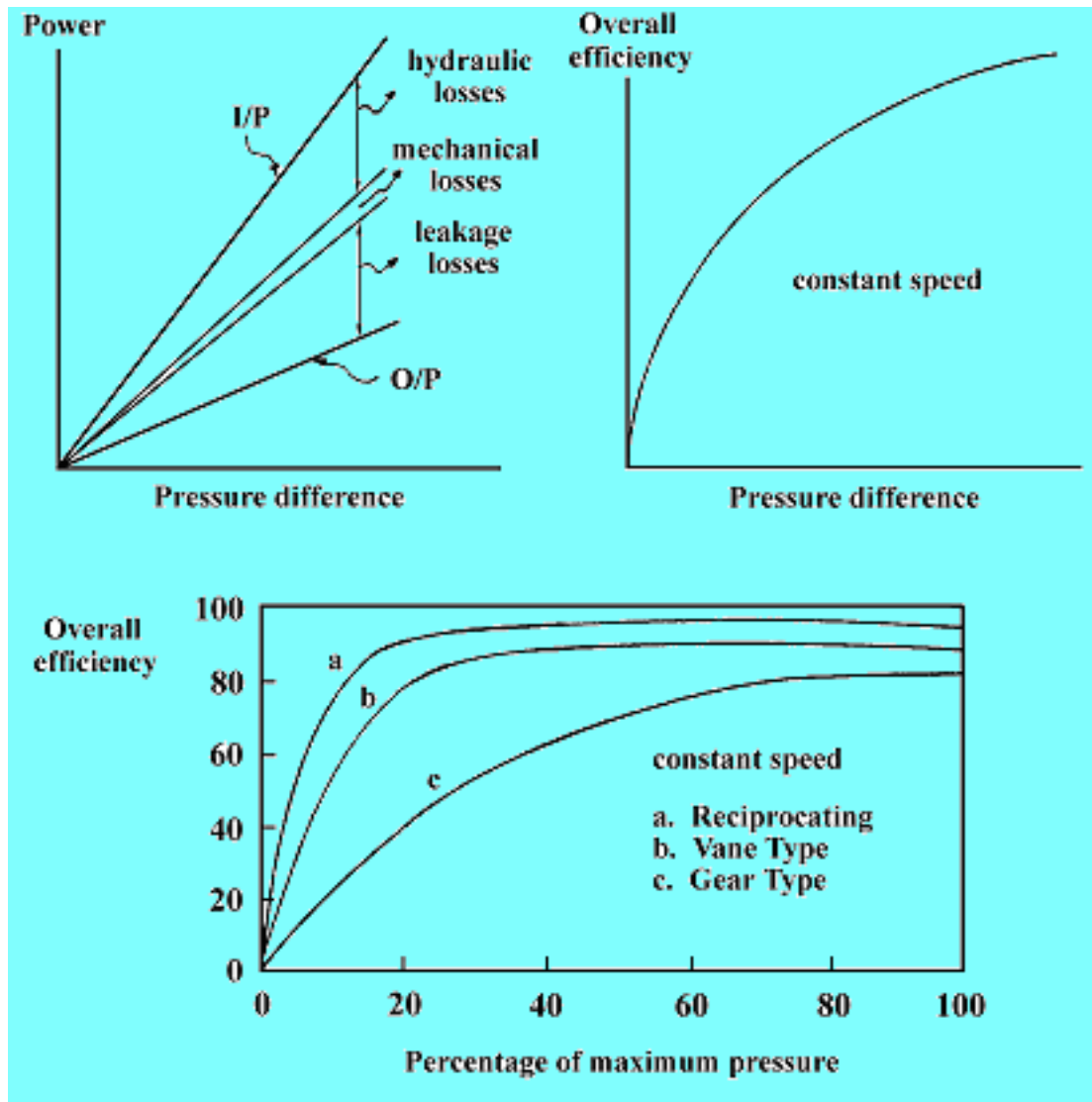
Fig. 8.11 Actual performance of positive pumps

As it could be seen from performance curves, the positive pumps are sensible to the speed variation and the discharge depends almost on the speed.

8.4 Inertia Pressure in Delivery and Suction Pipes:

Due to the fact of the discontinuity of the discharge from a reciprocating pump, inertia pressure will result. The inertia pressure is defined as follows; $P_i = \gamma \, l V_p / g.t$.

Consider a short time interval, thus substitute dV_p / dt for V_p / t, the acceleration of the water in the horizontal pipe $= dV_p / dt$;

$$dV_p / dt = (dV_p / d\theta)(d\theta / dt) = \omega.r.(D^2 / d^2).\cos\theta.(d\theta / dt)$$

and $d\theta / dt$ is the angular speed of crank shaft (ω), thus;

$$dV_p / dt = \omega^2.r.(D^2 / d^2).\cos\theta$$

Substitute in the inertia equation by this value;

$$P_i / \gamma = (l / g).\omega^2.r.(D^2 / d^2).\cos\theta \tag{8.7}$$

The maximum value of P_i will occur at $\theta = 0°$ and $180°$, or the ends of the stroke. The consequence of the pressure inertia rise in the delivery is the reduction in the pressure in the suction side. If the pressure in suction side is increased until it reaches the corresponding vapor pressure, cavitation will occur. The sign of cavitation will be the high noise and milky appearance of the water.
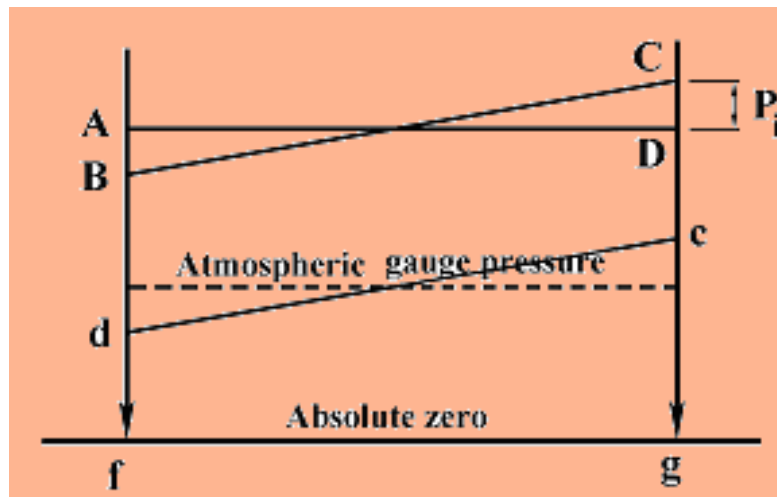
Fig. 8.12 Pressure in delivery line

It is clear from Figure 8.12 that the mean pressure in the delivery line is AD. If fd is smaller than the vapor pressure, cavitation will occur. It is important to notice that the work done is constant, hence the area fADg equals the area fBCg.

APPENDIX "I"

PRESSURE RECOVERY DEVICES
---

1. General:

The energy of the fluid leaving the blade consists of kinetic energy and pressure energy $(\dfrac{C^2}{2g}+\dfrac{P}{\gamma})$. Usually, any pump or blower is used to raise the fluid pressure, so the efficiency of the machine will be increased as much as one could convert the kinetic energy to pressure energy. The pressure recovery devices, as a general, consist of gradually expanded passages, which provide a gradual deceleration to the fluid motion. As a general, the ratio of the kinetic energy with reference to static pressure energy is higher in forward curved impeller than backward. This process of pressure recovery could be responsible of fairly high losses.

According to Bernoulli's equation, if (1) denotes the condition at the inlet of the diffuser and (2) denotes the condition at the exit of the diffuser, so:

$$\Delta P = P_2 - P_1 = \frac{\gamma\, C_1^2 (1 - A_1^2 / A_2^2)}{2g} \qquad \text{..........................} (1)$$

where A_1 and A_2 are the inlet and exit areas, respectively. The efficiency of the diffuser is defined as the ratio of the static pressure gain to the kinetic energy.

$$\eta_d = \frac{(\Delta P)_{actual}}{C_1^2 (1 - A_1^2 / A_2^2)(\gamma / 2g)} \qquad \text{..........................} (2)$$
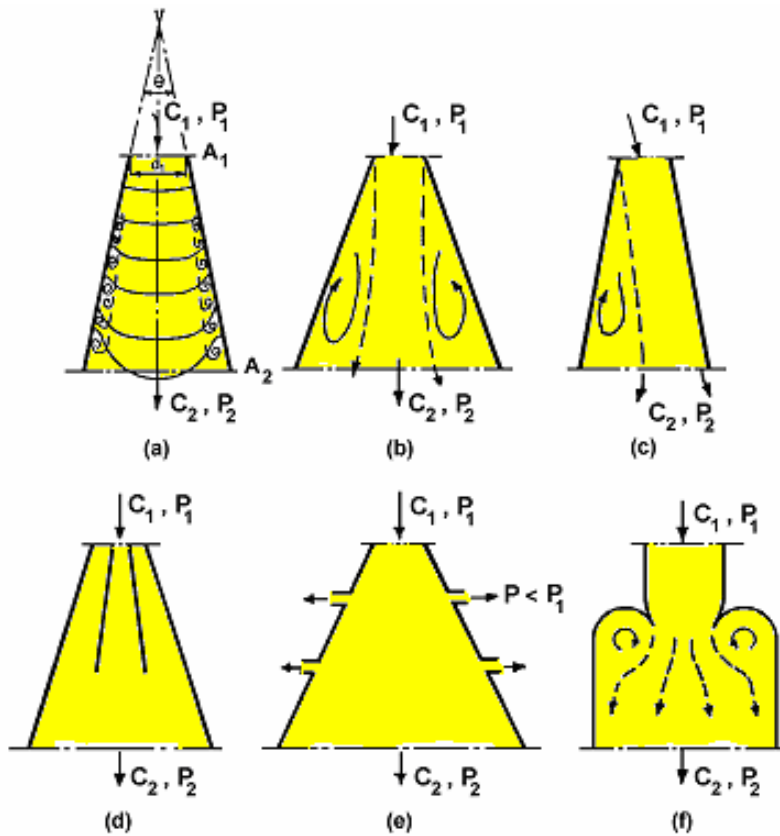
**Fig. 1 Diffuser. (a) Boundary-layer increase in diffuser. (b) and (c) Stall zones.
(d) Short vane dividers. (e) Boundary-layer absorption.
(f) Diffuser with standing vortices.**

Figure 1 shows some different diffuser types. A larger angle of divergence could lead to separation of flow from walls. The roughness of the internal wall of the diffuser is an important factor in determining losses as the creation and the development of boundary layer could be accelerated by higher degree of roughness.

Figure 2 shows some results of experiments on the relation between the angle of divergence θ, the diffuser length to width ratio, and the efficiency of the diffuser. Since the losses are mostly connected with the formation of boundary layers. Some particular behavior of boundary layers will be discussed in this Appendix.
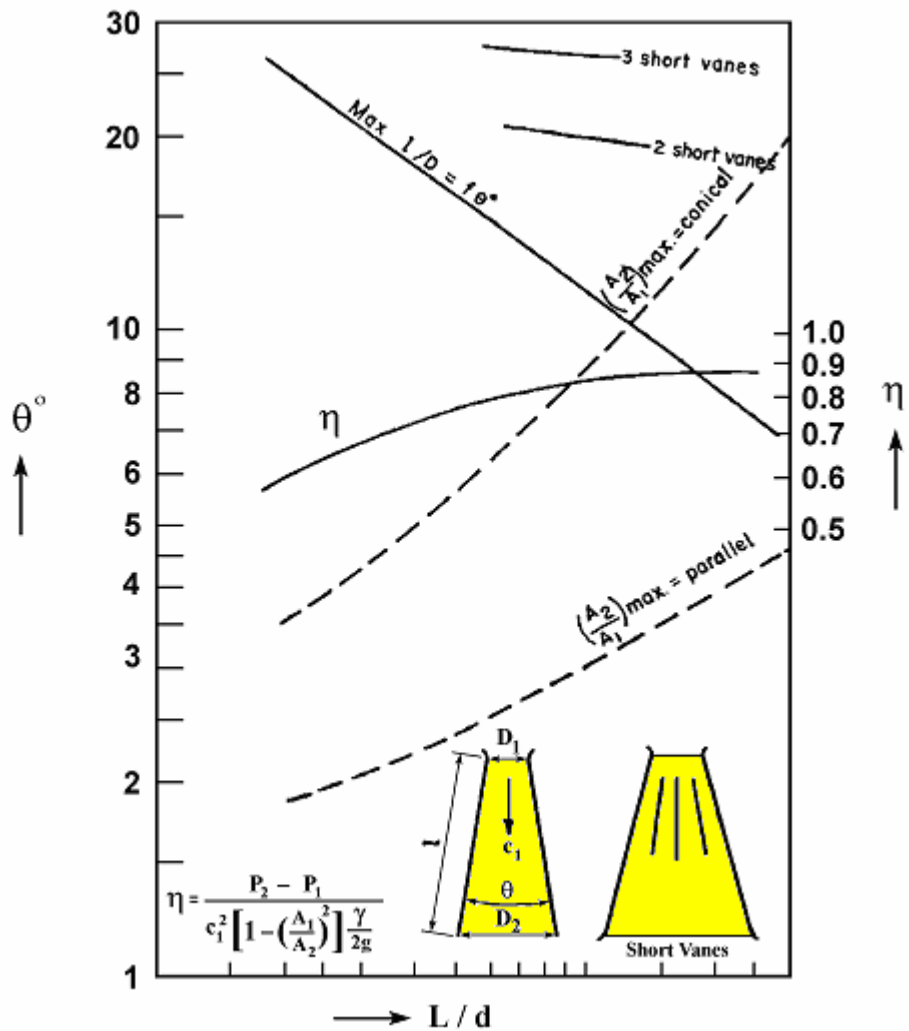
Fig. 2 Angle of divergence θ of diffusers versus *l/D* (at stall limits) and recovery value η. (Based on test result reported by Kline)

1.1 Calculation of Loss Coefficient:

Consider a straight cascade, as shown in Figure 3. The velocity distribution at the trailing edge will be deformed due to the deceleration of the flow adjacent to the blade, this will manifest by a depression right on the trailing edge, this depression will gradually disappear with increasing distance, this equalization process results in energy dissipation.
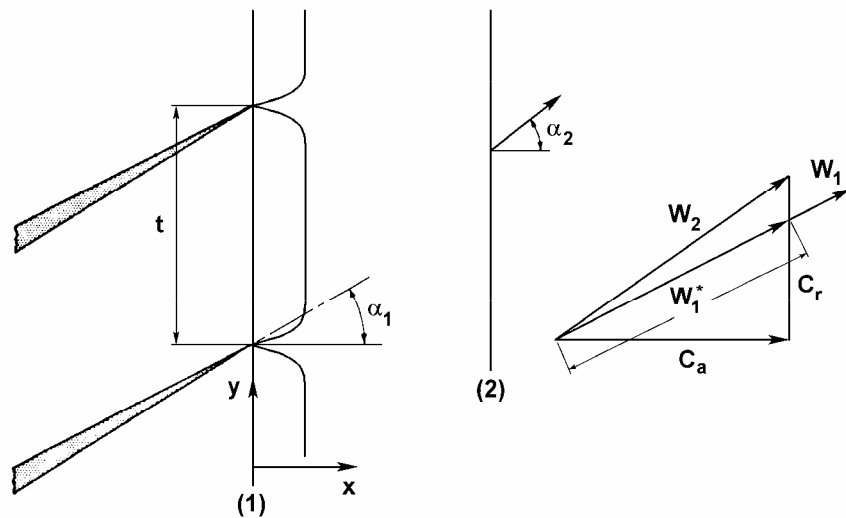
Fig. 3 Boundary layer effects at the exit of a cascade

This loss may be related to the boundary layer parameters. If W denotes the relative velocity in the cascade channel, due to the formation of boundary layer the velocity W_1 in the core region will be higher than the ideal W_1^*. Denote the condition at the exit of the cascade by (1) and further downstream in the diffuser by (2). The boundary layer at the trailing edge is characterized by its displacement thickness:

$$\delta_d = \int_{-\infty}^{+\infty} \frac{W_1 - W}{W_1} dn \qquad \text{... (3)}$$

and momentum thickness:

$$\delta_m = \int_{-\infty}^{+\infty} \frac{W}{W_1} \cdot \frac{W_1 - W}{W_1} dn \qquad \text{... (4)}$$

The through flow velocity C_a can be found after the continuity as follows:

$$C_a = \frac{1}{t} \int_{-t/2}^{t/2} W \cos \alpha_1 . dy \qquad \text{... (5)}$$

From equation (3) and substituting dn by $\cos \alpha_1 . dy$ and integrating equation (5):

$$C_a = W_1 \cos\alpha_1 \left(1 - \frac{\delta_d}{t\cos\alpha_1}\right) \quad \text{.................................} \quad (6)$$

Consider the momentum balance between (1) and (2) in tangential direction;

$$\rho \sin\alpha_1 \cos\alpha_1 \int_{-t/2}^{t/2} W^2 dy = \rho C_a C_r t \quad \text{........................} \quad (7)$$

with

$$W^2 = W_1^2 - (WW_1 - W^2) - W_1(W_1 - W) \quad \text{.....................} \quad (8)$$

Introducing the dimensionless displacement and momentum thickness;

$$\Delta = \frac{\delta_d}{t\cos\alpha_1}, \quad \theta = \frac{\delta_m}{t\cos\alpha_1} \quad \text{.................................} \quad (9)$$

then

$$W_1 \cos\alpha_1 = \frac{C_a}{1-\Delta} \quad \text{.................................} \quad (10)$$

The physical meaning of equation (10) is that the through flow velocity is increased by $1/(1-\Delta)$. After equations (7), (8), (9), and (10), one can write;

$$C_a C_r = W_1^2 \sin\alpha_1 \cos\alpha_1 (1 - \theta - \Delta) \quad \text{...........................} \quad (11)$$

or

$$W_1 \sin\alpha_1 = C_r \frac{1-\Delta}{1-\theta-\Delta} \quad \text{...............................} \quad (12)$$

The physical meaning of equation (12) is that the flow velocity is increased by $\left(\dfrac{1-\Delta}{1-\theta-\Delta}\right)$.

Apply now the momentum balance in *X*-direction between (1) and (2);

$$\frac{P_2 - P_1}{\rho} = \frac{\cos^2 \alpha_1}{t} \int_0^t W^2 dy - C_a^2 \qquad \text{............................} (13)$$

and similarly one can reach;

$$\frac{P_2 - P_1}{\rho} = C_a^2 \left(\frac{1 - \theta - \Delta}{(1 - \Delta)^2} - 1 \right) \qquad \text{............................} (13^*)$$

Apply Bernoulli's equation between (1) and (2):

$$E_L = \frac{P_1}{\rho} + \frac{W_1^2}{2} - \frac{P_2}{\rho} - \frac{W_2^2}{2} \qquad \text{............................} (14)$$

with

$$W_1^2 = \frac{C_a^2}{(1 - \Delta)^2} + \frac{C_r^2 (1 - \Delta)^2}{(1 - \theta - \Delta)^2}$$

$$W_2^2 = C_a^2 + C_r^2$$

then equation (13*) becomes:

$$E_L = \theta C_a^2 + \theta C_r^2 = \theta W_2^2 \qquad \text{............................} (14^*)$$

Now introducing the total energy loss coefficient, Eq. (3.6):

$$\zeta = \frac{E_L}{C_a^2 / 2} \qquad \text{or}$$

$$\zeta = \frac{2\theta}{\cos^2 \alpha_2} = \frac{2\delta_m}{t \cos^3 \alpha_2} \qquad \text{............................} (15)$$

2. Diffuser Types:

A brief information will be presented concerning the three main types of diffusers used in pumps, blowers, and compressors:
1. Vaneless Diffuser,
2. Vaned Diffuser,
3. Volute Type Diffuser.

2.1 Vaneless Diffuser

A vaneless diffuser is formed by two parallel circular surfaces as shown in Figure 4. This kind of diffusers is usually used in single stage blower. It has the advantage of a flatter efficiency curve, also the same diffuser could be used for different impellers, no need to new design as in the case of vaned diffuser. In the case of blowers and compressors, it has lower surge limit, on the other hand, the peak efficiency of the blowers with vaneless diffusers is about 3 to 4 points lower than with the vaned diffusers.

The vaneless diffuser has been extensively treated early by Snootal, Johnston, and Jansen. The stability limits of vaneless diffuser are strongly dependent on diffuser radius ratio if the conditions at diffuser inlet are such that low speed rotating stall patterns are generated in the diffuser. At high speed rotating patterns, the stability is more affected by the coupling conditions between the impeller and the diffuser than by the diffuser radius ratio.
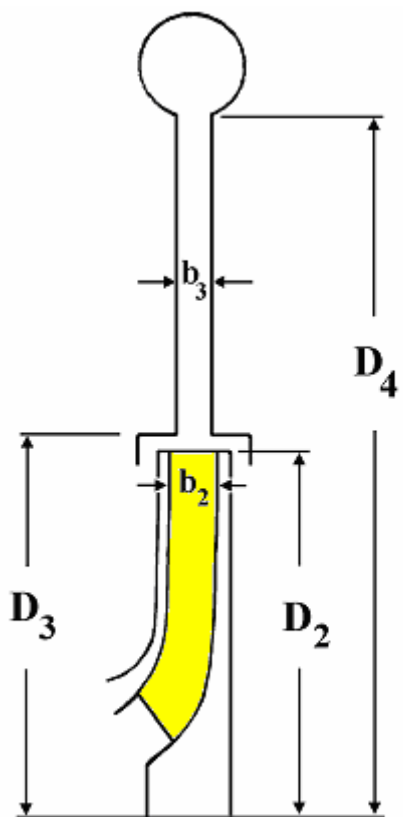
Fig. 4 Vaneless diffuser
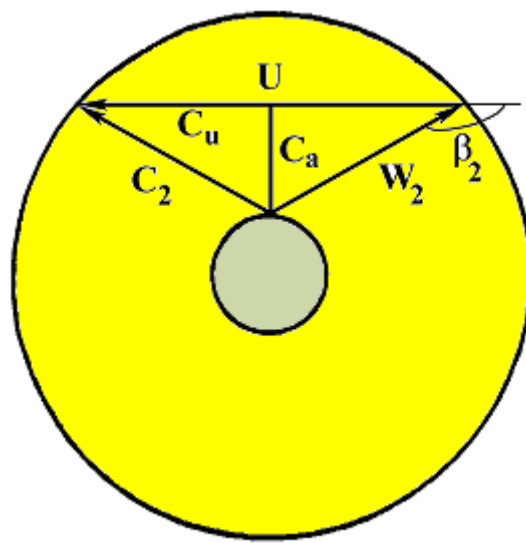
Fig. 5 Velocity triangle at diffuser inlet

The flow in the vaneless diffuser is assumed to be two-dimensional, incompressible, and inviscid. The equations governing the flow, Figure 5, are:

1) Continuity equation:

$$\partial(r.C_a)/\partial r + \partial C_u / \partial \theta = 0 \qquad\qquad \text{...................................... (16)}$$

2) Equation of motion in the radial direction:

$$\rho\left[\frac{\partial C_a}{\partial t} + C_a \frac{\partial C_a}{\partial r} + \frac{C_u}{r}.\frac{\partial C_a}{\partial \theta} - \frac{C_u^2}{r}\right] = -\frac{\partial P}{\partial r} \qquad \text{.......................... (17)}$$

3) Equation of motion in the tangential direction:

$$\rho\left[\frac{\partial C_u}{\partial t} + C_a \frac{\partial C_u}{\partial r} + \frac{C_u}{r}.\frac{\partial C_u}{\partial \theta} + \frac{C_a C_u}{r}\right] = -\frac{1}{r}.\frac{\partial P}{\partial \theta} \qquad \text{.................. (18)}$$

The main dimensions of the vaneless diffuser are its outer diameter D_4, impeller diameter D_2, the distance between the two parallel walls b_3, and the impeller width b_2. Following are the ratio between these dimensions:

$$D_4 / D_2 = 1.8, \qquad b_3 / b_2 = 0.8$$

2.2 Vaned Diffuser:

For this type of diffusers, the pressure recovery process occurs in vaned radial ring, Figure 6. To assure complete guidance of flow through the diffuser a guide vane is used. The angle of guide vanes is equal to α_2 or slightly lower (the absolute exit velocity angle).
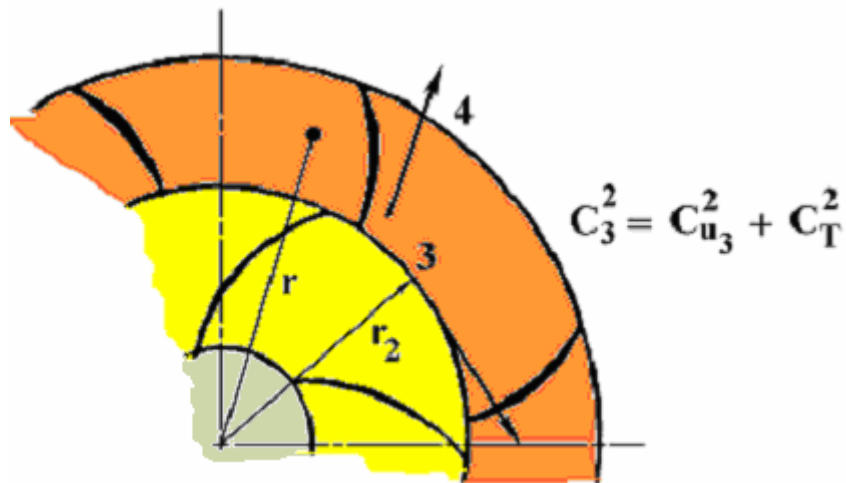
Fig. 6 Vaned diffuser

From continuity equation, one could easily write:

$$C_u = \frac{C_{u3} \cdot r_2}{r}, \qquad C_r = \frac{C_{r2} \cdot r_2}{r} \qquad \text{………………....... (19)}$$

where C_u and C_r are the tangential and the radial velocities of fluid, respectively. Consequently:

$$\tan \alpha = \frac{C_r}{C_u} = \frac{C_{r2}}{C_{u3}} = Const. \qquad \text{...................................... (20)}$$

Since the motion of fluid leaving the impeller is a logarithmic spiral, so the form of the vane could be found from the following equation:

$$\phi \tan \alpha = \ln(r/r') \qquad \text{... (21)}$$

where ϕ corresponds to the blade log spiral pitch. $\phi = \dfrac{2\pi}{Z}$ where Z is equal to number of blades. Z should not be equal to the number of impeller blades.
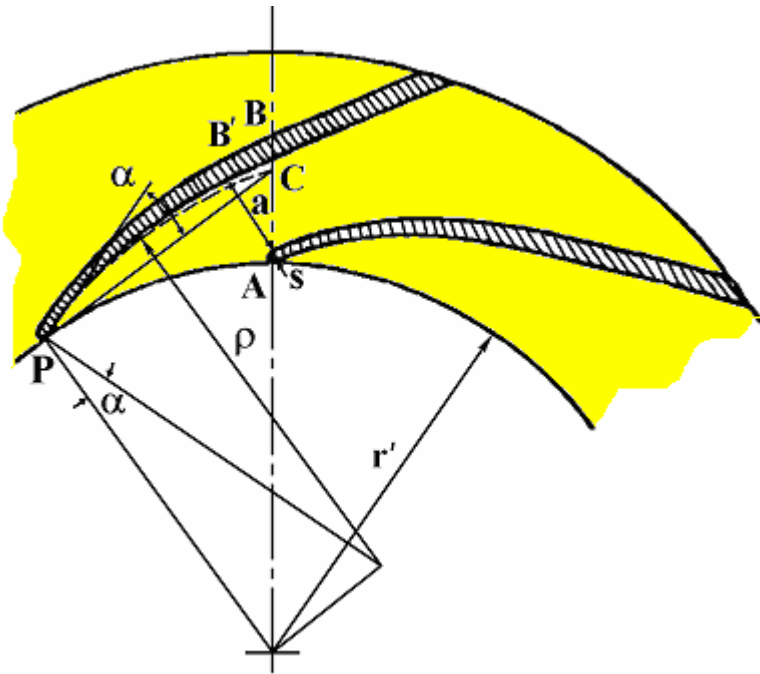
Fig. 7 Logarithmic spiral and its radius of curvature as guide blade inlet

The point B, Figure 7, should be previously calculated according to equation (21) and radius of curvature $\rho = r'/\cos\alpha$.

The passage width can easily calculated with $AB = r - r'$, $a + s = (r - r')$. $\cos\alpha$. For an approximation $\ln\dfrac{r}{r'} = \dfrac{r - r'}{r'}$ or $\dfrac{2\pi}{Z}.\tan\alpha = \dfrac{a + s}{r'}.\dfrac{1}{\cos\alpha}$ from which we can get:

$$a + s = r'\frac{2\pi}{Z}\sin\alpha = t\sin\alpha \qquad \text{................................... (22)}$$

then other point B. t is the blade pitch. A straight form of diffuser could be used of angle from 10° to 16°. To consider the blade thickness, one can use the following formula to calculate α_4:

$$\tan\alpha_4 = \tan\alpha_3 \frac{t_3}{t_3 - \sigma_3}\,, \qquad \sigma_3 = \frac{s}{\sin\alpha_3} \qquad \text{............. (23)}$$

2.3 Volute Type Diffuser

Many geometries exist, and the design procedure is applicable to all of them.

2.3.1 Parallel Walls:

The governing equation of motion is the free vortex

$$C_u.r = Const. \quad\quad\quad\quad\quad\quad\quad\quad\text{(24)}$$

and the continuity equation:

$$C_r.2\pi\, rb = C_{ro}.2\pi\, r_o b_o \quad\quad\quad\quad\quad\text{(25)}$$

where b is the width of the impeller at any radius r, b_o is the diffuser width at entry, and C_r is the radial velocity. o denotes the condition at inlet, Figure 8.
Thus we have;

$$C_r = C_{ro}\frac{r_o}{r} \quad\quad\quad\quad\quad\quad\quad\text{(26)}$$
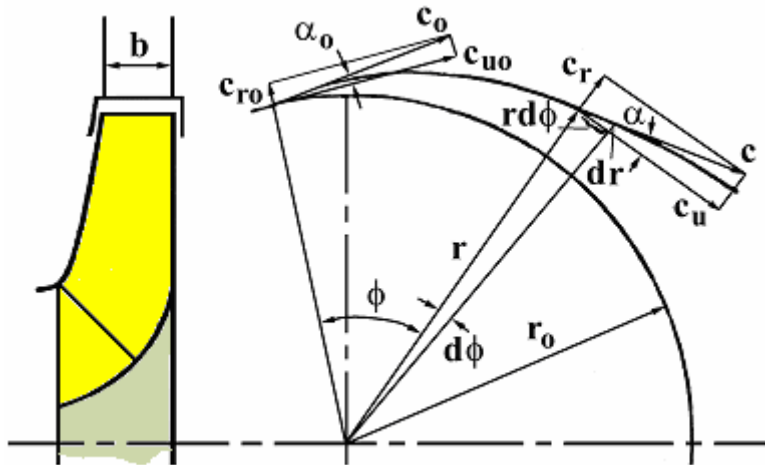
Fig. 8 Spiral space with parallel side walls

α should be constant throughout the diffuser.

i.e. $\quad \tan\alpha = \dfrac{C_r}{C_u} = \dfrac{C_{ro}}{C_{uo}} = Const. \quad\quad\quad\quad\text{(27)}$

The equation of the logarithmic spiral as defined before;

242

$$\tan \alpha = \tan \alpha_o = \frac{d\,r}{r d\phi} = \frac{C_{ro}}{C_{uo}} \quad \text{.......................…….............. (28)}$$

$$\ln \frac{r}{r_o} = \phi . \frac{C_{ro}}{C_{uo}} = \phi . \tan \alpha_o \quad \text{…..………….......................... (29)}$$

The above equation is the outside boundary curve for the volute. For the outline curvature, the following equation could be used;

$$R = \frac{r}{\cos \alpha} \quad \text{.............................……...……........... (30)}$$

The last solution is for constant width diffuser. In some cases, b_o does not equal b. This would result in an additional factor b_o / b, resulted from the continuity equation as follows:

$$C_r = C_{ro} \frac{r_o b_o}{r b} \quad \text{... (31)}$$

and thus, the equation of the spiral becomes:

$$\ln \frac{r}{r_o} = \phi . \tan \alpha_o . \frac{b_o}{b} \quad \text{..............……............... (32)}$$

2.3.2 *Tapering Side Walls:*

This type is shown in Figure 9. The principle as before could be applied and;

$$C_r = \frac{C_{ro} r_o b_o}{[b_o + 2(r - r_o) \tan \delta] r} \quad \text{...........................……..... (33)}$$

and;

$$\tan \alpha = \frac{C_r}{C_u} = \frac{d\,r}{r\,d\phi} = \frac{C_{ro} b_o}{C_{uo} [b_o + 2(r - r_o) \tan \delta]} \quad \text{................ (34)}$$

The solution to this differential equation is given by:

$$\phi = \frac{1}{\tan \alpha_o} \left[\left(1 - 2\frac{r_o}{b_o} \tan \delta \right) \ln \frac{r}{r_o} + 2\frac{r_o}{b_o} \left(\frac{r}{r_o} - 1 \right) \tan \delta \right] \quad \text{......} \quad (35)$$

and;

$$\phi = f(r) \quad \text{.......................................} \quad (36)$$
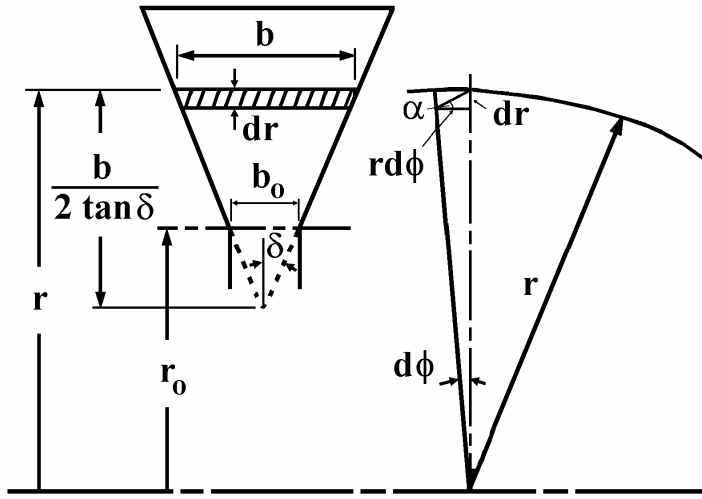
Fig. 9 Tapering side wall diffuser

The equation consists of a logarithmic and a linear term, the former disappears for;

$$1 - 2\frac{r_o}{b_o} \tan \delta = 0 \quad \text{...} \quad (37)$$

which means:

$$\tan \delta = \frac{b_o}{2 r_o}$$

δ is usually from 8° to 15°.

2.3.3 Rectangular Cross Section:

This type consists of gradually increasing rectangles, Figure 10. Thus, the area expands in axial and radial directions. We can put *h/b = Const.* At position *x*, $C_u = \frac{C_{uo} r_o}{r_o + x}$. Thus, we can consider a deviation from the line

244

$C_u.r = Const.$ with the angle ϕ, the volume $(\phi°/360)$ V flows through the section $b_\phi h_\phi$, thus:

$$\frac{\phi°}{360}V = \int_o^h \frac{C_{uo}r_o}{r_o + x}\frac{h}{c}dx \qquad\text{.. (38)}$$

which gives the equation

$$\phi = \frac{360\,C_{uo}\,r_o\,h}{V\,c}\ln\left(1 + \frac{h}{r_o}\right) \qquad\text{..................................... (39)}$$
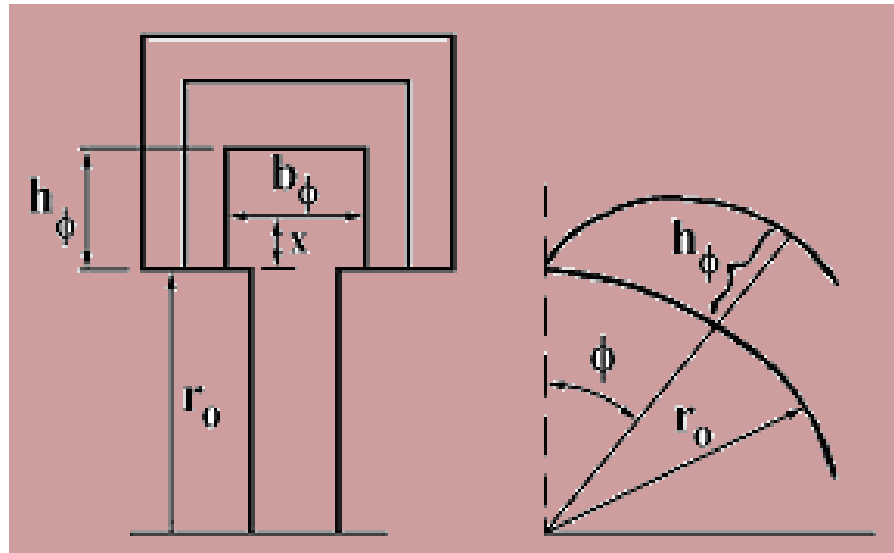
Fig. 10 Rectangular cross section diffuser

REFERENCES "Appendix I"

1. **ABDEL-HAMID, A.N.,** "Analysis of Rotating Stall in Vaneless Diffusers of Centrifugal Compressors", ASME PAPER 80-GT-184.
2. **CSANADY, G.T.,** "*Theory of Turbomachines*", McGraw-Hill, 1964.
3. **DEAN, R.C.,** "The Fluid Dynamic Design of Advanced Centrifugal Compressors", Creare Technical Notes, TN-185, July 1974.
4. **ECK, B.,** "*Fans: Design and Operation of Centrifugal, Axial Flow and Cross-Flow Fans*", Pergamon Press, 1973.
5. **JANSEN, W.,** "Rotating Stall in Radial Vaneless Diffusers", ASME Journal of Basic Engineering, Vol. 86, December 1964, pp. 750 – 758.
6. **JOHNSTON, J.P., and DEAN, R.C.,** "Losses in Vaneless Diffusers of Centrifugal Compressors and Pumps: Analysis, Experiments, and Design", Journal of Engineering for Power, Trans. ASME, Series A, Vol. 88, No. 1, January 1966, pp. 49 – 62.
7. **KOVATS, A.,** "*Theory and Design of Steam and Gas Turbines*", McGraw-Hill, 1954.
8. **RAYAN, M.A., and YANG, T.T.,** "An Investigation of Vane- Island Diffusers at High Spiral", ASME Paper 80-GT-148, March 1980.
9. **RUNSTADLER, P.W., and DEAN, R.C.,** "Straight Channel Diffusers Performance at High Inlet Mach Numbers", Journal of Basic Engineering, Trans. ASME, September 1969, pp. 397 – 422.
10. **SCHLICHTING, H.,** "*Boundary Layer Theory*", McGraw-Hill, 1964.

APPENDIX "II"

THEORY OF CAVITATION IN CENTRIFUGAL PUMPS

1. INTRODUCTION:

Cavitation is defined as the local vaporization of a liquid because of local pressure reductions due to dynamic action. In fact no other phase of hydraulic machinery design and operation has been given so much attention in technical literatures as cavitation. The reason for this was the use of higher specific speeds for both hydraulic turbines and centrifugal pumps, with the increased danger of cavitation.

The cavity is formed due to a liquid "rupture" when the hydrostatic pressure reduces to vapor pressure P_v. The liquid rupture is connected to the liquid tensile strength. Thus, the dissolved gases contribute to the reduction of the liquid tensile strength and its rupture allowing the formation of cavities.

NUCLEI: Liquids are often contain some weak spots, resulted from dissolved gasses or, the undissolved solids, immiscible liquids, and free gas. These are known as Nuclei.

The tensile strength of the interface between a solid impurity and the liquid depends upon the degree of wetting of the solid by the liquid. With a high degree of wetting, the inter-facial force is very high and even for a high degree of wetting (a "hydrophobic" particle) it is probably higher than the effective tensile strength observed in normal liquids. Figure 1 shows a very small gas bubble lodging in a crevice of a hydrophobic particle will be on the convex side of the liquid-gas interface, with the consequence that the pressure in the gas will be below that in the liquid.
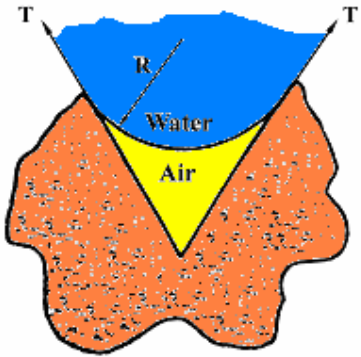
Fig. 1 A condition whereby an air bubble can remain stable indefinitely, without solution on a hydrophobic particle possessing a concave surface (after Liebermann)

The solid surfaces in contact with the liquid usually contain a plentiful supply of nuclei, so that boiling or cavitation readily takes place as soon as vapor pressure is reached, thus masking the fact that within the body of the liquid no cavities are initiated.

Thus an abundant supply of nuclei is in practice almost invariably ensured from the following potential sources:

1. Simple entrainment of relatively large air bubbles.
2. Hydrophobic particle possessing a concave surface.
3. Air bubbles attached to solid surfaces.

Some practically observed effects, which can be possibly explained by a relative scarcity of nuclei, are:

a- In high-pressure boiler feed pumps, the effects of cavitation are less serious than in the same pumps handling cold water under otherwise identical conditions. Modern boilers operate on a closed cycle with deaerated, distilled water, which is highly pressurized each time it passes through the boiler.

b- In the petroleum industry there is much less trouble from cavitation in hydraulic equipment than there is in comparable installations using water. Most petroleum products have a high wetting ability which would tend to decrease the number of available nuclei.

2. INCEPTION OF CAVITATION:

From the foregoing mentioned analysis, it is clear that the reduction of the hydrostatic pressure will initiate the formation of cavities. The vapor bubbles will grow until they reach a certain critical radius. They will be carried on with the stream until a high-pressure region reached where they will collapse producing a high-pressure chock on the adjacent walls. Thus the cavitation phenomenon may be treated as a bubble growth and collapse problem which has been treated theoretically by Rayleigh.

A reduction of the liquid hydrostatic pressure may be due to the following:

a- An increase in the static suction lift of the centrifugal pump.

b- A decrease in the atmospheric pressure with a rise in the altitude.

c- A decrease in the absolute pressure on the system, as in the case of pumping from vessels under vacuum.

d- An increase in the temperature of the pumping liquid, which will decrease the liquid tensile strength.

e- From airfoil theory (Fig. 2), when a flow around an airfoil occurs a region of low pressure is generated on the upper part and high pressure on the lower part. The inlet edge of impeller vanes acts in a manner similar to an airfoil, giving a local pressure rise on the leading face and a pressure reduction on the trailing face.

The amount of the pressure drop in the low-pressure region is function of the geometry and the speed ($\alpha.W^2/2g$). This fact was observed experimentally and is known as jet-wake flow pattern. The jet is corresponding to the driving edge with high static pressure energy. The wake is corresponding to the trailing edge with low static pressure energy.
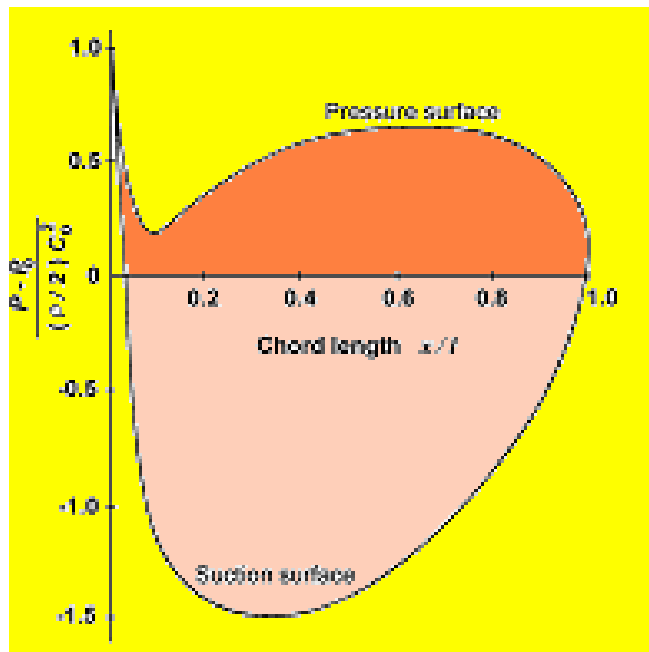
Fig. 2 (a) Actual pressure distribution on the airfoil designed
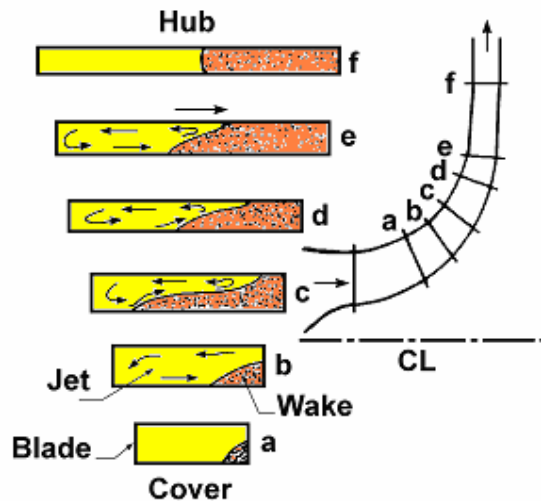
Fig. 2 (b) Development of the wake, secondary flow pattern
(obtained by Dean, Jr.)

Figure 3 shows some of the locations in as pump susceptible to cavitation. Cavitation occurs on blade surfaces, near the blunt trailing edge, at corners (such as the intersection of the blade and the wall), near the axial and radial gaps, in vortex regions such as the tip vortex, in the secondary vortex, in the scraping vortex, and in the trailing edge vortex.

Under extreme breakdown condition the entire passage may be dominated by cavitation bubbles.

(a) Centrifugal pump   **(b) Axial flow pump**
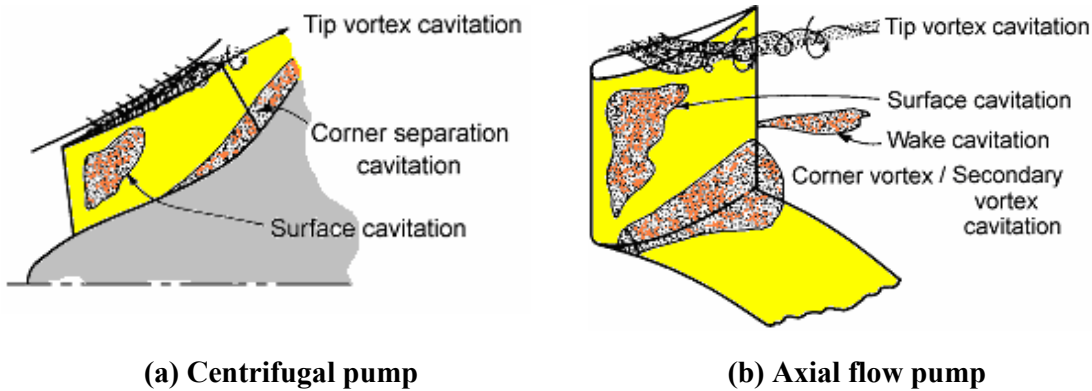
Fig. 3 Location of cavitation in centrifugal and axial flow pumps

3. SIGNS OF CAVITATION:

Cavitation is manifested by one or several of the following signs, all of which adversely affect the pump performance and may damage pump parts in severe cases.

3.1 NOISE AND VIBRATION:

This is owing to the collapse of the vapor bubbles as soon as they reach the high-pressure zones within the impeller. Noise and accompanying vibration are present in all pumps to a varying degree when they are operated at points far removed from the best efficiency point (b.e.p.) because of a bad angle of attack at the entrance to the impeller. By admitting small amounts of air into the pump suction, noise can be almost completely eliminated. In this way the air serves as a cushion when the vapor bubbles collapse.

3.2 DROP IN HEAD-CAPACITY AND EFFICIENCY CURVES:

This appears in varying degrees with pumps of different specific speeds. With low specific speed pumps, the head-capacity, the efficiency and the brake horsepower curves drop off suddenly when Q is increased to the point where cavitation is reached (Fig. 4). The degree of drop in the head-capacity and efficiency curves depends on the specific speed and on

250

the suction pressure, increasing for higher specific speed and lower suction pressure. The difference in the behavior of pumps of different specific speeds results from the difference in the impeller design. Low specific speed impeller vanes form a definite channel, the length of which depends on the vane angles, the number of vanes, and the ratio of the impeller eye diameter D_1 to the impeller outside diameter D_2 (Fig. 5 (a)).

When the pressure at the impeller eye reaches the vapor pressure, usually on the backside of the vane entrance tips, it extends very rapidly across the whole width of the channel, A-B, Fig. 5 (a)-(a), with a small increase in capacity and decrease in head.
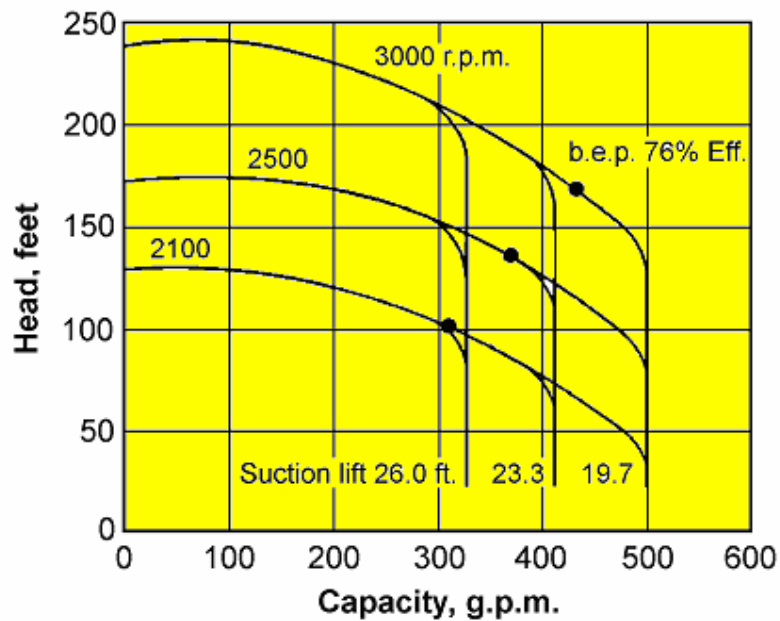
Fig. 4 Effect of speed and suction lift on cavitation of a single-suction pump, N_s = 1000
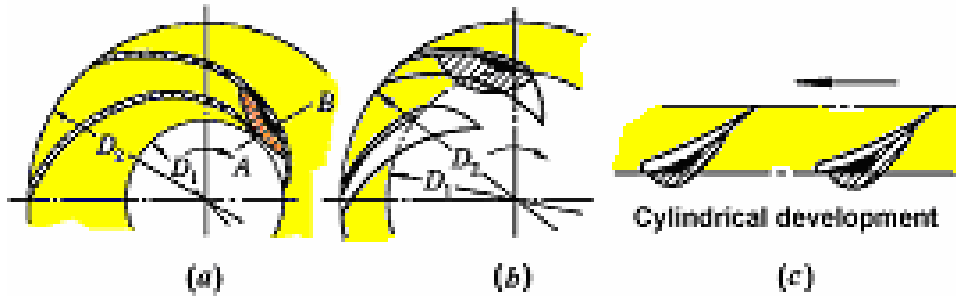
**Fig. 5 (a) Low pressure zones on back side of impeller vanes:
(a) low specific speed; (b) medium specific speed;
(c) propeller pump**
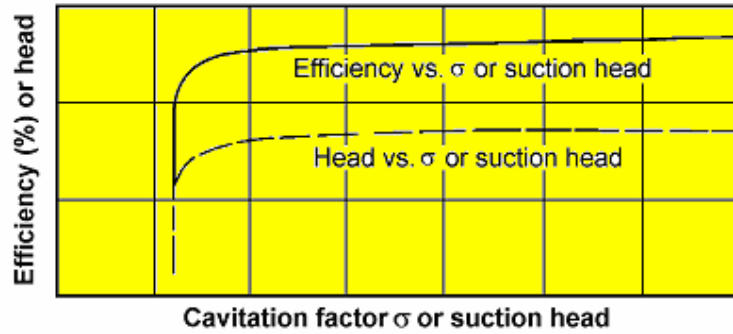
Fig. 5 (b) Cavitation characteristics at constant speed and capacity

A further drop in the discharge pressure does not produce any more flow because the pressure differential moving water to the impeller eye cannot be increased anymore. This differential is fixed by the suction pressure outside the pump, and the vapor pressure across the whole channel between any two vanes at the impeller entrance.

With high specific speed impellers, the channel between two vanes is wider and shorter, Fig. 5 (a)-(b). More drop in head and a greater increase in capacity are required to extend the vapor pressure zone across the whole channel. Therefore, the drop in the head-capacity curve extends through a wider range before the sudden break-off occurs. With propeller pumps the vanes do not overlap, Fig. 5 (a)-(c).

The results of cavitation tests can be represented graphically by plotting efficiency or head against cavitation factor σ or suction head at a

constant speed and capacity, Fig. 5 (b). The drop in efficiency and head curves indicates the beginning of cavitation.

3.3 IMPELLER VANE PITTING AND EROSION:

If a pump is operated under cavitation conditions for a sufficient length of time, impeller vane pitting appears, the amount of metal lost depending on the material in the impeller and the degree of cavitation. This will be discussed latter in details. Figure 6 shows an example of the weight loss rate versus time for a cavitating centrifugal pump impeller.
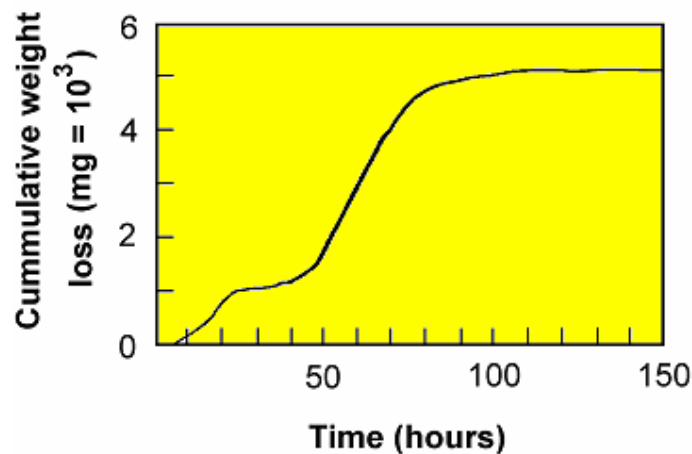
Fig. 6 Cumulative weight loss versus the pump running time

4. MECHANISMS OF DAMAGE:

Surface damage is a serious consequence of cavitation in pumps and turbines. Many studies have been made over the years of the causes and of the ways in which damage can be reduced. If chemical and corrosion effects are neglected, it seems reasonable to suppose that material removal in the erosion process must be due to the imposition on the surface of shear or normal stresses of sufficient magnitude to cause material failure, either through single blows or through fatigue-type effects. The existence of a microjet is proposed which, as the cavity collapses, bursts across the void of the bubble to hit the opposite surface at very high velocity (Fig. 7 (a)). The impact results in very high stresses, which are equal to or higher than the ultimate strength of the material in

many cases. There is a debate about the mechanism that leads to surface damage.

A combination of shock waves in the liquid, chemical, electrolytic actions and liquid "microjet" impact upon the eroded surface seems to represent, at this time, the most likely detailed mechanism for cavitation erosion. Figure 7 (b) shows bubble collapse adjacent to a surface with development of liquid microjet. The shock waves emitted during the bubble rebound (Fig. 7 (b)), which often follows original collapse, are believed to provide in many cases important assistance to the damaging process originating from the microjet impact. A suggested mechanism, based on the computed stresses being of the order of 2000 bar in some cases, is that work hardening with attendant temperature rise occurs in the material at the surface. This can lead to small changes in chemical composition and a spongy subsurface that leads to cracking of the hardened surface with subsequent penetration of the material. Eventually, the molecular bonding breaks down and erosion and corrosion occurs.
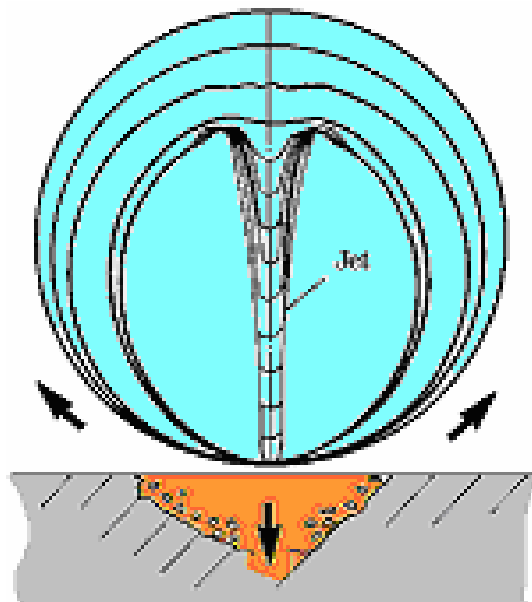
Fig. 7 (a) The jet collapse model for damage due to cavitation
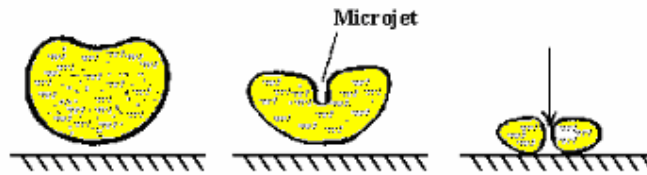
Fig. 7 (b) Schematic representation of successive stages of nonsymmetrical cavity collapse with microjet impingement against a metallic surface
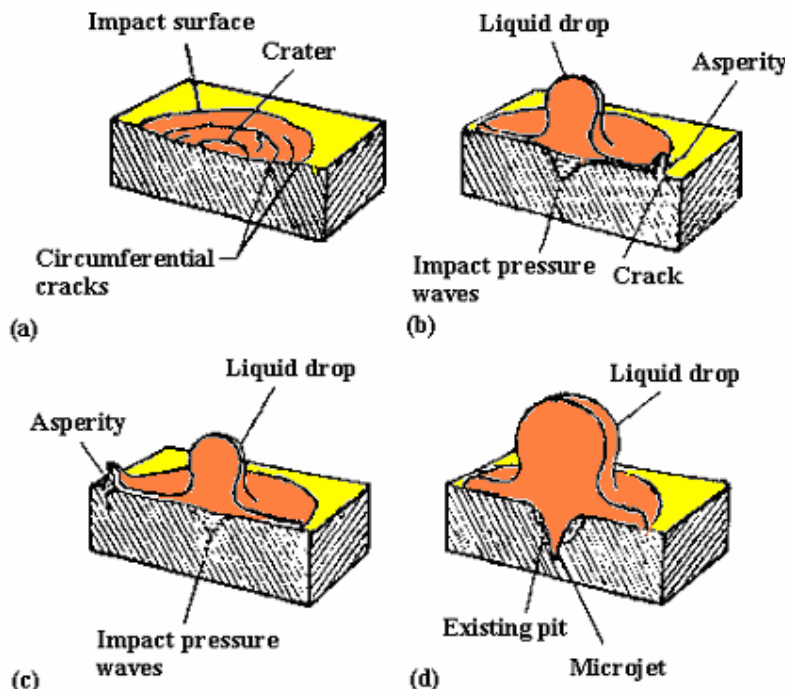
Fig. 8   Damaging mechanisms for liquid-impingement erosion [5]. (a) Solid surface showing initial impact of a drop of liquid that produces circumferential cracks in the area or impact, or produces shallow craters in very ductile material. (b) High-velocity radial flow of liquid away from the impact area by a nearby surface asperity, which cracks at its base. (c) Subsequent impact by another drop of liquid breaks the asperity. (d) Direct hit on a deep pit results in accelerated damage because shock waves bouncing off the sides of the pit cause the formation of a high-energy microjet within the pit [5].

Tillner et al. (1990) and Pearsall (1978) who show ways that damage can be produced in the laboratory for test and development purposes describe typical damage. The extent of the damage suffered depends on the fluid, the materials and the hydrodynamic system, and it has been found that even with advanced material loss the machine has developed the duty

required and damage has only been found during routine maintenance. In pumps, repair is usually by replacement, but in hydroelectric plant, it is a routine procedure to deposit metal in damaged areas and then to return the surface to the high finish required. Table 1 summarizes the resistance of common materials used in hydraulic machines.

Table 1 Relative losses of material under comparable conditions (obtained in a venturi test device using water at 20°C)

Material	Relative volumetric loss
Stellite	1
Cast stainless steel: 12.88% Cr, 0.17% Ni, 0.43% Mn, 0.38%Si	7
Stainless steel 18:8 Cr:Ni	5
Monel	16
0.33% carbon steel	37
14% Cr stainless steel (forged or drawn)	98
Manganese bronze	118
Gun metal	230
Cast iron (as cast without skin)	374
Typical cast aluminum alloy	1176

At least, the liquid pressures upon a neighboring wall during bubble collapse appear to be considerably less than that during rebound and appear to be of sufficient magnitude in fact to contribute to damage for most materials, Fig. 9.
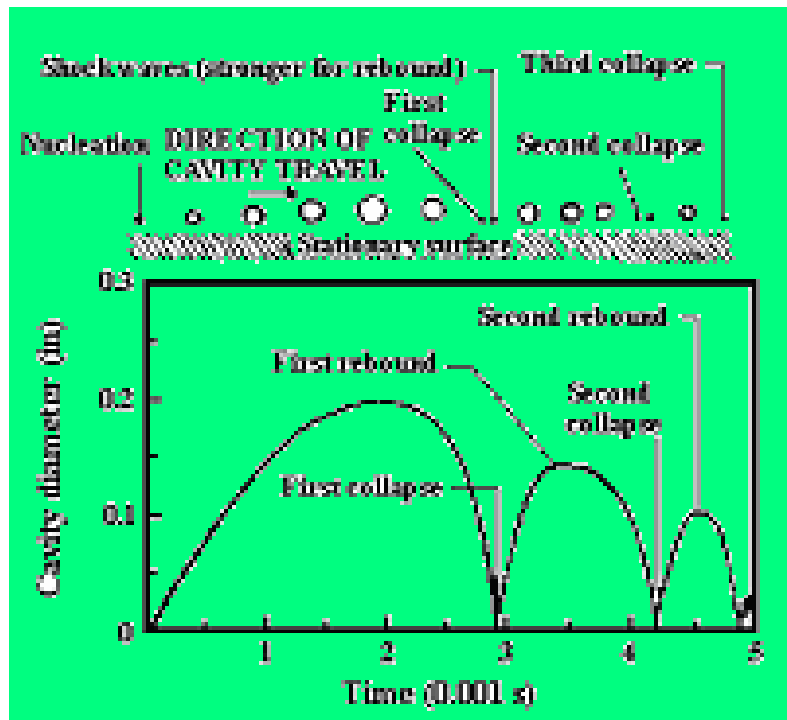
Fig. 9 (a) Schematic representation of successive ranges of growth, collapse, and rebound of a single traveling cavity.
(b) Graph of cavity diameter as a function of time for the cavity in (a)

5. *THERMODYNAMIC EFFECTS ON PUMP CAVITATION:*

The cavitation performance of a pump varies with the fluid condition. For example, when pumping water the required net positive suction energy (NPSE) is highest when passing cold water and decreases as the temperature rises. A similar effect is noted when other liquids are being pumped. The change is too large to be explained by the so-called Reynolds number effects. An empirical approach to this problem is known as the *B*-factor or *β*-factor method outlined by Knapp and Daily (1970) and Stahl and Stepannof (1956); the technique correlates suction hydraulic behavior with vapor volume in the cavitating region.

When examining bubbles in cold water it has always been assumed with some justification that all energy terms involving the vapor in the cavities are negligible compared with those of the surrounding liquid. When the temperature increases such an assumption may not be applied since the latent heat required to supply vapor to the cavity can no longer be ignored, and neither can the energy exchange during the expansion and contraction of the bubble. If they are neglected and the NPSE calculated

using cold data, the resulting value will be very conservative. As a consequence, boiler feed pumps in the 1950s began to be uneconomic in size as both pressures and temperatures rose with turbine steam conditions; eventually designers developed techniques to design for lower cavitation numbers than those for cold duties.

The heat required by vaporization must come from the liquid surrounding the cavity, thus casing a drop in temperature and vapor pressure in the immediate vicinity of the bubble. This has the effect of reducing the bubble size from that which would apply in cold liquid, thus reducing the effect on the flow. This reasoning has led to the approach of Stahl and Stepannof (1956). Figure 10 shows the conventional NPSE variation curves for a cold and a hot liquid. The two critical points where the 3% head drop applies are B and C. Point B is known for the cold test, and the NPSE reduction can be found to estimate point C.
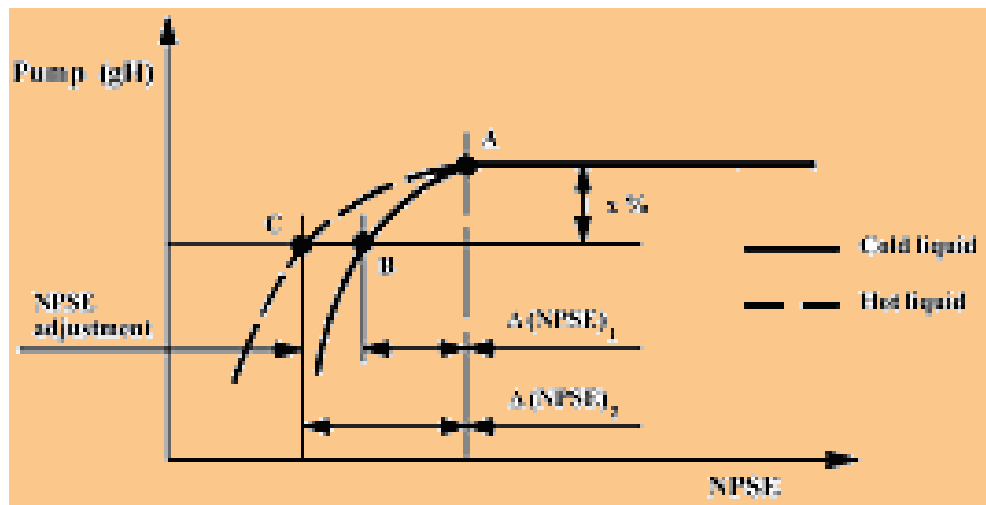
Fig. 10 The variation on NPSE required of liquid temperature

The volume ratio B or β is defined by Stahl and Stepannof as:

$$B = \frac{\text{volume of vapor}}{\text{volume of liquid}} \tag{1}$$

they showed that using the Claperyron-Clausius equation:

258

$$B = \Delta(NPSE)C_pT\left(\frac{v_v}{v_1 h_{fg}}\right)^2 \tag{2}$$

or

$$B` = \frac{B}{\Delta(NPSE)} = C_pT\left(\frac{v_v}{v_1 h_{fg}}\right)^2 \tag{3}$$

Figure 11, taken from Stahl and Stepannof (1956), plots $B`$ for a number of fluids based on refinery pumps of the double suction design and a 3% fall in gH. Also shown are lines of NPSE adjustment in the relation:

$$\sigma_{corrected} = \sigma \frac{- NPSE\ adjustment}{gH_{pump}} \tag{4}$$

The method is based on the assumptions that the cavities are uniformly distributed across the flow cross-section and that there is the 3% drop criterion. There are many other approaches but these indicate that there is a considerable difference in opinion (see for example Hutton and Furness, 1974).
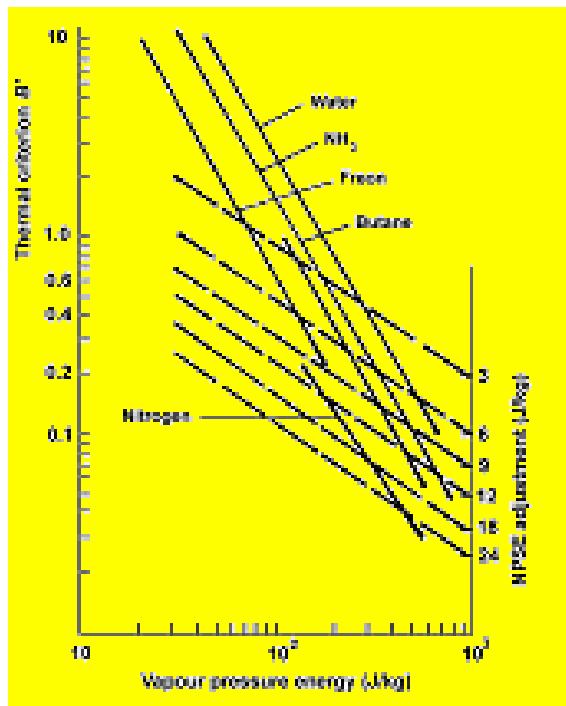
Fig. 11 Plot of thermodynamic adjustment factors
(from Stahl and Stepannof, 1956)

6. NET POSITIVE SUCTION HEAD:

The next problem is that of relating the occurrence of cavitation to other known hydraulic characteristics of the machine. Since cavitation is a function of the head at the low-pressure side of the machine, it is obvious that this "suction head" must be of paramount importance. This suction head may be defined with reference to Figure 12.
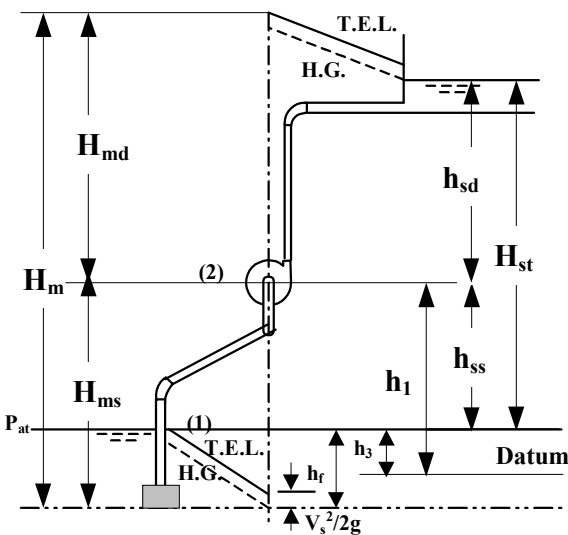
Fig. 12 Schematic Diagram of Pump Installation

H_m = Manometric head

H_{ms} = Manometric suction head

H_{md} = Manometric delivery head

h_{ss} = Static suction head

h_f = Friction head loss (included all losses such as entry losses

$V_s^2/2g$, so $h_f = h_{fs} + V_s^2/2g$).

Apply Bernoulli's equation between (1) and (2), (i.e. between the suction pipe flange and pump center assuming that point (2) is on impeller entrance).

$$\frac{P_2}{\gamma} + \frac{C_2^2}{2g} + h_1 = \frac{P_{at}}{\gamma} + \frac{C_1^2}{2g} + h_3 - h_f \qquad (\frac{C_1^2}{2g} = 0)$$

$$\frac{P_2}{\gamma} + \frac{C_2{}^2}{2g} = \frac{P_{at}}{\gamma} - h_{ss} - h_f \tag{5}$$

h_{ss} could be positive or negative depending on pump location. If it is above (+ve) or below (-ve) the suction reservoir. Cavitation occurs when L.H.S. of equation (5) is below the vapor pressure, or:

$$\left(\frac{P_2}{\gamma} + \frac{C_2{}^2}{2g} \right) - h_v \leq 0 \tag{6}$$

The above term is called "*Net Positive Suction Head*" 'NPSH' or H_{sv}, i.e.

$$H_{sv} = \frac{P_{at}}{\gamma} \pm h_{ss} - h_f - h_v \tag{7}$$

Two types of suction heads or NPSH to be considered in designing or purchasing a pump installation:
    i- Available suction head.
    ii- Required suction head.

The available suction head must be larger than the required suction head.

Available Suction Head:

This is determined by the plant designer and is based upon the conditions of the liquid handled, the pump location, and altitude … etc.

Example: Find the available NPSH for pump pumping water, if the pump is above the water surface by 3 m and h_f = 0.7 m and the atmospheric pressure is 1.03 kp/cm^2, vapor pressure is 0.0355 kp/cm^2 at 20°C, $\gamma = \rho g = 1000$ kp/m^3.

$$H_{sv} = \frac{1.03 \times 10^4}{1000} - 0.7 - 3 - \frac{0.0355 \times 10^4}{1000} = 6.24 \text{ m}$$

Required Suction Head:

Always calculated by pump manufacturer taking into consideration all types of losses between the suction flange and impeller entrance. Some of these losses will introduce as following:

1- Viscous friction losses $h_f \propto C^2 / 2g$ or $W_1^2 / 2g$.

2- By airfoil theory, when a flow around an airfoil occurs a region of low pressure is generated on the upper part and high pressure on the lower part.
   The inlet edge of the impeller vanes acts in a manner similar to an airfoil, giving a local pressure rise on the leading face and a pressure reduction on the trailing face. The amount of pressure drop in low-pressure region is function of speed $\propto W^2 / 2g$ also.

3- A sudden change in direction at impeller entrance increases the losses.

From the above points, all these losses occur between the pump suction flange and impeller entrance and are proportional to W^2 and could be equal to $K.W^2 / 2g$ where K is a coefficient. If the required suction head is larger than the available suction head cavitation will occur.

7. *NET POSITIVE SUCTION HEAD TEST:*

NPSH test must be conducted in the shop prior to shipment and installation; this test may be witnessed or unwitnessed according to the specification. Many standards exist to control this test; following is the section concerning the NPSH test in API standard 610 entitled "Centrifugal pumps for general refinery services".

The NPSH test shall be conducted with water as the pumped medium. The following formula shall be used to determine the vacuum to be maintained at the pump suction for the suppression test:

$$P_s = P_b - \left(P_v + \frac{30(H - h)\,sg}{34} \right) \qquad (8)$$

where:

P_s vacuum to be maintained at pump suction flange, inches of mercury.

P_b barometric pressure, inches of mercury.

P_v absolute vapor pressure of water at the temperature of test water, inches of mercury.

H NPSH, in feet of water as quoted by vendor.

h suction velocity head, feet of water at test conditions.

sg specific gravity of water at test temperature.

8. THOMA'S CAVITATION CONSTANT:

The experimental relationship between the impeller eye velocity at cut-off capacity and the suction pressure gives a satisfactory means for predicting cavitation for low specific speed pumps.

Thoma has suggested that the dynamic depression, including the velocity head at the impeller eye, can be expressed as a fraction of the total head H_m or:

$$NPSH = \sigma H_m \tag{9}$$

The coefficient σ is determined experimentally. It may be also written on the following form:

$$\sigma = \frac{\dfrac{P_{at}}{\gamma} \pm h_{ss} - h_f - h_v}{H_m} \tag{10}$$

The use of the cavitation constant σ is subject to a number of considerations:

1- The following relationship is given for the similarity regarding cavitation when it has progressed beyond the incipient stage:

$$\frac{\sigma_1 - \sigma_c}{\sigma_2 - \sigma_c} = \frac{H_{m2}}{H_{m1}}$$

where σ_c is the critical sigma coefficient which is constant for both model and prototype $\sigma_c = \sigma_{c1} = \sigma_{c2}$.

$$\sigma_1 = \frac{NPSH_1}{H_{m1}} \quad \text{is sigma for the model}$$

$$\sigma_2 = \frac{NPSH_2}{H_{m2}} \quad \text{is sigma for the prototype}$$

H_{m1} and H_{m2} are the operating heads of the model and prototype, respectively.

2- To make the discussion of cavitation more definite, the criterion of incipient cavitation should stated- whether it is the breaking off of the head-capacity curve, or the drop in efficiency, or noise and vibration, or the pitting of the impeller vane.

The drop in efficiency is more general because it applies to pumps irrespective of the specific speed and may be found while other signs of cavitation are not yet apparent.

9. SUCTION SPECIFIC SPEED:

Since cavitation is most likely to occur in the low-pressure regions of the machine, e.g. at the inlet of a pump impeller, it is natural to use the eye or throat diameter D_e of the runner as the representative dimension in the fundamental similarity considerations. In this manner, the kinematic condition for similarity of inlet flow and cavitation becomes:

$$\frac{Q}{D_e^{3} N} = Const$$

and the corresponding dynamic relations are:

$$\frac{NPSH.D_e^{4}}{Q^2} = Const$$

$$\frac{NPSH}{N^2 Q^2} = Const$$

By eliminating the dimension D_e in the same manner as that used previously to determine the specific speed N_s. The following equation is obtained:

$$S = \frac{N\sqrt{Q}}{NPSH^{3/4}} \tag{11}$$

This cavitation parameter *S* is called "*suction specific speed*".
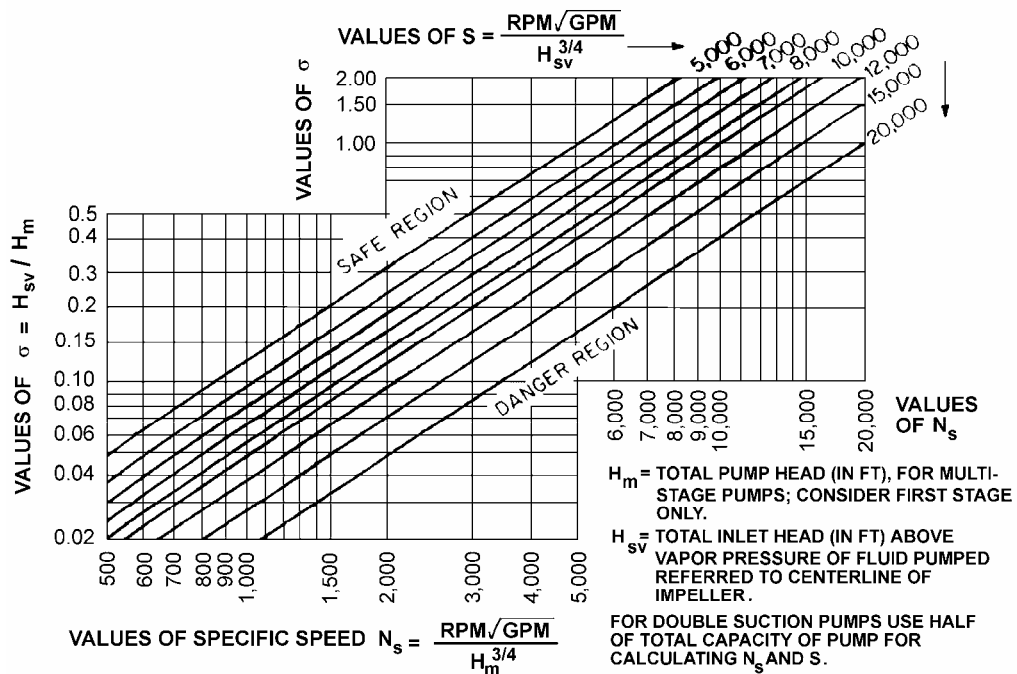
Since the two parameters σ and *S* are likely to have parallel use in the same field of application, it becomes necessary to state an analytic expression for the relation between them. This relation which may be derived from the explicit expressions for *S* and N_s, is:

$$\sigma = \left(\frac{N_s}{S}\right)^{4/3} \tag{12}$$

if the values of σ corresponding to a suitably defined cavitation limit are plotted against the specific speed (Figure 13), it is found that an average curve through such empirical points can well be approximated by the relation:

$$\sigma = Const.N_s^{4/3} \tag{13}$$

This equation is the empirical demonstration of the fact that *S* is practically independent of the specific speed.

Fig. 13 Cavitation limits of centrifugal and propeller pumps (Worthington Pump and Machinery Corporation)

The increase of the σ value in the diagram in the direction of increasing specific speed demonstrates that, for the same form of installation the head of the machine must decrease with increasing specific speed. For this reason, machines for high heads must be of low specific speed and machines of high heads may employ high specific speeds.

10. SOME DISCUSSIONS CONCERNING THE NPSH:

The net positive suction head problem is still very persistent. It is now compounded for large high head pumps by a new need for erosion avoidance at low flow rates. Admittedly, there have been few or rare problems arising from centrifugal pumps failing to deliver rated capacity and pressure in the field due to a NPSH shortcoming. Paradoxically, while NPSH requirements of the average pumps have been so well established, there are some new findings about cavitation effects on larger, high-head pumps that need considerable further research. Purchasers Users, and Contractors have all been "bearing down" on the pump manufacturers to achieve lower NPSH requirements on larger pumps to the point where other things are suffering, the pendulum has

sewing too far. This was resulted in large pumps operates at low speed. Also one of the recommendations usually used to avoid cavitation is the use of a larger pump than the size that would normally be chosen, one merely offers a "4 inches" pump instead of "3 inches" or one offers a double-suction impeller type pump instead of a single-suction, Figure 14. This practice thereby reduces the required NPSH to a significantly lower value and in this relatively painless manner pump application engineers have been falling into a trap lately.
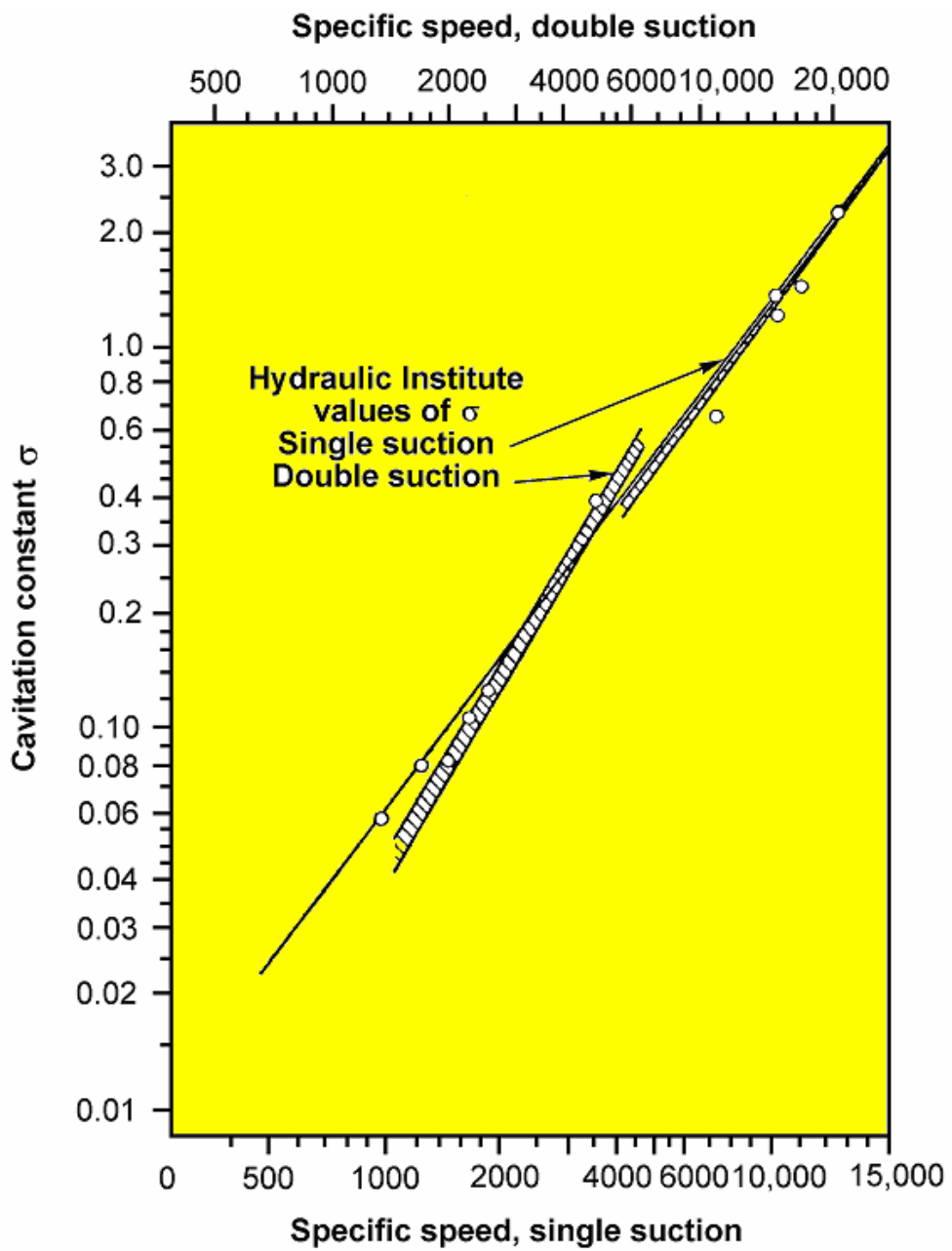
Fig. 14 Cavitation constant σ versus specific speed for best efficiency points

To understand the trap, it is necessary to show the shortcoming of the present definition of NPSH (required). Here is the issuance of the combined API and ASME definitions: "Net Positive Suction Head Required is determined by the vendor and is the total absolute head at the pump inlet less the vapor pressure head corresponding to the liquid temperature at the inlet required for the specified capacity" also "a drop

in head of 3 percent is usually accepted as evidence that cavitation is present". It is important to note that 3 percent head drop point is not always the start-of-cavitation point, neither is a 1 percent head drop point. At these head drop points, cavitation has already progressed sufficiently to affect the flow in the impeller passages.

The aforementioned "trap" is the excessive cavitation that can occur at low flows on high-energy pumps. Also the dangers of pulsation or surges due to rotating stall or unstable *H-Q* curve, the oversizing may cause the rated capacity to be below 60% the b.e.p. capacity for that size pump.

What should pump application engineers do to avoid partial-flow cavitation on high head pumps? If it becomes necessary to use an oversized pump for NPSH reasons, give more thought to the provisions to assure a higher minimum flow than usual. Table 2 gives approximate figures for minimum flows.

Table 2 Recommended minimum flows for high-energy pumps

LIQUID, & TYPE IMPELLER	ACTUAL RATIO, $NPSH_A/NPSH_{R3PC}$	RECOMMENDED MINIMUM, % OF B.E.P. FLOW
HYDROCARBON, Single-Suction or Double-Suction Impeller	1.1 and higher	25 %, or Manufacturer's recommendation if higher
WATER OR WATER SOLUTION, Single-Suction	2.0 or less 2.5 3.0 or more	35 ,, ,, 30 ,, ,, 25 ,, ,,
WATER OR WATER SOLUTION, Double-Suction	2.0 or less 2.5 3.0 or more	70 ,, ,, 60 ,, ,, 50 ,, ,,

11. CAVITATION NOISE IN CENTRIFUGAL PUMPS:

Nomenclature

*	Dimensionless
c	Velocity of sound in the fluid, (m/s)
C_L	Velocity of sound in casing material $\sqrt{E/\rho p}$, (m/s)
CNL	Acoustic cavitation pressure, (N/m^2)
CV	Solid-borne noise acceleration (effective value), (m/s^2)
CV*	Dimensionless solid-borne noise acceleration, CV* = CV (u_1^2 / D_1)

D_1	Impeller inlet diameter, (m)
ε	Relative erosion intensity
E_R	Maximum erosion rate, (m/s)
f	Frequency, (1/s)
F_{cor}	Corrosion factor
f_m	Frequency with the maximum energy density, (1/s)
F_{MAT}	Material factor
g	Acceleration due to gravity, (m/s^2)
h	Wall thickness
hD	Wall thickness of cover
HPF	High-pass filter
vac	Acoustic efficiency
I_{ac}	Acoustic intensity, (W/m^2)
I_R	Reference value for acoustic intensity, (W/m^2)
L	Length of cylinder
L_{cav}	Cavity length, (mm, m)
LPF	Low-pass filter
NF	Eigen frequency, (1/s)
NL	Total sound pressure in the liquid (RMS value), (N/m^2)
NL_0	Background noise level (as sound pressure), (N/m^2)
$NPSH_a$	Net positive suction head of the plant, referred to the middle of the pump, (m)
p	Static pressure, (N/m^2)
P_{ER}	Specific erosion power $P_{ER} = U_R\,E_R$, (W/m^2)
p_i	Implosion pressure, (N/m^2)
p_{sat}	Saturation vapour pressure, (N/m^2)
p_∞	Static pressure in the vicinity of the bubble, (N/m^2)
Q	Flow rate, (m^3/s)
Q_{Ref}	Flow rate at optimum efficiency, (m^3/s)
R	Radius of cylinder, (mm, m)
^-R	Reference value
ρ	Density of water, (kg/m^3)
R_m	Tensile strength, (N/m^2)
R_o	Radius of bubble at beginning of implosion, (m)
ρp	Density of casing material
S	Strouhal number
σ	Cavitation coefficient (general)
σ_{av}	Cavitation coefficient of installation
σ_i	Cavitation coefficient for visual inception of cavitation
σ_{rad}	Sound radiation coefficient
σ_{ul}	Cavitation coefficient of the pump
u_1	Circumferential speed at impeller inlet, (m/s)
U_R	Ultimate resilience, $U_R = Rm^2 / 2E$, (n/m^2)
ω	Angular frequency
w	Relative speed, (m/s)
Z_2	Number of blades
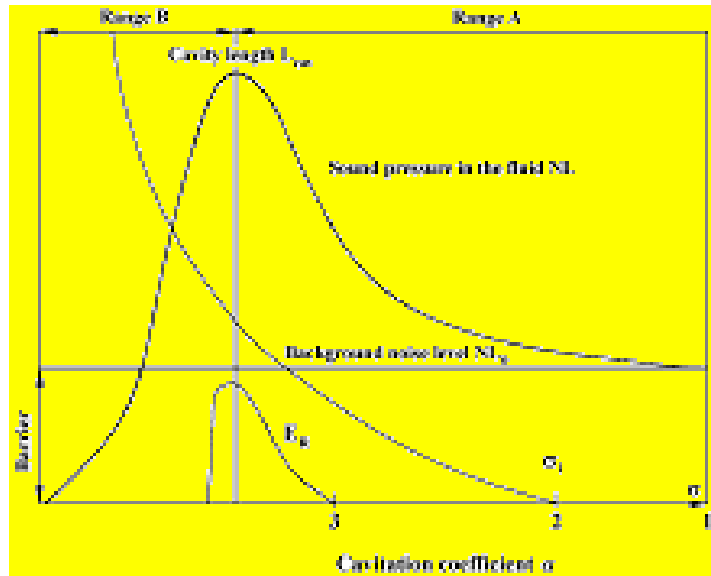
All types of cavitation can be quantified by means of cavitation noise measurements. This applies even to bubbles not in contact with a surface

and to cavitation on the pressure side. All parameters, which influence the hydrodynamic cavitation intensity, have also an influence on the cavitation noise.

During cavitation diagnosis by sound pressure measurements, the magnitude of the measured signal is a measure of the cavitation intensity, since the sound pressure increases with increasing number of imploding doubles. In this connection, it is necessary to establish when the cavitation begins and what interrelationships exist between cavitation noise and erosion.

If the inlet pressure is lowered during a suction test with constant flow quantity and constant speed of rotation, signals can be measured using a pressure transducer at the pump inlet. These signals are graphed in Figure 15.

A background noise level is measured at inlet pressures, which exceed the pressure at which cavitation starts. This noise level is independent of the inlet pressure and is caused by turbulences, unstable blade forces and mechanical machine noises. After cavitation has started, the noise level rises with decrease of the cavitation coefficient of the pump, first to a maximum (Figure 15, range A) and then drops steeply, often to lower than the background noise level (range B). It should be noted that the rate of cavitation-induced loss of material also has a similar graph (Figure 15).

1 Acoustic inception of cavitation
2 Visual inception of cavitation
3 Inception of erosion

**Fig. 15 Acoustic signal, cavity length and erosion rate as function of
the cavitation coefficient**

The maximum can be explained by that fact that, with decreasing cavitation coefficient, the volume of vapor (bubble size) and the number of bubbles both increase, with simultaneously linear decrease of the driving pressure difference. Superimposed on this process is the phenomenon that at small void fractions, the imploding bubbles (larger pressure difference) can reinforce each other [6], whereas at large void fractions, the local density and speed of sound, and thus the implosion pressure, decrease.

The lowering of the noise level in the range B can be explained by the following mechanisms:

-    When the bubble volume at the impeller inlet is large, a great part of the sound in these zones is absorbed with two phase flow: the bubbles can, for example, implode within the impeller ducts, whereby areas with two-phase flow between implosion zone and pressure transducer form an effective barrier.

-    At low inlet pressure, air can be precipitated in the pump inlet (or in the upstream throttle valve), so that a two-phase flow is again present, which makes the cavitation noise measurement completely unusable.

272

Basing on the fact that the noise in the range B sinks under the background noise level, the conclusion can be drawn that the main source of the background noise level is not in the inlet but in the impeller, i.e. in the unstable blade forces. Were the background noise level to be induced by flow processes in the inlet, it could not be blocked off from the sound pressure detectors by the two-phase flow in the impeller.

Hence where cavitation noise measurements are concerned, a distinction is to be drawn between the ranges A and B in Figure 15. In range A, cavitation is limited and the measured cavitation noise can be regarded as a measure of the cavitation intensity. On the order hand, in range B so much sound energy is absorbed by the two-phase flow that the measured sound pressure is no longer a reliable measure of the cavitation intensity.

A dimensionless representation of the reference sound pressure is chosen in order to be able to compare the measurements on different pumps and under different conditions better with each other. The effect of cavitation alone can be determined when the background noise level is subtracted from the total noise level. Since each blade is also a noise source, a conversion calculation to a reference number of blades is made. The cavitation noise arises from volume changes ("acoustic monopoly").

$$CNL_R = \sqrt{\frac{Z_2, R}{Z_2}\left(NL^2 - NL_0^2\right)}$$

$$CNL^* = \frac{2\, CNL}{\rho u_1^2}$$

Such standardization is thus physically appropriate and also confirmed by tests.

Frequency behavior of cavitation noise

Cavitation produces noise by periodic impulses, which are completely irregularly distributed as regards duration, height and sequence. The consequence is a continuous broad-band spectrum, the energy distribution of which has a broad maximum [20]. This arises from the most frequently occurring implosion time.

As is demonstrated by stroboscopic observations of cavities forming on impellers (Figure 16), the bubble fields fluctuate (less than 10 kHz) as the cavity length increases. They contribute apparently to the measured

cavitation noise and can be represented by Strouhal numbers ($S = 0.3 + 10\%$) [4, 5, 8]. The high frequency part originates from the implosions of the individual bubbles (frequency range: 10 kHz to 1 MHz).
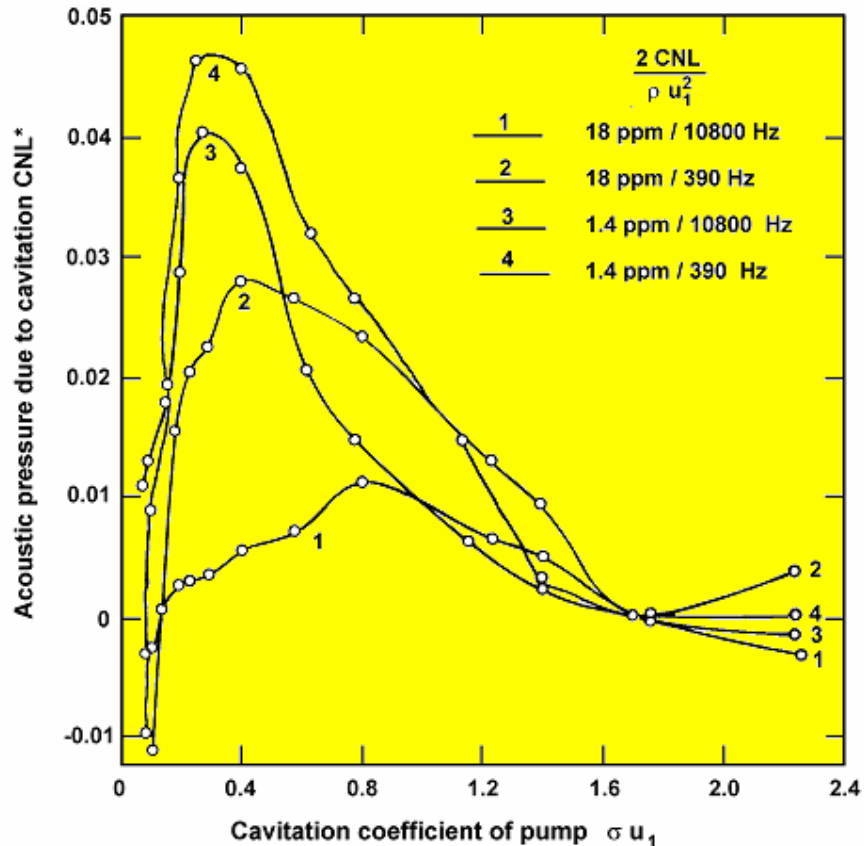
Fig. 16 Influence of the air content and of the frequency range on the cavitation noise (high-pass filter set in each case at the given frequency)

The bubble field fluctuations are caused by turbulences and by the instationary nature of impeller flow in the presence of incoming flow, which is not rotationally symmetrical. Such flow configurations occur in the inlets of multi-stage pumps, around ribs upstream of the impeller or at guide vanes. Presumably the bubble field variations modulate the implosion phenomena to a certain extent and influence the transport of bubbles from their place of origin to the implosion location.

Visual observations show that the bubble field fluctuations increase markedly with decreasing cavitation coefficient. Hence it is to be expected that the low frequency part of the cavitation noise spectrum increases as the cavitation coefficient decreases. Figure 16 confirms this.

274

Moreover, tests show that the gas content has a significant influence (particularly at frequencies of less than 10 kHz). A bubble implosion gives rise to a sharp pressure peak and lower pressure peaks in the rebound phase.

According to information published in the literature, the highest amplitudes in the cavitation noise spectrum occur at the following frequency:

$$f_m = \frac{1}{2R_o} \sqrt{\frac{p - p_\infty}{\rho}}$$
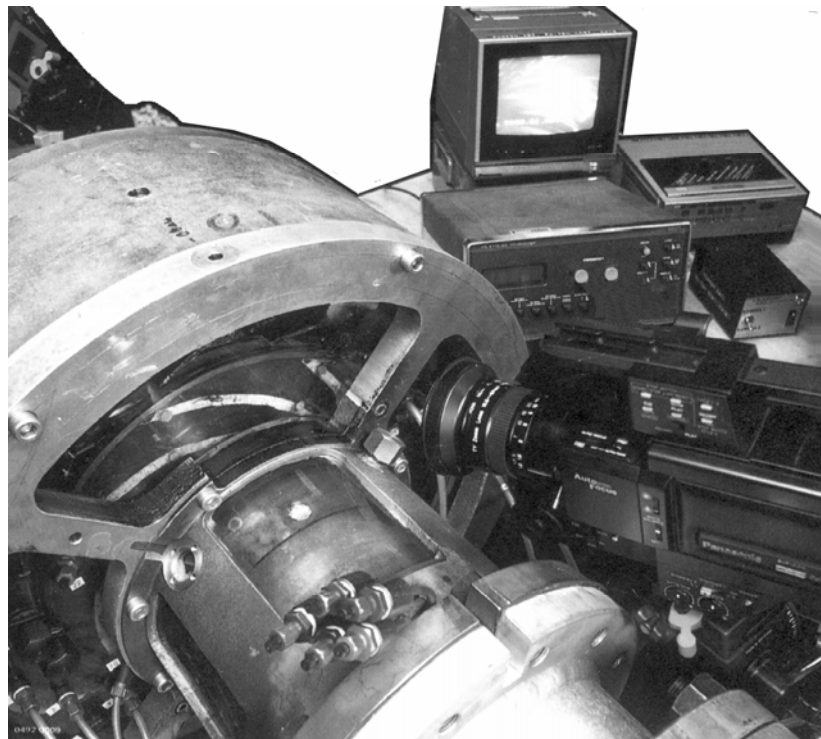
Fig. 17   Bubble field observations using the stroboscope require expensive modifications to the pumps. Cavitation noise measurements carried out at the same time provide clarifying information for use in the interpretation of fluid-borne and solid-borne noise

The bubble radius R_o and the local pressure p are unknown, but proportionality can be derived using the following equation [11]:

$$f_m \approx \frac{u_1 \sigma u_1^{3.5}}{D_1}$$

The frequency with the highest energy density is thus strongly dependent on the cavitation coefficient. As well as being indicated by the observations of Figure 16, this is also confirmed in the literature [10, 15]. Summarizing it can be established:

With increasing NPSH, increasing speed or increased cavitation coefficient, the maximum energy density of the cavitation noise spectrum is displaced to higher frequencies.

If it is intended to establish the cavitation intensity by cavitation noise measurements, it is necessary to measure in as broad a frequency spectrum as possible. Attention has also to be paid to the low frequency part since presumably bubble-field oscillation themselves contribute significantly to cavitation damage [1, 2]. If the cavitation noise is measured over a narrow frequency band, the band of maximum energy density might be displaced relative to the band measured when changing operation conditions so that incorrect conclusions might be drawn when interpreting the results. Information in the literature shows that measurements are frequently carried out only in a relatively narrow frequency band, the breadth of the frequency band being chosen at random. This renders comparison with other measurements more difficult.

If cavitation noise measurements are to be utilized in order to establish cavitation inception, then a frequency range, which is above that of the background noise level, is to be chosen.

Estimation of erosion risk basing on fluid-borne noise

In previous investigations, relationships between specific erosion power and the acoustic intensity in the range 1 to 180 kHz were developed.

Using the equations:

$$P_{ER} = 8,8.10^{-8} \frac{F_{cor}}{F_{Mat}} \left(\frac{I_{ac}}{I_R} \right)^{1.463}$$

$$I_{ac} = \frac{CNL_R^2}{\rho c}$$

the erosion rate can be estimated from the fluid-borne noise measurements. There is, however, a basic difficulty in that the inlet pressure can generally not be varied during measurements carried out in pumping installation. Hence it is also not possible to determine the background noise level. For approximation purposes, the total noise level can be utilized. This, however, implies the presence of developed cavitation.

The nearer the magnitude of the measured signal is to that of the background noising level, the greater the degree of unreliability of the measurement. If the characteristics of the installed impeller are known, visual cavitation commencement can be estimated approximately. Using the cavitation coefficient of the installation, it is possible to evaluate whether developed cavitation is to be expected or not.

In the case of large impeller inlet angles and unsuitable shaping of the runner blade inlet edges, a coefficient of 2 is no rarity. At an installation cavitation coefficient value of about 0.5, cavitation is generally to be expected. If the coefficient is between 0.2 and 0.3, it is possible that the range B (Figure 15) has already been attained and thus the measured acoustic pressure is no longer unquestionably a measure of the danger of cavitation.

When taking measurements on installations, an attempt could be made to utilize only the high-frequency sound (>10 kHz). However, when low frequency parts are filtered out, the characteristic and the level of the curves can differ markedly from the true values (Figure 16). The measured acoustic pressure is then no longer a measure of the hydrodynamic cavitation intensity.

When measurements are made on installations using different frequency bands, it can be established whether the low frequency sound constitutes a small proportion only of the total level. In that case, it is possible to use the sound pressure in the range of 10 to 180 kHz and regard this part of the spectrum as arising essentially from cavitation.

Evaluation of the erosion inception

The fluid-borne noise is a measure for the hydrodynamic cavitation intensity. Unfortunately, the measured sound pressure values are small in comparison with the implosion pressure. Hence, if erosion inception is to be determined, the absolute local material stressing (e.g. expressed via the

implosion pressure) is to be related to the cavitation resistance of the material used.

If the noise is measured at a defined spatial point, the sound power of the source can be calculated basing on the acoustic characteristics of the space concerned. By estimations of the acoustic efficiency (ratio of the radiated acoustic power to the mechanical power of the implosion process), the implosion pressure can be calculated approximately. Then the material stressing can be compared with the fatigue strength of the material.

Figure 18 shows the relationship between measured erosion and implosion pressures calculated from fluid-borne noise measurements. Since the absolute material stressing occurs due to the implosion pressure, the results from very different test setups can be entered into the diagram. In the case of drop impact erosion, the impact pressure can be calculated from $p_i = c\rho w$.

Using the data given in [27], a surprisingly good agreement with Figure 18 is found.
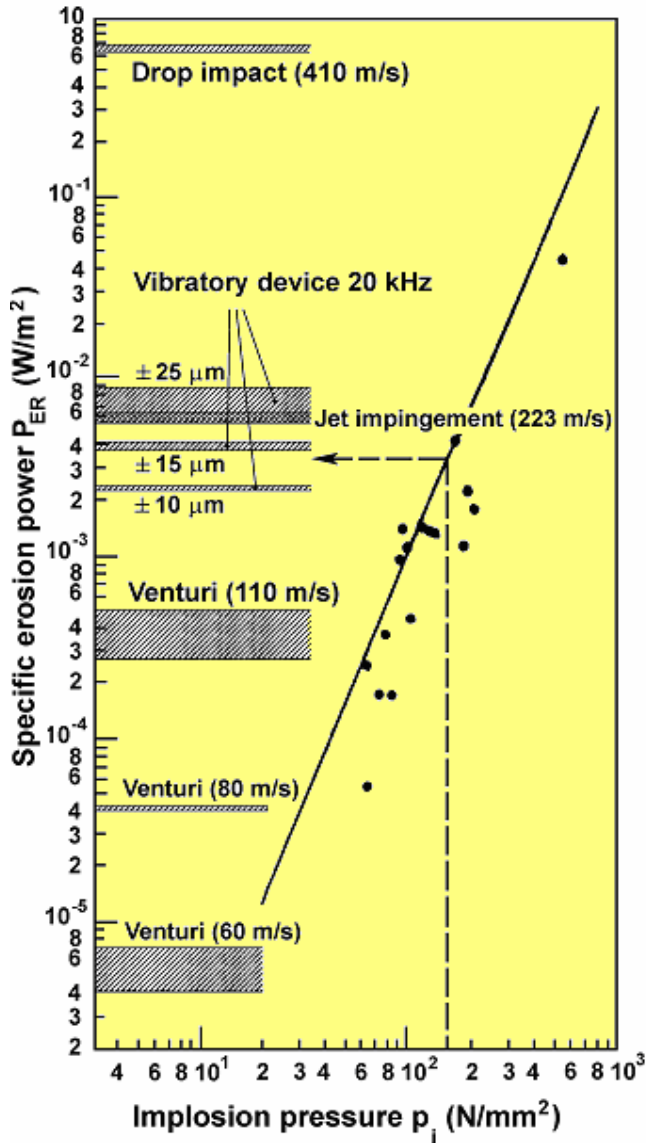
Fig. 18 Specific erosion power as a function of implosion pressure

Solid-borne noise measurements

When carrying out fluid-borne noise measurements, it is necessary to bore a hole in the inlet casing in order to fit the pressure transducer. Solid-borne noise measurements, on the other hand, can be accomplished very simply on the outer wall of the pump casing without any penetration into the system being necessary. Hence the measurement of solid-borne noise is to be recommended as an effective approach. As applies for fluid-borne noise measurements, such measurements should be made in a broad frequency band.

Figure 19 shows the solid-borne noise in the 10 to 30 kHz range and the fluid-borne noise measured simultaneously as a function of the cavitation coefficient. The curves of both fluid-borne and solid-borne noise have similar features as regards cavitation.
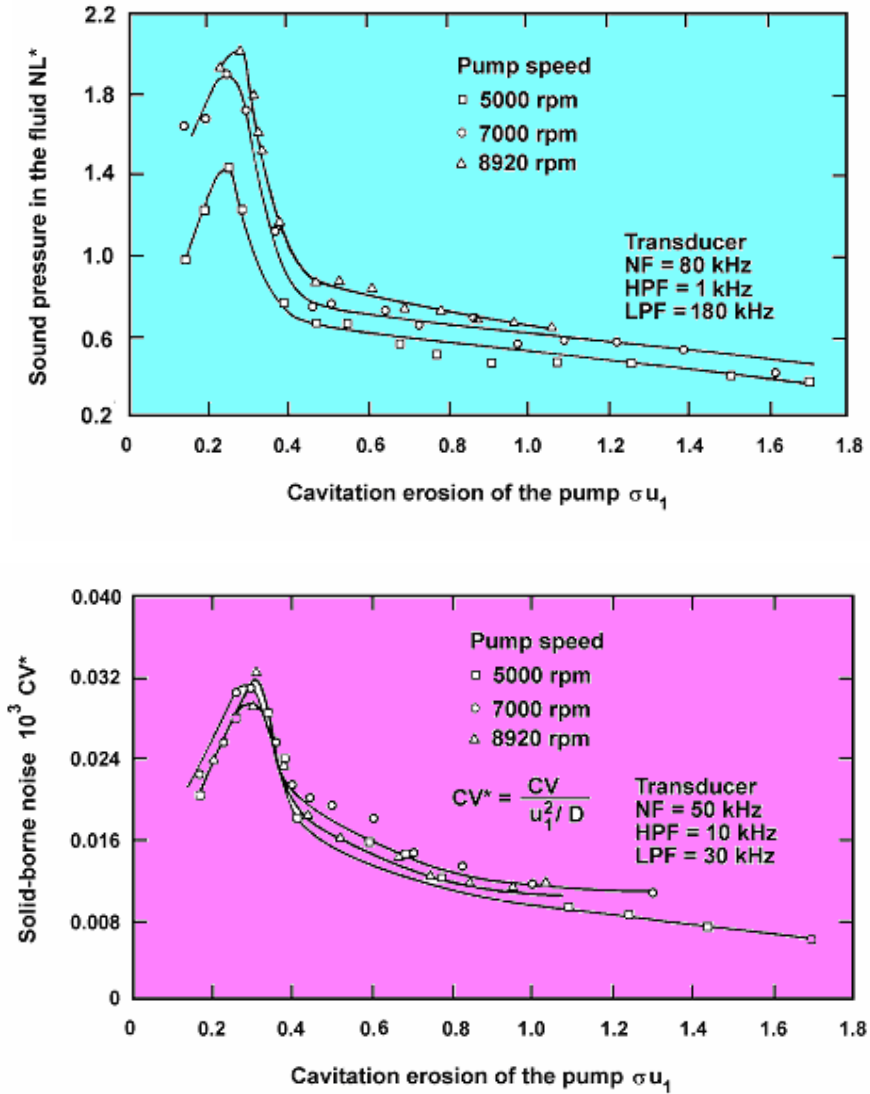
Fig. 19 Fluid-borne and solid-borne noise – high-pressure pump

In Figure 20 the specific erosion power is shown as a function of the solid-borne noise values measured [3, 4, 11, 22]. No universal relationship can be derived between erosion and measured acceleration. This is also not to be expected, since the transfer of the water-borne noise

into the casing wall and the transmission of solid-borne noise in the casing are dependent on the geometry and on the material (Figure 21). However, for a given system, there is a correlation between erosion and solid-borne noise.
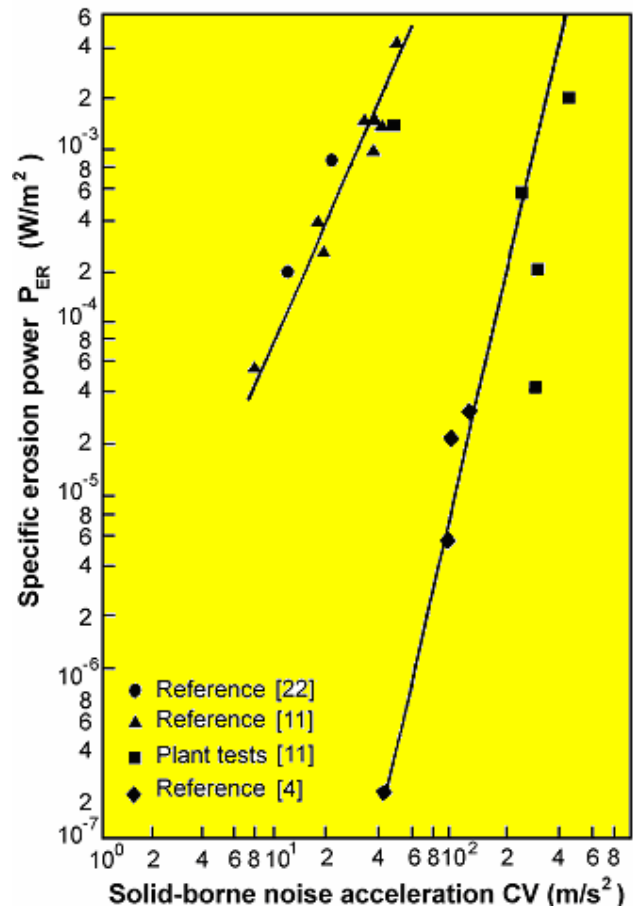
Fig. 20 Specific erosion power as a function of the solid-borne noise
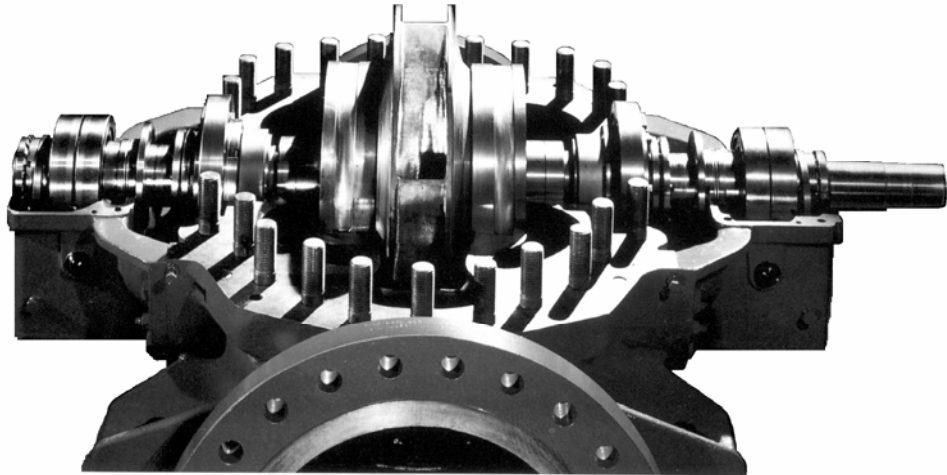
Fig. 21 Sophisticated design and modern materials technology are particularly called for when cavitation cannot be completely avoided due to the given operating conditions

In order to obtain a relationship, which is generally applicable between erosion and casing wall acceleration, an attempt can be made to calculate the fluid-borne noise from the measured acceleration basing on simple acoustic models. The statistical energy analysis method provides such a possibility [15]. It is based on the assumptions that the acoustic field in the liquid is of the broad band type and moreover diffuses and high frequency. Furthermore, it is assumed that in the frequency range under consideration there is a large number of independent modes, both of the fluid-filled space and also of the surrounding wall.

$$ NL = CV\rho\, h \sqrt{\frac{\rho\, p C_L}{\sqrt{3}\pi\,\rho\, C}\left(1 + \frac{R}{L}\cdot\frac{h_D}{h}\right)\left(1 + \frac{\eta}{\eta_{21}}\right)} $$

$$ \eta_{21} = \frac{\rho\, C \sigma_{rad}}{\rho\, p h \omega} $$

When using this method, the specific erosion power as function of the solid-borne sound (Figure 20) is transferred by calculation into the specific erosion power as a function of the fluid-borne sound (Figure 22), it is clear that the groups of data from the solid-borne measurements now group themselves round the erosion correlation as a function of the fluid-borne sound. This is particularly to be noted for the tests carried out on airfoils [4] (for these tests, it was not considered appropriate to normalize the CNL to the reference blade number).

282
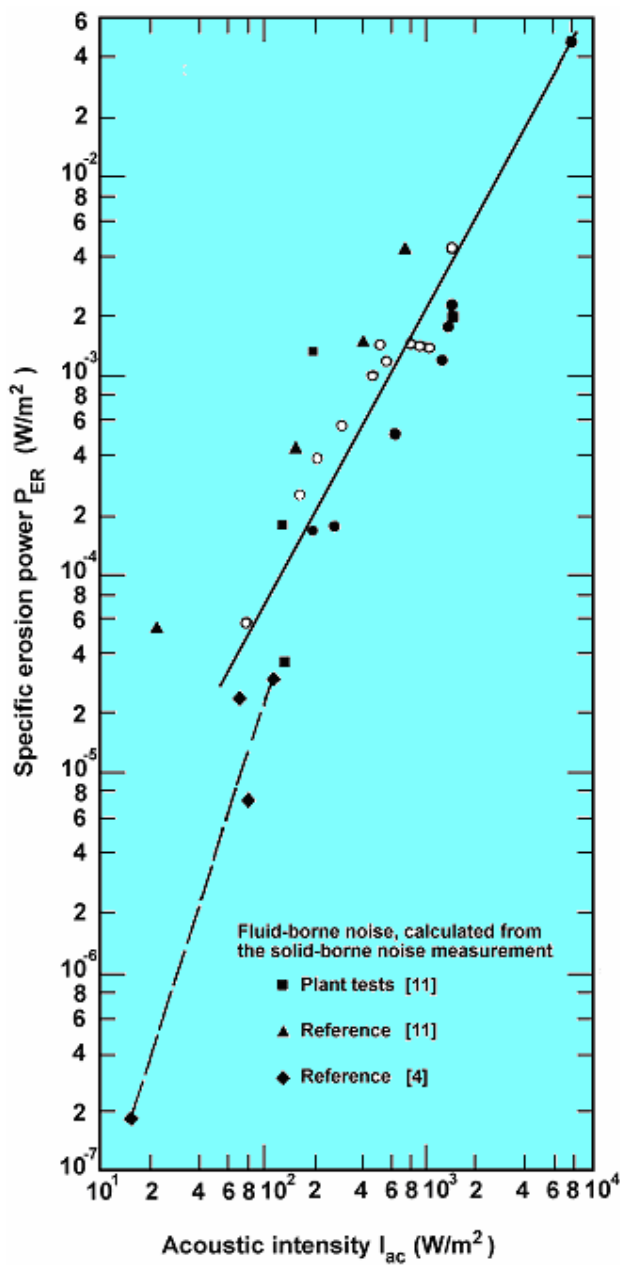
Fig. 22 Specific erosion power as a function of the fluid-borne noise

Since the acoustic models utilized are approximate and sound absorption as well as sound transmission are dependent on many parameters including pipeline connections and foundations, the degree of uncertainty and the amount of scatter associated with this calculation method are considerable. In addition, the measured data have been obtained from

various frequency bands since to date no unified measurement technique has come into being.

The precision of the process could be considerably improved if it were possible to measure the transfer functions between sound-borne and fluid-borne noise or at least spectra of such could be measured and the calculation carried out for each band.

The use of an acoustic model for the calculation of the fluid-borne noise from the solid-borne noise also has the advantage that the implosion pressure can be estimated and thus a value of absolute material loading is derived.

Measurements of the solid-borne noise spectrum indicate that the low frequency parts of it are of little account. Hence, here no attempt was made to establish a background level for solid-borne noise. The solid-borne noise level, however, was transformed to a reference blade number, since the number of noise sources (blades) must have a significant influence.

Relative erosion intensity

Since, to a first approximation, the sound pressure in the fluid is proportional to the measured acceleration, the same exponents for acceleration and sound pressure could be expected in the following relationship:

$$P_{ER} \sim CNL^x \sim CV^y$$

According to the measurements, [12], $x = y = 2.92$ would apply. Hence, for optimization purposes, a relative erosion intensity can be derived. This is defined as the erosion rate at a particular flow rate, referred to the erosion rate at the best point (or at any other reference point).

$$\varepsilon \equiv \frac{E_R(Q)}{E_R(Q_{ref})} = \left[\frac{CNL(Q)}{CNL(Q_{ref})} \right]^{2.92} = \left[\frac{CV(Q)}{CV(Q_{ref})} \right]^{2.92}$$

This relationship allows the erosion risk to be estimated at different loads under different operating conditions (e.g. temperatures, gas content, inlet pressure) or, after modifications (when the original condition was

measured previously) without the necessity of having to calculate to absolute values.

This procedure can, for example, be appropriate when another frequency range was used for the measurements.

Erosion rate and material loss

The possibilities of obtaining quantitative cavitation diagnosis basing on solid-borne or fluid-borne noise measurements are represented in Figure 23. According to this, a relatively simple diagnosis instrument can be constructed on the basis of solid-borne noise measurements. This instrument can also carry out all necessary cumulated operations. When determining erosion rate or load-dependent cumulated material loss, the following sources of error and uncertainties are to be taken into account:

Location of bubble implosion (on the impeller vanes within the liquid)
Air precipitation
Cavitation noise from foreign sources (for example valves, diffuser and labyrinths)
High background noise level masked by progressive cavitation
Impossibility of accurate determination of background noise level during measurement on installations
Uncertain determination of the acoustic cavitation pressure when it is only higher than the background noise level with a small amount.
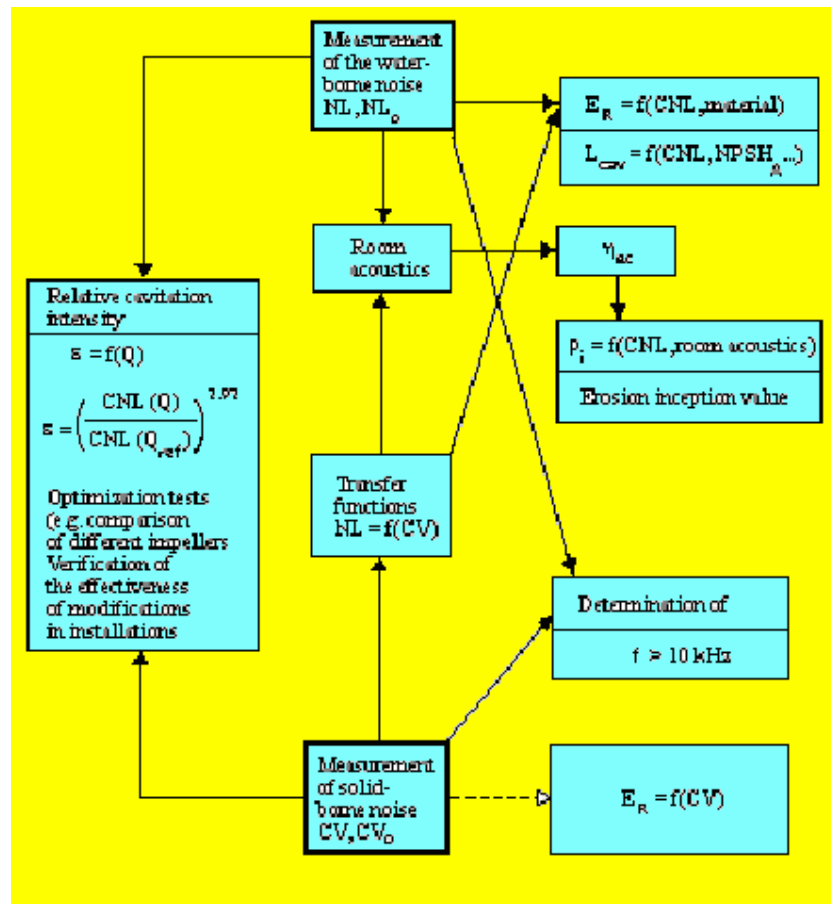
Fig. 23 Diagnosis possibilities available using fluid-borne and solid-borne noise

Fig. 24 Sheet and groove erosion on a pump impeller
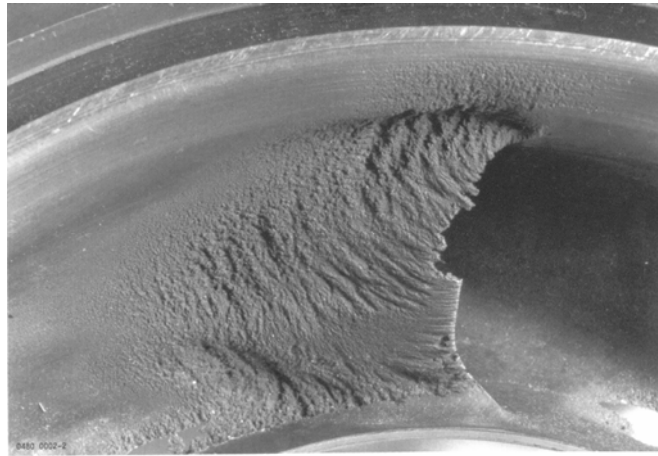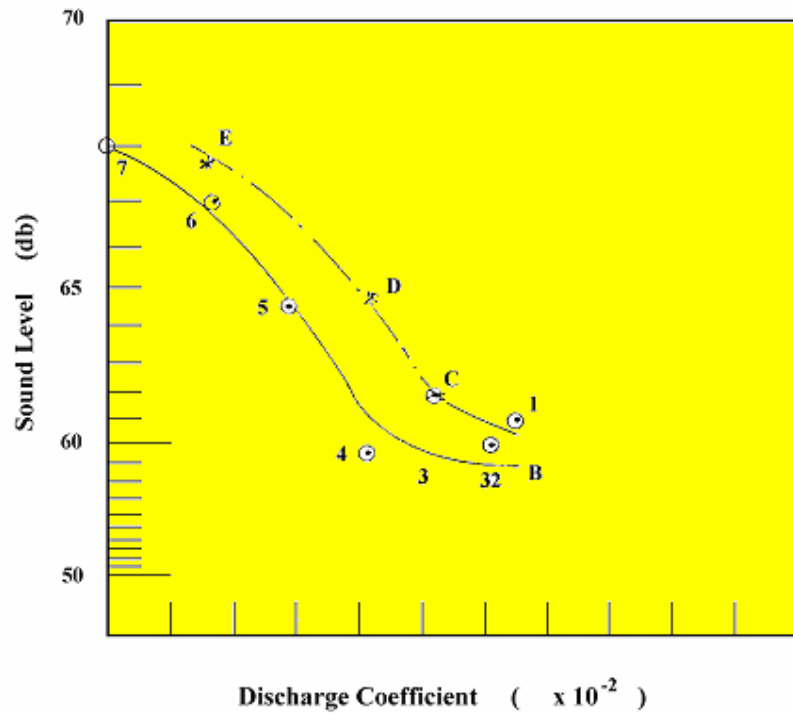
Fig. 25 Pump impeller showing cavitation erosion

12. *CAVITATION DETECTION BY DIGITAL ACOUSTIC EMISSION ANALYSIS:*

Up to now, digital acoustic emission analysis (AEA) has been used with success over a wide range of industrial applications. Figure 26 shows sound level measurements of centrifugal pump equipped with 5 blades impeller, the increase in sound level due to cavitation is clear. The (AEA) has proved to be a good tool for early detection and surveillance of cavitation damage. Also, the vibration measurements and analysis has been used long time for the cavitation detection. This text is not intended to cover this aspect, the reader may find detailed information in reference [21].

**Fig. 26 Sound level at frequencies 28600 and 14300 CPM
at impeller speed equals 2860   (5 blades)**
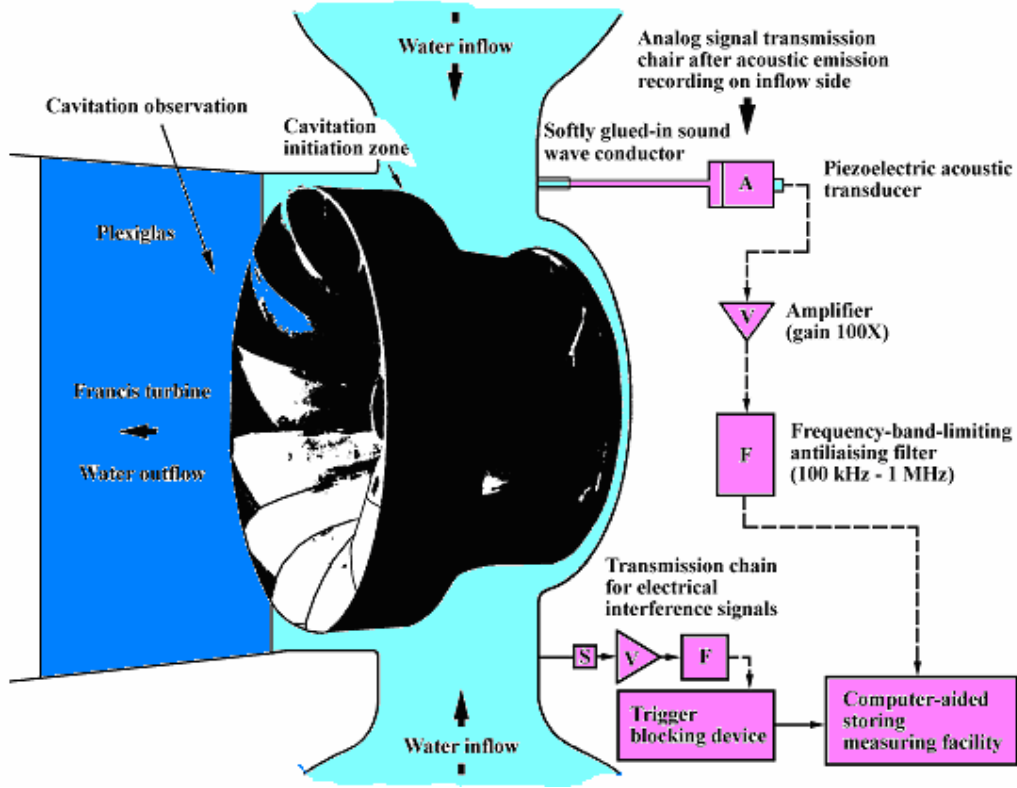
Fig. 27 AEA facility for cavitation investigation

13. HOW TO PREVENT CAVITATION:

1- A knowledge of the cavitation characteristics of pumps is the most important prerequisite of any cavitation problem study.

2- Second in importance is the knowledge of existing suction conditions of the plant at the time the pump selection is made.

3- An increase of suction pipe size, reduction of suction pipe length, elimination of turns, provision of a good suction bell - in other words, reduction of losses in the suction pipe - improve the suction conditions of a pump with regard to cavitation.

4- An increase in the number of vanes in high specific speed pumps, or the removal of parts of the vanes and opening the passages in the impeller eye of low specific speed pumps, will reduce the minimum suction head to meet fixed head-capacity conditions.

5- An ample suction approach area without excessive prerotation and a better streamlining of impeller approach are essential to obtain optimum cavitation characteristics of a pump.

6- Special materials may be used to reduce the pitting of pump parts due to cavitation, when justified, or when it is impossible to eliminate cavitation by any other means.

7- The impeller velocities, impeller vane load, and head per stage should be low for minimum suction head. All these factors lead to a bigger pump operated at a low speed, and possibly to location of the operating point to the left of the b.e.p.

8- A low impeller inlet angle β_1 leads to a reduction of NPSH requirements particularly at partial capacities.

9- A uniform velocity distribution through the impeller eye is important to obtain a minimum NPSH condition. Figure 28 shows a test of the same impeller in two casings; one has a straight tapered suction nozzle (full lines), the other has a flat elbow inlet nozzle (dotted lines). The advantages of the straight suction nozzle as to cavitation are quite obvious.
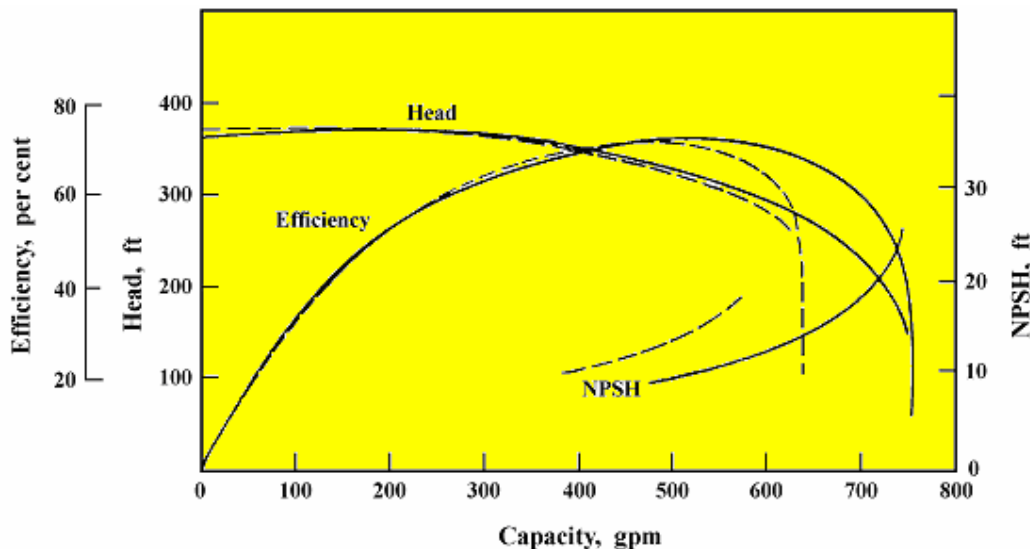
Fig. 28 Effect of suction nozzle on NPSH requirements. 3-in. pump, 3500 rpm.
    Full lines: straight end suction;
    Dotted lines: flat elbow suction nozzle

References "Appendix II"

1. **ABBOT, P.,** "Acoustic and Vibration Techniques for Cavitation Monitoring EPRI AP-5385", Sept. 1987. MEYER, E., NEUMANN, E. G., Physikalische und Technische Akustik, Vieweg Verlag, 1967.
2. **AVELLAN, F. and KARIMI, A.,** "Dynamics of Vortex Cavitation Involved in the Erosion of Hydraulic Machines", Proceedings 7th Conference on Erosion by Liquid and Solid Impact, Cambridge, Sept. 1987.
3. **AVELLAN, F., DUPONT, P. and FRAHAT, M.,** "Cavitation Erosion Power", ASME-JSME Fluids Engineering Conference, Portland, June 1991.
4. **BOURDON, P., SIMONEAU, R., AVELLAN, F. and FARHAT, M.,** "Vibratory Characteristics of Erosive Cavitation Vortices Downstream of a Fixed Leading Edge Cavity", IAHR Symposium, Belgrade 1990, Paper H3.
5. **CANAVELIS, R. and GRISON, P.,** "Aspects industriels de la cavitation", Revue française de Mécanique, 1986, No. 4, pp. 171-181.
6. **CHAHINE, G.L.,** "Pressure Generated by a Bubble Cloud Collapse", ASME Cavitation Forum, St. Louis 1982, pp. 27-30.
7. **CSANADY, G.T.,** "*Theory of Turbomachines*", McGraw-Hill Book Company, 1964.
8. **DURRER, H.,** "Cavitation Erosion and Fluid Mechanics", Sulzer Technical Review, Vol. 68, No. 3, 1986, pp. 55-61.
9. **FLORJANCIC, D.,** "Experimentelle Kavitationsuntersuchungen an einer Kreiselpumpe", Thesis, Swiss Federal Institute of Technology. Zurich, 1970
10. **FRANKLIN, R.E. and McMILLAN, J.,** "Noise Generation in Cavitating Flows of Submerged Jets", ASME Intl. Symposium on Cavitation Noise, Phoenix (AZ), Nov. 1982.

11. **GÜLICH, J.F.,** "Bestimmung der Kavitationserosion in Kreislepumpen auf Grund der Blasenfeldlänge und des Kavitationsschalls", Thesis, Technische Hochschule, Darmstadt, 1989.
12. **GÜLICH, J.F., "**Diagnosis of Cavitation in Centrifugal Pumps", Sulzer Technical Review, Vol. 74, No. 1, 1992, pp. 29-35.
13. **GÜLICH, J.F.,** "Guidelines for Prevention of Cavitation in Centrifugal Feedpumps", EPRI Report GS-6398, Nov. 1989.
14. **HAMMITT, F.G.,** "*Cavitation and Multiphase Flow Phenomena*", McGraw-Hill Book Company, 1980.
15. **HECKL, M. and MÜLLER, H.A.,** "*Taschenbuch der Technischen Akustik*", Springer Verlag, 1975.
16. **HUTTON, S.P. and FURNESS, R.A.,** "Thermodynamic Scale Effects in Cavitating Flows and Pumps", Proceedings of I. Mech. Eng. Conference: Cavitation, Sept. 1974, Edinburgh.
17. **KATO, H. et al.,** "Mechanism and Scaling of Cavitation Erosion", 12th Symposium on Naval Hydrodynamics, Washington, 1978, pp. 452-469.
18. **KNAPP, R.T. and DAILY, J.W.,** "*Cavitation*", Eng. Soc. Monograph, McGraw-Hill, New York, 1970.
19. **LAKSHMINARAYANA, B.,** "*Fluid Dynamics and Heat Transfer of Turbomachines*", John Wiley & Sons, Inc., 1996.
20. **LEDUC, D. and WEGNER, M.,** "Méthodes d'approche du bruit engendré par la cavitation", La Houille Blanche, 1985, No. 8, pp. 697-708.
21. **NERZ, K.P.,** "Early Detection and Surveillance of Material Damaging Processes by Digital Acoustic Emission Analysis", Sulzer Technical Review, Vol. 68, No. 3, 1986, pp. 62-64.
22. **OKAMURA, T. et al.,** "Intensity of Cavitation Erosion in Centrifugal Pumps Operating at Low Flow Rate", ASME Conference on Cavitation Hydraulic Structures and Turbomachinery, Albuquerque, 1985, pp. 63-70.
23. **PEARSALL, I.S., "**New Developments in Hydraulic Design Techniques", Proceedings of Pumps Conference: Inter-Flow 1978.
24. **RAMAMURTHY, A.S. et al.,** "Velocity Exponent for Erosion and Noise Due to Cavitation", ASME J. of Fluids Engineering, Vol. 101, March 1979, pp. 69-75.
25. **RAYAN, M.A., MAHGOB, M. and HASABO, N.,** "Cavitation Erosive Wear in Centrifugal Pump Impeller", ASME Cavitation and Multi-Phase Flow Forum, Publication ASME, July 1987.
26. **RAYAN, M.A.,** "Experimental Study of the Cavitation Erosion in Centrifugal Pump Impeller", Cavitation and Multiphase Flow Forum, Publication ASME, FED Vol. 23, 1985, pp. 82-83.
27. **RIEGER, H.,** "Kavitation und Erosion", VDI-Bericht No. 354, 1979, pp. 139-148.
28. **ROSS, D.,** "*Mechanics of Underwater Noise*", Pergamon Press, 1976.
29. **STAHL, H.A. and STEPANNOF, A.J.,** "Thermodynamic Aspects of Cavitation in Centrifugal Pumps", Trans. ASME, Vol. 78, 1956, pp. 1691-1693.
30. **STEPANOFF, A.J.,** "*Centrifugal and Axial Flow Pumps*", McGraw-Hill Book Company, 1975.
31. **TILLNER, W., FRITSCH, H., KRUFT, R., LEHMANN, W., LOUIS, H. and MASENDORF, G.,** "The Avoidance of Cavitation Damage", (ed. W.J. Bartz) (in German), 1990, English translation Maxwell, A.J. (ed. Turton, R.K.), 1993, MEP, London.

32. **TURTON, R.K.,** "*Principles of Turbomachinery*", 2nd edition, Chapman & Hall, London, 1995.
33. **VARGA, J.J., SEBESTYEN, G. and FAY, A.,** "Detection of Cavitation by Acoustic and Vibration-Measurement Methods", La Houille Blanche, 1969, No. 2, pp. 137-149.
34. **WISLICENUS, G.F.,** "*Fluid Mechanics of Turbomachinery*", Dover Publication Inc., New York, 1965.

APPENDIX "III"

SOLVED EXAMPLES AND PROBLEMS

CHAPTER I

BASIC THEORY

1.1 Velocity Diagram:

The velocity of the fluid particle moving through an impeller channel must satisfy the vectorial relationship.

$$\vec{C} = \vec{W} + \vec{U}$$

where:

C : is the absolute velocity
W : is the relative velocity tangent to the blade
U : is the tangential velocity
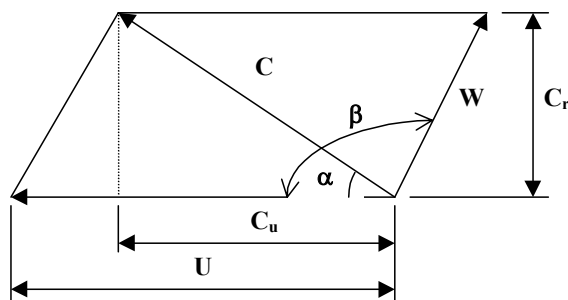
$$2 \, \omega.r = \frac{\pi DN}{60}$$

where:

N : the revolution per minute
D : the rotor diameter $= 2r$
ω : the angular velocity

C_r : the radial component of the absolute velocity
C_u : the tangential component of the absolute velocity
β : the blade angle
α : the angle between the tangential direction and the absolute velocity

The power generated from or by turbomachine rotor is defined by:

$$\text{Power} = \int\int \; r.\omega \; \vec{C}.dQ_m$$

The theoretical head generated $H_o = \dfrac{U_2 C_{u_2} - U_1 C_{u_1}}{g}$

The degree of reaction $\sigma = \dfrac{\left(U_1^2 - U_2^2\right) + \left(W_2^2 - W_1^2\right)}{\left(C_1^2 - C_2^2\right) + \left(U_1^2 - U_2^2\right) + \left(W_2^2 - W_1^2\right)}$

1.2 Coefficients and Efficiencies:

1.2.1 Circulatory Flow Coefficient

$$\eta_\infty = \overline{C}_{u_2} / C_{u_2}$$

where (the prime) to define the actual tangential velocity.

1.2.2 Manometric efficiency (Pump)

$$\eta_{man.} = \frac{\text{actual measured head}}{\text{head imparted to fluid by impeller}} = \frac{H_a}{H_o}$$

1.2.3 Mechanical efficiency

$$\eta_{mech.} = \frac{\gamma.QH_o}{Const.} / BHP \qquad \text{(Pump)}$$

or

$$\eta_{mech.} = BHP / \frac{\gamma.QH_o}{Const.} \qquad \text{(Turbine)}$$

1.2.4 Hydraulic efficiency (Turbine)

$$\eta_{hyd.} = H_o / H_{av}$$

Solved Examples

Example (1)

Derive an expression for the head created by the centrifugal forces only in a rotating element containing fluid such as pump impeller.

Solution

From Newton's second law of motion:

$$F = M.a = M\, r\, \omega^2$$

Consider a small element dM

$$dF = dM\, r\, \omega^2$$

where dF is the force produced due to the rotation of the mass dM in radial direction $\partial P = \dfrac{\partial F}{\partial A}$.

i.e.

$$\partial P = \partial\, r.rd\phi.dz.\rho.r\omega^2\, /\, dA \tag{1}$$

and $dA = r\, d\phi\, dz$, i.e.

$$\partial P = \rho\omega^2 r\partial r \tag{2}$$

Now apply Newton's second law of Motion on the Z direction, we obtain:
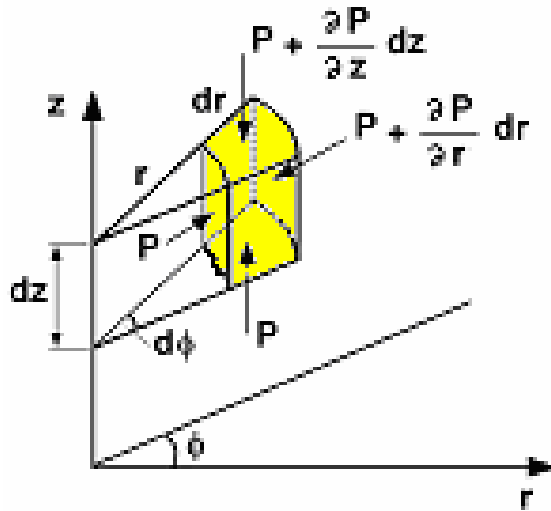
$$P.r.dr.d\phi - \left(P + \frac{\partial P}{\partial z}dz\right)r.dr.d\phi - \rho g.r.dr.d\phi.dz = 0$$

or

$$\frac{\partial P}{\partial z} = -\rho g \tag{3}$$

Note that P is a function of $r.z$

$$dP = \frac{\partial P}{\partial r}dr + \frac{\partial P}{\partial z}dz \tag{4}$$

294

From equations (2), (3) and (4):

$$dP = \rho\omega^2 r.dr - \rho g.dz$$

Integrate from r_1 to r_2

$$P_2 - P_1 = \frac{\rho\omega^2}{2}\left(r_2^2 - r_1^2\right) + \rho g\left(Z_1 - Z_2\right)$$

$P_2 - P_1$ represents the increment in total pressure due to centrifugal forces only. The last formula is important to the study of turbomachine. If Bernoulli's equation is applied, ($P_2 - P_1$) equals the difference in potential kinetic energy.

Example (2)

Starting from Bernoulli's equation for a steady flow, determine the head developed by a turbomachine.

Solution

Applying Bernoulli's equation on the relative path:

Consider also that the axis of reference rotate with the rotating element in such way, that we can consider that there is no power gained from the machine and vice-versa no power induced to the machine.

$$\left[\frac{P_1}{\rho g} + \frac{W_1^2}{2g} + V\right]_1 = \left[\frac{P_2}{\rho g} + \frac{W_2^2}{2g} + V\right]_2 \tag{1}$$

V_1 and V_2 represent the potential energy, which include the effect of centrifugal forces, which is calculated previously in the last example.

i.e.

$$\frac{P_1}{\rho g} - \frac{P_2}{\rho g} = \frac{W_2^2 - W_1^2}{2g} + \frac{\omega_1^2 r_1^2 - \omega_2^2 r_2^2}{2g} + Z_2 - Z_1 \tag{2}$$

$$U = \omega r$$

Applying Bernoulli's equation on the absolute path:

i.e.

$$H_o = \left[\frac{P_2}{\rho g} + \frac{C_2^2}{2g} + Z_2\right] - \left[\frac{P_1}{\rho g} + \frac{C_1^2}{2g} + Z_1\right] \tag{3}$$

From equations (2) and (3), we can find:

$$H_o = \frac{C_2^2 - C_1^2}{2g} + \frac{W_1^2 - W_2^2}{2g} + \frac{U_2^2 - U_1^2}{2g} \tag{4}$$

which is the general equation for the power delivered by the turbomachine.

The above equation could be also represented on the following form:

$$W^2 = U^2 + C^2 - 2UC \cos\alpha_2$$

Substitute in equation (4):

$$H_o = \frac{C_2 U_2 \cos\alpha_2 - C_1 U_1 \cos\alpha_1}{g}$$

Example (3)

A pump impeller rotating at 1400 rpm has an outside radius of 21 cm, the vane outlet angle β_2 is 158° and the radial velocity at the outlet C_{r2} is 4 m/s. Assuming radial flow at inlet, draw the theoretical outlet velocity diagram and calculate the various velocities and angles. What is the theoretical head H_o assuming that the circulatory flow coefficient $\eta_\infty = 1$.

Solution

$\beta_2 = 158°$

$\omega = \dfrac{2\pi N}{60} = 146.6$ rad/s

$U_2 = \omega\, r_2 = 146.6 \times 0.21 = 30.8$ m/s

$W_2 = \dfrac{C_{r_2}}{\sin(180 - \beta_2)} = \dfrac{4}{\sin 22°} = 10.66$ m/s

$C_{u_2} = U_2 - \dfrac{C_{r_2}}{\tan(180 - \beta_2)}$
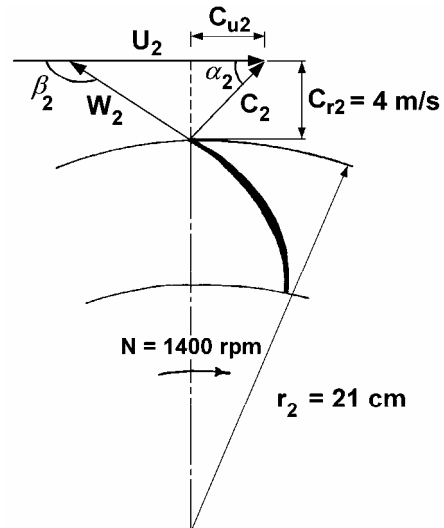
$= 30.8 - \dfrac{4}{\tan 22°} = 20.9$ m/s

$C_2 = \sqrt{C_{r2}^2 + C_{u2}^2}$

i.e. $C_2 = \sqrt{(4)^2 + (20.9)^2} = 21.3$ m/s

$\alpha_2 = \tan^{-1}\dfrac{C_{r_2}}{C_{u_2}} = 10° \, 50'$

$H_o = \dfrac{U_2 C_{u_2} - U_1 C_{u_1}}{g} = \dfrac{U_2 C_{u_2}}{g}$

C_{u2}
U_2
α_2
β_2 W_2 C_2 $C_{r2} = 4$ m/s
N = 1400 rpm
$r_2 = 21$ cm

296

$$H_o = \frac{30.8 \times 20.9}{9.81} = 65.6 \quad m$$

Example (4)

In the preceding example; assume a deviation of $10°$ applied to β_2 due to circulation after the modern theory, draw the velocity diagram and find the theoretical head H_o assuming radial flow at inlet, neglecting the deviation in inlet velocity diagram.

Assuming that the mechanical efficiency $\eta_{mech} = 0.95$, the hydraulic (or manometric) efficiency $\eta_{man} = 0.8$, find the required power to drive the pump. Also, calculate the water horsepower. The flow is 30 lit/s.

Solution

$$\eta_\infty = \frac{\overline{C}_{u_2}}{C_{u_2}}$$

i.e. $\overline{C}_{u_2} = 0.8 \times 20.9 = 16.7 \quad m/s$
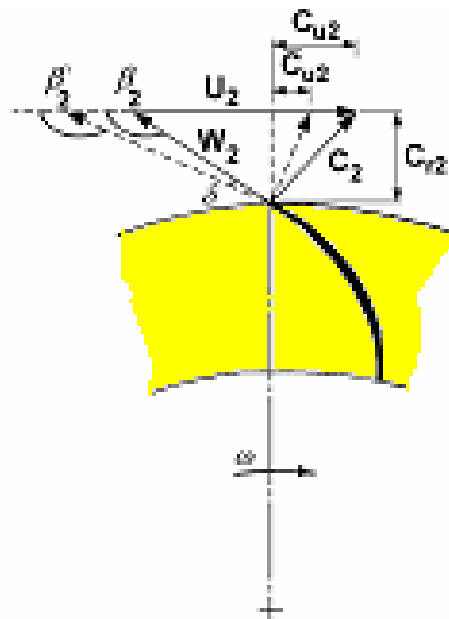
$$H_o = \frac{U_2 \overline{C}_{u_2}}{g} = \frac{30.8 \times 16.7}{9.81} = 52.5 \ m$$

$$\eta_{mech} = \frac{\gamma Q H_o}{75 \ B.H.P.}$$

i.e.
$$B.H.P. = \frac{1000 \times 0.030 \times 52.5}{75 \times 0.95} = 22.1 \quad hp$$

The power required to drive the pump = 22.1 hp

$$\eta_{man} = \frac{actual\ measured\ head}{head\ imparted\ to\ the\ fluid\ by\ impeller} = \frac{H_a}{H_o}$$

$$W.H.P. = \frac{\gamma Q H_a}{75} = \frac{1000 \times 0.030 \times 52.5 \times 0.80}{75} = 16.8 \quad hp$$

Example (5)

A turbine rotates at 150 rpm and discharges 0.8 m³/s. The radial velocity at inlet $C_{r_1} = 2$ m/s and equals 6 m/s at exit. The physical data are: $r_1 = 0.5$ m, $r_2 = 0.2$ m,

$\alpha_1 = 15°$, $\beta_2 = 135°$, $Z_1 = Z_2$, the pressure head at exit is 6 m. Assuming a loss of head of 2 m, calculate:

a) The head, power delivered by the turbine, (no draft tube are used) neglect circulatory flow and hydraulic losses.
b) The pressure head at entrance.
c) The degree of reaction.

Solution

a)

$$\omega = \frac{2\pi N}{60} = 15.7 \quad \text{rad/s}$$
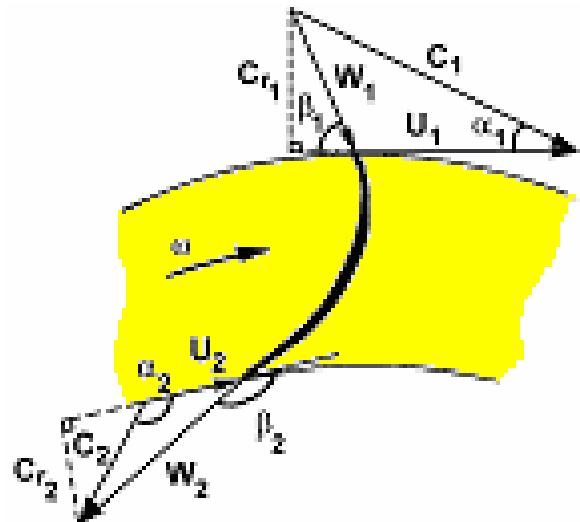
$$U_1 = \omega\, r_1 = 7.85 \quad \text{m/s}$$

$$U_2 = \omega\, r_2 = 3.14 \quad \text{m/s}$$

$$C_{u2} = \frac{C_{r_2}}{\tan(180 - \beta_2)} - U_2$$

$$= 6 - 3.14 = 2.86 \quad \text{m/s}$$

$$H_o = \frac{C_{u1}U_1 - C_{u2}U_2}{g} = 5.05 \quad \text{m}$$

$$Power = \frac{\gamma\, Q\, H_o}{75} = 53.9 \quad \text{hp}$$

b) Applying Bernoulli's equation between (1) and (2):

$$\frac{P_1}{\rho g} + Z_1 + \frac{C_1^2}{2g} - H_{loss} - H_o = \frac{P_2}{\rho g} + Z_2 + \frac{C_2^2}{2g} \qquad (Z_1 = Z_2)$$

$$C_1^2 = C_{u1}^2 + C_{r1}^2 = 57.65 \quad \text{m}^2/\text{s}^2$$

$$C_2^2 = C_{u2}^2 + C_{r2}^2 = 44.18 \quad \text{m}^2/\text{s}^2$$

$$\frac{P_1}{\rho g} + \frac{57.65}{2(9.81)} - 2 - 5.05 = 6 + \frac{44.18}{2(9.81)}$$

i.e. pressure head at entrance $P_1 / \rho g = 12.36$ m

c) The degree of reaction $= \dfrac{\left(\dfrac{P_1}{\rho g} + Z_1\right) - \left(\dfrac{P_2}{\rho g} + Z_2\right)}{H_o}$

In this case, we must subtract the entry losses from $P_1 / \rho g$ to obtain the real pressure head at entrance.

$$\sigma = \frac{(12.36 - 2) - 6}{5.05} = 0.864$$

298

The turbine is reaction type.

<u>N.B.:</u> We can find the same value for σ using the following form of σ.

$$\sigma = \frac{\left(U_1^2 - U_2^2\right) + \left(W_2^2 - W_1^2\right)}{\left(U_1^2 - U_2^2\right) + \left(W_2^2 - W_1^2\right) + \left(C_1^2 - C_2^2\right)}$$

$$W_1^2 = U_1^2 + C_1^2 - 2U_1 C_{u1}$$
$$= 61.62 + 57.65 - 2 \times 7.46 \times 78.5 = 2.146$$

i.e. $W_1 = 1.465$ m/s

$$W_2^2 = U_2^2 + C_2^2 - 2U_2 C_{u2} = 36.08$$
$$W_2 = 6 \text{ m/s}$$

$$\sigma = \frac{(61.62 - 9.86) + (36 - 2.1)}{(61.62 - 9.86) + (36 - 2.1) + (57.6 - 44.18)}$$
$$\sigma = 0.864$$

Example (6)

It is desired to pump 100 lit/s of water to the top of a cooling tower, the required manometric head was 19 meters. A radial centrifugal pump type was selected to give the required manometric head. The pump technical data are as following: impeller outside diameter $D_2 = 21$ cm, vane outlet angle $\beta_2 = 158°$, impeller tip width $= 5$ cm and rotating speed $N = 1750$ rpm. Find the following:

a) The theoretical head, manometric (hydraulic) efficiency, the required power to drive the pump if the mechanical efficiency $\eta_{mech} = 0.95$. Neglect the circulatory flow.

b) If the circulatory flow coefficient is 0.8, find the tangential component of the absolute velocity at exit due to the modern theory $\bar{C}_{u2}$. Also, calculate the deviation angle δ.

Solution

a)
$$H_o = \frac{U_1 C_{u_1} - U_2 C_{u_2}}{g} = \frac{U_2 C_{u_2}}{g}$$

$$\omega = \frac{2\pi N}{60} = 183.25 \quad \text{rad/s}$$
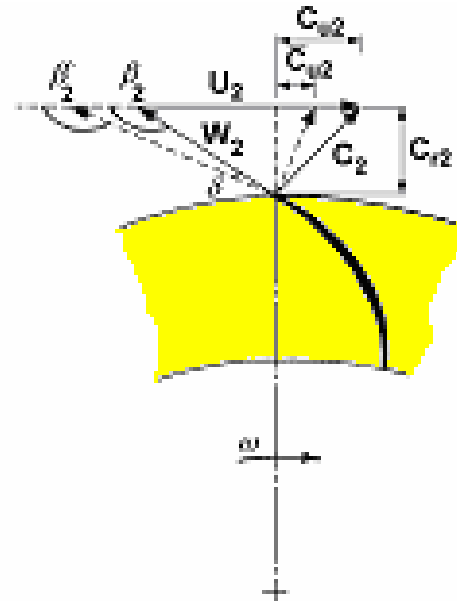
$$U_2 = \omega r_2 = 183.25 * 0.21/2 = 19.24 \quad \text{m/s}$$

$$C_{u_2} = U_2 - \frac{C_{r_2}}{\tan(180 - \beta_2)}$$

$$C_{r2} = \frac{Q}{\pi D_2 b_2} = \frac{0.1}{\pi \times 0.21 \times 0.05} = 3.03 \quad \text{m/s}$$

$$C_{u_2} = 19.24 - 7.5 = 11.74 \quad \text{m/s}$$

$$H_o = \frac{19.24 \times 11.74}{9.81} = 23 \quad \text{m}$$

$$\eta_{man} = \frac{\text{actual head measured}}{\text{head imparted to the fluid by the impeller}} = \frac{19}{23} = 0.83$$

$$\eta_{mech} = \frac{\gamma Q H_o}{75 B.H.P.}$$

$$\therefore B.H.P. = \frac{1000 \times 0.1 \times 23}{0.95 \times 75} = 32.2 \quad \text{hp}$$

b)
$$\eta_\infty = \frac{\overline{C}_{u_2}}{C_{u_2}}$$

$$\overline{C}_{u_2} = 0.8 \times 11.74 = 9.39 \quad \text{m/s}$$

$$\overline{C}_{u_2} = U_2 - \frac{C_{r_2}}{\tan(180 - \beta_2')}$$

$$\tan(180 - \beta_2') = \frac{C_{r_2}}{U_2 - \overline{C}_{u_2}} = \frac{3.03}{19.24 - 9.29} = 0.307$$

$$\beta_2' = 162° \, 54'$$

$$\delta = \beta_2' - \beta_2 = 4° \, 54'$$

Problems

1- Determine the expression of the degree of reaction and show that the propeller pump is a reaction machine.

2- A turbine rotates at 100 rpm and discharges 0.84 m^3/s, the hydraulic efficiency under these conditions is 75.5 %. The physical data are: $r_1 = 0.46$ m, $r_2 = 0.22$ m, $\alpha_1 = 15°$, $\beta_2 = 135°$, $A_1 = 0.12$ m^2, $A_2 = 0.078$ m^2. Neglect the circulatory flow coefficient and take the mechanical efficiency $\eta_{mech} = 0.95$. Determine the power delivered by the turbine.
(39 HP)

3- A centrifugal pump rotates at 600 rpm. The following data are taken: $r_1 = 5.08$ cm, $r_2 = 20.3$ cm, radial area $A_1 = 769$ cm^2, radial area $A_2 = 295$ cm^2, $\beta_1 = 135°$, $\beta_2 = 120°$ and assume radial flow at entrance to blades. Neglecting friction, calculate the relative velocities at entrance and exit and the power transmitted to the water.

4- A reaction turbine is working under a head of 25 meters running at 300 rpm. The velocity of the periphery of the wheel is 30 m/s and the radial velocity C_{r_1} is 4 m/s. If the hydraulic losses are 20 % of the available head and the discharge is radial, find:
     i) the inlet angle β_1 and guide blade angle at inlet α_1.
     ii) the rotor diameter.
(170° 18′, 31° 27′, 1.9 m)

5- An impeller rotating at 1150 rpm has the following dimensions:
$b_1 = 3.175$ cm	$b_2 = 1.9$ cm
$D_1 = 17.8$ cm	$D_2 = 38$ cm
$\beta_1 = 162°$	$\beta_2 = 160°$

(b_1, b_2 are the passage widths at inlet and outlet, respectively).
Cross-sectional area $A = \pi D b$ (if vane thickness is neglected). Assuming radial inlet flow and neglecting vane thickness draw the virtual velocity diagrams and calculate the rated capacity in lit/min and the virtual head neglecting the circulatory flow.

6- A pump impeller is 0.3 m in diameter, discharges 0.15 m^3/s when running at 1200 rpm. The blade angle β_2 is 160° and the exit area A_2 is 0.023 m^2. Assuming losses of 2.8 (W_2^2/2g) and 0.38 (C_2^2/2g), compute the efficiency of the pump (exit area A_2 is measured normal to W_2).
(62.1 %)

7- A centrifugal pump having an effective blade angle at outlet of 135° is required to lift water against a head of 22 m, the speed of the shaft being 800 rpm and the velocity of flow is 2 m/s. Calculate the diameter of impeller required if:
(i) The whole of the energy corresponding to velocity of wheel at exit is wasted.
    (ii) 40 % of this energy is converted into useful pressure energy.

Neglect friction in case (ii). State also the width of the mouth of the impeller if the discharge is 150 lit/s. Blade thickness may be disregarded.
(0.546 m, 0.476 m, 0.05 m)

8- An inward flow reaction turbine discharges radially and the velocity of flow is constant and equal to the velocity of discharge from the suction tube. Show that the hydraulic efficiency can be expressed by:

$$\eta_h = \cfrac{1}{1 - \cfrac{0.5\tan^2\alpha_1}{\left[\left(\cfrac{\tan\alpha_1}{\tan\beta_1}\right) - 1\right]}}$$

where α_1 and β_1 are the guide and vane angles at inlet.
(A.M.I.E., May 1969)

9- A centrifugal pump has 50 cm outside diameter and 25 cm inside diameter rotating at 1000 rpm. The vanes are set forward at an angle of $\beta_2 = 45°$. If the radial velocity of the water through the wheel be maintained constant at 2 m/s, find the angle of the vanes at inlet, the velocity and the direction of the water at exit and the work done by the wheel per kg of water.

******

CHAPTER II

DIMENSIONAL ANALYSIS

2.1 Hydraulic Similarity

a- Geometric similitude:
$$\frac{L_{model}}{L_{prototype}} = L_{ratio}$$

b- Kinematic similitude: $V_{model} / V_{prototype} = V_m / V_p = L_r / T_r$

c- Dynamic similitude: $F_{model} / F_{prototype} = M_m.a_m / M_p.a_p$

2.2 Application of Dimensional Analysis in Turbomachines

Apply the Buckingham π theorem considering a series of geometrically similar pumps or turbines of different sizes but having similar flow patterns.

The following π terms can be found:
$\pi_1 = gH_o / D^2N^2$ Manometric coefficient.
$\pi_2 = Q / ND^3$ Analogue to discharge coefficient.
$\pi_3 = ND^2 / \nu$ Reynolds number.

2.3 Reynolds Number Effect

To avoid the problems arise when a machine is originally designed at certain Reynolds number and tested in the shop at different Reynolds numbers, the following formula is used:
$$\frac{1 - \eta_1}{1 - \eta_2} = \left(\frac{Re_2}{Re_1} \right)^n$$
where n varies from 0.1 to 0.25.

2.4 Affinity Laws

For the same machine at different speeds and flows:
$H_1 / H_2 = (N_1 / N_2)^2$ $(Q_1 / Q_2 = N_1 / N_2)$

$$Q_1 / Q_2 = (H_1 / H_2)^{1/2}$$

2.5 Non-Dimensional Coefficients

- Specific Speed: Universal $N_s = \dfrac{N \sqrt{Q}}{(gH)^{3/4}}$

- Pressure Coefficient $\phi = H / (U_2^2 / 2g)$

- Flow Coefficient $\psi = (Q / A) / U$

- Specific Diameter $D_{sp} = \dfrac{D(gH)^{1/4}}{\sqrt{Q}}$

Solved Examples

Example (1)

Show that the specific speed expression $\left(N_s = \dfrac{N\sqrt{Q}}{(gH)^{3/4}} \right)$ depends upon the proportions of the wheel rather than the operating speed, consider pump impeller and radial flow.

Solution

$$N_s = \frac{N(Q)^{1/2}}{(gH)^{3/4}} \tag{1}$$

$$Q = A_1 C_{r_1} = \pi . D_1 b_1 C_{r_1}$$
$$= \pi . D_1 b_1 U_1 \tan(180 - \beta_1)$$

i.e. $\quad Q = \pi^2 D_1^2 \tan(180 - \beta_1) b_1 N \tag{2}$

$$H = \frac{C_{u_2} U_2}{g} \quad \text{radial flow at inlet.}$$

$$= \frac{U_2}{g}\left[U_2 - \frac{C_{r_2}}{\tan(180 - \beta_2)} \right]$$

$$C_{r_2} = \frac{Q}{A_2} = \frac{Q}{\pi . D_2 b_2} = \frac{\pi^2 D_1^2 \tan(180 - \beta_1) b_1 N}{\pi . D_2 b_2} \tag{3}$$

i.e. $\quad H = \dfrac{U_2^2}{g}\left[1 - \dfrac{\pi^2 D_1^2 \tan(180 - \beta_1) b_1 N}{\pi . D_2 b_2 \tan(180 - \beta_2) \pi D_2 N} \right]$

$$H = \frac{\pi^2 D_2^2 N^2}{g}\left[1 - \left(\frac{D_1}{D_2}\right)^2 \left(\frac{b_1}{b_2}\right)\left(\frac{\tan(180 - \beta_1)}{\tan(180 - \beta_2)}\right) \right] \tag{4}$$

From equations (4), (2) and (1), we find:

$$N_s = \frac{N\left[\pi^2 D_1^2 \tan(180 - \beta_1) b_1 N\right]^{1/2}}{\left(\pi^2 D_2^2 N^2\right)^{3/4}\left[1 - \left(\dfrac{D_1}{D_2}\right)^2 \left(\dfrac{b_1}{b_2}\right)\left(\dfrac{\tan(180 - \beta_1)}{\tan(180 - \beta_2)}\right) \right]^{3/4}}$$

$$
\text{i.e.} \quad N_s = \frac{\dfrac{D_1}{D_2}\sqrt{\dfrac{b_1}{D_2}\tan\left(180 - \beta_1\right)}}{\sqrt{\pi}\left[1 - \left(\dfrac{D_1}{D_2}\right)^2\left(\dfrac{b_1}{b_2}\right)\left(\dfrac{\tan\left(180 - \beta_1\right)}{\tan\left(180 - \beta_2\right)}\right)\right]^{3/4}}
$$

Example (2)

A centrifugal pump pumps water at 0.240 m³/s rotating at 1200 rpm, a prototype pump using 10 lit/s is to be tested. If the diameter of the model is 3 times the diameter of the prototype, at what speed should the prototype run, if the pump pumps oil at a head of 30 meters. What would be the required power to drive the model and the prototype? Take the model efficiency = 0.8.

Solution

$$
\pi_1 = \left.\frac{Q}{ND^3}\right|_1 = \left.\frac{Q}{ND^3}\right|_2
$$

$$
\frac{0.240}{1200\left(3\right)^3} = \frac{0.01}{N} \qquad\qquad N = 1350 \text{ rpm}
$$

$$
\pi_2 = \left.\frac{gH}{N^2 D^2}\right|_1 = \left.\frac{gH}{N^2 D^2}\right|_2
$$

$$
\frac{30}{\left(1200\right)^2\left(3\right)^2} = \frac{H_2}{\left(1350\right)^2} \qquad\qquad H_2 = 3.75 \quad \text{m}
$$

$$
P_1 = \frac{\gamma Q_1 H_1}{75\,\eta} = \frac{1000\times0.240\times30}{75\times0.8} = 120 \quad hp
$$

$$
\frac{1 - \eta_1}{1 - \eta_2} = \left(\frac{D_2}{D_1}\right)^{0.25}
$$

$$
\frac{1 - 0.80}{1 - \eta_2} = \left(\frac{1}{3}\right)^{0.25} \qquad\qquad \eta_2 = 0.736
$$

$$
P_2 = \frac{1000\times0.01\times3.75}{75\times0.736} = 0.68 \quad hp
$$

Example (3)

It is required to construct a hydraulic turbine (inward Francis type) for a hydraulic power plant to operate under the following conditions: rotating speed $N = 110$ rpm, discharge $Q = 11$ m³/s, the radial velocity at the inlet $C_{r1} = 2$ m/s, the radial velocity at exit $C_{r2} = 9.5$ m/s and the physical data are: the outside diameter $D_1 = 4.5$ m, the absolute inlet angle $\alpha_1 = 15°$, the absolute exit angle $\alpha_2 = 90°$ (radial flow at exit). Assume that the potential energy is constant ($Z_1 = Z_2$), the pressure head at exit equal 6 m and the hydraulic losses are 2 m. Calculate:

(i) The head and power delivered by the turbine, (assume no draft tube). Calculate also the specific speed.
(ii) The pressure head at entrance.
(iii) It's required to construct a prototype to predict the actual machine performance, the assumed outside diameter D_2 of the prototype was 0.3 m and the hydraulic circuit in the laboratory has the following specifications: Available head = 5.5 m, Hydraulic efficiency = 0.8. Find the required speed and flow, also calculate the specific speed N_s.

(B.Sc., Elec. Eng., June 1977)

Solution

$D_1 = 4.5$ m $\qquad\qquad$ $C_{r2} = 9.5$ m/s $\qquad\qquad$ $C_{r1} = 2$ m/s
$Q = 11$ m³/s $\qquad\qquad$ $N = 110$ rpm

i) $\omega = \dfrac{2\pi N}{60} = 11.5$ rad/s

$U_1 = \omega R_1 = 25.9$ m/s

$C_{u_1} = \dfrac{C_{r_1}}{\tan \alpha_1} = \dfrac{2}{\tan 15} = 7.46$ m/s

$H_o = \dfrac{C_{u_1} U_1 - C_{u_2} U_2}{g}$

$H_o = \dfrac{7.46 \times 25.9}{9.81} = 19.7$ m

$Power = \dfrac{1000 \times 11 \times 19.7}{75} = 2889$ hp

$N_s = \dfrac{N\sqrt{B.H.P.}}{H^{5/4}} = 142$

ii) $\dfrac{P_1}{\rho g} + \dfrac{C_1^2}{2g} + Z_1 = \dfrac{P_2}{\rho g} + \dfrac{C_2^2}{2g} + Z_2 + h_{loss} + h_o$

$C_1^2 = \sqrt{C_{u1}^2 + C_{r1}^2} = 7.7$ m/s

$C_2 = C_{r2} = 9.5$ m/s

$\dfrac{P_1}{\rho g} + \dfrac{(7.7)^2}{2*9.81} = 6 + \dfrac{(9.5)^2}{2*9.81} + 2 + 19.7$

$$\frac{P_1}{\rho g} = 29.3 \quad \text{m} \quad \text{or} \quad 2.9 \text{ kg/cm}^2$$

iii) $D_2 = 0.3$ m $\qquad\qquad H_2 = 5.5$ m $\qquad\qquad \eta_h = 0.8$

$$\left.\frac{H}{N^2 D^2}\right|_1 = \left.\frac{H}{N^2 D^2}\right|_2$$

$$\frac{19.7}{(110)^2 (4.5)^2} = \frac{5.5 \times 0.8}{N^2 (0.3)^2} \qquad \therefore N = 780 \quad \text{rpm}$$

$$\left.\frac{Q}{N.D^3}\right|_1 = \left.\frac{Q}{N.D^3}\right|_2$$

$$\frac{11}{110(4.5)^3} = \frac{Q}{780(0.3)^3} \qquad \therefore Q = 0.025 \quad \text{m}^3/\text{s}$$

$$P = \frac{1000 \times 0.025 \times 5.5 \times 0.8}{75} = 1.13 \quad \text{hp}$$

$$N_s = \frac{N\sqrt{B.H.P.}}{H^{5/4}} = 142$$

Example (4)

A turbine develops 144 HP running at 100 rpm under a head of 7.7 meters. What power would be developed under a head of 11 meters? At what speed should the turbine run?

Solution

$$\pi_2 = \left.\frac{H}{N^2 D^2}\right|_1 = \left.\frac{H}{N^2 D^2}\right|_2$$

For the same machine: $\qquad\qquad \left.\dfrac{H}{N^2}\right|_1 = \left.\dfrac{H}{N^2}\right|_2$

$$\frac{7.7}{(100)^2} = \frac{11}{N_2^2} \qquad\qquad N_2 = 120 \quad \text{rpm}$$

$P \alpha \rho g Q H \qquad\qquad\qquad Q \alpha ND^3$

i.e. $\qquad\qquad P \alpha ND^3 H$

i.e. $\qquad\qquad \dfrac{P_1}{P_2} = \dfrac{N_1 H_1}{N_2 H_2}$

$$\frac{144}{P_2} = \frac{100 \times 7.7}{120 \times 11}$$

$$\therefore P_2 = 247 \text{ HP}$$

Example (5)

At a hydraulic plant the propeller type turbine are rated at 48,000 HP at 82 rpm under a 14 meters head, the diameter is 7 meters, for a geometrical similar turbine to develop 36,000 HP under a 11 meters head, what speed and diameter should be used? What percentage change in flow is probable?

Solution

$$P = \frac{\gamma \, QH}{Const.} \qquad\qquad \frac{P_1}{P_2} = \frac{Q_1 H_1}{Q_2 H_2}$$

i.e. $\quad \dfrac{Q_1}{Q_2} = \dfrac{P_1}{P_2}\dfrac{H_2}{H_1} = \dfrac{48,000}{36,000}\dfrac{11}{14} = 1.05$

The flow will be reduced by 5 %.

$$\left.\frac{Q}{N.D^3}\right|_1 = \left.\frac{Q}{N.D^3}\right|_2$$

$$N_2 D_2^3 = \frac{Q_2}{Q_1} N_1 D_1^3$$

$$= 0.95 \times 82 \times (7)^3 = 26720$$

$$\left.\frac{H}{N^2 D^2}\right|_1 = \left.\frac{H}{N^2 D^2}\right|_2$$

$$N_2^2 D_2^2 = \frac{H_2}{H_1} N_1^2 D_1^2 = \frac{11}{14}(82)^2 (7)^2 = 258874$$

$$N_2 D_2 = 509$$

$$D_2 = \sqrt{\frac{26720}{509}} = 7.25 \quad \text{m}$$

$$N_2 = \frac{509}{7.25} = 70 \quad \text{rpm}$$

$$N_2 = \frac{509}{7.25} = 70 \quad \text{rpm}$$

Problems
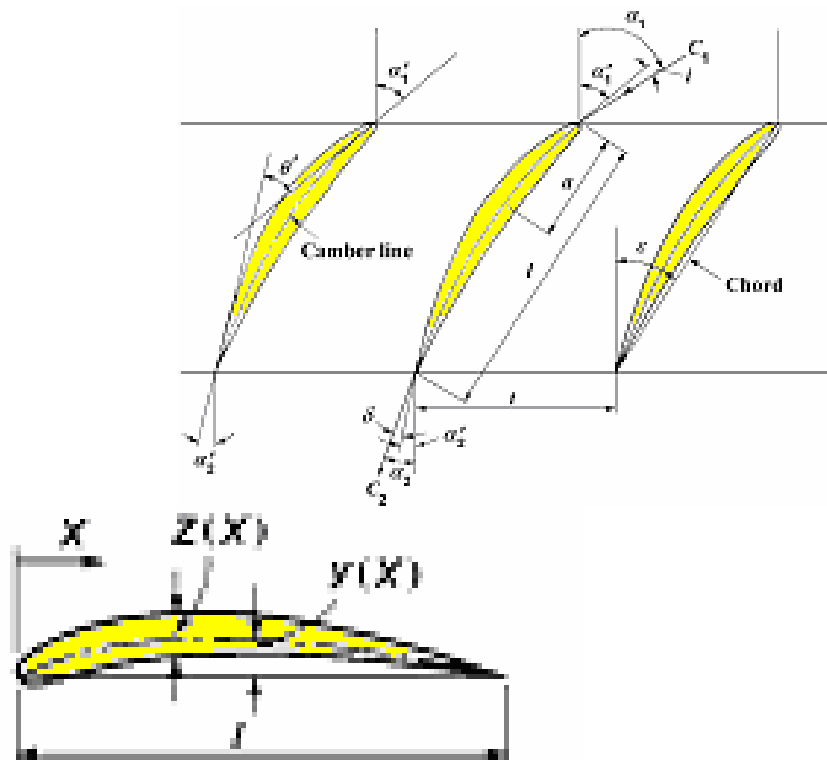
1- An impulse wheel at best speed produced 125 HP under a head of 85 m. By what percent should the speed be increased for a 90 m head? Assuming equal efficiencies, what power would result?
(2.9 %, 136.1 hp)

2- Assuming the power delivered to a pump is a function of the specific weight of the fluid, the flow in lit per minute, and the head delivered, establish an equation by dimensional analysis [power equation].

3- A centrifugal pump discharged 65 lit/min against a head of 17 meters when the speed was 1500 rpm. The diameter of the impeller was 30 cm and the brake horsepower was 6 HP. A geometrically similar pump 38 cm in diameter is run at 1750 rpm. Assuming equal efficiencies, what head will be developed? How much water will be pumped and what brake horsepower will be required?
(37.1 m, 154 1it/min, 31.7 hp)

4- A turbine model, built to a scale of 1:5 was found to develop 4.5 BHP at a speed of 400 rpm under a head of 2 meters. Assuming the overall efficiency of the full-size turbine = 0.8, find the speed and the power of the full-size turbine under a head of 9 meters.
(169.7 rpm, 1073.8 hp)

5- Seawater of specific gravity 1.03 is to be circulated through condensers by a propeller pump 120 cm in diameter, it is found that a scale model of the pump 25 cm in diameter gives its best efficiency when pumping 97 lit/s of fresh water against a head of 4 meters at a speed of 2060 rpm. What should be the speed of the full size pump to deliver 90 tons per minute and what pressure difference would it generate?
(279.6 rpm, 17177 Pa)

6- A centrifugal pump of diameter 30 cm (throat diameter) running at 1450 rpm delivers 74 lit/s of water against a head of H = 46 m at optimum efficiency of 81 %. Investigate the operation of the pump handling:
    (a) oil of sp. gr. 0.86, viscosity $0.857*10^{-5}$ m^2/s,
    (b) fuel oil of sp. gr. 0.94, viscosity $0.232*10^{-5}$ m^2/s.

7- The same model pump of Problem (6) is now built to a scale 2.5 times larger and used to pump oil (b) of the previous problem. Find at a speed of 1450 rpm head capacity, power, and efficiency at the optimum point.

8- A centrifugal pump of impeller 25 cm diameter revolving at 1450 rpm delivers at its best efficiency point 29 lit/s of water ($v = 0.9*10^{-6}$ m^2/s) against a head of 20 meters at an efficiency of 80 percent. A geometrically similar pump is to be built to produce a head of 25 m when handling oil of specific gravity 0.89 and kinematic viscosity $4.5*10^{-5}$ m^2/s at the best efficiency point, at the same speed, what will the diameter of the pump have to be and what will be the quantity delivered, power consumption, and efficiency at the same optimum operating point?
(Mans. Univ., B.Sc., 1978)

<div align="center">******</div>

CHAPTER III

CASCADE MECHANICS

3.1 CASCADE NOMENCLATURE:

Blade inlet angle	α_1'		Position of	
Blade outlet angle	α_2'		maximum camber	a
Fluid inlet angle	$\alpha_1 = \alpha_1' + i$		Chord	ℓ
Fluid outlet angle	$\alpha_2 = \alpha_2' + \delta$		Spacing	t
Blade camber angle	$\theta' = \alpha_1' - \alpha_2'$		Space-chord ratio	t/ℓ
Stagger angle	ε		Solidity	ℓ/t
Deflection	$\theta = \alpha_1 - \alpha_2$			
Incidence angle	$i = \alpha_1 - \alpha_1'$			
Deviation angle	$\delta = \alpha_2 - \alpha_2'$			

The head-capacity curve:

$$H = BU^2 - AUQ$$

where A and B are constants and equal as follows:

$$A = \frac{\ell}{t}(\tan\alpha_1 - \tan\alpha_2)$$
$$B = 1$$

3.2 Cascade Coefficients:

Total pressure loss coefficient $\qquad \zeta = \dfrac{\Delta P_o}{\dfrac{1}{2}\rho C_a^{\ 2}}$

Pressure rise coefficient $\qquad C_p = \dfrac{\Delta P}{\dfrac{1}{2}\rho C_a^{\ 2}}$

Tangential force coefficient $\qquad C_f = 2\,(\tan\alpha_1 - \tan\alpha_2)$

Mean angle $\qquad \tan\alpha_m = \frac{1}{2}\,(\tan\alpha_1 + \tan\alpha_2)$

Lift coefficient $\qquad C_L = 2\,(t/\ell)\cos\alpha_m\,(\tan\alpha_1 - \tan\alpha_2) - C_D\tan\alpha_m$

Drag coefficient $\qquad C_D = \zeta\,(t/\ell)\cos^3\alpha_m$

Discharge coefficient $\qquad \psi = C_a\,/\,U$

Cascade efficiency $\qquad \eta = 1 - \zeta\,\psi/C_f$

Deviation from ideal direction $\qquad \delta = \alpha_2 - \alpha_2'$

Nominal deviation $\qquad \delta^* = m\,\theta'\,(t/\ell)^n$

where $\qquad m = 0.23\,(2\,a/\ell)^2 + \alpha_2^*/500$

$\qquad a:$ the distance of maximum camber from leading edge,

$\qquad \alpha_2^*:$ the nominal exit angle.

$\qquad n = 0.5$ for compressor cascades,

$\qquad n = 1$ for compressor inlet guide vanes.

Solved Examples

Example (1)

A compressor cascade has a space-chord ratio of unity and blade inlet angle of 45°, stagger angle $\varepsilon = 28°$, using the NACA results, Fig (3.5), find the loss coefficient ζ, C_f, the drag coefficient, the lift coefficient and pressure rise coefficient. Also, find the pressure rise across the cascade for $\rho = 9.5$ x 10^{-6} kg/m³, $C_a = 47$ m/s. If the above cascade is for an axial air compressor of tangential velocity U = 150 m/s, find its efficiency and construct the velocity diagrams (Adapted from Csanady).

Solution

Inlet angle $\alpha_1 = 45°$, from Figure 3.5 at $\alpha_1 - \varepsilon = 17°$
$\theta = \alpha_1 - \alpha_2 = 30°$
i.e. $\alpha_2 = 15°$

$\tan \alpha_m = 0.5 (\tan \alpha_1 + \tan \alpha_2)$ $\alpha_m = 32.37°$
$C_D (\cos^2 \alpha_1 / \cos^2 \alpha_m) = 0.055$
$C_D = 0.078$

From equation (3.8) $C_f = 2 (\tan \alpha_1 - \tan \alpha_2) = 1.46$
From equation (3.16) $C_L = 2 (t/\ell) \cos \alpha_m (\tan \alpha_1 - \tan \alpha_2) = 1.24$

It is easy to notice that the term $C_D \tan \alpha_m$ can be easily neglected since C_D is small and equals zero for ideal lift.

From equation (3.15) $C_D = \zeta (t/\ell) \cos^3 \alpha_m$
$\zeta = 0.129$
From equation (3.9) $\zeta = C_f \tan \alpha_m - C_p$
      $C_p = 0.796$

From equation (3.1) $C_p = \dfrac{\Delta P}{\frac{1}{2} \rho C_a^2}$

i.e. $\Delta P = 1/2 \rho C_a^2 C_p$
      $\Delta P = 1/2$ x 9.5 x 10^{-6} x $(47)^2$ x $0.796 = 8.35$ x 10^{-3} N/m²
which is corresponding to the static pressure rise or
         $P / \rho g = 8.35$ x $10^{-3} / (9.5$ x 10^{-6} x $9.81)$
            $= 89.6$ meters of air
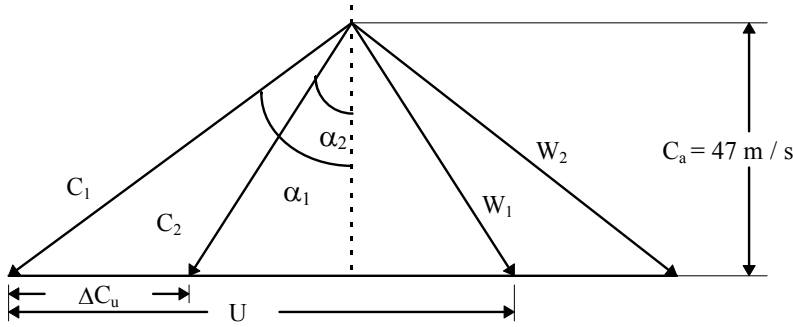
$\Delta C_u = C_a (\tan \alpha_1 - \tan \alpha_2) = 34.4$ m/s
$H = U \Delta C_u / g = 526$ m
$\psi = C_a / U = 0.313$
$\eta = 1 - \zeta \psi/C_f = 0.97$

Example (2)

A compressor cascade has a space-chord ratio of unity and blade inlet and outlet angles of 45° and 15°, respectively. If the blade camber line is a circular arc (i.e. $a/\ell = 0.5$) where a is the distance of maximum camber from leading edge. The cascade is designed to operate at Howell's nominal condition. Determine the fluid deflection, incidence and ideal lift coefficient at the design point (Adapted from Dixon).

Solution

The turning angle $\theta' = \alpha_1' - \alpha_2' = 30°$

$\qquad$ (α_1' and α_2' are the blade angles at inlet and outlet)

The nominal fluid outlet angle $\qquad\qquad \alpha_2^* = \alpha_2' + \delta^*$

$\qquad$ From equation (3.28): $\qquad\qquad \delta^* = m\theta'(t/l)^n$

$\qquad$ From equation (3.29): $\qquad\qquad m = 0.23(2a/l)^2 + \alpha_2^*/500$

Combining these three equations and solving for α_2^*, the following expression can be obtained:

$$\alpha_2^* = \frac{\alpha_2' + 0.23(2a/l)^2\theta'(t/l)^n}{1 - \theta'(t/l)^n/500}$$

Putting $a/l = 0.5$, $t/l = 1$ and $n = 0.5$, then $\alpha_2^* = 23.3°$

The nominal deflection $\theta^* = \alpha_1^* - \alpha_2^*$ (No turning)

From Figure 3.7: $\theta^* = 24°$

Hence $\alpha_1^* = 47.3°$ and the nominal incidence $i^* = \alpha_1^* - \alpha_1' = 2.3°$

The ideal lift coefficient corresponding to zero drag (i.e. $C_D = 0.0$)

From relation (3.16):

$\qquad$ $C_L = 2 \, (t/\ell) \cos \alpha_m \, (\tan \alpha_1 - \tan \alpha_2) - C_D \tan \alpha_m$ (The second term = 0.0)

$\qquad\qquad = 1.04$

Note that angles α_1 and α_2 correspond to the nominal Howell condition.

Example (3)

Experimental compressor cascade results suggest that the stalling lift coefficient of a cascade blade may be expressed as $C_L \left(\dfrac{C_1}{C_2} \right)^3 = 1.8$ where C_1 and C_2 are the entry and exit velocities. Find the stalling inlet angle for a compressor cascade of space/chord ratio of unity if the outlet air angle is 30°. If the total pressure loss coefficient at zero incidence i = 0 (corresponding to minimum pressure loss) $\zeta = 0.02$, find the corresponding pressure coefficient.

Solution

NOTE: Stall point is arbitrarily specified as the incidence at which the total pressure loss is twice the minimum loss in total pressure.

Assume $\alpha_1 = 40°$ From relation (3.16)

$C_L = 2 (t/\ell) \cos \alpha_m (\tan \alpha_1 - \tan \alpha_2) - C_D \tan \alpha_m$ (The second term = 0.0)   (1)

       $\tan \alpha_m = \tfrac{1}{2} (\tan \alpha_1 + \tan \alpha_2) = 0.708$

       $\alpha_m = 35° \ 18'$

Then from equation (1): $C_L = 0.427$

$C_1 \cos \alpha_1 = C_2 \cos \alpha_2 = C_a$

i.e. $\dfrac{C_1}{C_2} = \dfrac{\cos \alpha_2}{\cos \alpha_1}$

$$ C_L = 1.8 \left(\frac{C_2}{C_1} \right)^3 \qquad\qquad (2) $$

$$ C_L = 1.8 \left(\frac{\cos \alpha_1}{\cos \alpha_2} \right)^3 = 1.51 $$

Assume $\alpha_1 = 48°$

       $\tan \alpha_m = 0.84$ and $\alpha_m = 40° \ 06'$

From equation (1) $C_L = 0.82$ and from equation (2) $C_L = 0.83$ which is acceptable.

From relation (3.8)

       $C_f = 2 (\tan \alpha_1 - \tan \alpha_2)$

       $C_f = 1.066$

and ζ stalling equal twice of minimum, i.e. $\zeta = 2 \times 0.02 = 0.04$

From relation (3.9)

       $\zeta = C_f \tan \alpha_m - C_p$

i.e. $C_p = C_f \tan \alpha_m - \zeta = 0.857$

Example (4)

The cascade shown in Figure 3.5, is to be used for an axial flow propeller pump impeller. The cascade has a space-chord ratio of unity and blade inlet angle of 45° and stagger angle $\varepsilon = 28°$, find the pressure rise coefficient if the net positive suction head (total pressure at inlet minus vapor pressure) is 7 meters of water. Specify the maximum allowable axial velocity with regard to cavitation danger. The maximum surface velocity may be taken as 25 percent above inlet velocity C_1. Also, find Euler head and the efficiency.

Solution

Inlet angle $\alpha_1 = 45°$, from Figure 3.5 at $\alpha_1 - \varepsilon = 17°$

$\theta = \alpha_1 - \alpha_2 = 30°$ i.e. $\alpha_2 = 15°$

$\tan \alpha_m = 0.5 (\tan \alpha_1 + \tan \alpha_2)$ $\qquad \alpha_m = 32.37°$

$C_D (\cos^2 \alpha_1 / \cos^2 \alpha_m) = 0.055$

$C_D = 0.078$

From equation (3.8) $\qquad C_f = 2 (\tan \alpha_1 - \tan \alpha_2) = 1.46$

From equation (3.16) $\qquad C_L = 2 (t/\ell) \cos \alpha_m (\tan \alpha_1 - \tan \alpha_2) = 1.24$

From equation (3.15) $\qquad C_D = \zeta (t/\ell) \cos^3 \alpha_m$

$\zeta = 0.129$

From equation (3.9) $\qquad \zeta = C_f \tan \alpha_m - C_p$

$C_p = 0.796$

From the definition of the NPSH:

$$NPSH = \left(\frac{P_1}{\rho g} + \frac{C_1^{\,2}}{2g} \right) - \frac{P_v}{\rho g} = 7 \text{ m}$$

The cavitation occurs when $P_1 \le P_v$, so to prevent the pump from cavitation danger $\dfrac{C_1^{\,2}}{2g}$ must be equal or less than 7 meters.

i.e. $\dfrac{C_1^{\,2}}{2g} \le 7$ or $C_1 = 11.72$ m/s then $C_2 = 8.57$ m/s

and the maximum allowable surface velocity being $W_1 = 1.25 \, C_1$
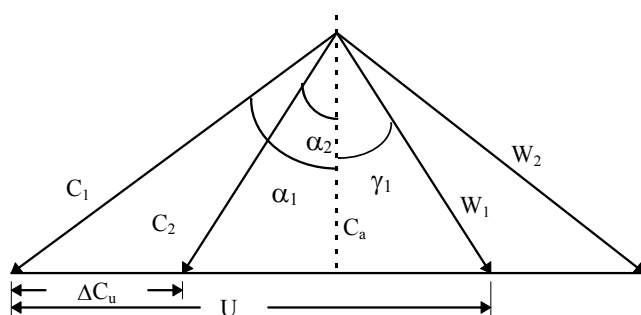
$$\cos \gamma_1 = \frac{C_a}{W_1} = \frac{C_a}{1.25 \, C_1}$$

also

$C_a = C_1 \cos \alpha_1 = C_2 \cos \alpha_2$

i.e. $\cos \gamma_1 = \dfrac{\cos \alpha_1}{1.25} = 0.566$

and $\gamma_1 = 55° 30'$

Maximum $C_a = C_1 \cos \alpha_1 = 8.28$ m/s

$U = C_a (\tan \alpha_1 + \tan \gamma_1) = 20.34$ m/s

317

$$\Delta C_u = C_a (\tan \alpha_1 - \tan \alpha_2) = 6.06 \text{ m/s}$$
$$H_o = U \, \Delta C_u/g = 12.56 \text{ m}$$

Discharge coefficient $\psi = C_a / U = 0.41$

Ideal cascade efficiency based on perfect fluid
$$\eta = 1 - \zeta \, \psi/C_f = 1 - 0.129*0.41/1.46 = 96 \%$$

The static pressure rise $\Delta P / \rho g$

$$C_p = \frac{\Delta P}{\frac{1}{2}\rho C_a^2}$$

$$\Delta H = C_p \frac{C_a^2}{2g} = 2.78 \text{ m}$$

The change in dynamic head $\dfrac{C_1^2 - C_2^2}{2g} = 3.26 \text{ m}$

The total expected gain = 2.78 + 3.26 = 6.04 m and the hydraulic efficiency = 6.04/12.56 = 0.48 which is low due to the limitation imposed by the NPSH.
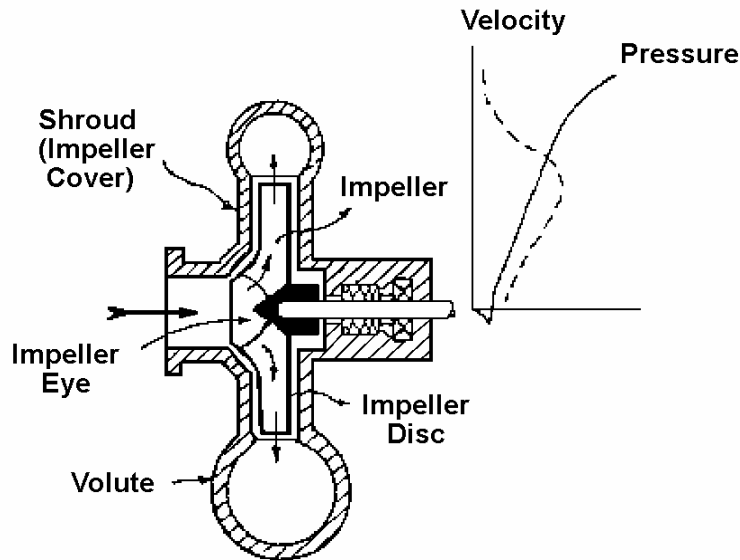
Problems

1- For the cascade data shown in Example 1, choose the optimum (ψ / C_f a minimum) operating point, and find the corresponding pressure rise and tangential force per centimeter height of blade, if axial velocity of 80 m/s, density of $9.5*10^{-6}$ kg/m^3, blade spacing 10 cm.

(0.022 Pa, 3.04 x 10^{-5} N/cm)

2- Explore one or two other possible choices of stagger angle in Example 1 with a view to ascertaining the most favorable design possibility with regard to efficiency.

3- A compressor cascade has the following data of $t/\ell = 1.0$, $\alpha_1' = 45°$, $\alpha_2' = 15°$. The nominal conditions were $\theta^* = 24°$ and $i^* = 2.3$, the off-design performance of this cascade is required at an incidence $i = 3.8°$ (referring to Fig. 3.8).

4- A compressor cascade has a space-chord ratio of unity, blade angle of 45° and stagger angle $\varepsilon = 28°$, find the loss coefficient, the drag coefficient, the lift coefficient, and the pressure rise coefficient. Also, find the pressure rise across the cascade for $\rho = 0.00001$ kg/m^3, $C_a = 47$ m/s (using NACA data: $\theta = \alpha_1 - \alpha_2 = 30°$ and $C_D \cos^2 \alpha_1 / \cos^2 \alpha_m = 0.0065$).

(B.Sc., Mans. Univ., 1982)

******

CHAPTER IV

INCOMPRESSIBLE FLOW TURBOMACHINES

4.1 Centrifugal Pumps (Performance Curve)

Theoretical head:

$$H_o = \frac{\left(U_1 C_1 \cos\alpha_1 - U_2 C_2 \cos\alpha_2\right)}{g}$$

Assuming radial inlet and substitute $C_2 \cos\alpha_2$ by $U_2 + (C_{r2} / \tan\beta_2)$

$$H_o = \frac{U_2^2}{g} + \frac{U_2 C_{r_2}}{g \tan\beta_2} \qquad \text{and} \qquad Q = \pi . D_2 b_2 C_{r_2}$$

Then:
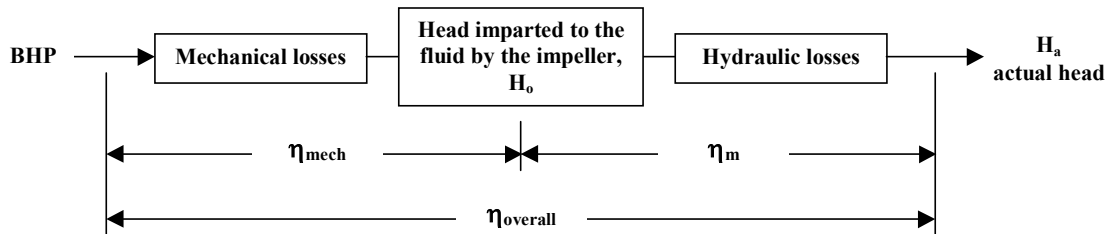
$$H_o = \frac{U_2^2}{g} + \frac{U_2 Q}{g \pi . D_2 b_2 \tan \beta_2}$$

4.2 Efficiencies and Coefficients of Centrifugal Pumps:

η_m = Manometric efficiency = $\dfrac{H_a \left(measured\ head\right)}{H_o}$

$\eta_{mech.}$ = Mechanical efficiency = $\dfrac{\gamma Q H_o}{Const. \times BHP}$

$\eta_{overall} = \eta_{mech.} \cdot \eta_m$

ψ = Discharge coefficient = $\dfrac{Q/A}{U}$ or $Q / \left(D^2 . \sqrt{2gH}\right)$

Universal specific speed $N_s = \dfrac{N\sqrt{Q}}{\left(gH\right)^{3/4}}$ in SI units

The net positive suction head NPSH

$$NPSH = \frac{P_{at}}{\rho g} \pm h_{ss} - h_f - h_v$$

where:

h_{ss} : Static suction head

h_f : Friction loss

h_v : Vapour pressure

Thoma cavitation factor $\sigma = \dfrac{NPSH}{H_m}$

4.3 Design Features of Centrifugal Pumps:

- Leakage Calculation

$$Q_L = C_v A_p \sqrt{2gh}$$

where:

C_v = Velocity coefficient

A_p = Clearance area

h = Head across the orifice = $0.75 \dfrac{U_2^2 - U_1^2}{2g}$

- Disk Friction

Disk friction losses = $K.D^2 U^2 \rho$
where K is a constant

- Axial Thrust $= \left(P_2 - P_1\right)\dfrac{\pi}{4}\left(D_1^2 - D_s^2\right)$

where subscripts 1, 2 and s indicate inlet, exit and shaft, respectively.

- Shaft diameter $\quad D_s = \sqrt[3]{\dfrac{16\,T}{\pi\,S_s}}$

where:

T is the torque,

S_s is the allowable shear stress.

- Eye Diameter D_o

$$D_o^2 = \frac{4}{\pi}\frac{Q}{U_o} + D_H^2$$

where D_H is the hub diameter.

$$b_1 = \frac{Q}{\pi.D_1.\varepsilon.C_{r_1}}$$

where ε is the contraction ratio.

Then, assume ϕ between 0.9 and 1.2

$$\phi = \frac{U_2}{\sqrt{2gH}} \quad \text{to find } D_2 \text{ and assume } \beta_2 \text{ is slightly lower than } \beta_1$$

322

The number of blades $Z_n = 6.5 \dfrac{D_2 + D_1}{D_2 - D_1} \sin(180 - \beta_m)$

where $\beta_m = (\beta_1 + \beta_2)/2$

$$\varepsilon = \frac{\pi D - t Z_n}{\pi D}$$

where t is the impeller thickness.

Solved Examples

Example (1)

Test results on a single stage single suction centrifugal mixed flow type pump operating at 375 rpm designed to deliver 2.4 m³/min of water are given in curve form as follows:

Flow (m³/min)	0	4	8	12	16	20	24	28	34
Head (m)	12	11.3	10.6	9.9	9.1	8.2	7.2	5.9	4.9
η (%)	0	23	45	62	75.5	84	88	85	81
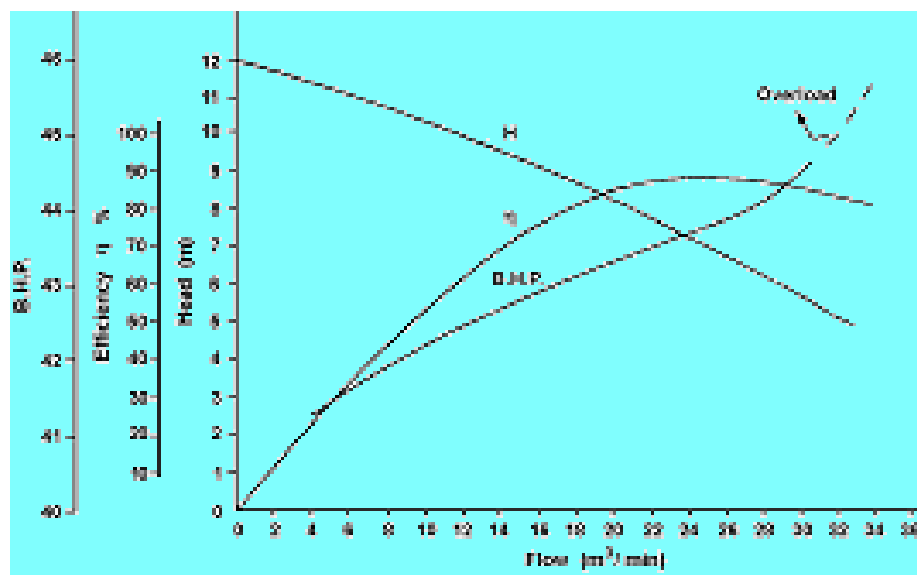
a- Plot these curves and draw the BHP curve.
b- On the same sheet, draw the same three curves in dotted lines if the liquid pumped has a specific gravity of 0.9 but otherwise the same as water, give a brief discussion of your reason for each curve.
c- Draw the performance curve for the pump when it rotates at 500 rpm.

Solution

(a) The horsepower $= \dfrac{\gamma \, QH}{\eta.Const} = \dfrac{1000 \; QH}{60 * 75 * \eta}$

Thus the power will be:

B.H.P.   41.8   42.5   42.8   43.3   43.6   43.9   45.7

(b) If the fluid density changes, this should not affect the head-discharge curve, so the head-discharge will remain constant, the delivery pressure will change only, ($P = \rho g h$).

324

The power should be reduced as it could be seen from the power relation.

$$\text{Power} = \frac{\gamma Q H}{\eta . Const.}$$

The efficiency is a relation between the head delivered and the power consumed which practically will alter (The hydraulic losses will change, as it is a function of the density and the viscosity of water), but it could be assumed constant.

(c) To draw the performance of the pump at different speeds, one can make use of the affinity laws as follows:

$$\frac{Q_1}{Q_2} = \frac{N_1}{N_2} \qquad \text{i.e.} \qquad Q_2 = \frac{N_2}{N_1} Q_1 \qquad \therefore Q_2 = \frac{500}{375} Q_1$$

$$\frac{H_1}{H_2} = \frac{N_1^2}{N_2^2} \qquad \text{i.e.} \qquad H_2 = \left(\frac{N_2}{N_1}\right)^2 H_1 \qquad \therefore H_2 = \left(\frac{500}{375}\right)^2 H_1$$

Example (2)

A pump whose performance is given by:

Q (lit/s)	0	150	300	450	600
H (m)	15.5	15	14	12	9

is interposed in a pipe in which the loss in suction pipe = 1/3 loss in delivery line when the static lift was 6 m, the maximum possible discharge was found to be 300 lit/s. Find the highest possible position of pump above sump level, given that $h_v = 0.3$ m, $h_{at} = 10.3$ m, cavitation factor = 0.5. Neglect the effect of kinetic energy loss in pipe.

Solution

The Thoma cavitation factor is defined by:

$$\sigma = \frac{H_{sv}}{H_m} \quad \text{where } H_{sv} \text{ is the NPSH}$$

i.e. $H_{sv} = 0.5\, H_m$

The manometric head at $Q = 300$ lit/s could be taken from the performance curve,
i.e. $H_m = 14$ m
i.e. $H_{sv} = 14 \times 0.5 = 7$ m

$$H_{sv} = \frac{P_{at}}{\rho g} - h_{ss} - h_f - h_v$$

$$7 = 10.3 - h_{ss} - h_f - 0.3$$

i.e. $h_{ss} + h_f = 3$ (1)

From the figure, we can write:

$$H_m = h_f(suction) + h_{ss} + h_{sd} + h_{fd}$$ (2)

we have: $h_s = h_{ss} + h_{sd} = 6$ m

and the losses in suction line equal 1/3 the losses in delivery line. If we put the loss in delivery line equal h_f

i.e. the loss in suction line = $h_f / 3$

Thus, from equation (2):

$$14 = 6 + h_f + h_f / 3$$

$$= 6 + \frac{4}{3} h_f$$

i.e. $h_f = 6$ m

The losses in suction pipe = $\frac{1}{3} \times 6 = 2$ m

From equation (1) $h_{ss} = 1$ m
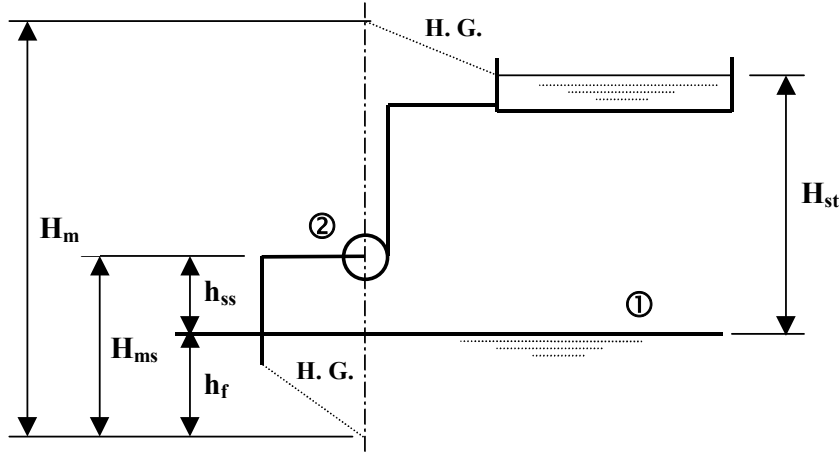
i.e. the highest possible position of the pump above the sump level would be 1 meter.

Example (3)

During a laboratory test on a pump, appreciable cavitation began when the pressure plus velocity head at inlet was reduced to 3.26 m while the total head change across the pump was 36.5 m and the discharge was 48 liters/s. Barometric pressure was 750 mm Hg and the vapour pressure of water 1800 Pa. What is the value of σ_c? If the pump is to give the same total head and discharge in a location where the normal atmospheric pressure is 622 mm Hg and the vapour pressure of water 830 Pa, by how much must the height of the pump above the supply level be reduced?

(Mans. Univ., B.Sc., 1978)

326

Solution

(a) Applying Bernoulli's equation between (1) and (2):

$$\frac{P_1}{\rho g} + \frac{C_1^2}{2g} + Z_1 = \frac{P_2}{\rho g} + \frac{C_2^2}{2g} + Z_2 + h_f , \qquad (C_1 = 0)$$

From the figure $Z_1 = 0, \ Z_2 = h_{ss}$

$$\frac{P_2}{\rho g} + \frac{C_2^2}{2g} = 3.26 \ \text{m} \ \text{(Given)}$$

and P_1 is the atmospheric pressure P_{at}, thus:

$$\frac{P_{at}}{\rho g} = \frac{P_2}{\rho g} + \frac{C_2^2}{2g} + h_{ss} + h_f \qquad\qquad (1)$$

$P_v = 1800 \ \text{Pa} \ \text{or} \ 1800 \ \text{N/m}^2 \ \text{or} \ 1800/9.8 = 183.6 \ \text{kg/m}^2$

$P_{at} = 75*13.6*10^4/1000 = 10200 \ \text{kg/m}^2$

i.e. $\quad h_{ss} + h_f = \dfrac{10200}{1000} - 3.26 = 6.94 \quad \text{m}$ $\qquad\qquad (2)$

We have $\sigma_c = \dfrac{H_{sv}}{H_m}$ and

$$H_{sv} = \frac{P_{at}}{\rho g} - h_{ss} - h_f - h_v \qquad\qquad (3)$$

$$h_v = \frac{183.6}{1000} = 0.1836 \quad \text{m}$$

From equations (2) and (3):

$$H_{sv} = \frac{10200}{1000} - 6.94 - 0.1836 = 3.076 \quad \text{m}$$

$$\therefore \sigma_c = \frac{3.076}{36.5} = 0.0843$$

(b) $\quad P_v = \dfrac{830}{9.8} = 84.69 \quad \text{kg/m}^2$

$$P_{at} = \frac{62.2*13.6*10^4}{1000} = 8459.2 \quad \text{kg/m}^2$$

$$\sigma_c \ H_m \ = \ H_{sv} \ = \ \frac{P_{at}}{\rho g} - (h_{ss} + h_f) - h_v$$

$$3.076 \ = \ \frac{8459.2}{1000} - (h_{ss} + h_f) - \frac{84.69}{1000}$$

$$h_{ss} + h_f \ = 5.3 \quad m$$

From equation (2) if h_f does not change:

$\therefore$ The pump height must be reduced by $6.94 - 5.3 = 1.64$ m.

Example (4)

It is required to pump 40 lit/s of water to the top of a cooling tower, the manometric head was 19 meters, a radial centrifugal pump was selected to develop the required manometric head, assume the eye diameter equal to the inlet diameter, the hub diameter $D_H = 7$ cm, the water velocity in the suction pipe $V_o = 4$ m/s. The contraction ratios at inlet and exit ε_1, $\varepsilon_2 = 0.9$, the pressure coefficient $\phi = 1.08$, the flow coefficient $\psi = 0.21$, the vane outlet angle $\beta_2 = 158°$, impeller tip width at inlet $= 2.3$ cm, the pump is direct driven by an electric motor at a speed of 1750 rpm, calculate: (assume radial flow at inlet)

i-   Approximate eye diameter, vane inlet angle β_1.

ii-   The theoretical (virtual) head developed, neglect all mechanical losses.

iii- The circulatory flow coefficient, the tangential component of the absolute velocity C_{u2} (after the modern theory) at exit, find also the angle of deviation (neglect the hydraulic losses).

iv- If the pump is placed 8 meters above the water level in suction line what would be the NPSH, does the pump cavitate? Calculate also the Thoma cavitation factor, assume the losses equal to 2.5 meters, the vapour pressure equal to 0.5 m and the atmospheric pressure $= 10.3$ m.

   (Mans. Univ., B.Sc., 1977)

Solution

a) $Q = AV_o = \dfrac{\pi}{4}\left(D_o^{\,2} - D_H^{\,2}\right)V_o$

i.e. D_o = eye diameter $= D_1$

$$D_1 = \sqrt{\frac{4}{\pi}\frac{Q}{V_o} + D_H^{\,2}} = 0.133 \quad m$$

$D_1 = 13.3$ cm

$\alpha_1 = 90°$

$$\tan(180 - \beta_1) = \frac{C_1}{U_1} = \frac{C_{r_1}}{U_1}$$

$$C_{r_1} = \frac{Q}{\pi D_1 b_1 \varepsilon_1}$$

$$= \frac{40}{1000 \times \pi \times 0.133 \times 0.023 \times 0.9} = 4.6 \quad \text{m/s}$$

$$\tan(180 - \beta_1) = \frac{4.6}{\dfrac{\pi \times 0.133 \times 1750}{60}} = 0.3770$$

i.e. $\quad \beta_1 = 159° 18'$

b) $\quad \phi = \dfrac{U_2}{\sqrt{2gH}}$

$$U_2 = \frac{\pi D_2 N}{60} = 1.08\sqrt{2 \times 9.81 \times 19} = 20.85 \quad \text{m/s}$$

$D_2 = 0.228$ m $\quad$ or $\quad$ 22.8 cm

$$\psi = \frac{C_{r_2}}{\sqrt{2gH}} = 0.21$$

$C_{r_2} = 4.05$ m/s

$$C_{u_2} = U_2 - \frac{C_{r_2}}{\tan(180 - \beta_2)} = 20.85 - \frac{4.05}{\tan 22°} = 10.9 \quad \text{m/s}$$

$$H_o = \frac{U_2 C_{u_2}}{g} = \frac{20.85 \times 10.9}{9.81} = 23.2 \quad \text{m}$$

$$Power = \frac{\gamma Q H_o}{Const.} = \frac{1000 \times 40 \times 23.2}{1000 \times 75} = 12.37 \quad \text{hp}$$

$$\eta = \frac{19}{23.2} = 0.815$$

c) $\quad \eta_\infty = \dfrac{\overline{C_{u_2}}}{C_{u_2}} = \dfrac{gH_2}{U_2} \cdot \dfrac{U_2}{gH_o} = 0.815$ (Neglecting all mechanical losses and friction

losses).

Thus, we can say that $\eta_\infty = \eta_h$ only if we neglect the mechanical losses and hydraulic losses in the pump. This is a theoretical case which does not exist actually.

$$\overline{C_{u_2}} = 8.924 \quad \text{m/s}$$

$$\tan(180 - \beta_2') = \frac{C_{r_2}}{U_2 - \overline{C_{u_2}}}$$

i.e. $\quad \beta_2' = 161°15'$

$\delta = \beta_2' - \beta_2 = 161°15' - 158° = 3°15'$

d) $NPSH = \dfrac{P_{at}}{\rho g} - h_{ss} - h_f - h_v$

$= 10.3 - 8 - 2 - 1 = -0.7$

i.e., the pump cavitate.

$\sigma = \dfrac{NPSH}{H_m} = \dfrac{-0.7}{19} = -0.0368$

Example (5)

Competitive bids from three companies for a water circulating pump to handle 2000 lit/min of water with a head of 50 meters and operates 8 hours/day, 300 day/year, are as follows:

Company	A	B	C
Price in £	230	410	260
Efficiency %	71	77	73
Estimated life in years	10	15	10

The annual fixed charges are 20 % of the initial price and the power costs 2 piasters per kW.hr, which pump could be selected?

Solution

Water horsepower $= \dfrac{\gamma Q H}{Const.}$

$= \dfrac{1000 \times 2000 \times 50}{1000 \times 60 \times 75} = 22.2$ hp

Cost of power = 0.746 x 2 = 1.49 piaster per HP-hr

Company	A	B	C
B.H.P.	31.2	28.8	30.4
B.H.P.-hr/year	74,800	69,100	73,000
Power cost/year	1115	1030	1080
Fixed charges/year	46	82	52
Depreciation	23	27.3	26
Total annual cost	1184	1139	1158

It may be seen from the above example that the total annual cost are about the same for the bids A, B, and C, despite the differences between their initial prices, but if the operation time is increased, the bid B will be in a better position.

Example (6)

A pump is to operate 2400 hours a year with a guaranted efficiency of 75 %, the water horsepower is 50, annual fixed charges including depreciation are 20 % of the contract price and power costs 2 piasters per BHP-hr. What penalty should be involved for each point that the efficiency is below the guaranted value?

Solution

Guaranted horsepower = 50/0.75 = 66.7
Each point of efficiency below the guaranted efficiency represents = 66.7/75 = 0.89 BHP.
The extra cost per year = 0.89 x 2400 x 0.02 = 42.72 if the depreciation is 20% of the contract price.
Thus, the pump is expected to have 5 year life.
The penalty P = 42.72 x 5 = 214 £

Example (7)

A centrifugal pump, which runs at 16.6 rev/s, is mounted so that its centre is 2.4 m above the water level in the suction sump. It delivers water to a point 19 m above its centre; the friction loss in the suction pipe is 68 Q^2 meter and that in the delivery pipe is 650 Q^2 meter where Q in m^3/s is the rate of flow. The impeller of the pump is 350 mm diameter, and the width of the blade passages at outlet is 18 mm. The blades themselves occupy 5 % of the circumference and are backward facing at 35° to the tangent. At inlet, the flow is radial and the radial component of velocity remains unchanged through the impeller. Assuming that 50 % of the velocity head of the water leaving the impeller is converted to pressure head in the volute, and that friction and shock losses in the pump, the velocity heads in the suction and delivery pipes are negligible, calculate the rate of flow and the manometric efficiency of the pump.

Solution

N = 16.6 rev/s
H_s = 2.4 m, H_d = 19 m
H_{fs} = 68 Q^2, H_{fd} = 650 Q^2
D_2 = 35 cm
b_2 = 1.8 cm
ε_2 = 0.95
β_2 = 145°
C_{u1} = 0
C_{r1} = C_{r2}

$$U_2 = \pi D_2 N = 18.25 \quad \text{m/s}$$
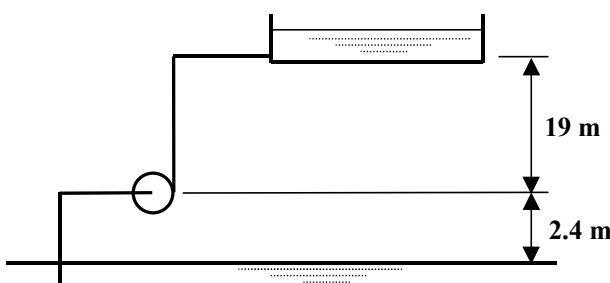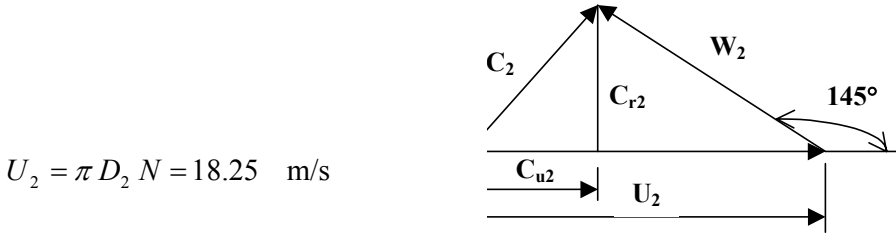
$$H_m = H_s + H_d + H_{fs} + H_{fd} = 2.4 + 19 + 68Q^2 + 650Q^2 = 21.4 + 718Q^2 \qquad (1)$$

$$C_{r2} = \frac{Q}{\pi D_2 b_2 \varepsilon_2} = \frac{Q}{\pi (0.35)(0.018)(0.95)} = 53.18Q \qquad (2)$$

$$C_{u2} = U_2 - \frac{C_{r2}}{\tan(180° - \beta_2)} = 18.25 - \frac{53.18Q}{\tan(180° - 145°)} = 18.25 - 75.95Q \qquad (3)$$

$$C_2^2 = C_{r2}^2 + C_{u2}^2 = (53.18Q)^2 + (18.25 - 75.95Q)^2$$

$$\therefore C_2^2 = 333.1 - 2772.2Q + 8596.5Q^2 \qquad (4)$$

$$C_1 = C_{r1} = C_{r2} = 53.18Q \qquad (5)$$

Applying Bernoulli's equation between the inlet and exit of impeller:

$$\left(\frac{P_1}{\gamma} + \frac{C_1^2}{2g} + Z_1\right) + H_o = \left(\frac{P_2}{\gamma} + \frac{C_2^2}{2g} + Z_2\right) + h_L \qquad (h_L = 0, Z_1 = Z_2)$$

$$\frac{P_2 - P_1}{\gamma} = \frac{C_{u2} U_2}{g} - \frac{C_2^2 - C_1^2}{2g} \qquad (6)$$

Total pressure rise = Pressure rise in impeller + Gain of pressure in the volute

$$H_m = \frac{P_2 - P_1}{\gamma} + 0.5\frac{C_2^2}{2g}$$

$$H_m = \frac{C_{u2} U_2}{g} + \frac{C_1^2}{2g} - \frac{0.5C_2^2}{2g}$$

From equations (1), (4) and (5):

$$21.4 + 718Q^2 = \frac{18.25(18.25 - 75.95Q)}{9.81} + \frac{(53.18Q)^2}{2(9.81)} - \frac{0.5(333.1 - 2772.2Q + 8596.5Q^2)}{2(9.81)}$$

$$792.94Q^2 + 70.64Q - 4.06 = 0$$

$$\therefore Q = 0.0397 \ \text{m}^3/\text{s}$$

$$H_m = 21.4 + 718Q^2 = 22.53 \ \text{m}$$

$$H_o = \frac{C_{u2}U_2}{g} = \frac{18.25(18.25 - 75.95Q)}{9.81} = 28.34 \ \text{m}$$

$$\therefore \eta_m = \frac{H_m}{H_o} = \frac{22.53}{28.34} = 0.795$$

Problems

1- A centrifugal pump lifts water against a static head of 37 m of which 4 m is the static suction lift. The suction and delivery pipes are both 15 cm diameter, the head loss in the suction pipe is 2.2 m and in the delivery pipe is 7.25 m. The impeller is 38 cm diameter, and 2.5 cm wide at the exit. It revolves at 1200 rpm and its effective exit blade angle is 145°. If the manometric efficiency of the pump is 82 % and the overall efficiency is 70 %, what discharge would you expect, and what horsepower would be needed to drive the pump? What would be the pressure head indicated at the suction and delivery branches of the pump?
(12.8 lit/s, 11.3 hp)

2- If the static lift for a centrifugal pump is h_s in meter, speed of rotation N, rpm, and the exit diameter of the impeller is D meters, show that $N = 84.6\sqrt{h_s} / D$ for the speed at which the pumping begins.
(Mans. Univ., B.Sc., 1980)

3- It is required to deliver 1000 lit/min against a head of 131 m at 3600 rpm. Assuming acceptable efficiency of pump at specific speeds of the impeller between 22 and 75 where Q is in m^3/s and H in meters, how many pumping stages should be used?
(3 stages)

4- Gasoline at 100°F is being drawn from a closed tank having a pressure of 0.7 kg/cm^2 in a plant located 1000 m above the sea level, the pump centreline is located 2 m below the gasoline level in the tank. The suction line friction and turbulence head losses are 0.8 meter. The vapour pressure of the gasoline is 0.5 kg/cm^2 and the specific gravity is 0.72, the atmospheric pressure for an altitude of 1000 m is 68.5 Hg, what is the available suction head of the system?
(3.97 m)

5- A centrifugal pump impeller has an external diameter of 30 cm and discharge area of 0.108 m^2. The blades are bent backwards so that the direction of the relative velocity at outlet makes an angle of 145° with the tangent to the direction of impeller rotation. The diameters of the suction and delivery pipes are 30 cm and 22 cm, respectively. Gauges at points on the suction and delivery pipes close to the pump read heads of 3.6 m below and 18.6 m above atmospheric pressure. The pump is 1.5 m above sump level and delivers 720 m^3/hr of water at 1200 rpm, the SHP required is 96. Find:
 (a) The overall efficiency.
 (b) The manometric efficiency, assuming that water enters the impeller without shock or whirl.
 (c) The loss of head in the suction pipe.
(61.7 %, 71.3 %, 1.7 m)   (Alex. Univ., B.Sc., 1971)

6- A centrifugal pump impeller is of 250 mm external diameter and 32 mm wide at exit. The circumference is reduced by 12 % because of the vane thickness. The vanes are inclined at 140° to the tangent at exit. If the discharge is 2860 lit/min,

the hydraulic efficiency is 83 % and the pump revolves at 1000 rpm, calculate the fraction of the kinetic energy of discharge from the impeller which is recovered in the volute. Assume no losses in the impeller.

(59 %)

7- A centrifugal pump, having 4 stages in parallel, delivers 180 lit/s of liquid against a head of 25 m, the diameter of impellers $D_2 = 23$ cm and the speed is 1700 rpm. A pump is to be made up with a number of identical stages in series to run at 1250 rpm and to deliver 240 lit/s against a head of 250 m. Find the diameter of the impellers and the number of stages required if these impellers are of similar construction to those of the first pump.

(5 stages, 44.5 cm)

8- A single-stage centrifugal pump is to be used to pump water through a vertical distance of 30 m at the rate of 45 liters/s. Suction and delivery pipes will have a combined length of 36 m, and a friction factor f of 0.006, both will be 150 mm diameter. Losses at valves, etc., are estimated to total 2.4 times the velocity head in the pipes. The basic design of pump has a dimensionless specific speed of 0.074 rev, forward curved impeller blades with an outlet angle of 65° to the tangent and a width of impeller passages at outlet equal to one-tenth of the diameter. The blades themselves occupy 5 % of the circumference. If a manometric efficiency (neglecting whirl slip) of 75 % may be expected, determine a suitable impeller diameter.

(Mans. Univ., B.Sc., 1981)

9- For a specified duty, 55 tons of water per minute are required to be pumped against a head of 3 meters, it is desired to compare the probable speeds, overall dimensions of a centrifugal pump and a propeller pump. Give an estimate of these values assuming that the maximum diameter of the centrifugal pump casing is 2.5 times the impeller diameter and that the maximum diameter of the propeller pump casing is 1.25 times the propeller diameter.

10- Two centrifugal pumps have the head-discharge characteristic as follows:

(lit/s)	0	4	8	12	16	20	24
Pump I $_m$ **(m)**	50.0	51.8	50.8	48.0	47.5	32.5	18.3
Pump II $_m$ **(m)**	46.5	45.9	44.2	40.3	40.3	26	17

Both pumps are installed together and are required to pump water through a pipe 15 cm diameter having $f = 0.02$. Calculate the heads under which pumps are working and discharges in lit/s pumped by them if:

(a) The pumps are connected in series, static lift is 65 m and suction and delivery pipes are 800 m long.

(b) The pumps are connected in parallel, static lift is 15 m and suction and delivery pipes are 360 m long.

(39 m, 31 m, 17.8 l/s; 28 m, 21 l/s, 19 l/s)

11- A pump operating continuously (8760 hours a year) has an efficiency of 70 percent and circulates 8000 lit/min against a head of 100 m. A new pump costing 1000 LE and having an efficiency of 82 % can be purchased. If power costs 2

piasters per kW-hr and the annual fixed charges are 20 percent of the initial cost, would you advise purchasing the pump?

12- The performance curves of a centrifugal pump are:

Q (lit/s)	50	100	150	200	250	300
H (m)	21	20	19	17.5	15	12.5
η_m (%)	38	67.5	70	83	80	70

When this pump is used with a long pipeline 50 cm diameter, it gave a maximum discharge as 150 lit/s with static lift 10 meters. If another pipeline 40 cm has the same length as the first one is used in parallel with the first line, calculate the approximate pump discharge and SHP. Neglect the effect of suction pipe K.E., (f = 0.03 for all pipes).
(B.Sc., Alex. Univ., 1982)

13- A centrifugal pump is used to deliver water from a water main at point A to the atmosphere at a height of 23 m above pump level. The suction pipe, which is horizontal is of length 5 m and diameter 5 cm, the delivery pipe has 3 bends (C = 0.8) and is of length 45 m and diameter 5 cm. If the water is collected in a tank of dimensions 3 m x 2 m x 2 m, find the minimum time to fill the tank given that the water main pressure at point A is 2 kg/cm^2, coefficient of friction of both pipes = 0.03, and the performance of the pump is given by:

Q (lit/s)	0	3	6	9	12
H (m)	22	22.5	20	16	10
η_m (%)	0	40	70	85	65

(B.Sc., Alex. Univ., 1978)

14- A centrifugal pump having 3 stages and delivers 100 lit/s of liquid against a head of 30 m, the diameter of impellers are D_e = 10 cm, D_2 = 22 cm, the speed is 1750 rpm. Find the diameter of the balance drum if it has to be connected to the suction pipe, what would be the drum diameter if the impellers are to be arranged in a way back to back? (The third impeller is in opposite direction to the 1st and 2nd).

******

CHAPTER V

INCOMPRESSIBLE FLOW TURBINES
" HYDRAULIC TURBINES "

5.1 Impulse Turbines (*Pelton Wheel*)

$$\text{Power} = \frac{\gamma Q}{g}\left(1 - \frac{\cos \beta}{\sqrt{1+k}}\right)\left(UC_1 - U^2\right)$$

where:
   k is the friction coefficient
   C_1 is the jet velocity $= C_v \sqrt{2gh}$

The maximum power $= \dfrac{\gamma Q}{g}\left(C_1^2 / 4\right)\left(1 - \cos \beta\right)$

The ideal efficiency $\eta_{ideal} = 1/2\ (1 - \cos \beta)$

Pressure coefficient $\phi = \dfrac{U}{\sqrt{2gh}}$

Specific speed $N_s = N\sqrt{B.H.P}\,/\,H^{5/4}$

5.2 Reaction turbines (*Francis, Propeller, Kaplan*)

$$Power = \frac{\gamma Q}{g}\left(U_1 C_{u_1} - U_2 C_{u_2}\right)$$

Pressure coefficient $\phi = U_1 / \sqrt{2gh}$

Flow coefficient $\psi = C_{r_1} / \sqrt{2gh}$

$\eta_{hyd} = H_o / H_{available}$
$\eta_{mech} = BHP / \left(\gamma Q H_o / Const.\right)$
$\eta_{overall} = \eta_{hyd} . \eta_{mech} = BHP / WHP$

Draft tube efficiency $= \dfrac{h_g}{\dfrac{V_1^2 - V_e^2}{2g}}$

where:

h_g is the actual head gained,

Subscripts 1 and e denotes inlet and exit of draft tube.

The maximum allowable height of the turbine above tail race Z:

$$Z = P_a / \gamma - P_v / \gamma - \sigma_g H$$

5.3 Torque Converter

$$\eta = \frac{T_2 N_2}{T_1 N_1}$$

Solved Examples

Example (1)

Calculate how many jets would be required for a Pelton wheel, which is to develop 12200 BHP under 264 m head at a speed of 500 rpm. Assuming that the jet diameter is not to exceed 1/9 wheel diameter, state also the diameter of the jets, the diameter of the wheel and the quantity of water required, taking the overall efficiency as 87 %. Assume head coefficient $\phi = 0.45$ and discharge coefficient $C_v = 0.98$.

Solution

$$WHP = BHP / \eta_h = 12200 / 0.87 = \gamma QH / 75$$

Then: $Q = 3.99 \text{ m}^3/\text{s}$

Jet velocity $C_1 = C_v \sqrt{2gh} = 0.98\sqrt{2 \times 9.81 \times 264} = 70.6 \quad \text{m/s}$

Wheel velocity:

$$U = \phi\sqrt{2gh} = 0.45\sqrt{2 \times 9.81 \times 264} = 32.4 \quad \text{m/s}$$

$$U = \pi D N / 60$$

$$32.4 = 3.14 \times D \times 500 / 60$$

i.e. D = Wheel diameter = 1.24 m

$d/D = 1/9$ so, $d = 1.24/9 = 0.1378 \text{ m}$

Area of jet = $(\pi / 4) (0.1378)^2 = 0.0149 \text{ m}^2$

Total required jet area = $Q/C_1 = 3.99/70.6 = 0.0564 \text{ m}^2$

Hence, the number of jets = 0.0564/0.0149 = 3.78 ≈ 4

Therefore, 4 jets are needed each having a diameter of:

$$\sqrt{0.0546 / (4 \times 3.14/4)} = 0.134 \quad \text{m}$$

The actual ratio d/D is thus 0.134/1.24 = 1/9.25 which is about the same.

Example (2)

It is desired to construct a hydraulic turbine for a hydraulic power plant to operate under the following conditions: discharge Q = 3.5 m³/s of water, the available net head = 290 meters, the hydraulic efficiency = 0.8, the rotating speed = 300 rpm. A Pelton wheel impulse turbine was selected with the following specifications: the bucket angle $\beta_2 = 160°$, the coefficient of velocity for the nozzle is 0.98. Determine:

(a) The brake horsepower, Pelton wheel diameter (assume the friction coefficient k = 0.2).

(b) The required number of jets, comment if the ratio of jet diameter to wheel diameter = 1/10, also calculate the head coefficient ϕ and the specific speed N_s.

(Mansoura University, 1977)

Solution

a) $BHP = \eta_h \times WHP$

$BHP = 0.8 \times 1000 \times 3.5 \times 290/75 = 10827$ HP

$$BHP = \gamma Q H / 75 = \frac{\gamma Q}{75g}\left(\left(1 - \frac{\cos \beta_2}{\sqrt{1+k}}\right)\left(C_1 U_1 - U_1^2\right)\right)$$

$C_1 = 0.98\sqrt{2gh} = 73.9$ m/s

$$\frac{0.8 \times 1000 \times 3.5 \times 290}{75} = \frac{1000 \times 3.5}{75g}\left(\left(1 - \frac{\cos \beta_2}{\sqrt{1+k}}\right)\left(73.9U - U^2\right)\right)$$

$U^2 - 73.9U + 1225 = 0$

$U = \frac{-b \pm \sqrt{b^2 - 4c}}{2a}$

$(U - 48.8)$ *or* $(U - 25.1) = 0$

$U = 48.8$ m/s   *or*   25.1 m/s

Total required area $= Q/C_1 = 3.5 / 73.9 = 0.0474$ m^2 or 474 cm^2

If d_j not exceed 1/10 D take $d_j = 0.1D$

$D = \frac{U \times 60}{\pi \times N}$

i.e. $D = \frac{25.1 \times 60}{\pi \times 300} = 1.6$ m

b) $d_j = 0.1 \times 1.6 = 0.16$ m

Area of jet $= \pi (0.16)^2/4 = 0.02$ m^2

No. of jets $= 0.04774 / 0.02 = 2.37$ take 3

Diameter of jet $d_j = \sqrt{\frac{0.0474 \times 4}{3 \times \pi}} = 0.14$ m $= 14$ cm

or $d_j/D = 0.14 / 1.6 = 0.088$ which is about the same.

$\phi = U/C_1 = 25.1 / 73.9 = 0.34$

$$N_s = \frac{N\sqrt{Power}}{H^{5/4}} = \frac{300\sqrt{10827}}{(290)^{1.25}} = 26 \quad \text{in M.K.S.}$$

$$N_s = \frac{N\sqrt{Q}}{(gH)^{3/4}} = \frac{300\sqrt{3.5}}{60(9.8 \times 290)^{3/4}} = 0.0239$$

Example (3)

It is required to construct a hydraulic turbine for a hydraulic power plant, the available net head is 57 m, and the available discharge is 10 m³/s. The proposed turbine type is inward Francis, the turbine runner has the following dimensions: the rotor outside diameter D_1 = 5 m, assume the rotating speed N = 200 rpm. The hydraulic efficiency = 85 %. Find:

(a) The maximum permissible height of the turbine above the tail race, given that the atmospheric pressure P_a = 1.03 kg/cm², vapor pressure is 0.05 kg/cm², and the relation between the specific speed and the critical Thoma cavitation factor is given by:

Specific speed	100	250	400	600
Critical Thoma cavitation factor	0.04	0.15	0.35	0.8

(b) It is required to construct a prototype to predict the actual machine performance. The assumed outside diameter D_1 for the prototype was 0.5 m and the hydraulic circuit in the laboratory has the following specifications:
Available net head = 6 meters, Hydraulic efficiency = 0.85.
Assume the mechanical efficiency equal 0.95, find the required speed and also calculate the specific speed.

Solution

(a) $P = \gamma Q H / 75$

$$\eta_{overall} = \eta_m \eta_h = 0.85 \times 0.95 = 0.808$$

$$P = 1000 \times 10 \times 57 / 75 = 7600 \quad HP$$

$$\eta_{overall} = BHP / WHP$$

i.e. $BHP = 0.808 \times 7600 = 6140$ H.P.

$$N_s = \frac{N\sqrt{BHP}}{H^{5/4}} \quad \text{(metric units)}$$

$$= 200\sqrt{6140} / 57^{5/4} = 100$$

From table σ_c at $N_s = 100 \quad \therefore \sigma_c = 0.04$

$$Z = \frac{P_a}{\gamma} - \frac{P_v}{\gamma} - \sigma_c H$$

$$= 1.03 \times 10^4 / 1000 - 0.05 \times 10^4 / 1000 - 0.04 \times 57$$

$$\therefore \ Z = 7.52 \text{ meters}$$

The height portion of the turbine above the tailrace is 7.5 m

(b) $\quad \dfrac{gH}{D^2 N^2}\bigg|_1 = \dfrac{gH}{D^2 N^2}\bigg|_2$

$$N_2^2 = N_1^2 \times \frac{D_1^2 H_2}{D_2^2 H_1} = 40000 \left(\frac{5}{0.5}\right)^2 \left(\frac{6}{57}\right)$$

$$N_2 = 649 \ \text{rpm}$$

$$\frac{Q}{ND^3}\bigg|_1 = \frac{Q}{ND^3}\bigg|_2$$

$$Q_2 = \frac{Q}{ND^3}\bigg|_1 N_2 D_2^3 = \frac{10 \times 649}{200}\left(\frac{0.5}{5}\right)^3$$

$$Q_2 = 0.0325 \ \text{m}^3/\text{s} \qquad \text{or} \qquad 32.5 \ \text{lit/s}$$

Power = 1000 x 0.0325 x 6 / (75 x 0.808) = 2.127 H.P.

$$N_s = \frac{649\sqrt{2.1267}}{6^{5/4}} = 100$$

Example (4)

The following data refer to a Pelton wheel: the bucket angle $\beta = 165°$, the coefficient of discharge for the nozzle $C_v = 0.98$, the friction coefficient k = 0.2. Assume that the optimum speed ratio differs from 0.5 as a result of losses due to windage and bearing friction, which are proportional to the square of the rotational speed (take the proportionality constant equal to 0.2), obtain a formula for the optimum speed ratio, hence calculate it for the above given data and also calculate the maximum overall efficiency.
(B.Sc., Mansoura University, 1981)

Solution

Given $\qquad \beta = 165°, \qquad C_v = 0.93, \qquad k = 0.2$
Assume the relative velocity $W_2 = \text{Constant} \times W_1$

$$\text{Constant} = J = \frac{1}{\sqrt{1+k}} \qquad\qquad \text{i.e.} \quad W_2 = J\,W_1$$

$$\text{Power} = \frac{\gamma Q}{g}\left(C_{u_1} U_1 - C_{u_2} U_2\right) - \text{Losses in bearing, ... etc.}$$

The losses are proportional to U^2 or $P.U^2$, where P is the proportionality constant.

i.e. $\quad Power = \dfrac{\gamma Q}{g}\left(C_1\cos\alpha_1 U_1 - C_2\cos\alpha_2 U_2 - PU^2\right)$ $\hspace{3cm}$ (1)

$U_1 = U_2 = U, \quad W_2 = JW_1$ $\hspace{5cm}$ (2)

$C_1\cos\alpha_1 = C$

$C_{u_2} = C_2\cos\alpha_2 = U - W_2\cos(180-\beta)$

$W_2 = JW_1 = J(C-U)$

$C_{u_2} = U + J(C-U)\cos\beta$ $\hspace{5cm}$ (3)

From equations (1), (2) and (3):

$$Power = \frac{\gamma Q}{g}\left\{U\left[C-(U+J(C-U)\cos\beta)\right]-PU^2\right\}$$

$$Power = \frac{\gamma Q}{g}\left[UC(1-J\cos\beta)-U^2(1-J\cos\beta)-PU^2\right]$$

$$\frac{d\,Power}{dU}=0=C(1-J\cos\beta)-2U(1-J\cos\beta)-2UP$$

$$\frac{U}{C}=0.5\;\frac{1-J\cos\beta}{1-J\cos\beta+P}\;,\qquad\qquad J=\frac{1}{\sqrt{1+0.2}}=0.913$$

$$\frac{U}{C}=0.5\;\frac{1-0.913\times\cos163°}{1.2-0.913\times\cos163°}=0.4519$$

$$\eta_{overall}=\frac{B.H.P.}{W.H.P.}$$

$$B.H.P.=\frac{\gamma Q}{g}\left[U\,C(1-J\cos\beta)-U^2(1-J\cos\beta)-PU^2\right]$$

When $\quad U/C = 0.45 = \phi \qquad\qquad$ i.e. $\qquad\qquad U = 0.45\,C$

$$\eta_{overall}=\frac{B.H.P.}{W.H.P.}$$

$$\eta_{max}=\frac{1}{gH}\left[\phi C^2(1-J\cos\beta)-\phi^2 C^2(1-J\cos\beta)-P\phi^2 C^2\right]$$

$$=\frac{C^2}{gH}\left[\phi(1-J\cos\beta)-\phi^2(1-J\cos\beta)-P\phi^2\right]$$

$$=\frac{C_v^2.2gH}{gH}\left[(1-J\cos\beta)(\phi-\phi^2)-P\phi^2\right]$$

$$=2C_v^2\left[(1-J\cos\beta)(\phi-\phi^2)-P\phi^2\right]$$

$$=2\times(0.98)^2\left[1.88\times0.2475-0.2\times(0.45)^2\right]=0.832$$

342

Example (5)

A Pelton wheel with a needle-controlled nozzle develops 950 hp when the total head is 200 m and the jet diameter is 10 cm. The nozzle discharge coefficient $C_v = 0.98$. Assuming that the total head and wheel efficiency remain constant, determine the percentage reduction in Q when the horsepower is reduced to 500 hp by (a) needle regulation, (b) partial closure of throttle valve on the pipeline, also obtain the loss of head across the valve in case (b).

Solution

$$(BHP)_1 = 950 \text{ H.P.} \qquad h = 200 \text{ m} \qquad d_3 = 10 \text{ cm.}$$
$$(BHP)_2 = 500 \text{ H.P.}$$
$$C = C_v\sqrt{2gh} = 0.98\sqrt{2 \times 9.8 \times 200} = 61.4 \text{ m/s}$$
$$Q_1 = \pi(0.1)^2(61.4)/4 = 0.481 \text{ m}^3/\text{s}$$

a)
$$\eta = \frac{(BHP)_1}{\gamma\, Q_1\, H/75} = \frac{(BHP)_2}{\gamma\, Q_2\, H/75}$$

i.e. $\dfrac{950}{Q_1} = \dfrac{500}{Q_2}$ $\qquad$ i.e. $\qquad Q_2/Q_1 = 0.526$

b)
$$\eta = \frac{(BHP)_1}{\gamma\, Q_1\, H/75} = \frac{(BHP)_2}{\gamma\, Q(H - H_e)/75}$$

$$\frac{950}{Q_1\, H} = \frac{500}{Q_2(H - H_e)} \tag{1}$$

$$Q_2 = (\pi/4)(0.1)^2(0.98)\sqrt{2 \times 9.81 \times (200 - H_e)}$$
$$= 0.034\sqrt{200 - H_e} \tag{2}$$

From equation (1):

$$Q_2(200 - H_e) = 50.6$$

From equation (2):

$$0.034\sqrt{200 - H_e}\,(200 - H_e) = 50.6$$
$$(200 - H_e)^{1.5} = 1488$$
$$200 - H_e = 130.4$$
$$H_e = 69.6 \text{ m}$$

From equation (1):

$$Q_2/Q_1 = 0.807$$

Example (6)

In a vertical shaft inward flow reaction turbine, the sum of the pressure and kinetic heads at entrance to the spiral casing is 120 m and the vertical distance between this section and the tail race level is 3 m. The peripheral velocity of the runner at entry is 30 m/s, the radial velocity of the water is constant at 9 m/s and the discharge from the runner is without whirl. The estimated hydraulic losses are:

      (1) between turbine entrance and exit from the guide vanes 4.8 m.
      (2) in the runner 8.8 m.
      (3) in the draft tube 790 mm.
      (4) kinetic head rejected to the tail race 460 mm.

Calculate the guide vane angle, the runner blade angle at inlet and the pressure head at entry to the runner.
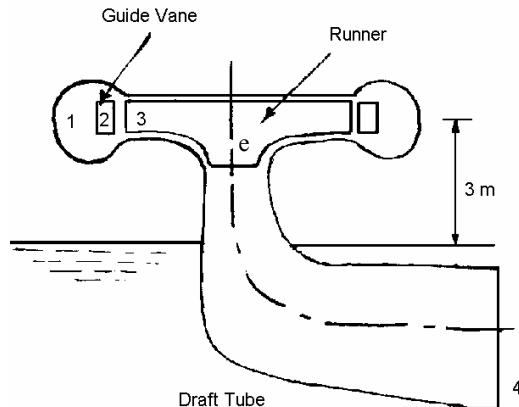
Solution

$U_1 = 30$ m/s

$C_{r3} = C_{re} = 9$ m/s

$\dfrac{P_1}{\gamma} + \dfrac{C_1^2}{2g} = 120$ m

Losses$_{1\text{-}2}$ = 4.8 m

Losses$_{3\text{-}e}$ = 8.8 m

Losses$_{e\text{-}4}$ = 0.79 m

Kinetic energy rejected = 0.46 m

$$H_o = \frac{P_1}{\gamma} + \frac{C_1^2}{2g} + Z - \text{Losses}$$

$$H_o = 120 + 3 - \text{Losses}$$

$$= 123 - (4.8 + 8.8 + 0.79 + 0.46)$$

$$= 108.15 \text{ m}$$

$$H_o = \frac{U_3 C_{u3} - U_e C_{ue}}{g} \quad \text{(The second term} = \text{zero)}$$

$$108.15 = \frac{U_3 . C_{u3}}{g}$$

i.e. $C_{u3} = 35.36$ m/s

$\tan \alpha_3 = \dfrac{C_{r3}}{C_{u3}} = 0.2545$ $\therefore \; \alpha_3 = 14° \; 17'$

$\tan \beta_3 = \dfrac{C_{r3}}{C_{u3} - U_3} = 1.677$ $\therefore \; \beta_3 = 59° \; 12'$

$C_3 = \sqrt{C_{u3}^2 + C_{r3}^2} = 36.49$ m/s

Applying Bernoulli's equation between points 1 and 3:

$$\frac{P_1}{\gamma} + \frac{C_1^2}{2g} = \frac{P_3}{\gamma} + \frac{C_3^2}{2g} + \text{Losses}_{1-2}$$

$$120 = \frac{P_3}{\gamma} + \frac{(36.49)^2}{2(9.81)} + 4.8$$

Pressure head $\quad \dfrac{P_3}{\gamma} = 120 - \dfrac{(36.49)^2}{2(9.81)} - 4.8$

$$= 47.3 \quad \text{m}$$

Example (7)

A vertical shaft inward flow Francis turbine is to be installed in a situation where a much longer draft tube than usual must be used, the turbine runner is 760 mm diameter and the circumferential area of flow at inlet is 0.2 m². The overall operating head is 30 m and the speed is 6.25 rev/s. The guide vane angle is 15° and the inlet angle of the runner blades is 75°. At outlet, water leaves the runner without whirl. The axis of the draft tube is vertical, its diameter at the upper end is 450 mm. The friction loss plus the kinetic energy rejected to the tail race is given by:

$$h_{loss} \ (\text{meters}) = 0.03 \ Q^2 \ L$$

where Q (m³/s) is the flow rate and L (m) the length. If the absolute pressure head at the top of the tube is not to fall below 3.6 m of water, calculate the hydraulic efficiency of the turbine and show that the maximum permissible length of draft tube above the level of the tail race is about 5.35 m. (The length of the tube below tail water level may be neglected. Atmospheric pressure = 10.3 m water head).

Solution

$A_1 = 0.2 \ \text{m}^2$

$H = 30 \ \text{m} \qquad\qquad N = 6.25 \ \text{rev/s}$

$\alpha_1 = 15° \qquad\qquad\quad \beta_1 = 75°$
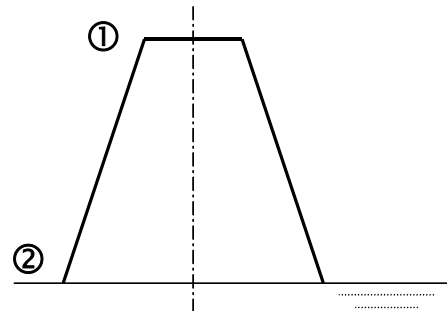
$D = 0.76 \ \text{m} \qquad\qquad D_{draft} = 45 \ \text{cm}$

$h_{loss} = h_f + \dfrac{V_2^2}{2g} = 0.03 \ Q^2 L$
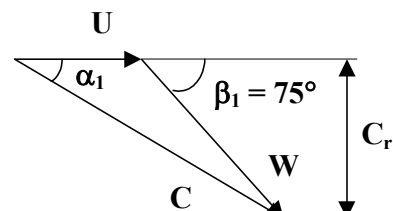
$$U = \pi D N = \pi \times 0.76 \times 6.25 = 14.9 \quad \text{m/s}$$

$$\tan \beta_1 = \frac{C_r}{C_u - U}$$

i.e. $\quad C_u = U + \dfrac{C_r}{\tan \beta_1} = 14.9 + 0.268 \ C_r$

$$\tan \alpha_1 = \frac{C_r}{C_u} = \frac{C_r}{14.9 + 0.268 \ C_r}$$

$$C_r = 4.269 \quad \text{m/s}$$

$$C_u = 16.04 \quad \text{m/s}$$

$$Q = C_r.A = 0.853 \quad \text{m}^3/\text{s}$$

$$\eta_h = \frac{H_o}{H_{av}}, \qquad\qquad H_o = \frac{C_u U}{g} = 24.36 \quad \text{m}$$

$$\eta_h = \frac{24.36}{30} = 0.812 \approx 0.81$$

Applying Bernoulli's equation between (1) and (2):

$$\frac{P_1}{\rho g} + \frac{V_1^2}{2g} + Z = \frac{P_2}{\rho g} + \frac{V_2^2}{2g} + h_f$$

$$3.6 + \frac{Q^2}{2g A_1^2} + L = 10.3 + 0.03 Q^2 L$$

$$3.6 + 1.467 + L = 10.3 + 0.03(0.853)^2 L \qquad\qquad \text{i.e.} \qquad\qquad L = 5.35 \text{ m}$$

Problems

1- For the following two-nozzles Pelton wheel, calculate its maximum efficiency and output. Pitch circle diameter of runner is 2.5 m, nozzle diameter is 0.15 m, head on the nozzle is 1600 m, C_v for nozzle is 0.98, bucket angle at exit is 173°, horsepower lost in disk friction is 6.6 $\times$ 10^{-6} N^3, horsepower lost in bearing friction is 2.1 $\times$ 10^{-3} N^2, where N is the speed of wheel in rpm, speed ratio is 0.45, the relative velocity is reduced by 10 % of its magnitude before leaving the buckets due to friction in buckets.
(88.5 %, 115981 hp)   (Alex. Univ., B.Sc., 1970)

2- An inward Francis turbine rotates at 150 rpm and discharges 0.8 m^3/s. The radial velocity at inlet C_{r1} = 2 m/s and equal 6 m/s at exit, the physical data are: r_1 = 0.5 m, r_2 = 0.2 m, α_1 = 15°, β_2 = 135°, the pressure head at exit is 6 m. Assuming a loss of head of 2 m, find:
(a) The head, power delivered by the turbine (no draft tube), neglect hydraulic losses.
  (b) The pressure head at entrance.

3- A Kaplan turbine develops 2000 H.P. under a head of 6 m. The turbine is set 2.5 m above the tail water level. A vacuum gauge inserted at the turbine outlet records a suction head of 3.1 m. If the turbine efficiency is 85 %, what will be the efficiency of the draft tube, having inlet diameter of 3 m ? Neglect hydraulic losses (Neglect hydraulic losses in the draft tube).

4- The hydro-power station comprises three propeller turbine sets, each develops 10,000 HP at full load and has the following characteristics at constant speed:

Head available is 20 m

Load in % of maximum load	20	40	60	80	100
Overall efficiency (%)	35	58	73	85	92

If the average monthly load on the station during a certain year is:

Months	1,2,3,4	5,6,7	8,9,10,11,12
Average load H.P.	16,000	8,000	22,000

Determine the total amount of water passing in station during this year in the above case, and in the case when one turbine only of 30,000 HP capacity is used having the same above characteristics, which case would you prefer and why?

5- A Francis turbine installation is working under a head of 20 m develops 1500 H.P. when running at 355 rpm. The efficiency of the draft tube is expressed as the ratio of head gained to the inlet kinetic energy. The cross-sectional area of draft tube outlet is four times the inlet area, loss in divergence is 0.2/2g (inlet velocity – outlet velocity)^2 .
(a) Draw the turbine installation, showing the highest position possible of the turbine relative to the tail race, assume the hydraulic efficiency = 0.85.
(b) Calculate the efficiency of the draft tube.
(c) What will be the reading of a pressure gauge set at the inlet of the draft tube, if the inlet area of the draft tube = 3 m^2. (Assume atmospheric pressure = 1.03 kg/cm^2, vapour pressure = 0.05 kg/cm^2).

	Specific speed (metric)	100	250	400

Cavitation factor (critical)   0.04   0.15   0.35
(2.8 m, 0.825, 7.23 m)

6- In order to predict the performance of a turbine which is to work under 77 m head, a model to scale of 1/6 is tested, this model gave the following results on test: N = 100 rpm, head = 3 m, Q = 267 lit/s, output = 5.26 HP. What would be the speed and the output of the prototype when working under its designed head?

Use Moody's formula $\dfrac{1-\eta}{1-\eta_m} = \left(\dfrac{D_m}{D}\right)^{0.2}$.

7- A Kaplan turbine is rated at 34000 H.P. when working under 30 m of head at 160 rpm. Find the diameter of the runner? The overall efficiency of the turbine equals 0.9, the flow ratio = 0.65 and the hub diameter equals 0.3 of the external diameter of runner. Find the specific speed of turbine.

8- A vertical shaft Francis turbine has an overall efficiency of 90 % and runs at 428 rpm with a water discharge of 15.5 m³/s. The flow velocity (C_{r1}) at the inlet of the runner is 8.5 m/s and the pressure head and kinetic head at this point is 140 m, the centerline of the casing being 3 m above the tail water level. The peripheral velocity of the runner is 30 m/s. The hydraulic efficiency is 90 %. Determine:
        (a) The output power in kW.
        (b) The dimensionless specific speed.
        (c) The guide vane angle.
        (d) The runner blade angle at inlet.

9- A fluid coupling is to be used to transmit 150 kW between an engine and a gear box when the engine speed is 40 rev/s. The mean diameter at the outlet of the primary member is 380 mm and the cross-sectional area of the flow passage is constant at 0.026 m². The relative density of the oil is 0.85 and the efficiency of the coupling is 96.5 %. Assuming that the shock losses under steady conditions are negligible and that the friction loss round the fluid circuit is four times the mean velocity head, calculate the mean diameter at inlet to the primary member.

10- A Francis turbine has a runner diameter 2 m, outlet diameter 1 m, outer width 0.5 m, running at 310 rpm under a net head of 90 m. If at full load, flow velocity is 6 m/s, mechanical and hydraulic efficiencies are 80 and 86 %, respectively, calculate the output and speed ratio.
If the velocity of flow is reduced by the use of guide vanes to 3 m/s, draw carefully the inlet and outlet velocity triangles for the above two cases. Estimate approximately the values of mechanical and hydraulic efficiencies.
(Alex. Univ., B.Sc., 1982)

******

CHAPTER VII

FANS, BLOWERS AND TURBO-COMPRESSORS

7.1 Coefficients and Efficiencies of Centrifugal Compressors:

The polytropic head

$$H_{poly} = \frac{R.T_1}{m}\left[\left(\frac{P_2}{P_1}\right)^m - 1\right]$$

with

$$m = \frac{n-1}{n} = \frac{k-1}{k\,\eta_p}$$

$$H_o = \frac{U_2 C_{u_2} - U_1 C_{u_1}}{g}$$

Pressure coefficient $\phi = U_2/\sqrt{2gh}$

Slip factor $= C_{u2}/U_2$

Nominal meter cube (N m^3) is the volume of a gas at 0°C and 760 mm Hg.

A standard cubic foot per minute SCFM is the volume of a gas at 66°F (520°R) and 1497 psia.

Solved Examples

Example (1)

A sewage aeration blower running at 3500 rpm is designed to deliver 34000 m³/hour of air from 20°C and 1.03 kg/cm² atmospheric pressure to a discharge pressure of 1.56 kg/cm² with an efficiency of 70 %. On a hot summer day, the atmospheric temperature rises to 43°C but the barometric pressure does not change. It is desired to vary the blower speed to maintain the same discharge pressure.
Determine:
  (a) blower speed for the summer operation.
  (b) corresponding flow in nominal meter cube per month.
(c) brake horsepower required, assuming that the efficiency remains constant and
   assume a mechanical efficiency of 0.9. (k = 1.4 for air).

Solution

(a)   The polytropic head: $H_{poly} = \dfrac{R.T_1}{m}\left[\left(\dfrac{P_2}{P_1}\right)^m - 1\right]$

where $m = \dfrac{k-1}{k\,\eta_p}$

P_2 remains constant, thus,

$$\frac{H_{poly\,1}}{H_{poly\,2}} = \frac{P_1 v_1}{P_2 v_2} = \frac{T_1}{T_2}, \qquad Pv = RT$$

and $R = \overline{R}/MW = 848/29 = 29.25 \text{ m/K}$

$$H_1 = \frac{29.25\times(20+273)}{\dfrac{1.4-1}{1.4\times0.7}}\left[\left(\frac{1.56}{1.03}\right)^{\frac{1.4-1}{1.4\times0.7}} - 1\right]$$

$H_1 = 21005\,(1.1845) = 3876 \quad \text{m}$

i.e. $H_2 = H_1(T_2/T_1) = 3876(316/293) = 4180 \quad \text{m}$

From affinity laws:

$$\frac{H_1}{H_2} = \frac{N_1^2}{N_2^2}$$

Then $N_2 = \sqrt{4180\times3500/3876} = 3635 \quad \text{rpm}$

(b)   From affinity laws:
       $Q_1/Q_2 = N_1/N_2$
   i.e. $Q_2 = 3635 \times 34000/3500 = 35311 \text{ m}^3/\text{hr}$

The nominal meter cube is the volume of a gas at atmospheric pressure and 0°C

       $Q = v_o\, Q_2 / v_2$

v_o is the specific volume of air at 0°C = R.T$_o$ / P_a

$P_o = P_1$ inlet pressure, then:

$Q = Q_2\, T_o/T_2$ in Nominal m³/hr

$\quad = 35311 \times 273/316 = 30506$ Nominal m³/hr

The power $= \gamma\, QH\,/(\eta \times 75) = QH\,/(v\eta \times 75)$

$\qquad P.v = R.T$

$$v = RT_1\,/\,P_1 = \frac{29.25 \times 316}{1.03 \times 10^4} = 0.899 \quad m^3/kg$$

i.e. $Power = \dfrac{4180 \times 35311}{3600 \times 0.899 \times 0.7 \times 75} = 869\ H.P.$

The brake horsepower $= \dfrac{869}{0.9}$ $\therefore\ B.H.P. = 965$ H.P.

Example (2)

The impeller of a centrifugal fan has an inner radius of 250 mm and width of 187.5 mm; the values at exit are 375 mm and 125 mm, respectively. There is no whirl at inlet, and at outlet the blades are backward facing at 70° to the tangent. In the impeller there is a loss by friction of 0.4 times the kinetic head corresponding to the relative outlet velocity, and in the volute there is a gain equivalent to 0.5 times the kinetic head corresponding to the absolute velocity at exit from the runner. The discharge of air is 5.7 m³/s when the speed is 13.5 rev/s. Neglecting the thickness of the blades and whirl slip, determine the head across the fan and the power required to drive it if the density of the air is sensibly constant at 1.25 kg/m³ throughout and mechanical losses account for 220 W.

Solution

r_1 = 250 mm
b_1 = 187.5 mm
r_2 = 375 mm
b_2 = 125 mm
N = 13.5 rev/s
180° − β_2 = 70°
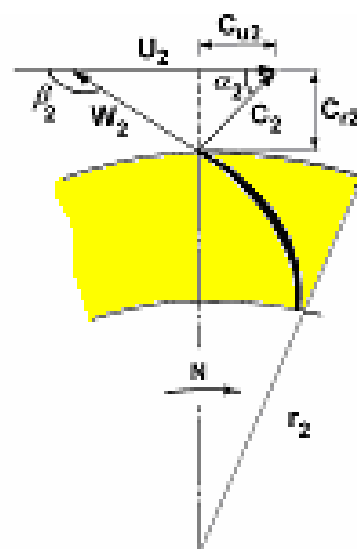
Losses: $0.4\ \dfrac{W_2^2}{2g}$, $0.5\ \dfrac{C_2^2}{2g}$

Q = 5.7 m³/s
$\rho_{air} = 1.25$ kg/m³
Mechanical Losses = 220 W

$$U_2 = \frac{2\pi r_2 N}{60} = 31.79 \quad \text{m/s}$$

$$H_o = \frac{C_{u_2} U_2}{g}$$

$$C_{r_2} = \frac{Q}{2\pi r_2 b_2} = \frac{5.7}{2\pi \times 0.375 \times 0.125} = 19.35 \quad \text{m/s}$$

$$C_{u_2} = U_2 - \frac{C_{r_2}}{\tan 70°} = 24.74 \quad \text{m/s}$$

$$W_2 = \frac{C_{r_2}}{\sin 70°} = 20.59 \quad \text{m/s}$$

$$C_2 = \sqrt{C_{r_2}^2 + C_{u_2}^2} = 31.4 \quad \text{m/s}$$

$$H_o = \frac{C_{u_2} U_2}{g} = 80.1 \quad \text{m}$$

$$\textit{Losses in impeller} = 0.4 \times \frac{W_2^2}{2g} = 8.6 \quad \text{m}$$

$$\textit{Losses in volute} = 0.5 \times \frac{C_2^2}{2g} = 25.1 \quad \text{m}$$

Total losses = 25.1 + 8.6 = 33.7 m

Head gained = 80.1 − 33.7 = 46.4 m

$$\text{Power} = \frac{\gamma Q H_o}{\textit{Const.}} = \frac{1.25 \times 5.7 \times 80.1}{75} = 7.61 \quad \text{hp}$$

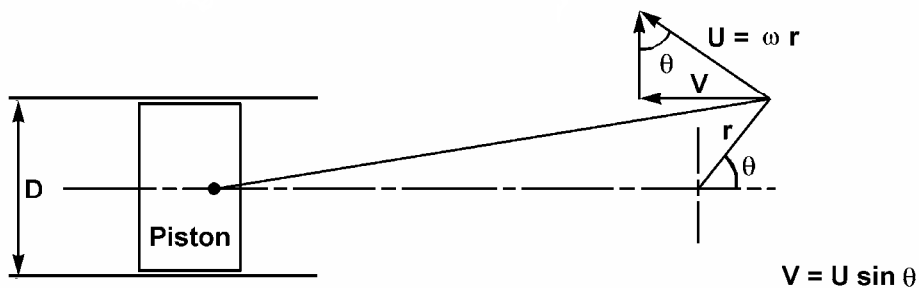B.H.P. = $7.61 + 220 \times 10^{-3} \times 1.34 = 7.9$ hp

Problems

1- In a centrifugal compressor the inlet absolute flow to the runner is radial, and the exit relative flow from the runner is radial and the runner operates at 22000 rpm and has an outside diameter of 28 cm, the used gas is air and the inlet temperature is 18°C. If the pressure coefficient $\phi = 0.5$, find the pressure ratio.

2- A centrifugal fan runner consists of some blades, two parallel circular disks and a short length of circular pipe in an axial direction at inlet. Assume an incompressible fluid with a certain density in slugs per cubic meter. The runner speed is N (rpm), the outside diameter of the runner is D (meter), and the inlet diameter is 0.4 D, assume that the area of the inlet pipe equals the circumferential area (between the parallel disks) at the inlet diameter, the relative velocity of exit is radial, with a magnitude 0.3 of the velocity. Develop an expression for the torque in meter-kg of the runner on the fluid in terms of density, N, D, and some numerical constants.

3- A blower is designed to draw in 2000 m^3/hr of carbon dioxide at 32°C and 1.24 kg/cm^2 and compress it to 1.4 kg/cm^2 when operating at 4000 rpm. It is to be tested with air at 1.03 kg/cm^2 and 20°C and driven by a motor running at 3550 rpm. Determine the flow discharge and pressure, which the machine should deliver at the design point on test to be acceptable.

4- A two-stage radial airplane supercharger is designed to deliver 4000 kg of air per hour at a pressure of 77 cm of Hg when operating at an altitude of 5000 meter where the temperature is −15°C and the pressure is 42 cm Hg. It rotates at 18000 rpm and is to have a polytropic efficiency of 0.72. It is to be tested at sea level (75 cm Hg and 26°C) at a speed of 14000 rpm. Assuming that the efficiency at the design point does not change, determine for the design point under test conditions:
    (a) the cubic meter of air taken in per minute.
    (b) the discharge pressure in cm of mercury absolute.
    (c) the horsepower required to drive it.

******

CHAPTER VIII

VOLUMETRIC MACHINES

8.1 Piston Pump

$$Q = \frac{\pi}{4}D^2 2r \frac{N}{60} \qquad\qquad \text{Stroke} = 2\,r$$

The swept volume $= \dfrac{\pi}{4}D^2 2r$

$$\eta_v = Q_a / Q$$

The velocity in the delivery pipe $V_p = \dfrac{2\pi\,n.r}{60}\dfrac{D^2}{d^2}\sin\theta$,   where d is the pipe diameter.
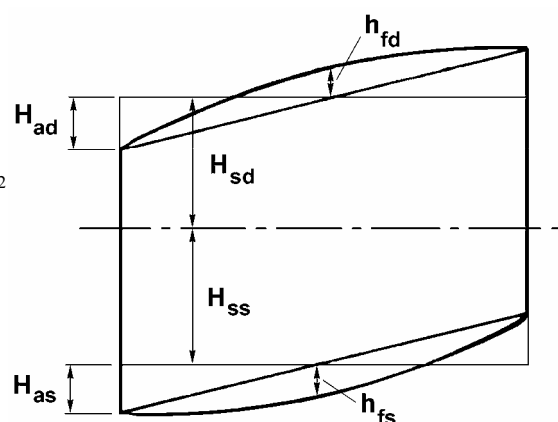
8.2 Inertia Pressure

$$\frac{P_1}{\rho g} = \left(\frac{l}{g}\right)\omega^2 r\left(\frac{D^2}{d^2}\right)\cos\theta$$

8.3 Effect of Friction

$$h_f = f\frac{L}{d}\frac{V_p^2}{2g} = \frac{f.L}{2g\,d}\left(\omega r\frac{D^2}{d^2}\sin\theta\right)^2$$

$$H_{ma} = H_{ss} + H_{sd} + \frac{2}{3}\left(h_{fs} + h_{fd}\right)$$

354

8.4 Gear Wheel Pump

$$Q = \frac{2a.l.n.N}{60}$$

where a area enclosed between any two teeth and the casing,
  l axial length of teeth,
  n number of teeth in each gear,
  N speed in rpm.

Solved Examples

Example (1)

Estimate the dimensions of the rotors of a gear wheel pump for the following duty: liquid oil of viscosity $4*10^{-4}$ m^2/s, overall efficiency = 0.6, volumetric efficiency = 0.9, number of teeth per rotor = 12, ratio of l/D = length/diameter = 1.5, ratio of D/C (where C is the distance between axes) = 1.18, discharge 350 lit/min, speed 750 rpm, pressure generated 10.5 kg/cm^2, what power input would be required?

Solution

Discharge per revolution = 350 x 1000 /750 = 466.6 cm^3 / revolution

Q = 466.6 / 0.9 = 518.4 cm^3 / revolution

$Q = KC(D-C)l$

$Q = 2.98\,C(D-C)l$

$Q = 2.98\,\dfrac{D}{1.18}\left(D-\dfrac{D}{1.18}\right)(1.5D)$

Q is the discharge per revolution, from which the rotor diameter D = 9.65 say 10 cm.

L = Length = 15 cm

Power output = $\gamma\,Q\,H\,/75$ = 10.5 x 10^4 x 350 /(1000 x 60 x 75)

= 8.16 H.P.

B.H.P. = 8.16 / 0.6 = 13.6 H.P.

Example (2)

A single-acting reciprocating water pump, with a bore and stroke of 150 mm and 300 mm respectively, runs at 0.4 rev/s. Suction and delivery pipes are each 75 mm diameter. The former is 7.5 m long and the suction lift is 3 m. There is no air vessel on the suction side. The delivery pipe is 300 m long, the outlet (at atmospheric pressure) being 13.5 m above the level of the pump, and a large air vessel is connected to the delivery pipe at a point 15 m from the pump. Calculate the absolute pressure head in the cylinder at beginning, middle and end of each stroke. Assume that the motion of the piston is simple harmonic, that losses at inlet and outlet of each pipe are negligible, that the slip is 2 % and that f for both pipes is constant at 0.01. (Atmospheric pressure is 10.34 m water head).

Solution

Single acting, single cylinder
D = 15 cm
Stroke $L = 2r = 30$ cm
N = 0.4 rps
$d_s = d_d = 7.5$ cm
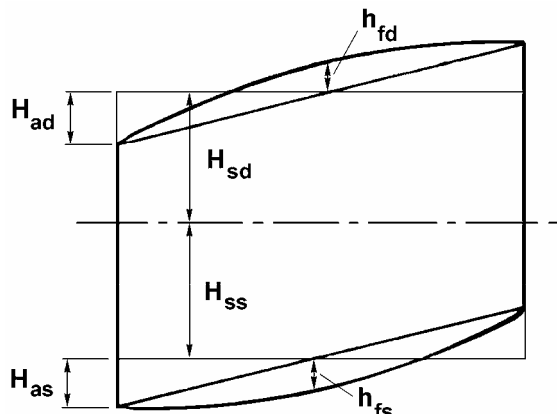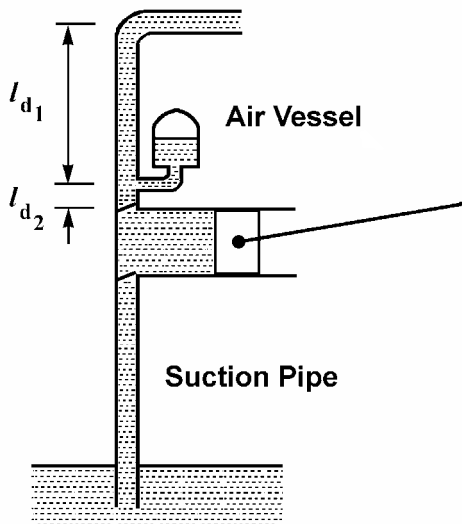$l_s = 7.5$ m
$l_d = 300$ m
$H_{ss} = 3$ m
$H_{sd} = 13.5$ m
$l_{d2} = 15$ m

$$slip = 2\% = \frac{Q - Q_a}{Q} \times 100$$

$f = 0.01$
$H_{at} = 10.34$ m water

Air Vessel

Suction Pipe

I. Suction Stroke

Absolute Pressure $= H_{at} - H_{ss} - H_{as} - h_{fs}$

$$H_{as} = \frac{l_s}{g}\frac{A}{a_s}\omega^2 r \cos\theta$$

$$= \frac{7.5}{9.81}\left(\frac{0.15}{0.075}\right)^2 (2\pi \times 0.4)^2 \times 0.15 \cos\theta$$

$$= 2.9\cos\theta$$

$$h_{fs} = f\frac{l_s}{2gd_s}\left(\frac{A}{a_s}\right)^2 (\omega r)^2 \sin^2\theta$$

$$= 0.01\frac{7.5}{2 \times 9.81 \times 0.075}\left(\frac{0.15}{0.075}\right)^4 (2\pi \times 0.4 \times 0.15)^2 \sin^2\theta$$

$$= 0.116\sin^2\theta$$

Absolute Pressure $= 10.34 - 3 - 2.9\cos\theta - 0.116\sin^2\theta$
$\quad = 7.34 - 2.9\cos\theta - 0.116\sin^2\theta$

357

- At the beginning $\qquad \theta = 0$

$\qquad$ Absolute Pressure = 4.44 m water
- At the middle $\qquad \theta = \pi/2$

$\qquad$ Absolute Pressure = 7.22 m water
- At the end $\qquad \theta = \pi$

$\qquad$ Absolute Pressure = 10.24 m water

II. Delivery Stroke

$\qquad$ Absolute Pressure $= H_{at} + H_{sd} + h_{fd1} - h_{fd2} - H_{ad2} + V_d^2/2g$ (The last term = 0)

$$Q = \frac{ALN}{60} = (\pi/4)(0.15)^2 \times 0.30 \times 0.4 = 2.12 \times 10^{-3} \quad m^3/s$$

$\because slip = 2\% = \dfrac{Q - Q_a}{Q} \times 100$

$\therefore Q_a = 0.98Q = 0.98(2.12 \times 10^{-3}) = 2.0776 \times 10^{-3} \quad m^3/s$

$$V_d = \frac{Q_a}{A_p} = \frac{2.0776 \times 10^{-3}}{(\pi/4)(0.075)^2} = 0.47 \text{ m/s}$$

$$h_{f\,d_1} = f\frac{l_{d_1}}{d_d}\frac{V_d^2}{2g} = 0.01 \times \frac{(300-15)}{0.075} \times \frac{(0.47)^2}{2 \times 9.81}$$

$$= 0.428 \text{ m}$$

$$h_{f\,d2} = f\frac{l_{d_2}}{2g\,d_d}\left(\frac{A}{a_d}\right)^2 (\omega r.\sin\theta)^2$$

$$= 0.01 \times \frac{15}{2 \times 9.81 \times 0.075}\left(\frac{0.15}{0.075}\right)^4 \times (2\pi \times 0.4 \times 0.15)^2 \sin^2\theta$$

$$= 0.232 \sin^2\theta$$

$$H_{ad2} = \frac{l_{d2}A}{g\,a_d}\omega^2 r\cos\theta = \frac{15 \times \pi/4(0.15)^2}{9.81 \times \pi/4(0.075)^2}(2\pi \times 0.4)^2 \times 0.15 \cos\theta$$

$$= 5.795 \cos\theta$$

Absolute Pressure $= 10.34 + 13.5 + 0.428 - 0.232 \sin^2\theta - 5.795 \cos\theta$

$\qquad\qquad\qquad = 24.268 - 0.232 \sin^2\theta - 5.795 \cos\theta$

- At the beginning of delivery stroke $\theta = \pi$

$\qquad$ Absolute Pressure $= 24.268 - 0 + 5.795 = 30.063$ m water

- At the middle $\theta = 3\pi/2$

$\qquad$ Absolute Pressure $= 24.268 + 0.232 - 0 = 24.5$ m water

- At the end $\theta = 2\pi$

$\qquad$ Absolute Pressure $= 24.268 - 0 - 5.795 = 18.473$ m water

Problems

1- A plunger pump works against a total static head of 96 m and when running at 42 rpm. It is required to force 45 lit/s of water along a delivery pipe 25 cm diameter and 130 m long, there are no air vessels, the stroke of plungers is twice the diameter. If the number of cylinders chosen were 1, 2, 3 and 4, calculate in each case:

     i) the plunger diameter,

    ii) the maximum pressure in the pipe.

2- A gear wheel pump is required to deliver 4 lit/s of oil of specific gravity of 0.94 when running at 700 rpm. The suction pressure is 0.2 kg/cm^2 and the delivery pressure is 6 kg/cm^2, the overall efficiency is 90 %. The length of the gear wheels or rotors is 2 x maximum diameter, and in shape they are geometrically similar to those shown in the figure (Chapter VIII), what would be their outside diameter and what would be the power input to the pumps?

3- A reciprocating pump has two double acting cylinders each 200 mm bore, 450 mm stroke, the cranks being at 90° to each other and rotating at 20 rev/min. The delivery pipe is 100 mm diameter, 60 m long and there are no air vessels. Assuming simple harmonic motion for the piston, determine the maximum and mean water velocities in the delivery pipe and the inertia pressure in the delivery pipe near the cylinders at the instant of minimum water velocity in the pipe.

(2.666 m/s, 2.4 m/s, ± 236.9 kPa)

****

******